High Voltage Engineering

J Rohan Lucas

Senior Professor in Electrical Engineering

BScEng, MSc, PhD, FIEE, CEng, FIE(SL), MCS(SL)

2001

Department of Electrical Engineering
University of Moratuwa, Sri Lanka

First Produced in Cyclostyled form 1970
[Revised and Reproduced periodically]

New Edition 1995
Revised Edition 2001

Printed in Sri Lanka

Contents

Preface

This book has arisen out of the need to include many of the major aspects of high voltage engineering in a single volume. The book is intended primarily as a basic text book in high voltage engineering at the Final Year level of a four year undergraduate course specialising in Electrical Engineering, with emphasis on heavy current engineering. It is also expected to be of immense value to practising electrical engineers, especially to those in the electricity supply industry.

The substance of this book is organised in the following major sections. (i) Review of breakdown of insulating materials, (ii) Surge phenomena and their analysis, (iii) Generation of high voltages for testing purposes, (iv) measurement of high voltages and testing procedure, and (v) Co-ordination of insulation in a power system.

A prior knowledge of basic electrical engineering theory and electric power system analysis has been considered as a pre-requisite in writing this book. However, important background material is reviewed as a refresher where ever considered necessary.

Information for this book has been collated over a period of over 25 years from various sources, a record of which has not been maintained, during the teaching of high voltage engineering as a subject to electrical engineering undergraduates at the University of Moratuwa and its predecessors. The author is grateful to each of these sources, but regrets his inability to thank them individually.

This book, although it has not come out as a complete text book before the 1995 edition, it has nevertheless come out in parts, mainly as lecture handouts over the period of time. In fact, the original complete edition in cyclostyled form came out during the period July-September 1971 and has undergone continuous revisions.

October 2001 J. R. Lucas

Breakdown of Gaseous Insulation

1.1 Ionisation of Gases

Electrical Insulating Materials (or Dielectrics) are materials in which electrostatic fields can remain almost indefinitely. These materials thus offer a very high resistance to the passage of direct currents. However, they cannot withstand an infinitely high voltage. When the applied voltage across the dielectric exceeds a critical value the insulation will be damaged. The dielectrics may be gaseous, liquid or solid in form.

Gaseous dielectrics in practice are not free of electrically charged particles, including free electrons. The electrons, which may be caused by irradiation or field emission, can lead to a breakdown process to be initiated. These free electrons, however produced, on the application of an electric field are accelerated from the cathode to the anode by the electric stress applying a force on them. They acquire a kinetic energy (½ mu^2) as they move through the field. The energy is usually expressed as a voltage (in electron-volt, eV, where e is the charge on an electron) as the energies involved are extremely small. [The energy $E_i = e\ V_i$ is expressed in electron volt. 1 e V = 1.6×10^{-19} J]. These free electrons, moving towards the anode collide with the gas molecules present between the electrodes. In these collisions, part of the kinetic energy of the electrons is lost and part is transmitted to the neutral molecule. If this molecule gains sufficient energy (more than the energy E_i necessary for ionisation to occur), it may ionise by collision. The (mean) number of ionising collisions by one electron per unit drift across the gap is not a constant but subject to statistical fluctuations. The newly liberated electron and the impinging electron are then accelerated in the field and an electron avalanche is set up. Further increase in voltage results in additional ionising processes. Ionisation increases rapidly with voltage once these secondary processes take place, until ultimately breakdown occurs.

It is worth noting that in uniform fields, the ionisation present at voltages below breakdown is normally too small to affect engineering applications. In non-uniform fields, however, considerable ionisation may be present in the region of high stress, at voltages well below breakdown, constituting the well known corona discharge.

1.1.1 Ionisation processes in gas discharges

The electrical breakdown of a gas is brought about by various processes of ionisation. These are gas processes involving the collision of electrons, ions and photons with gas molecules, and electrode processes which take place at or near the electrode surface [Electrons can be emitted from the cathode if the stress is around 100 - 1000 kV/cm due to field emission].

Ionisation is the process by which an electron is removed from an atom, leaving the atom with a nett positive charge (positive ion). Since an electron in the outermost orbit is subject to the least attractive force from the nucleus, it is the easiest removed by any of the collision processes. The energy required to remove an outer electron completely from its normal state in the atom to a distance well beyond the nucleus is called the first ionisation potential.

The reciprocal process of an electron falling from a great distance to the lowest unoccupied orbit is also possible. In this case, a photon will be emitted having the same energy as previously absorbed.

1.1.2 Relevant gas ionisation processes

(i) Ionisation by simple collision

When the kinetic energy of an electron (½ mu²), in collision with a neutral gas molecule exceeds the ionisation energy ($E_i = e V_i$) of the molecule, then ionisation can occur.
(i.e. when ½ mu² > E_i)

$$M + e^- (½ mu^2) \rightarrow M^+ + 2 e^-$$

In general, a positive ion and 2 slow moving electrons will result. The probability of this process is zero for electron energies equal to the ionisation energy E_i, but increases almost linearly at first, and then gradually with electron energy up to a maximum.

When the gas molecules are bombarded with electrons, other electrons bound to atoms may be freed by the collision with the high energy electron. The ratio of the electrons given by collision to the primary electrons depend, mainly on the energy of the primaries. This is maximum at primary electron energies of about 200 - 500 eV. For lower energy values, the energy transferred may not be sufficient to cause electrons to escape from the surface of the molecules, and thus the probability of ionisation is small. For much higher values of primary energies, the energy of the impinging electron would be sufficient for this electron to penetrate the surface deeper into the molecule, so that again the chance of escape of other electrons decreases.

Thus the variation of the ionisation probability in air with increase of electron energy is as shown in figure 1.1.

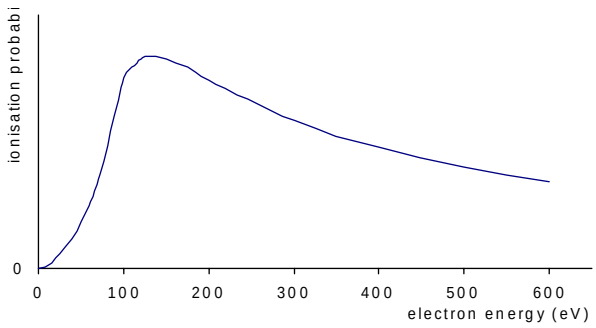

Figure 1.1 - Ionisation probability curve in air

(ii) Excitation

In the case of simple collision, the neutral gas molecule does not always gets ionised on electron impact. In such cases, the molecule will be left in an excited state M^*, with energy E_e.

$$M + e^- (½ mu^2) \rightarrow M^* + e^-$$

This excited molecule can subsequently give out a photon of frequency v with energy emitted h v. The energy is given out when the electron jumps from one orbit to the next.

$$M^* \rightarrow M + h v$$

where h = Planck's constant = 6.624×10^{-34} J s

(iii) Ionisation by Double electron impact

If a gas molecule is already raised to an excited state (with energy E_e) by a previous collision, then ionisation of this excited molecule can occur by a collision with a relatively slow electron. This electron would need less energy than the ionisation energy, but the energy must exceed the additional energy required to attain the ionisation energy.

(i.e. $\frac{1}{2} mu^2 > E_i - E_e$)

$$M^* + e^- (\tfrac{1}{2} mu^2) \rightarrow M^+ + 2\, e^-$$

(iv) Photo-ionisation

A molecule in the ground state can be ionised by a photon of frequency v provided that the quantum of energy emitted h v (by an electron jumping from one orbit to another), is greater than the ionisation energy of the molecule.

(i.e. $h\,v > E_i$, where h = Plank's constant = 6.624×10^{-34} joule)

$$M + h\,v \rightarrow M^+ + e^-$$

(v) Electron Attachment

If a gas molecule has unoccupied energy levels in its outermost group, then a colliding electron may take up one of these levels, converting the molecule into a negative ion M^-.

$$M + e^- \rightarrow M^-$$

The negative ion thus formed would be in an excited state, caused by the excess energy.

Note: Electron attachment decreases the number of free electrons, unlike ionisation which increases the free electrons.

(vi) Electron detachment

This occurs when a negative ion gives up its extra electron, and becomes a neutral molecule.

$$M^- \rightarrow M + e^-$$

(vii) Other Processes

The above processes are the most important in relation to the gas discharge phenomena. Other possible gas processes include ion-atom collisions, excited atom-molecule collisions, and atom-atom collisions. It should be noted that collisions between ions and atoms rarely result in ionisation, due to the relatively slow interaction time, which allows the internal motion of the atomic system to adjust itself gradually to the changing condition without any energy transition occurring.

In order to cause ionisation of a neutral unexcited atom of its own kind, a positive ion must possess energy of at least 2 eV. Normally ions and atoms having such energies are encountered only in high current arcs and thermonuclear discharges.

1.2 Breakdown Characteristic in gases

Two mechanisms of breakdown in gasses is known. These are the **avalanche** and **streamer** mechanisms.

1.2.1 Electron Avalanche Mechanism (Townsend Breakdown Process)

One of the processes which are considered in breakdown is the Townsend breakdown mechanism. It is based on the generation of successive secondary avalanches to produce breakdown.

Suppose a free electron exists (caused by some external effect such as radio-activity or cosmic radiation) in a gas where an electric field exists. If the field strength is sufficiently high, then it is likely to ionize a gas molecule by simple collision resulting in 2 free electrons and a positive ion. These 2 electrons will be able to cause further ionization by collision leading in general to 4 electrons and 3 positive ions. The process is cumulative, and the number of free electrons will go on increasing as they continue to move under the action of the electric field. The swarm of electrons and positive ions produced in this way is called an electron avalanche. In the space of a few millimetres, it may grow until it contains many millions of electrons. This is shown in Figure 1.2.

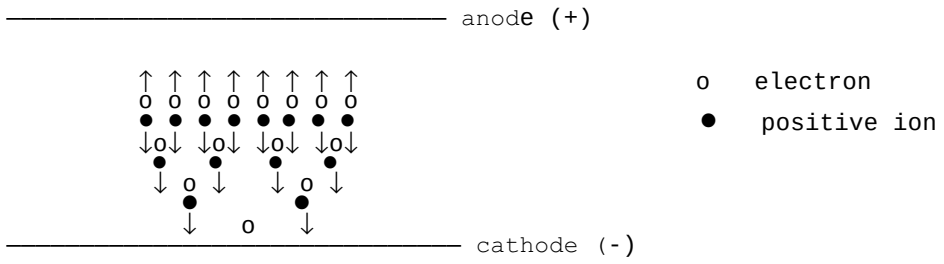

Figure 1.2 - Electron Avalanche

1.2.1.1 Mathematical Analysis

When the voltage applied across a pair of electrodes is increased, the current throughout the gap increases slowly, as the electrons emitted from the cathode move through the gas with an average velocity determined by their mobility for the field strength existing for the particular value of voltage. Impact ionization by electrons is probably the most important process in the breakdown of gasses, but this process alone is not sufficient to produce breakdown.

Let n_0 = number of electrons/second emitted from the cathode,

n_x = number of electrons/second moving at a distance x from the cathode
[$n_x > n_0$ due to ionising collisions in gap]

α = number of ionising collisions, on average, made by one electron per unit drift in the direction of the field. [Townsend's first ionisation coefficient]

then $1/\alpha$ = average distance traversed in the field direction between ionising collisions.

Consider a laminar of thickness dx at a distance x from the cathode. The n_x electrons entering the laminar will traverse it in the presence of the applied field E. The ionising collisions generated in the gas gap will be proportional to both dx and to n_x.

Thus

$$dn_x \propto n_x$$

$$\propto dx$$

Therefore $dn_x = \alpha \, . \, n_x \, . \, dx$ (from definition of α)

Rearranging and integrating gives

$$\int_{n_0}^{n_x} \frac{d\, n_x}{n_x} = \alpha \int_0^x dx$$

$$\log_e (n_x / n_0) = \alpha \,.\, x$$

$$n_x = n_0 \cdot e^{\alpha x}$$

If the anode is at a distance x = d from the cathode, then the number of electrons n_d striking the anode per second is given by

$$n_d = n_0 \,.\, e^{\alpha d}$$

Therefore, on the average, each electron leaving the cathode produces $(n_d - n_0)/n_0$ new electrons (and corresponding positive ions) in the gap.

In the **steady state**, the number of positive ions arriving at the cathode/second must be exactly equal to the number of newly formed electrons arriving at the anode. Thus the circuit current will be given by

$$I = I_0 \,.\, e^{\alpha d}$$

where I_0 is the initial photo-electric current at the cathode.

In the actual breakdown process, the electron impact ionization is attended by secondary processes on the cathode, which replenish the gas gap with free electrons, with every newly formed avalanche surpassing the preceding one in the number of electrons.

Consider now the current growth equations with the secondary mechanism also present.

Let γ = number of secondary electrons (on average) produced at the cathode per ionising collision in the gap. [Townsend's second ionisation coefficient]

n_0 = number of primary photo-electrons/second emitted from the cathode

n_0' = number of secondary electrons/second produced at the cathode

n_0'' = total number of electrons/second leaving the cathode

Then $n_0' = n_0 + n_0''$

On the average, each electron leaving the cathode produces $[e^{\alpha d} - 1]$ collisions in the gap, giving the number of ionising collisions/second in the gap as $n_0'' (e^{\alpha d} - 1)$. Thus by definition

$$\gamma = \frac{n_0'}{n_0''(e^{\alpha d} - 1)}$$

giving $n_{0'} = \gamma\, n_0''(e^{\alpha d} - 1)$

but $n_0'' = n_0 + n_{0'}$

so that $n_0'' = n_0 + n_0''(e^{\alpha d} - 1).\gamma$

This gives the result

$$n_0'' = \frac{n_0}{1 - \gamma (e^{\alpha d} - 1)}$$

Similar to the case of the primary process (with α only), we have

$$n_d = n_0'' \, e^{\alpha d} = \frac{n_0 \, e^{\alpha d}}{1 - \gamma (e^{\alpha d} - 1)}$$

Thus, in steady state, the circuit current I will be given by

$$I = \frac{I_0 \, e^{\alpha d}}{1 - \gamma (e^{\alpha d} - 1)}$$

This equation describes the growth of average current in the gap before spark breakdown occurs.

As the applied voltage increases, $e^{\alpha d}$ and $\gamma e^{\alpha d}$ increase until $\gamma e^{\alpha d} \rightarrow 1$, when the denominator of the circuit current expression becomes zero and the current $\mathbf{I \rightarrow \infty}$. In this case, the current will, in practice, be limited only by the resistance of the power supply and the conducting gas.

This condition may thus be defined as the breakdown and can be written as

$$\gamma (e^{\alpha d} - 1) = 1$$

This condition is known as the **Townsend criteria for spark breakdown**.

The avalanche breakdown develops over relatively long periods of time, typically over 1 μs and does not generally occur with impulse voltages.

1.2.1.2 Determination of Townsend's Coefficients α and γ

Townsend's coefficients are determined in an ionisation chamber which is first evacuated to a very high vacuum of the order of 10^{-4} and 10^{-6} torr before filling with the desired gas at a pressure of a few torr. The applied direct voltage is about 2 to 10 kV, and the electrode system consists of a plane high voltage electrode and a low voltage electrode surrounded by a guard electrode to maintain a uniform field. The low voltage electrode is earthed through an electrometer amplifier capable of measuring currents in the range 0.01 pA to 10 nA. The cathode is irradiated using an ultra-violet lamp from the outside to produce the initiation electron. The voltage current characteristics are then obtained for different gap settings. At low voltage the current growth is not steady. Afterwards the steady Townsend process develops as shown in figure 1.3.

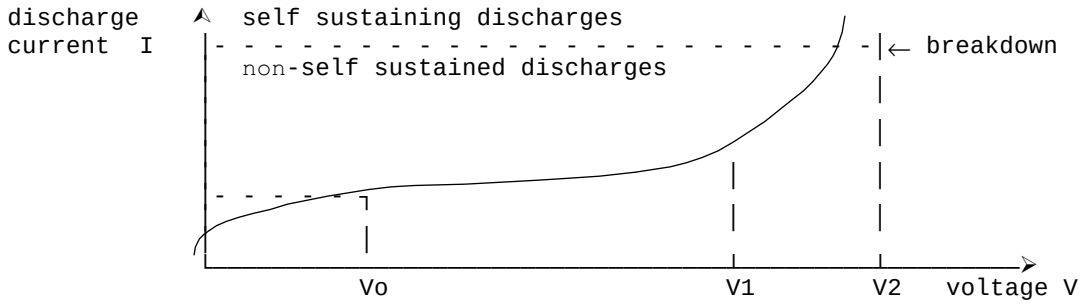

Figure 1.3 - Typical Current growth

From the Townsend mechanism, the discharge current is given by

$$I = \frac{I_0 \, e^{\alpha d}}{1 - \gamma (e^{\alpha d} - 1)} \approx I_0 \, e^{\alpha d} \quad \text{when } \alpha d \gg 1$$

This can be written in logarithmic form as

$$\ln I = \alpha d + \ln I_0$$

$$y = m x + c$$

From a graph of ln I vs d, the constants α and I_0 can be determined from the gradient and the intercept respectively, as in figure 1.4.

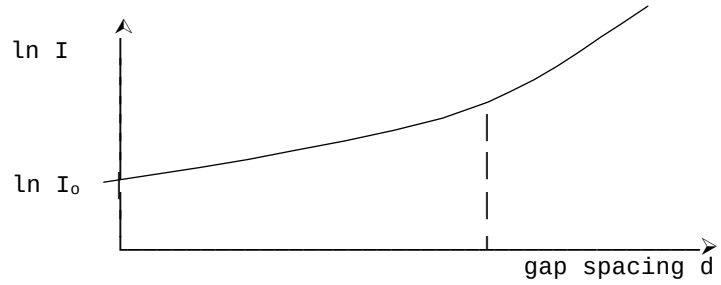

Figure 1.4 - Variation of ln I vs d

Once I_0 and α are known, γcan be determined from points on the upward region of the curve. The experiment can be repeated at different pressures if required.

1.2.1.3 Breakdown in electronegative gases

In the above analysis, electron attachment to neutral molecules was not considered. Electron attachment removes free electrons and thus gives gases very high dielectric strengths. The gases in which electron attachment occurs are electro-negative gases.

An attachment coefficient η can be defined, analogous with α, as the number of attachments per electron per unit drift in the direction of the field. Under these conditions, the equation for the average current growth in a uniform field can be shown to be as follows.

$$I = I_0 \frac{\left[\frac{\alpha}{\alpha-\eta} e^{(\alpha-\eta)d} - \frac{\eta}{\alpha-\eta}\right]}{1-\gamma\frac{\alpha}{\alpha-\eta}\left[e^{(\alpha-\eta)d}-1\right]}$$

The corresponding criteria for spark breakdown is

$$\gamma\frac{\alpha}{\alpha-\eta}\left[e^{(\alpha-\eta)d}-1\right]=1$$

1.2.2 Paschen's Law

When electrons and ions move through a gas in a uniform field E and gas pressure p, their mean energies attain equilibrium values dependant on the ratio E/p; or more precisely

$\alpha/p = f_1(E/p)$ and $\gamma = f_2(E/p)$

For a uniform field gap, the electric field E = V/d. Thus applying Townsend's criterion for spark breakdown of gases gives

$$\gamma (e^{\alpha d} - 1) = 1$$

which may be written in terms of the functions as

$$f_2\left(\frac{V}{p\,d}\right)\left[e^{p\,d\,f_1\left(\frac{V}{p\,d}\right)} - 1\right] = 1$$

This equation shows that the breakdown voltage V is an implicit function of the product of gas pressure p and the electrode separation d.

That is V = f (p.d)

In the above derivation the effect of temperature on the breakdown voltage is not taken into account. Using the gas equation **pressure . volume = mass . R . absolute Temperature**, we see that **pressure = density . R . absolute Temperature**. Thus the correct statement of the above expression is **V = f(ρ.d)**, where ρ is the gas density. This is the statement of **Paschen's Law**.

Under constant atmospheric conditions, it is experimentally found that the breakdown voltage of a uniform field gap may be expressed in the form

$$V = A \,.\, d + B \,.\, \sqrt{d}$$ where **d** is the gap spacing

For air, under normal conditions, A = 24.4 kV/cm and B = 6.29 kV/cm$^{1/2.}$

[The breakdown voltage gradient is about 30 kV/cm in uniform fields for small gaps of the order of 1 cm, but reduces to about 6 kV/cm for large gaps of several meters]

Figure 1.5 shows a typical breakdown vs spacing characteristic.

Figure 1.5 - Breakdown characteristic

This variation with spacing can be modified using Paschen's Law to include the variation with gas density as follows.

$$V = \frac{A}{\rho_0} \,.\, \rho\, d + \frac{B}{\rho_0^{1/2}} \,.\, (\rho\, d)^{1/2}$$

$$= A(\delta\, d) + B(\delta\, d)^{1/2}$$

where δ = relative density (or gas density correction factor).

This equation is true for gap spacings of more than 0.1 mm at N.T.P. However, with very low products of **pressure x spacing**, a minimum breakdown voltage occurs, known as the **Paschen's minimum**. This can be explained in the following manner.

Consider a gap of fixed spacing, and let the pressure decrease from a point to the right of the minimum (Figure 1.6).

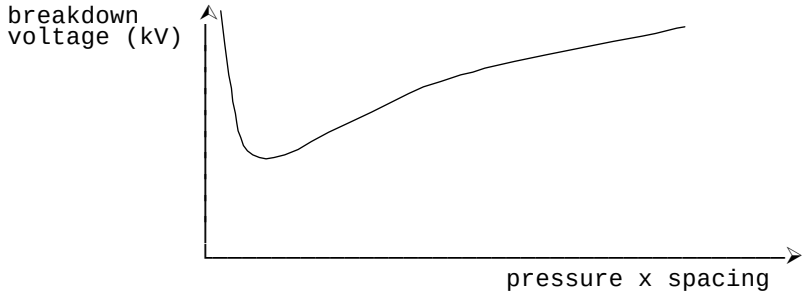

Figure 1.6 - Breakdown characteristic

The density therefore, decreases and an electron moving in the field consequently makes fewer collisions with gas molecules as it travels towards the anode. Since each collision results in a loss of energy, it follows that a lower electric stress suffices to impart to electrons the kinetic energy (½ m u^2) required to ionize by collision.

Gas	V_{min} (V)	p.d at V_{min} (torr-cm)
Air	327	0.567
Argon	137	0.9
Hydrogen	273	1.15
Helium	156	4.0
Carbon dioxide	420	0.51
Nitrogen	251	0.67
Nitrous oxide	418	0.5
Oxygen	450	0.7
Sulphur dioxide	457	0.33
Hydrogen Sulphide	414	0.6

Table 1.1 - Minimum sparking voltages

Near the minimum of the characteristic, the density is low and there are relatively few collisions. It is necessary now to take into account the fact that an electron does not necessarily ionize a molecule on collision with it, even if the energy of the electron exceeds the ionisation energy. The electrons have a finite chance of ionizing, which depends upon its energy. If the density and hence the number of collisions is decreased, breakdown can occur only if the chance of ionising is increased, and this accounts for the increase in voltage to the left of the minimum.

It is worth noting that if the density is fixed, breakdown to the left of the minimum occurs more readily (i.e. at lower voltage) at longer distances. Typically the voltage minimum is 300 V and occurs at a product or **p.d** of **5 torr mm**, or at a gap of about 0.06 mm at N.T.P.

At very low pressures, and at very high pressures (compared with atmospheric), Paschen's Law fails. Also, Paschen's Law is valid for temperatures below about 1100^0C. A further increase in temperature ultimately results in the failure of Paschen's Law because of thermal ionisation.

It can be seen from the breakdown characteristic, that for a constant gap spacing, the breakdown voltage, and hence the breakdown stress required, is very much higher than at atmospheric conditions, under very high pressure and under very low pressures (high vacuum) conditions. Thus both high vacuum as well as high gas pressure can be used as insulating media. [The vacuum breakdown region is that in which the breakdown voltage becomes independent of the gas pressure] Under normal conditions, operation is well to the right of Paschen's minimum.

The table 1.1 gives the minimum sparking potential for various gases.

1.2.3 Streamer Mechanism

This type of breakdown mainly arises due to the added effect of the space-charge field of an avalanche and photo-electric ionization in the gas volume. While the Townsend mechanism predicts a very diffused form of discharge, in actual practice many discharges are found to be filamentary and irregular. The Streamer theory predicts the development of a spark discharge directly from a single avalanche. The space charge produced in the avalanche causes sufficient distortion of the electric field that those free electrons move towards the avalanche head, and in so doing generate further avalanches in a process that rapidly becomes cumulative. As the electrons advance rapidly, the positive ions are left behind in a relatively slow-moving tail.The field will be enhanced in front of the head. Just behind the head the field between the electrons and the positive ions is in the opposite direction to the applied field and hence the resultant field strength is less. Again between the tail and the cathode the field is enhanced. (Figure 1.7)

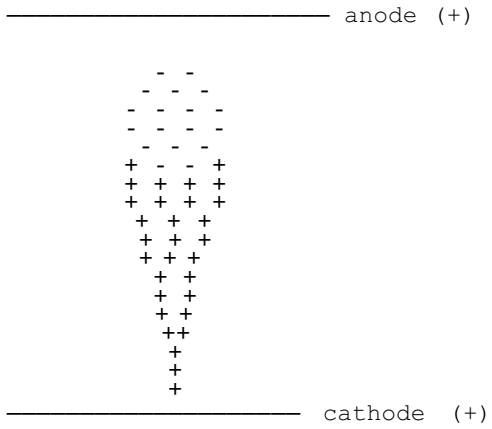

Figure 1.7 - Streamer Mechanism

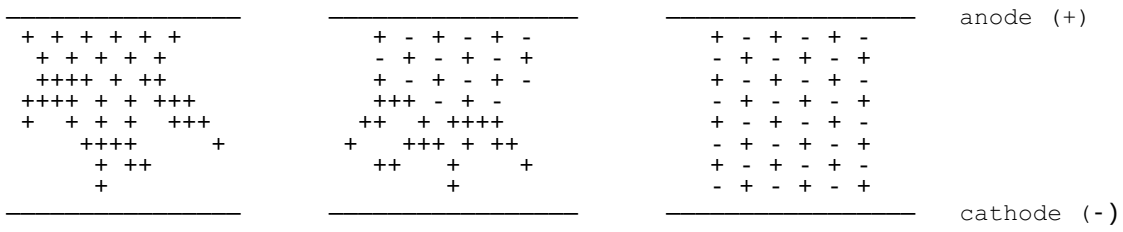

Figure 1.8 - Streamer breakdown

Due to the enhanced field between the head and the anode, the space charge increases, causing a further enhancement of the field around the anode. The process is very fast and the positive space charge extends to the cathode very rapidly resulting in the formation of a streamer. Figure 1.8 shows the breakdown process.

1.2.4 Factors affecting the breakdown voltage a Vacuum gap

Vacuum is ideally the best insulator, with breakdown strengths of the order of 10^4 kV/c. The breakdown voltage of a high vacuum is the voltage which when increased by a small amount will cause the breakdown of the gap that was held at that voltage for an infinite time. However, this definition is not always practicable as the breakdown is affected by many factors.

(i) Electrode Separation

For vacuum gaps less than about 1 mm, the breakdown voltage is approximately proportional to the length, all other parameters remaining constant. This gives a constant breakdown strength. For these small gaps, the breakdown stress is relatively high, being of the order of 1 MV/cm. Field emission of electrons probably plays an important part in the breakdown process.

$$V = k \cdot d \qquad \text{for } d < 1 \text{ mm}$$

For gaps greater than about 1 mm, the breakdown voltage does not increase at an equal rate and the apparent breakdown stress for longer gaps is much reduced, being about 10 kV/cm at a spacing of 10 cm. [Apparent stress is defined as the voltage required to cause breakdown divided by the distance between the electrodes]. Figure 1.9.

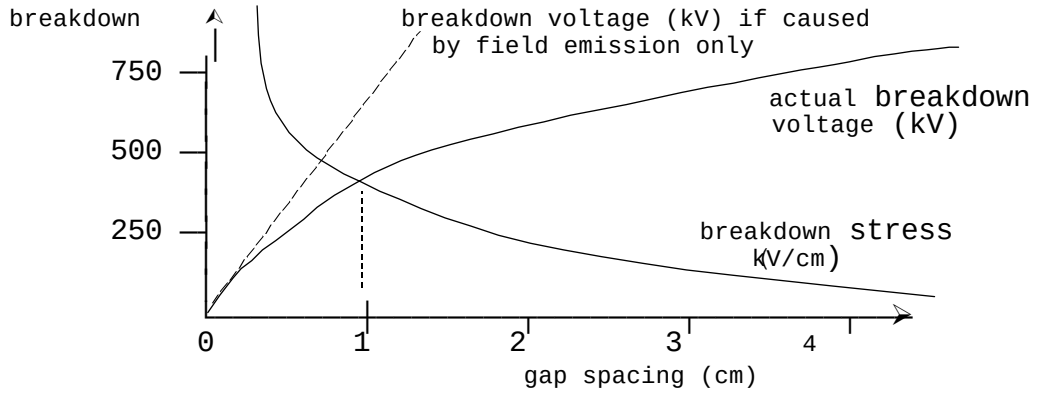

Figure 1.9 - Breakdown characteristic

Cranberg has shown theoretically that for longer gaps, it is the product of breakdown voltage and breakdown stress that remains constant.

$$V \cdot E = k_1 \qquad \text{for } d > 1 \text{ mm.}$$

where the constant k_1 depends on the material and surface conditions of the electrodes.

For an **Uniform field gap**, E = V/d, so that

$$V = k_2 \, d^{1/2}$$

Or in a more general form, both regions can be expressed by the equation

$$V = k \, d^{x} \qquad \text{where } x = 0.5 \text{ for long gaps} > 1 \text{ mm}$$
$$= 1 \quad \text{for gaps} < 1\text{mm}$$

(ii) Electrode Effects

Conditioning

The breakdown voltage of a gap increases on successive flashovers, until a constant value is reached. The electrodes are then said to be conditioned. This increase in voltage is ascribed to the burning off by sparking of microscopic irregularities or impurities which may exist on the electrodes. When investigating the effect of various factors on breakdown, the electrodes must first be conditioned in such a way that reproducible results are obtained.

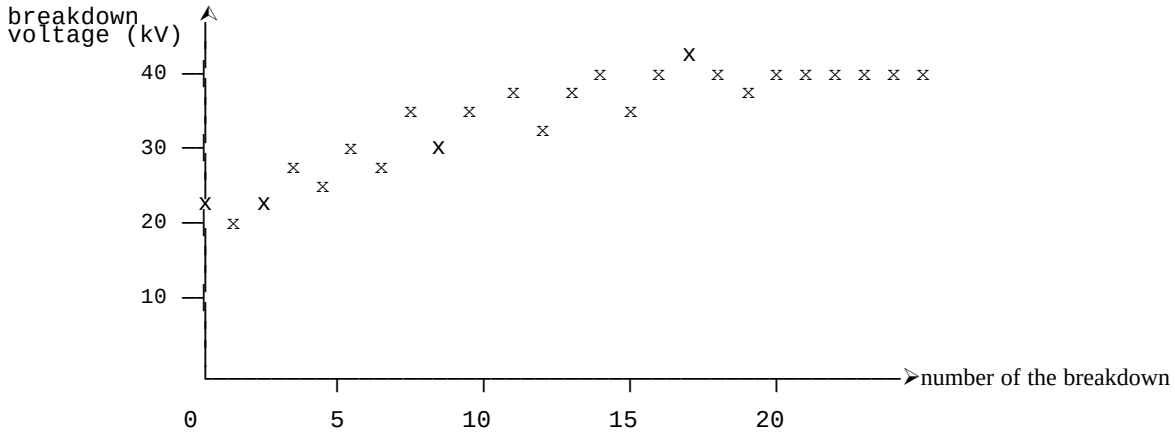

Figure 1.10 - Breakdown characteristics

The effect of conditioning is shown in figure 1.10. The breakdown voltage of conditioned electrodes or gaps is very much reproducible than otherwise, and hence breakdown values that are normally obtained experimentally are those of conditioned electrodes. Unconditioned electrodes may have breakdown values a low as 50% of the breakdown voltage with conditioned electrodes.

(iii) Material and Surface Finish

Electrode Material	Voltage across 1 mm gap (kV)
Steel	122
Stainless Steel	120
Nickel	96
Monel metal	60
Aluminium	41
Copper	37

Table 1.2 - Effect of electrode material on breakdown

The electrode surfaces form the physical boundaries between which the breakdown finally takes place. Thus it is not surprising to find that the breakdown strength of a given size of gap is strongly dependant on the material of the electrodes. In general, the smoother the surface finish, the greater the breakdown voltage.

(iv) Surface contamination

Presence of contamination in the test cell reduces the breakdown voltage sometimes by as much as 50% of the clean electrode value.

(v) Area and configuration of electrodes

Increasing the area of the electrodes makes it more difficult to maintain a given breakdown voltage. Thus breakdown voltage decreases slightly with increase in surface area. For example, electrodes of 20 cm^2 area gives the breakdown voltage across a 1 mm gap of 40 kV, whereas electrodes of the same material of area 1000 cm^2 gives a breakdown voltage across the same 1 mm gap as 25 kV.

Up to 1 mm gap, the more convex electrodes have higher breakdown voltage than the more nearly plane electrodes even though at the same voltage they carried a higher electric field at the surface.

(vi) Temperature

The variation of the breakdown voltage with temperature is very small, and for nickel and iron electrodes, the strength remains unchanged for temperatures as high as 500^0C. Cooling the electrodes to liquid Nitrogen temperature increases the breakdown voltage.

(vii) Frequency of applied voltage

It is known that a given gap stands a higher impulse voltage than an alternating voltage, and a higher alternating voltage than a direct voltage. However, it has been shown that for a small gap (2 mm) there is no dependence of the breakdown voltage on the frequency in the range 50 Hz to 50 kHz.

(viii) Vacuum Pressure

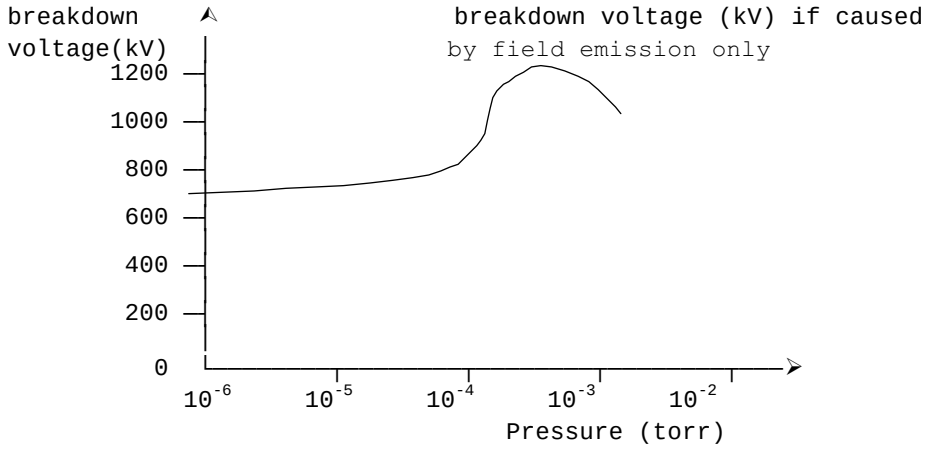

Figure 1.11 - Breakdown characteristic

For small gaps, increasing the degree of vacuum increases the breakdown voltage until below a certain pressure there is no change. The vacuum breakdown region is the region in which the breakdown voltage becomes independent of the nature of the pressure of the gap between the electrodes.

However, for large gaps (about 200 mm spacing) it is found that below a certain pressure the breakdown voltage starts decreasing again, so that the breakdown stress at this stage could in fact be improved by actually worsening the vacuum.

For example, using a 1.6 mm diameter sphere opposite a plane cathode and a gap of 200 mm, the characteristics shown in figure 1.11 was obtained. The breakdown voltage was constant for pressure less than 5×10^{-4} torr, but rose with increasing pressure to a maximum at 5×10^{-4} torr, with further increase in pressure the voltage fell sharply.

1.2.5 Time lags of Spark breakdown

In practice, particularly in high voltage engineering, breakdown under impulse fields is of great importance. On the application of a voltage, a certain time elapses before actual breakdown occurs even though the applied voltage may be much more than sufficient to cause breakdown.

In considering the time lag observed between the application of a voltage sufficient to cause breakdown and the actual breakdown the two basic processes of concern are the appearance of avalanche initiating electrons and the temporal growth of current after the criterion for static breakdown is satisfied.

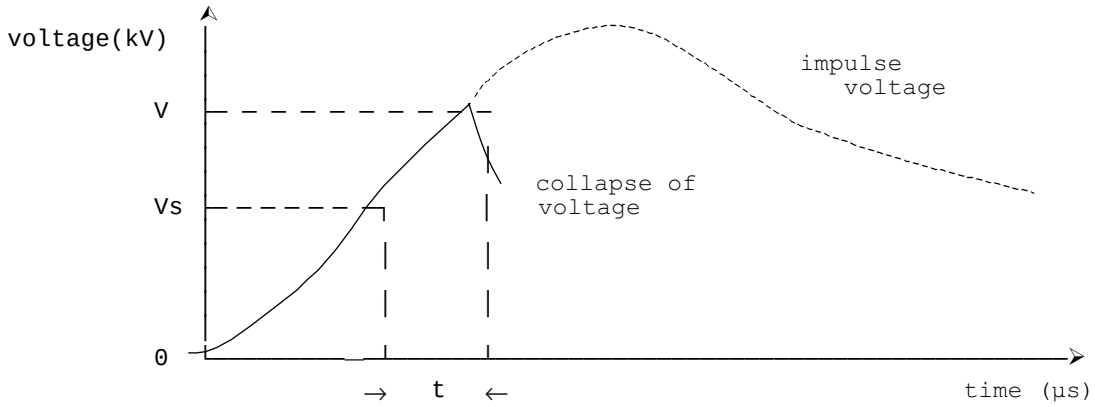

Figure 1.12 - Time lag of impulse breakdown

In the case of slowly varying fields, there is usually no difficulty in finding an initiatory electron from natural sources (ex. cosmic rays, detachment of gaseous ions etc). However, for impulses of short duration (around 1 μs), depending on the gap volume, natural sources may not be sufficient to provide an initiating electron while the voltage is applied, and in the absence of any other source, breakdown will not occur. Figure 1.12 shows the time lag for an impulse voltage waveform.

The time t_s which elapses between the application of a voltage greater than or equal to the static breakdown voltage (V_s) to the spark gap and the appearance of a suitably placed initiatory electron is called the statistical time lag of the gap, the appearance being usually statistically distributed.

After such an electron appears, the time t_f required by the ionisation processes to generate a current of a magnitude which may be used to specify breakdown of the gap is known as the formative time lag. The sum $t_f + t_s = t$ is the total time lag, and is shown in the diagram. The ratio V/V_s, which is greater than unity, is called the impulse ratio, and clearly depends on $t_s + t_f$ and the rate of growth of the applied voltage.

The breakdown can also occur after the peak of the voltage pulse, (i.e. on the wavetail). Depending on the time lag, the breakdown may occur in the wavefront or the wavetail of the impulse waveform.

(i) Statistical Time lag t_s

The statistical time lag is the average time required for an electron to appear in the gap in order that breakdown may be initiated.

If β = rate at which electrons are produced in the gap by external irradiation
P_1 = probability of an electron appearing in a region of the gap where it can lead to a spark
P_2 = probability that such an electron appearing in the gap will lead to a spark

then, the average time lag $$t_s = \frac{1}{\beta P_1 P_2}$$

If the level of irradiation is increased, β increases and therefore t_s decreases. Also, with clean cathodes of higher work function β will be smaller for a given level of illumination producing longer time lags.

The type of irradiation used will be an important factor controlling P_1, the probability of an electron appearing in a favourable position to produce breakdown. The most favourable position is, of course near the cathode.

If the gap is overvolted, then the probability of producing a current sufficient to cause breakdown rapidly increases. P_2 therefore increases with overvoltage and may tend to unity when the overvoltage is about 10%. As $P_2 \rightarrow 1$ with increasing overvoltage, $t_s \rightarrow 1/\beta P_1$.

(ii) Formative time lag

After the statistical time lag, it can be assumed that the initiatory electron is available which will eventually lead to breakdown. The additional time lag required for the breakdown process to form is the formative time lag. An uninterrupted series of avalanches is necessary to produce the requisite gap current (μA) which leads to breakdown, and the time rate of development of ionisation will depend on the particular secondary process operative. The value of the formative time lag will depend on the various secondary ionisation processes. Here again, an increase of the voltage above the static breakdown voltage will cause a decrease of the formative time lag tf.

(iii) Time lag characteristic

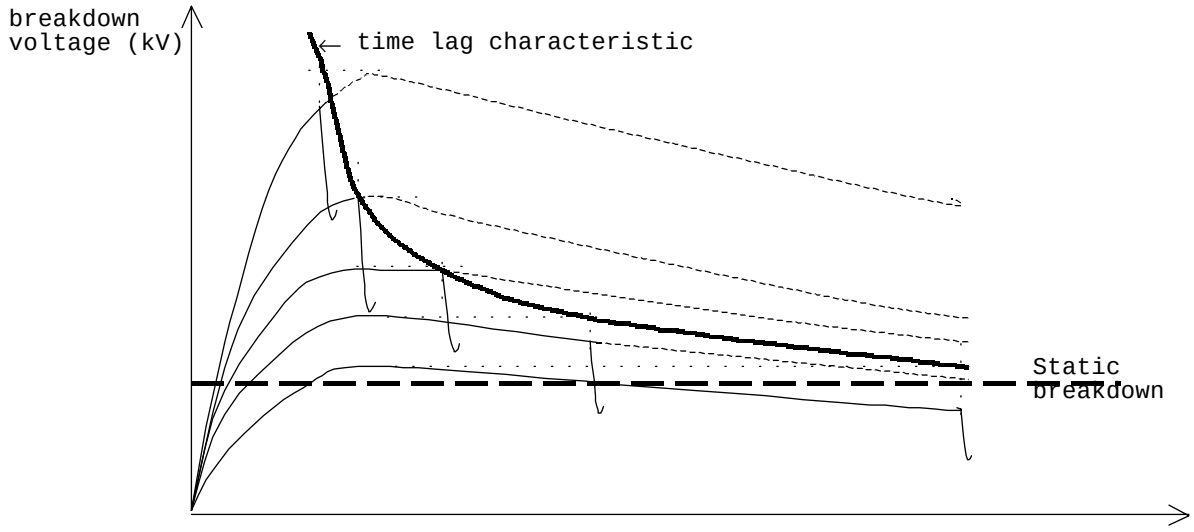

Figure 1.13 - Time-lag characteristics

The time lag characteristic is the variation of the breakdown voltage with time of breakdown, and can be defined for a particular waveshape. The time lag characteristic based on the impulse waveform is shown in figure 1.13.

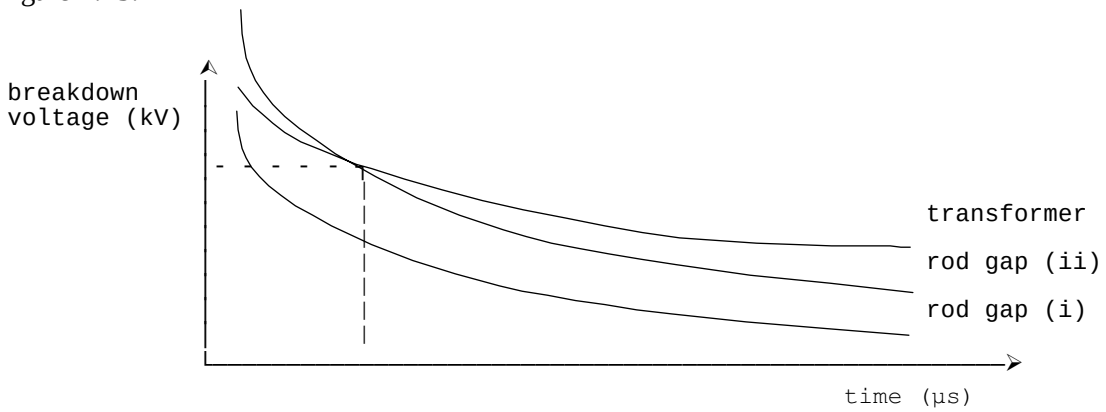

Figure 1.14 - Typical Time lag characteristics

The time lag characteristic is important in designing insulation. If a rod gap is to provide secondary protection to a transformer, then the breakdown voltage characteristic of the rod gap must be less than that of the transformer at all times (gap i) to protect it from dangerous surge voltages. This will ensure that the gap will always flashover before the protected apparatus. This is shown in figure 1.14.

However, with such a rod gap, the gap setting will be low, as the sharpness of the two characteristics are different. Thus it is likely that there would be frequent interruptions, even due to the smallest overvoltages which would in fact cause no harm to the system. Thus it is usual to have the rod gap characteristic slightly higher (gap ii) resulting in the intersection of the characteristics as shown. In such a case, protection will be offered only in the region where the rod gap characteristic is lower than that of the transformer. This crossing point is found from experience for a value of voltage which is highly unlikely to occur. The other alternative is of course to increase the transformer characteristic which would increase the cost of the transformer a great deal. [This decision is something like saying, it is better and cheaper to replace 1 transformer a year due to this decision than have to double the cost of each of 100 such transformers in the system.]

1.2.6 Corona Discharges

In a uniform electric field, a gradual increase in voltage across a gap produces a breakdown of the gap in the form of a spark without any preliminary discharges. On the other hand, if the field is non-uniform, an increase in voltage will first cause a localised discharge in the gas to appear at points with the highest electric field intensity, namely at sharp points or where the electrodes are curved or on transmission line conductors. This form of discharge is called a corona discharge and can be observed as a bluish luminance. This phenomena is always accompanied by a hissing noise, and the air surrounding the corona region becomes converted to ozone. Corona is responsible for considerable power loss in transmission lines and also gives rise to radio interference.

1.2.6.1 Mechanism of Corona formation on a 2 conductor line

When a gradually increasing voltage is applied across two conductors, initially nothing will be seen or heard. As the voltage is increased, the air surrounding the conductors get ionised, and at a certain voltage a hissing noise is heard caused by the formation of corona. This voltage is known as the disruptive critical voltage (**dcv**). A further increase in the voltage would cause a visible violet glow around the conductors. This voltage is the visual corona inception voltage.

If the applied voltage is direct, the glow observed will be uniform on the positive conductor, while the negative conductor will be more patchy and often accompanied by streamers at rough points. In the case of alternating voltages, both conductors appear to have a uniform glow, but when observed stroboscopically the effect is seen to be similar to the direct voltage case.

If the voltage is further increased, the corona increases and finally spark over would occur between the two conductors. If the conductors are placed quite close together, corona formation may not occur before the spark over occurs. The condition for this will be considered later.

The formation of corona causes the current waveform in the line, and hence the voltage drop to be non-sinusoidal. It also causes a loss of power.

There is always some electrons present in the atmosphere due to cosmic radiation etc. When the line voltage is increased, the velocity of the electrons in the vicinity of the line increases, and the electrons acquire sufficient velocity to cause ionisation.

To prevent the formation of corona, the working voltage under fair weather conditions should be kept at least 10% less than the disruptive critical voltage.

Corona formation may be reduced by increasing the effective radius. Thus steel cored aluminium has the advantage over hard drawn copper conductors on account of the larger diameter, other conditions remaining the same. The effective conductor diameter can also be increased by the use of bundle conductors.

Corona acts as a safety valve for lightning surges, by causing a short circuit. The advantage of corona in this instance is that it reduces transients by reducing the effective magnitude of the surge by partially dissipating its energy due to corona.

The effect of corona on radio reception is a matter of some importance. The current flowing into a corona discharge contains high-frequency components. These cause interference in the immediate vicinity of the line. As the voltage is gradually increased, the disturbing field makes its appearance long before corona loss becomes appreciable. The field has its maximum value under the line and attenuates rapidly with distance. The interference fails to about a tenth at 50 m from the axis of the line.

1.2.6.2 Waveform of Corona Current

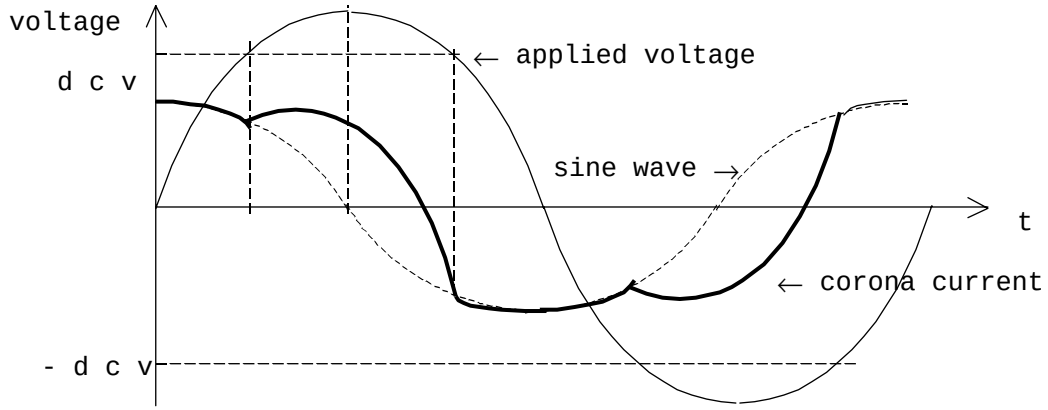

Figure 1.15 Waveform of corona current

The shunt current in a line is almost purely capacitive under normal conditions, and leads the applied voltage by 90^0, and there is no power loss in the line under no-load conditions. When the applied voltage is increased and corona is formed, the air is rendered conducting, and power loss occurs. The shunt current would no longer be leading the voltage by 90^0. Thus the current waveform would consist of two components. The lossy component would be non-sinusoidal and would occur only when the disruptive critical voltage is exceeded in either polarity. This resultant waveform is shown in figure 1.15. The corona current can be analysed and shown to possess a strong third harmonic component.

1.2.6.3 Mechanism of corona formation

The stress surrounding the conductor is a maximum at the conductor surface itself, and decreases rapidly as the distance from the conductor increases. Thus when the stress has been raised to critical value immediately surrounding the conductor, ionisation would commence only in this region and the air in this region would become conducting. The effect is to increase the effective conductor diameter while the voltage remains constant. This results in two effects. Firstly, an increase in the effective sharpness of the conductor would reduce the stress outside this region, and secondly, this would cause a reduction of the effective spacing between the conductors leading to an increase in stress. Depending on which effect is stronger, the stress at increasing distance can either increase or decrease. If the stress is made to increase, further ionisation would occur and flashover is inevitable.

Under ordinary conditions, the breakdown strength of air can be taken as 30 kV/cm. Corona will of course be affected by the physical state of the atmosphere. In stormy weather, the number of ions present is generally much more than normal, and corona will then be formed at a much lower voltage than in fair weather. This reduced voltage is generally about 80% of the fair weather voltage.

The condition for stable corona can be analysed as follows.

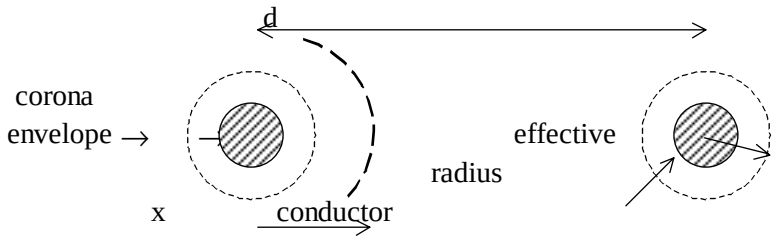

Figure 1.16 - Electric Stress in two conductor system

The electric stress ξ at a distance x from a conductor of radius x, and separated from the return conductor by a distance d is given by

$$\xi = \frac{1}{\varepsilon_0} . \frac{q}{2\pi x l}$$

where q is the charge on each conductor in length *l*.

Thus the potential V can be determined from $V = \int \xi \, dx$

$$V = \int_r^{d-r} \frac{q}{2\pi x \varepsilon_0} . dx$$

Since both charges (+q and -q) produce equal potential differences, the total potential difference between the two conductors is double this value. Thus the conductor to neutral voltage, which is half the difference would be equal to this value. Thus the conductor to neutral voltage is

$$V = \frac{q}{2\pi \varepsilon_0} . \log_e \left(\frac{d-r}{r} \right)$$

Therefore the electric stress at distance x is given by

$$\xi_x = \frac{V}{x \log_e \frac{d-r}{r}}$$

$$\xi_x = \frac{V}{x \log_e \frac{d}{r}} \quad \text{if } d \ll r$$

[Note; ξ_x and V can both be peak values or both rms values]

For three phase lines, with equilateral spacing, it can be shown that the stress is still given by the same expression when V is the voltage to neutral and d is the equilateral spacing.

For air, ξ_{max} = 30 kV/cm, so that ξ_{rms} = 30/√2 = 21.2 kV/cm.

Since there is no electric stress within the conductor, the maximum stress will occur when x is a minimum, that is at x = r.

Thus if $E_{0,rms}$ is the rms value of the disruptive critical voltage to neutral,

$$\xi_{rms} = 21.2 = \frac{E_{0,rms}}{r \log_e \frac{d}{r}}$$

When the surface of the conductor is irregular, it is more liable to corona. Thus an irregularity factor m_0 is introduced to account for this reduction. Typical values of this factor are

m_0 = 1.0 for smooth polished conductors,
= 0.98 to 0.93 for roughened conductors,
≈ 0.90 for cables of more than 7 strands, and
= 0.87 to 0.83 for 7 strand cables.

Since the corona formation is affected by the mean free path, and hence by the air density, a correction factor δ is introduced. This air density correction factor is given by the usual expression, with **p** being the pressure expressed in **torr** and **t** being the temperature expressed in ^{0}C.

$$\delta = \frac{p}{760} \cdot \frac{273 + 20}{273 + t} = \frac{0.386\ p}{273 + t}$$

The disruptive critical voltage can then be written as in the following equation.

$$E_{0,rms} = 21.2\ \delta\ m_0\ r \log_e (d/r) \qquad \text{kV to neutral}$$

1.2.6.4 Visual Corona

Visual corona occurs at a higher voltage than the disruptive critical voltage. For the formation of visual corona, a certain amount of ionization, and the raising of an electron to an excited state are necessary. The production of light by discharge is not due to ionisation, but due to excitation, and subsequent giving out of excess energy in the form of light and other electromagnetic waves. To obtain the critical voltage for visual corona formation, the disruptive critical voltage has to be multiplied by a factor dependant on the air density and the conductor radius. Further the value of the irregularity factor is found to be different.

The empirical formula for the formation of visual corona is

$$E_{v,rms} = 21.2\ m_v\ \delta\ r \left[1 + \frac{0.3}{\sqrt{\delta\ r}}\right] . \log_e \frac{d}{r}$$

The values of the irregularity factor m_v for visual corona is given by

m_v = 1.0 for smooth conductors,
= 0.72 for local corona on stranded wires (patches)
= 0.82 for decided corona on stranded wires (all over the wire)

1.2.6.5 Stable Corona formation

Consider two conductors, just on the limit of corona formation. Assume that there is a thin layer Δr of ionised air around each conductor, so that the effective radius becomes $(r + \Delta r)$. The change in electric stress $\Delta\xi$ due to this layer can be determined using differentiation.
Thus

$$\Delta\xi = \Delta\left(\frac{E}{r\log_e\frac{d}{r}}\right)$$

$$\Delta\xi = \left[\frac{-E}{\left(r\log_e\frac{d}{r}\right)^2}.\left(\log_e\frac{d}{r} + r.\frac{r}{d}.\frac{-d}{r^2}\right)\right].\Delta r$$

$$\Delta\xi = \frac{E\left(1-\log_e\frac{d}{r}\right).\Delta r}{\left(r\log_e\frac{d}{r}\right)^2}$$

When $\log_e > 1$, the above expression is negative. i.e. $d/r > e$ (=2.718)

Under this condition, the effective increase in diameter lowers the electric stress and no further stress increase is formed, and corona is stable. If on the other hand, $d/r < e$, then the effective increase in the diameter raises the electric stress, and this causes a further ionisation and a further increase in radius, and finally leads to flash-over.

In practice, the effective limiting value of d/r is about 15 and not **e** (=2.718). For normal transmission lines, the ratio d/r is very much greater than 15 and hence stable corona always occurs before flashover.

For example, in a 132 kV line with a spacing of 4 m and a radius of conductor of 16 mm, the ratio has a value $d/r = 4/16\text{x}10^{-3} = 250 >> 15$.

1.2.6.6 Power Loss due to Corona

The formation of corona is associated with a loss of power. This loss will have a small effect on the efficiency of the line, but will not be of sufficient importance to have any appreciable effect on the voltage regulation. The more important effect is the radio interference.

The power loss due to corona is proportional to the square of the difference between the line-to-neutral voltage of the line and the disruptive critical voltage of the line. It is given by the empirical formula

$$P_c = \frac{243}{\delta}.(f+25).\sqrt{\frac{r}{d}}.(E-E_{0,rms})^2.10^{-5} \text{ kW/km/phase}$$

where $E_{0,rms}$ = disruptive critical voltage (kV)
f = frequency of supply (Hz)
E = Phase Voltage (line to neutral) (kV)

For storm weather conditions, the disruptive critical voltage is to be taken as 80% of disruptive critical voltage under fair weather conditions.

Example

Determine the Disruptive Critical Voltage,the Visual Corona inception voltage, and the power loss in the line due to corona, both under fair weather conditions as well as stormy weather conditions for a 100 km long 3 phase, 132 kV line consisting of conductors of diameter 1.04 cm, arranged in an equilateral triangle configuration with 3 m spacing. The temperature of the surroundings is 40^0 C and the pressure is 750 torr. The operating frequency is 50 Hz. [The irregularity factors may be taken as $m_o = 0.85$, $m_v = 0.72$]

The Air density correction factor δ is given by

$$\delta = \frac{p}{760}.\frac{273+20}{273+t} = \frac{0.386\ p}{273+t}$$

$$\delta = \frac{750}{760}.\frac{293}{313} = 0.925$$

$\therefore$ Disruptive critical voltage = 21.2 δ m_0 r $\log_e$ (d/r) kV to neutral
= 21.2 x 0.925 x 0.85 x 0.52 x $\log_e$ (3/0.0052)
= 55.1 kV

Similarly,
Visual corona voltage = 21.2 x 0.925 x 0.72 x 0.52 x $\log_e$ (3/0.0052) x [1 + 0.3/(0.895 x 0.52)^{½}]
= 67.2 kV

Power loss under fair weather condition is given by

$$P_c = \frac{243}{0.925}.(50+25).\sqrt{\frac{0.0052}{3}}.\left(\frac{132}{\sqrt{3}} - 55.1\right)^2.10^{-5}.100 \quad \text{kW/phase}$$

$$= 365 \ \text{kW/phase}$$

Similarly, power loss under stormy weather condition is given by

$$P_c = \frac{243}{0.925}.(50+25).\sqrt{\frac{0.0052}{3}}.\left(\frac{132}{\sqrt{3}} - 55.1*0.8\right)^2.10^{-5}.100 \quad \text{kW/phase}$$

$$= 847 \ \text{kW/phase}$$

2

Breakdown of Liquid and Solid Insulation

2.1 Breakdown in Liquids

In highly purified liquid dielectrics, breakdown is controlled by phenomena similar to those for gasses and the electric strength is high (of the order of 1 MV/cm).
Unfortunately, liquids are easily contaminated, and may contain solids, other liquids in suspension and dissolved gasses. The effect of these impurities is relatively small for short duration pulses (10 μs).

However, if the voltage is applied continuously, the solid impurities line up at right angles to equipotentials, and distort the field so that breakdown occurs at relatively low voltage. The line up of particles is a fairly slow process, and is unlikely to affect the strength on voltages lasting for less than 1 ms.

Under the action of the electric field, dissolved gasses may come out of solution, forming a bubble. The gas in the bubble has a lower strength than the liquid, so that more gas is produced and the bubble grows, ultimately causing breakdown. Because, of the tendency to become contaminated, liquids are not usually used alone above 100 kV/cm in continuously energised equipment, however, they are used at much higher tresses (up to 1 MV/cm) in conjunction with solids, which can be made to act as barriers, preventing the line-up of solid impurities and localising of any bubbles which may form. The main function of the liquid in such arrangements is to fill up the voids.

2.1.1 Breakdown of Commercial liquids

When a difference of potential is applied to a pair of electrodes immersed in an insulating liquid, a small conduction current is first observed. If the voltage is raised continuously, at a critical voltage a spark passes between the electrodes. The passage of a spark through a liquid involves the following.

(a) flow of a relatively large quantity of electricity, determined by the characteristics of the circuit,
(b) a bright luminous path from electrode to electrode,
(c) the evolution of bubbles of gas and the formation of solid products of decomposition (if the liquid is of requisite chemical nature)
(d) formation of small pits on the electrodes,
(e) an impulsive pressure through the liquid with an accompanying explosive sound.

Tests on highly purified transformer oil show that

(a) breakdown strength has a small but definite dependence on electrode material,
(b) breakdown strength decreases with increase in electrode spacing,
(c) breakdown strength is independent of hydrostatic pressure for degassed oil, but increases with pressure if oil contains gases like nitrogen or oxygen in solution.

In the case of commercial insulating liquid, which may not be subjected to very elaborate purifying treatment, the breakdown strength will depend more upon the nature of impurities it contains than upon the nature of the liquid itself.

These impurities which lead to the breakdown of commercial liquids below their intrinsic strength, can be divided into the following 3 categories.

(a) Impurities which have a breakdown strength lower than that of the liquid itself (ex: bubbles of gas). Breakdown of the impurities may trigger off the total breakdown of the liquid.
(b) Impurities which are unstable in the electric field (ex: globules of water). Instability of the impurity can result in a low resistance bridge across the electrodes and in total breakdown.
(c) Impurities which result in local enhancement of electric field in a liquid (ex: conducting particles). The enhanced field may cause local breakdown and therefore initiate complete breakdown.

These will be considered in turn in the following sections.

2.1.2 Breakdown due to gaseous inclusions

Gas or vapour bubbles may exist in impure liquid dielectrics, either formed from dissolved gasses, temperature and pressure variations, or other causes.

The electric field E_b in a gas bubble which is immersed in a liquid of permittivity ε_1 is given by

$$E_b = \frac{3\varepsilon_1}{2\varepsilon_1 + 1} E_0$$

where E_0 is the field in the liquid in the absence of the bubble.

The electrostatic forces on the bubble cause it to get elongated in the direction of the electric field. The elongation continues, when sufficient electric field is applied, and at a critical length the gas inside the bubble (which has a lower breakdown strength) breaks down. This discharge causes decomposition of the liquid molecules and leads to total breakdown.

2.1.3 Breakdown due to liquid globules

If an insulating liquid contains in suspension a globule of another liquid, then breakdown can result from instability of the globule in the electric field.

Consider a spherical globule of liquid of permittivity ε_2 immersed in a liquid dielectric of permittivity ε_1. When it is subjected to an electric field between parallel electrodes, the field inside the globule would be given by

$$E = \frac{3\varepsilon_1}{2\varepsilon_1 + \varepsilon_2} E_0$$

where E_0 is the field in the liquid in the absence of the globule.

The electrostatic forces cause the globule to elongate and take the shape of a prolate spheroid (i.e. an elongated spheroid). As the field is increased, the globule elongates so that the ratio γ of the longer to the shorter diameter of the spheroid increases. For the same field E, the ratio γ is a function of $\varepsilon_2/\varepsilon_1$.

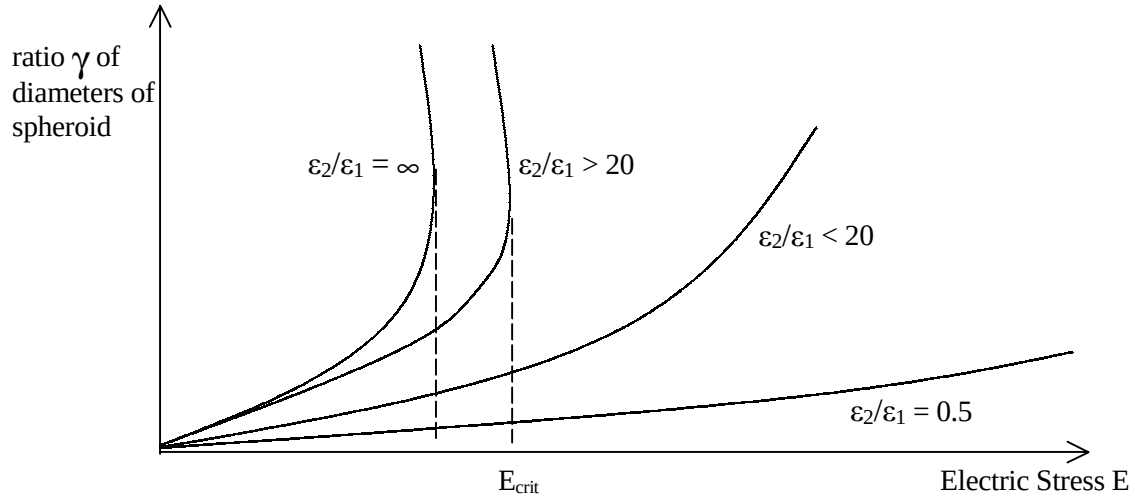

Figure 2.1 - Variation of ratio of diameters of spheroid

When $\varepsilon_2 >> \varepsilon_1$ (generally when $\varepsilon_2/\varepsilon_1 > 20$), and the field exceeds a critical value, no stable shape exists, and the globule keeps on elongating eventually causing bridging of the electrodes, and breakdown of the gap. When $\varepsilon_2/\varepsilon_1 >> 20$, the critical field at which the globule becomes unstable no longer depends on the ratio, and is given by $E_{crit.}$

$$E_{crit} = 1.542\left(\frac{\sigma}{R\,\varepsilon_1}\right)^{1/2} \quad kV/cm$$

where σ = surface tension of the globule (N/m)
ε_1 = relative permittivity of the insulating liquid
R = initial radius of globule (m).

Example 2.1

For a droplet of water (R = 1 μm , $\varepsilon_2 = 90$) in an insulating oil ($\varepsilon_1 = 2$); $\varepsilon_2 >> \varepsilon_1$.
Also σ = 0.043 N/m.

Thus E_{crit} = $1.542\,(0.043/10^{-6} \times 2)^{½}$ kV/cm = 226 kV/cm.
= 0.226 MV/cm

Thus we see that a droplet of water even as small as 1 μm in radius (quite unobservable) can greatly reduce the breakdown strength of the liquid dielectric. In fact, a globule of water of radius of only 0.05 μm, which is quite unobservable, will be disrupted at a value of about 1 MV/cm which is the breakdown strength of the pure liquid. Thus even submicroscopic sources of water, such as condensed breakdown products, or hygroscopic solid impurities, may greatly influence breakdown conditions. A globule which is unstable at an applied value of field elongates rapidly, and then electrode gap breakdown channels develop at the end of the globule. Propagation of the channels result in total breakdown.

2.1.4 Breakdown due to solid particles

In commercial liquids, solid impurities cannot be avoided and will be present as fibres or as dispersed solid particles. If the impurity is considered to be a spherical particle of permittivity ε_2 and is present in a liquid dielectric of permittivity ε_1, it will experience a force

$$\frac{(\varepsilon_2 - \varepsilon_1)}{\varepsilon_2 + 2\,\varepsilon_1}\,\Delta E^2$$

where E = applied field, r = radius of particle.

Generally $\varepsilon_2 > \varepsilon_1$, so that the force would move the particle towards the regions of stronger field. Particles will continue to move in this way and will line up in the direction of the field. A stable chain of particles would be produced, which at a critical length may cause breakdown.

Because of the tendency to become contaminated, liquids are seldom used alone above 100 kV/cm in continuously energised equipment. However they may be used up to 1 MV/cm in conjunction with solids which can be made to act as barriers, preventing the line-up of solid impurities and localising bubbles which may form.

2.1.5 Purification of a liquid for testing

(a) **Removal of dust**

Small dust particles can become charged and cause local stresses which can initiate breakdown. They can also coalesce to form conducting bridges between electrodes. Careful filtration can remove dust particles greater in size than 1 μm. The strength of the liquid then increases and greater stability is achieved.

(b) **Removal of dissolved gasses**

Liquid insulation will normally contain dissolved gas in small but significant amounts. Some gases such as Nitrogen and Hydrogen do not appear to upset the electrical properties to a great extent, but oxygen and carbon dioxide can cause the strength to change significantly. Thus it necessary to control the amount of gases present. This is done by distillation and degassing.

(c) **Removal of ionic impurities**

Ionic impurities in the liquid (particularly residual water which easily dissociates) leads to abnormal conductivity and heating of the liquid. Water can be removed by drying agents, vacuum drying, and by freezing out in low temperature distillation.

For measurements on liquid dielectrics, where test cells are small, electrode preparation is much more critical than it is for measurements on gases or solids. Not only is the surface smoothness important, but surface films, particularly oxides can have a marked influence on the strength.

2.2 Breakdown of Solid Insulating Materials

In solid dielectrics, highly purified and free of imperfections, the breakdown strength is high, of the order of 10 MV/cm. The highest breakdown strength obtained under carefully controlled conditions is known as the "intrinsic strength" of the dielectric. Dielectrics usually fail at stresses well below the intrinsic strength due usually to one of the following causes.

(a) electro-mechanical breakdown
(b) breakdown due to internal discharges
(c) surface breakdown (tracking and erosion)
(d) thermal breakdown
(e) electro-chemical breakdown
(f) chemical deterioration

These will now be considered in the following sections.

2.2.1 Electro-mechanical breakdown

When an electric field is applied to a dielectric between two electrodes, a mechanical force will be exerted on the dielectric due to the force of attraction between the surface charges. This compression decreases the dielectric thickness thus increasing the effective stress. This is shown in figure 2.2.

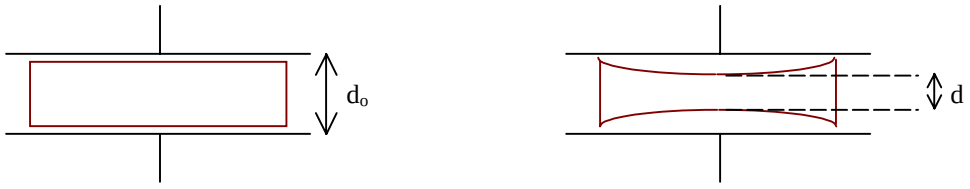

Figure 2.2 - Process of breakdown

Compressive force $P_c = ½ D E = ½ \varepsilon_o \varepsilon_r V^2/d^2$,
and From Hooke's Law for large strains, $P_c = Y \ln (d_o/d)$

At equilibrium, equating forces gives the equation,

$$V^2 = \frac{2Y}{\varepsilon_o \varepsilon_r} d^2 \ln\frac{d_o}{d}$$

By differentiating with respect to d, it is seen that the system becomes unstable when $\ln (d_o/d) > ½$ or $d < 0.6\ d_o$.

Thus when the field is increased, the thickness of the material decreases. At the field when $d < 0.6\ d_o$, any further increase in the field would cause the mechanical collapse of the dielectric. The apparent stress (V/d_o) at which this collapse occurs is thus given by the equation

$$E_a = 0.6\left[\frac{Y}{\varepsilon_o \varepsilon_r}\right]^{\frac{1}{2}}$$

2.2.2 Breakdown due to internal discharges

Solid insulating materials sometimes contain voids or cavities in the medium or boundaries between the dielectric and the electrodes. These voids have a dielectric constant of unity and a lower dielectric strength. Hence the electric field strength in the voids is higher than that across the dielectric. Thus even under normal working voltages, the field in the voids may exceed their breakdown value and breakdown may occur. The mechanism can be explained by considering the following equivalent circuit of the dielectric with the void, shown in figure 2.3.

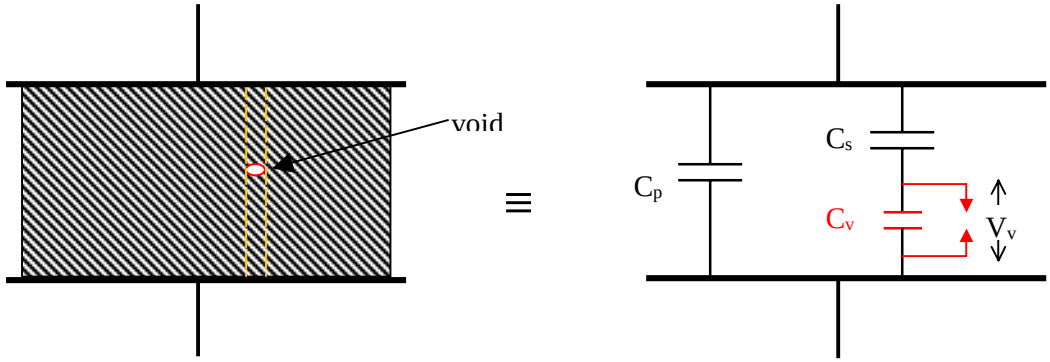

Figure 2.3 - Equivalent circuit of dielectric with void

When the voltage V_v across the void exceeds the critical voltage V_c, a discharge is initiated and the voltage collapses. The discharge extinguishes very rapidly (say 0.1 μs). The voltage across the void again builds up and the discharges recur. The number and frequency of the discharges will depend on the applied voltage. The voltage and current waveforms (exaggerated for clarity) are shown in figure 2.4.

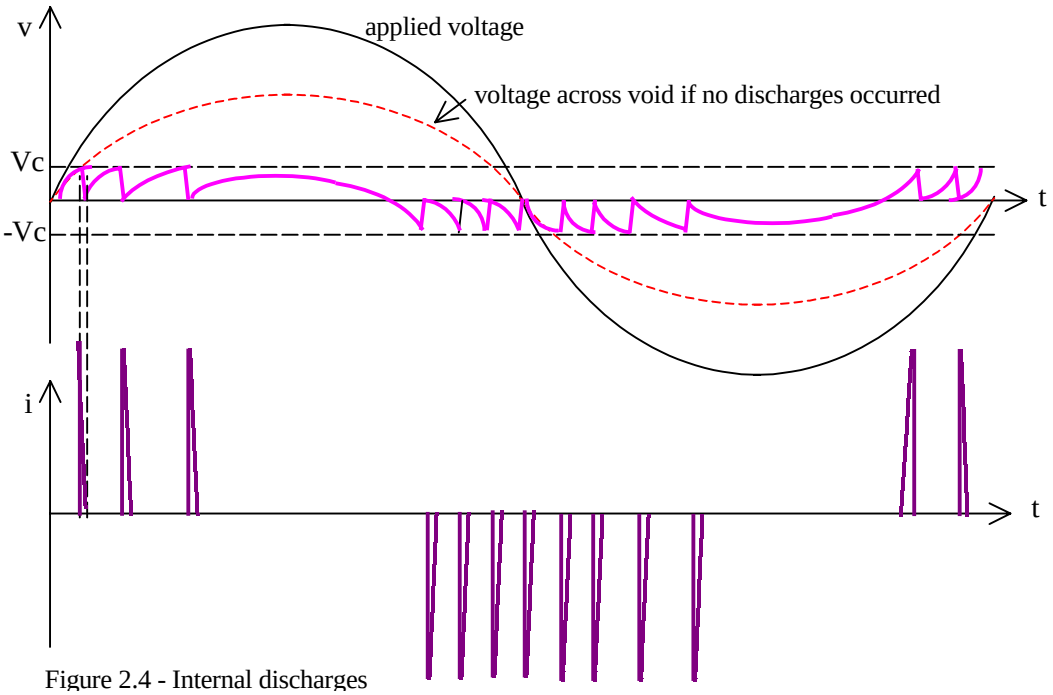

Figure 2.4 - Internal discharges

In each of the discharges, there will be heat dissipated in the voids which will cause carbonization of the surface of the voids and erosion of the material. The gradual erosion of the material and consequent reduction in the thickness of the insulating material eventually leads to breakdown.
Breakdown by this process is slow and may occur in a few days or may take a few years.

Deterioration due to internal discharges

In organic liquid-solid dielectrics, internal discharges produce gradual deterioration because of

(a) disintegration of the solid dielectric under the bombardment of electrons set free by the discharges
(b) chemical action on the dielectric of the products of ionization of the gas
(c) high temperatures in the region of the discharges.

All voids in the dielectric can be removed by careful impregnation and this results in an increase in the discharge inception stress E_i. The final value E_i then depends on electrical processes which lead to gas formation.

In oil impregnated paper these are

(a) decomposition of moisture in paper
(b) local electrical breakdown of the oil.

The stress at which gas is evolved from paper containing appreciable quantities of moisture can be less than 10 V/μm, but increases continuously with increasing dryness and can be higher than 100 V/μm when the paper is thoroughly dry. Except in very dry conditions, the gas first formed arises from electrochemical decomposition of water held in the paper.

When a gas bubble is formed in an oil-paper dielectric at the discharge inception stress E_i, discharges in the bubble decompose the molecules of the oil, resulting in further gas formation and a rapid growth of the bubble. As long as the bubble remains in the dielectric, the inception stress E_i is low, often lower than the rated stress, but resting the dielectric long enough for the gas to dissolve in the oil restores the initial high discharge inception stress. Although on resting E_i improves, permanent damage has been caused by the discharges and this manifests itself in an increase of loss angle and is due to the formation of ions by the discharges. Also, due to the discharges, widespread carbonization occur.

2.2.3 Surface Breakdown

Surface flashover

Surface flashover is a breakdown of the medium in which the solid is immersed. The role of the solid dielectric is only to distort the field so that the electric strength of the gas is exceeded.

If a piece of solid insulation is inserted in a gas so that the solid surface is perpendicular to the equipotentials at all points, then the voltage gradient is not affected by the solid insulation. An example of this is a cylindrical insulator placed in the direction of a uniform field. Field intensification results if solid insulation departs even in detail from the cylindrical shape. In particular if the edges are chipped, or if the ends of the cylinder are not quite perpendicular to the axis, then an air gap exists next to the electrode, and the stress can reach up to ε_r times the mean stress in the gap. [ε_r is the dielectric constant of the cylinder]. Discharge may therefore occur at a voltage approaching $1/\varepsilon_r$ times the breakdown voltage in the absence of the cylinder, and these discharges can precipitate a breakdown.

The three essential components of the surface flashover phenomena are

(a) the presence of a conducting film across the surface of the insulation

(b) a mechanism whereby the leakage current through the conducting film is interrupted with the production of sparks,

(c) degradation of the insulation must be caused by the sparks.

The conducting film is usually moisture from the atmosphere absorbed by some form of contamination. Moisture is not essential as a conducting path can also arise from metal dust due to wear and tear of moving parts. Sparks are drawn between moisture films, separated by drying of the surface due to heating effect of leakage current, which act as extensions to the electrodes. {For a discharge to occur, there must be a voltage at least equal to the Paschen minimum for the particular state of the gas. For example, Paschen minimum in air at N.T.P it is 380 V, whereas tracking can occur at well below 100 V. It does not depend on gaseous breakdown.] Degradation of the insulation is almost exclusively the result of heat from the sparks, and this heat either carbonises if tracking is to occur, or volatilises if erosion is to occur. Carbonization results in a permanent extension of the electrodes and usually takes the form of a dendritic growth. Increase of creepage path during design will prevent tracking, but in most practical cases, moisture films can eliminate the designed creepage path.

Tracking

Tracking is the formation of a permanent conducting path across a surface of the insulation, and in most cases the conduction (carbon path) results from degradation of the insulation itself leading to a bridge between the electrodes. The insulating material must be organic in nature for tracking to occur.

Erosion

In a surface discharge, if the products of decomposition are volatile and there is no residual conducting carbon on the surface, the process is simply one of pitting. This is erosion, which again occurs in organic materials.

If surface discharges are likely to occur, it is preferable to use materials with erosion properties rather than tracking properties, as tracking makes insulation immediately completely ineffective, whereas erosion only weakens the material but allows operation until replacement can be made later.

2.2.4 Thermal Breakdown

Heat is generated continuously in electrically stressed insulation by dielectric losses, which is transferred to the surrounding medium by conduction through the solid dielectric and by radiation from its outer surfaces. If the heat generated exceeds the heat lost to the surroundings, the temperature of the insulation increases.

The power dissipated in the dielectric can be calculated as follows.

Uniform direct stress

Power dissipated/volume = ξ^2/ρ W/m^3 where ξ = uniform direct stress V/m
ρ = resistivity of insulation Ω m

Uniform alternating stress

Power dissipated P = V . I cos φ where V = applied voltage V
= V . VCω tan δ ω = supply frequency Hz
C = dielectric capacitance F
Capacitance C = A ε_r ε_0 / d δ = loss angle rad
ε = dielectric constant
Therefore P = V^2 (A ε_r ε_0 / d) ω tan δ ξ = alternating stress V/m

Re-arranging terms gives the result

$$P = (V/d)^2 . \varepsilon_r \varepsilon_0 . 2 \pi f . \tan \delta . A . d$$

Since A.d is the volume of the dielectric, and V/d is the uniform applied stress,

Power dissipated/volume = $\xi^2 \varepsilon_r \varepsilon_0 2 \pi f \tan \delta$ W/m^3

$= 2 \pi \times 8.854 \times 10^{-12} \xi^2 \varepsilon_r f \tan \delta$ W/m^3

$= 5.563 \times 10^{-11} \xi^2 \varepsilon_r f \tan \delta \times 10^{10}$ W/m^3 if ξ is in kV/cm

Power dissipated/volume = $0.556 \xi^2 f \varepsilon_r \tan \delta$ W/m^3 with ξ in kV/cm

The simplest case is where the loss of heat by cooling is linearly related to the temperature rise above surroundings, and the heat generated is independent of temperature. (i.e. the resistivity and the loss angle do not vary with temperature).

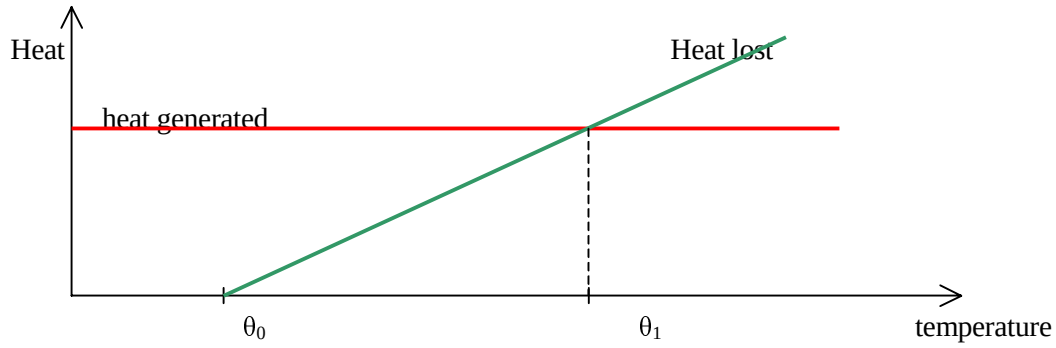

Figure 2.5 Thermal breakdown

Heat lost = k (θ - θ_0), where θ = ambient temperature

Equilibrium will be reached at a temperature θ_1 where the heat generated is equal to the heat lost to the surroundings, as shown in figure 2.5.

In practice, although the heat lost may be considered somewhat linear, the heat generated increases rapidly with temperature, and at certain values of electric field no stable state exists where the heat lost is equal to the heat generated so that the material breaks down thermally. The rapid increase is due to the fact that with rise in temperature, the loss angle of the dielectric increases in accordance with an exponential law (loss $\propto e^{-A/T}$, where T is the absolute temperature).

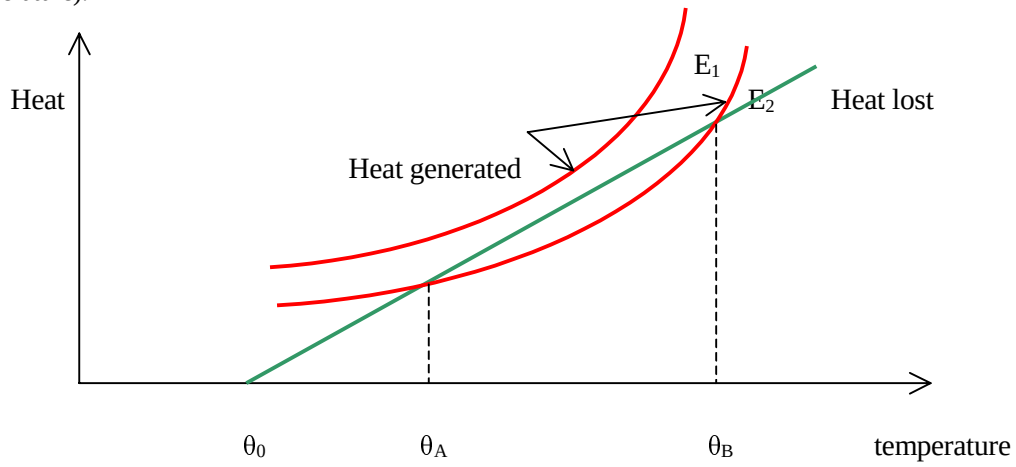

Figure 2.6 Thermal breakdown

Figure 2.6 shows the variation of heat generated by a device for 2 different applied fields and the heat lost from the device with temperature.

For the field E_2, a stable temperature θ_A exists (provided the temperature is not allowed to reach θ_B). For the field E_1, the heat generated is always greater than the heat lost so that the temperature would keep increasing until breakdown occurs.

The maximum voltage a given insulating material can withstand cannot be increased indefinitely simply by increasing its thickness. Owing to thermal effects, there is an upper limit of voltage V_θ, beyond which it is not possible to go without thermal instability. This is because with thick insulation, the internal temperature is little affected by the surface conditions. Usually, in the practical use of insulating materials, V_θ is a limiting factor only for high-temperature operation, or at high frequency failures.

2.2.5 Electro-chemical Breakdown

Since no insulant is completely free of ions, a leakage current will flow when an electric field is applied. The ions may arise from dissociation of impurities or from slight ionisations of the insulating material itself. When these ions reach the electrodes, reactions occur in accordance with Faraday's law of electrolysis, but on a much smaller scale. The insulation and the electrode metal may be attacked, gas may be evolved or substance may be deposited on the electrodes. The products of the electrode reaction may be chemically or electrically harmful and in some cases can lead to rapid failure of the insulation. The reactions are much slower than in normal electrolytic processes due to the much smaller currents. The products of the reactions may be electrically and chemically harmful because the insulation and electrodes may be attacked, and because harmful gases may be evolved.

Typically a 1 μF paper capacitor operating at 1 kV at room temperature would require 2 to 3 years to generate 1 cm^3 hydrogen. At elevated temperatures, the products of electrolysis would be formed much more rapidly. Also since impurities give rise to an increase in the ion concentration, care must be taken to prevent contamination during manufacture.

The rate of electrolysis is much greater with direct stress than with alternating stress. This is due to the fact that the reactions may be wholly or partially reversed when the polarity changes and the extent of reaction depends on the reaction rate and the time for diffusion of the reaction products away from the electrodes as well as on the nature of the reaction products. However at power frequency, electrochemical effects can be serious and are often responsible for long-term failure of insulation. The most frequent source of ions is ionizable impurities in the insulation. Thus contamination of insulation during manufacture and during assembly into equipment must be avoided with great care. Also, contamination in polar insulating materials should be avoided with still greater care because of the greater degree of dissociation of ionic substance in solution.

The long term lives of capacitors containing chlorinated impregnants under direct stress may be greatly extended by adding small quantities of certain **stabilizers**, which are hydrogen acceptors and act as depolarizers at the cathode. Hydrogen ions discharged at the cathode readily react with the stabilizer rather than with the impregnant, a more difficult chemical process. In the absence of the stabilizer, the hydrogen reacts with the chlorine of the impregnant to produce hydrochloric acid, and rapid deterioration occurs due to attack of the acid on the electrodes and cellulose. The extension of the life caused by the stabilizers is proportional to the amount of stabilizer added. For example, with 2% of the stabilizer Azobenzene, mean life may be extended 50 times.

2.2.6 Chemical Deterioration

Progressive chemical degradation of insulating materials can occur in the absence of electric stress from a number of causes.

Chemical Instability

Many insulating materials, especially organic materials, show chemical instability. Such chemical changes may result from spontaneous breakdown of the structure of the material. Under normal operating conditions, this process is very slow, but the process is strongly temperature dependant. The logarithm of the life **t** of paper insulation can be expressed as an inverse function of the absolute temperature **θ**.

$$\log_{10} t = A/\theta + B \qquad \text{where A \& B are constants}$$

If t is expressed in weeks, for vacuum dried paper immersed in oil in contact with Nitrogen, the constants have values A = 7000 and B = - 16.0.

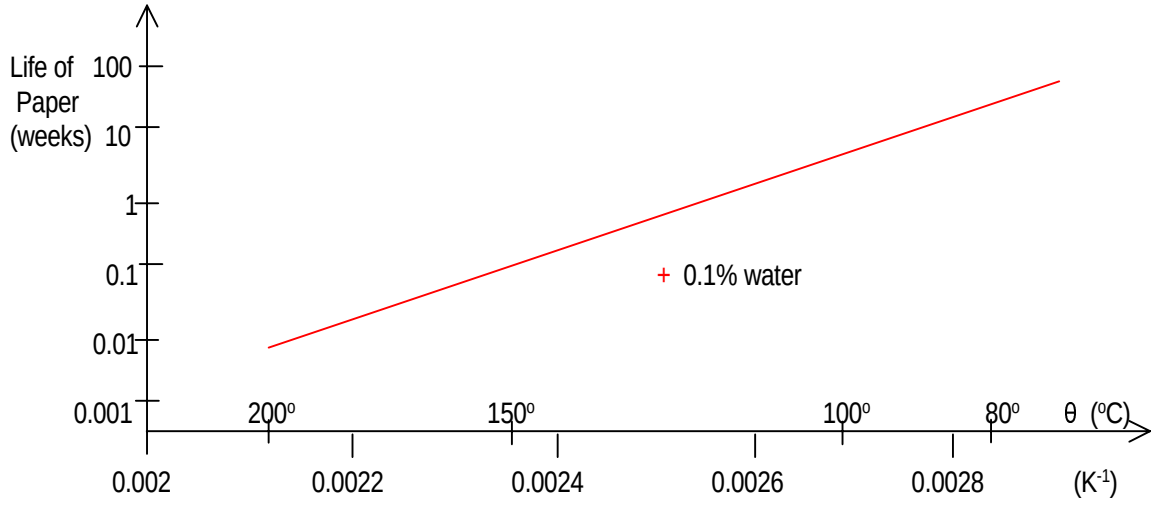

Figure 2.7 - Dependence of life of paper on temperature

In the presence of oxygen or moisture, the life of the insulation decreases much more rapidly.
With increase in amount of moisture present, B decreases so that the life of the paper also decreases. With about 0.1% moisture present, B decreases by as much as 0.8, so that **t** decreases by a factor of about 6. This means that presence of about 0.1% moisture reduces the life of the insulation by as much as 6 times. Figure 2.7 shows the variation.

Oxidation

In the presence of air or oxygen, especially ozone, materials such as rubber and polyethylene undergo oxidation giving rise to surface cracks, particularly if stretched and exposed to light. Polythene also oxidises in strong day light unless protected by an opaque filler.

Hydrolysis

When moisture or water vapour is present on the surface of a solid dielectric, hydrolysis occurs and the materials lose their electrical and mechanical properties. Electrical properties of materials such as paper, cotton tape, and other cellulose materials deteriorate very rapidly due to hydrolysis. Polyethylene film may lose its mechanical strength in a few days if kept at 100 % relative humidity.

Other processes

Progressive chemical degradation of insulating materials can also occur due to a variety of processes such as, incompatibility of materials (ex: rubber ages more rapidly at elevated temperatures in the presence of copper, and cellulose degrades much more rapidly in the presence of traces of acidic substances), and leaching (washing out of a soluble constituent) of chemically active substances (ex: glass fabrics made from glasses of high sodium content lose their strength rapidly due to leaching of sodium to the surface of the fibres and the subsequent chemical attack of the strong alkali on the glass surface).

2.3 Breakdown of Composite Insulation

Almost no complete electrical insulation consists of one insulating phase. Usually more than one insulating material will be involved, either in series, parallel or both.

The simplest form of composite insulation system consists of 2 layers of the same material. In this case advantage is taken of the fact that two thin sheets have a higher electric strength than a single sheet of the same total thickness.
In other cases, composite dielectrics occur either due to design considerations (ex: paper with an impregnating liquid) or due to practical difficulties of fabrication (ex: air in parallel with solid insulation).
In certain cases, the behaviour of the composite insulation could be predicted from the behaviour of the components. But in most cases, the system as whole has to be considered. The following considerations determine the performance of the system as a whole.

(i) The stress distribution at different parts of the insulation system is distorted due to the component dielectric constants and conductivities,

(ii) the breakdown characteristics at the surface are affected by the insulation boundaries of various components,

(iii) the internal or partial discharge products of one component invariably affect the other components in the system, and

(iv) the chemical ageing products of one component also affect the performance of other components in the system.

2.3.1 Matching dielectric constants

When composite insulation has components with different dielectric constants, utilisation of the materials may be impaired. This is especially true in the oil/transformerboard dielectric. This is because the oil has a lower dielectric constant and lower dielectric strength compared to that of transformerboard.

Since the dielectrics are in series,

$$\frac{V_1}{V_2} = \frac{C_2}{C_1} = \frac{A\varepsilon_2}{d_2}.\frac{d_1}{A\varepsilon_1} = \frac{\varepsilon_2 d_1}{\varepsilon_1 d_2}$$

$$V = V_1 + V_2$$

$$\frac{V_1}{V} = \frac{V_1}{V_1 + V_2} = \frac{\varepsilon_2 d_1}{\varepsilon_1 d_2 + \varepsilon_2 d_1}$$

$$\xi_1 = \frac{V_1}{d_1} = \frac{\varepsilon_2}{\varepsilon_1 d_2 + \varepsilon_2 d_1}.V$$

$$\xi_2 = \frac{V_2}{d_2} = \frac{\varepsilon_1}{\varepsilon_1 d_2 + \varepsilon_2 d_1}.V$$

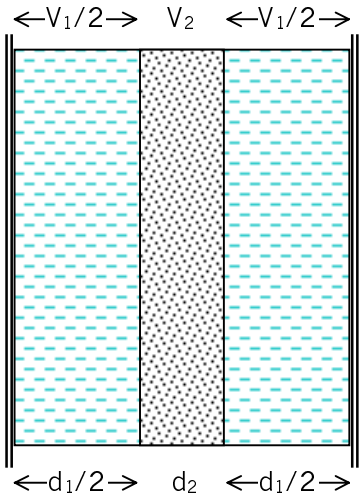

Figure 2.8 - Composite Dielectric

Example

A transformer oil having a dielectric constant of 2.2 and a dielectric strength of 25 kV/mm, is used as an insulation in a of spacing 8 mm. Determine the maximum applicable voltage. A barrier of thickness 3 mm of transfomerboard with a higher dielectric strength of 50 kV/mm (dielectric constant 4.4) is used in this space to increase the strength. Does the transformerboard serve this purpose in this case ?

With only transformer oil, the maximum applicable voltage is given by

$$V = 25 \times 8 = 400 \text{ kV}$$

If a barrier of thickness 3 mm is placed in the space with the oil, the maximum applicable voltage is given by

$$50 = \frac{4.4}{2.2 \times 2 + 4.4 \times 6} \times V$$

$$V = \frac{50 \times 14}{2} = 350 \text{ kV}$$

It can be seen that the maximum applicable voltage in fact reduces below that of only oil.
It is thus important, when barriers have to be used, to match the permittivities of the component insulations. Thus great gains could be achieved if a transformerboard with a dielectric constant of 2.6 could be used instead of one with 4.4.

Lightning Phenomena

3.1 Mechanism of Lightning

Lightning is an electric discharge in the form of a spark or flash originating in a charged cloud. It has now been known for a long time that thunder clouds are charged, and that the negative charge centre is located in the lower part of the cloud where the temperature is about - 5^0C, and that the main positive charge centre is located several kilometres higher up, where the temperature is usually below - 20^0C. In the majority of storm clouds, there is also a localised positively charged region near the base of the cloud where the temperature is 0^0C. Figure 3.1 shows such a cloud located above a overhead transmission line.

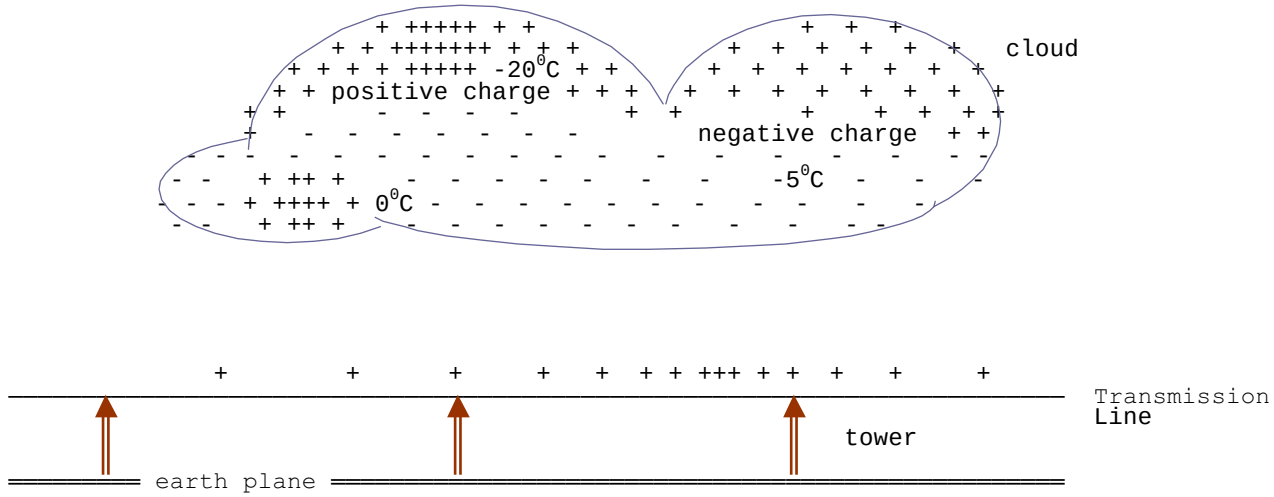

Figure 3.1 - Induced charges on transmission line

Fields of about 1000 V/m exist near the centre of a single bipolar cloud in which charges of about 20 C are separated by distances of about 3 km, and indicate the total potential difference between the main charge centres to be between 100 and 1000 MV. The energy dissipated in a lightning flash is therefore of the order of 1000 to 10,000 MJ, much of which is spent in heating up a narrow air column surrounding the discharge, the temperature rising to about 15,000 ^{0}C in a few tens of microseconds. Vertical separation of the positive and negative charge centres is about 2 - 5 km, and the charges involved are 10 - 30 C. The average current dissipated by lightning is of the order of kilo-amperes. During an average lightning storm, a total of the order of kilo-coulombs of charge would be generated, between the 0^0C and the -40 ^{0}C levels, in a volume of about 50 km^3.

3.1.1 Breakdown Process

Under the influence of sufficiently strong fields, large water drops become elongated in the direction of the field and become unstable, and streamers develop at their ends with the onset of corona discharges. Drops of radius 2 mm develop streamers in fields exceeding a 9 kV/cm - much less than the 30 kV/cm required to initiate the breakdown of dry air. The high field need only be very localised, because a streamer starting from one drop may propagate itself from drop to drop under a much weaker field.

When the electric field in the vicinity of one of the negative charge centres builds up to the critical value (about 10 kV/cm), an ionised channel (or streamer) is formed, which propagates from the cloud to earth with a velocity that might be as high as one-tenth the speed of light. Usually this streamer is extinguished when only a short distance from the cloud.

Forty micro-seconds or so after the first streamer, a second streamer occurs, closely following the path of the first, and propagating the ionised channel a little further before it is also spent. This process continues a number of times, each step increasing the channel length by 10 to 200 m. Because of the step like sequence in which this streamer travels to earth, this process is termed the **stepped leader** stroke. This process is shown diagrammatically in figure 3.2.

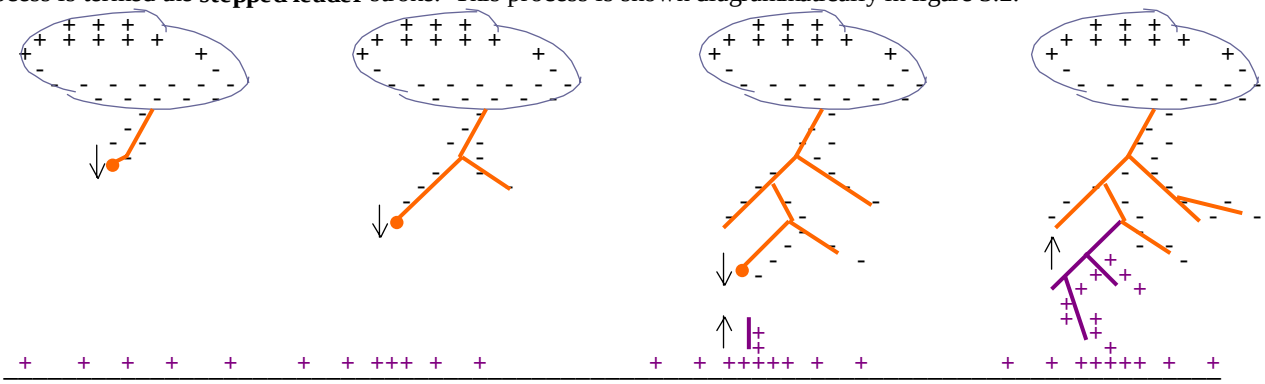

Figure 3.2 - Propagation of lightning channel

When eventually the stepped leader has approached to within 15 to 50 m of the earth, the field intensity at earth is sufficient for an upward streamer to develop and bridge the remaining gap. A large **neutralising** current flows along the ionised path, produced by the stepped leader, to neutralise the charge. This current flow is termed the **return** stroke and may carry currents as high as 200 kA, although the average current is about 20 kA.

The luminescence of the stepped leader decreases towards the cloud and in one instances it appears to vanish some distance below the cloud. This would suggest that the current is confined to the stepped leader itself. Following the first, or main stroke and after about 40 ms, a second leader stroke propagates to earth in a continuous and rapid manner and again a return stroke follows. This second and subsequent leader strokes which travel along the already energised channel are termed **dart leaders**.

What appears as a single flash of lightning usually consist of a number of successive strokes, following the same track in space, at intervals of a few hundredths of a second. The average number of strokes in a multiple stroke is four, but as many as 40 have been reported. The time interval between strokes ranges from 20 to 700 ms, but is most frequently 40-50 ms. The average duration of a complete flash being about 250 ms.

The approximate time durations of the various components of a lightning stroke are summarised as follows.

Stepped leader	=	10 ms
Return stroke	=	40 μs
period between strokes	=	40 ms
duration of dart leader	=	1 ms

For the purpose of surge calculations, it is only the heavy current flow during the return stroke that is of importance. During this period it has been found that the waveform can be represented by a double exponential of the form

$$i = I(e^{-\alpha t} - e^{-\beta t})$$

with wavefront times of 0.5 - 10 μs, and wavetail times of 30 - 200 μs. (An average lightning current waveform would have a wavefront of the order of 6 μs and a wavetail of the order of 25 μs).
The standard voltage waveform used in high voltage testing has a 1.2/50 μs waveform to take into account the most severe conditions. For the standard waveform, the coefficients α and β in the double exponential have values of $\alpha = 1.426 \times 10^4\ s^{-1}$, and $\beta = 4.877 \times 10^6\ s^{-1}$.

3.1.2 Frequency of occurrence of lightning flashes

A knowledge of the frequency of occurrence of lightning strokes is of utmost importance in the design of protection against lightning. The frequency of occurrence is defined as the flashes occurring per unit area per year.

However, this cannot be measured very easily, and without very sophisticated equipment. This information is difficult to obtain. However, the keraunic level at any location can be quite easily determined. The **keraunic level** is defined as the number of days in the year on which thunder is heard. It does not even distinguish between whether lightning was heard only once during the day or whether there was a long thunderstorm. Fortunately, it has been found by experience that the keraunic level is linearly related to the number of flashes per unit area per year. In fact it happens to be about twice the number of flashes/square mile/year. By assuming this relationship to hold good throughout the world, it is now possible to obtain the frequency of occurrence of lightning in any given region quite easily.

The isokeraunic level map, which shows contours of equal keraunic level, for Sri Lanka is shown in figure 3.3.

Figure 3.3 - Isokeraunic Level map of Sri Lanka

The map is based on the findings of the study “Lighning conditions in Ceylon,, and measures to reduce damage toelectrical equipment” by Dr Gi-ichi Ikeda in 1968 (Asian Productivity organization report, May 1969 – AP) Project TES/68)

3.2 Lightning Problem for Transmission Lines

The negative charges at the bottom of the cloud induces charges of opposite polarity on the transmission line. These are held in place in the capacitances between the cloud and the line and the line and earth, until the cloud discharges due to a lightning stroke. The figure 3.4 shows the problems facing the transmission engineer caused by lightning. There are three possible discharge paths that can cause surges on the line.

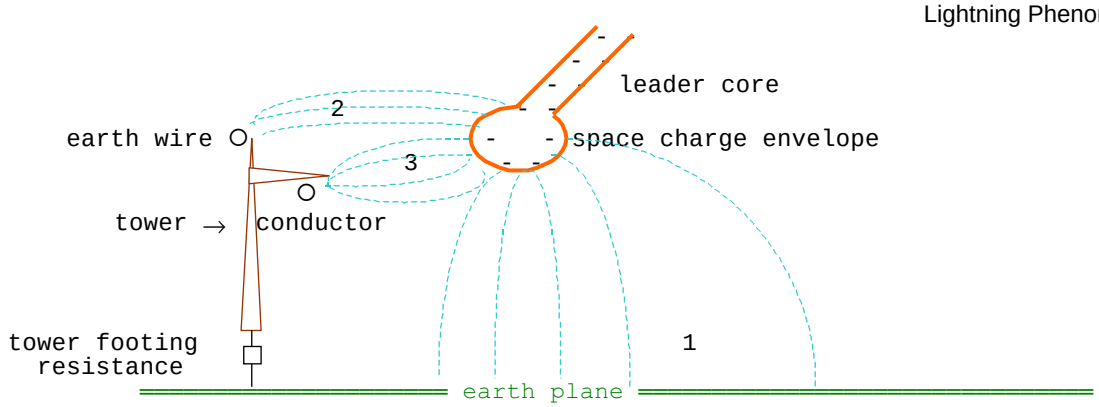

Figure 3.4 - Geometry of lightning leader stroke and transmission line

(a) In the first discharge path (1), which is from the leader core of the lightning stroke to the earth, the capacitance between the leader and earth is discharged promptly, and the capacitances from the leader head to the earth wire and the phase conductor are discharged ultimately by travelling wave action, so that a voltage is developed across the insulator string. This is known as the **induced voltage due to a lightning stroke to nearby ground**. It is not a significant factor in the lightning performance of systems above about 66 kV, but causes considerable trouble on lower voltage systems.

(b) The second discharge path (2) is between the lightning head and the earth conductor. It discharges the capacitance between these two. The resulting travelling wave comes down the tower and, acting through its effective impedance, raises the potential of the tower top to a point where the difference in voltage across the insulation is sufficient to cause flashover from the tower back to the conductor. This is the so-called **back-flashover** mode.

(c) The third mode of discharge (3) is between the leader core and the phase conductor. This discharges the capacitance between these two and injects the main discharge current into the phase conductor, so developing a surge-impedance voltage across the insulator string. At relatively low current, the insulation strength is exceeded and the discharge path is completed to earth via the tower. This is the **shielding failure** or direct stroke to the phase conductor.

The protection of structures and equipment from the last mode of discharge by the application of lightning conductors and/or earth wires is one of the oldest aspects of lightning investigations, and continue to do so.

3.2.1 Shielding by overhead ground wires

Overhead ground wires are provided on transmission lines to intercept direct strokes of lightning and thus keep it off the phase conductor, and to reduce the surge current and hence the overvoltage on a phase conductor by having currents induced in it.

The proportion of lightning flashes capable of causing sparkover of line insulation decreases as the system voltage increases. This is due to the fact that the magnitude of the overvoltage caused by lightning strokes are almost independent of the system voltage. Of course there is a slight dependence as the height of the towers also increase with the increase in voltage and a taller tower is more liable to a lightning strike. For a given magnitude of lightning overvoltage, the per unit value based on system voltage decreases as the system voltage increases. Thus as the system voltage increases, there are lesser number of flashovers caused by lightning.

Not only does the tall tower attract more lightning strokes, but also it requires a much better earth-wire coverage for a given degree of protection. The figure 3.5 illustrates this geometrically, by considering two identical configurations of conductors, but with the height of the tower different.

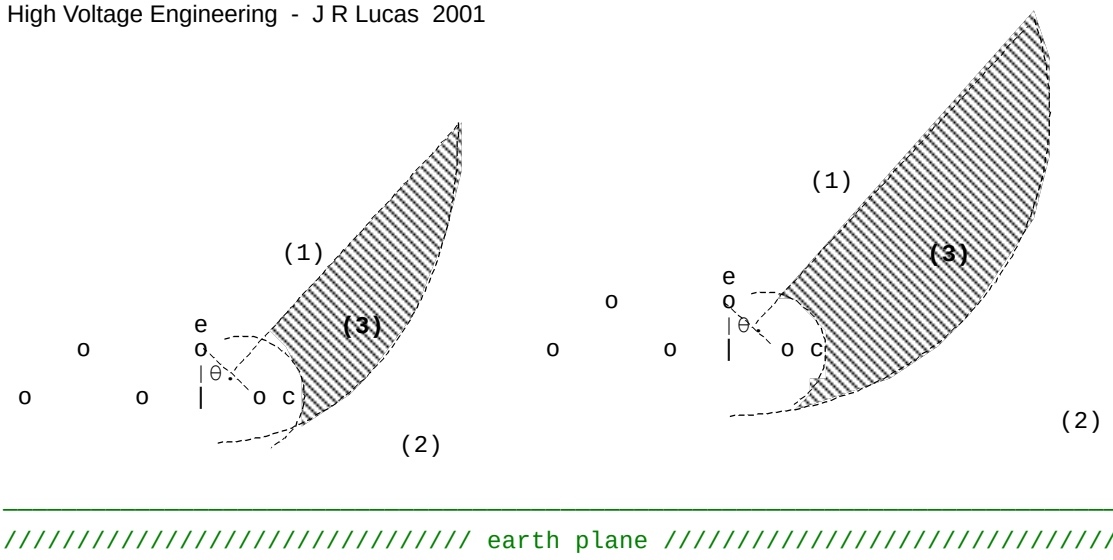

Figure 3.5 - Earth wire shielding - geometric model

The region marked (1) on the diagram, represents the region in which lightning will most likely strike the earth wire and thus provide protection against direct strikes. The locus of the lower boundary of this region is approximately defined by the perpendicular bisector of the line joining the phase conductor (the outermost for a horizontal arrangement and the uppermost in the case of a vertical arrangement) and the earth wire.

The region marked (2) on the diagram, represents the region in which lightning avoids both the overhead conductor as well as the earth wire but strikes some nearby object. The region has the upper boundary defined approximately by a parabolic locus. This locus is taken as equidistant from both the earth plane as well as the phase conductor. {This assumption is not exactly true as the phase conductor is a better attractor of lightning due to its sharper configuration).

Depending on the strength of the charge on the leader core, lightning will be initiated at a distance away from the object struck. Thus if the leader core could approach very close to the phase conductor before it discharges, then that particular stroke will be weak. This defines a minimum region within which lightning strikes terminating on the line does not do any damage. This region thus has a circular locus around the conductor, which need not be considered.

The region marked (3) on the diagram is the balance region, demarcated by the locus of region (1), the locus of region (2) and the circular locus where the stroke is too weak to cause damage. In this region (3) the lightning stroke is most likely to terminate on the phase conductor. The area (3) is thus a measure of the efficiency of the earth-wire protection. The smaller this region is the better the shielding provided by the overhead earth wires. It can be seen that for the same semi-vertical shielding angle θ, the taller the tower the lesser the efficiency of protection provided by the earth wire. Further it can be seen that if the semi-vertical angle of shielding is reduced, the area (3) reduces giving better protection. Thus to obtain the same degree of protection, taller towers require smaller protection angles.

3.2.2 Calculation of Shielding angle

The shielding angle of an overhead earth wire is defined as the semi-vertical angle between the line joining the most exposed conductor and the earth wire.

Consider the electrostatic interaction between the core of the downward lightning stroke and a single conductor and a single earth wire as shown in figure 3.6. As the leader channel propagates downwards, its equipotential lines will interact with both phase conductor as well as the earth wire. The earth wire may be at a lower potential than the phase conductor or vice versa. In the former case (a) protection will be afforded, and the shielding is effective. In the latter case (b) no protection will be afforded and non-effective shielding will occur.

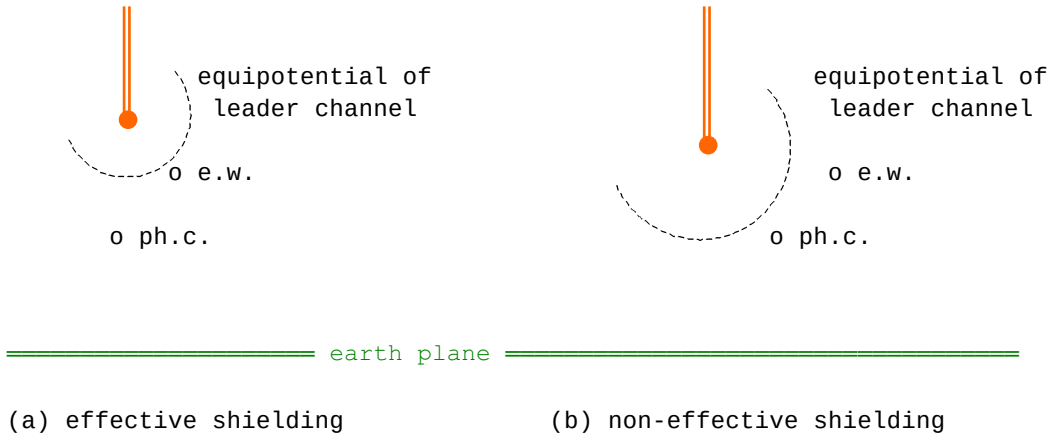

Figure 3.6 - Equipotentials of downward leader

For the same conductor configuration, both effective shielding and non-effective shielding could occur depending on how close the leader channel gets to the phase conductor. Thus it is necessary to know the critical distance at which various charges discharge. These have been obtained by various investigators and is illustrated in figure 3.7.

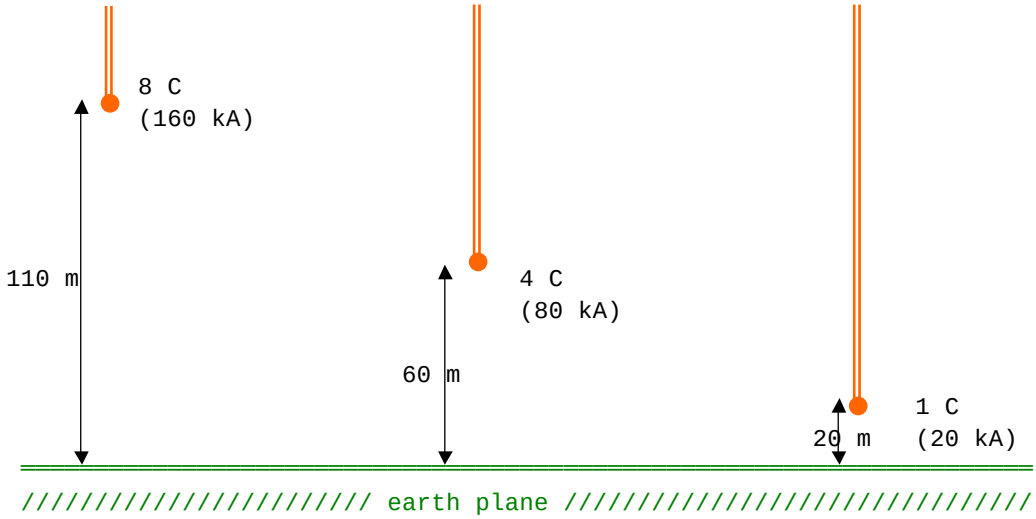

Figure 3.7 - Critical Distances associated with charges in stroke

The peak value of the return stroke current is approximately proportional to the leader charge, and the corresponding values are shown alongside the value of the charge on the diagram.

Figure 3.8 shows the distribution of magnitudes of the charges (and currents), in terms of the percentage of strokes exceeding a given current.

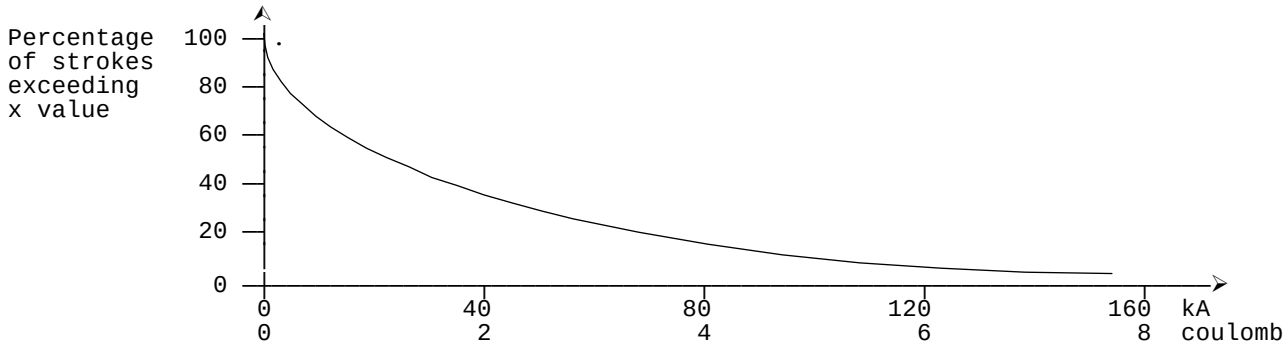

Figure 3.8 - Charge concentration in lightning

Based on the above, it has been found that a shielding angle of the order of 30^0 would give almost complete protection, where as an angle of nearly 90^0 would give almost no protection. Typical values used for the shielding angle are in the range of 22^0 to 48^0.

3.3 Area of attraction of transmission systems to lightning

Protective zone of lightning conductor: The area over which a lightning stroke will be attracted to and will terminate on a lightning conductor in preference to earth is termed the **protection range** or **protective zone**. Figure 3.9 shows this zone.

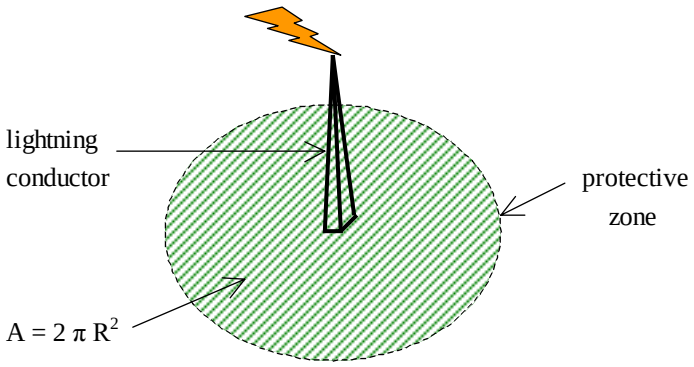

Figure 3.9 - protective zone of lightning conductor

The calculation of the area is based on a gradient of 3 kV/cm at the tower at which the upward streamer is initiated from the tower. It has been found that for the **average** stroke the **protective ratio** is approximately two for a lightning conductor or tower.

$$R = 2H \text{ (approx) at 20 kA}$$

That is, the area of attraction of a lightning conductor may be expected to be equal to an area around the base of the conductor with a radius of twice the conductor height. In the case of transmission lines, the earth wire is positioned to protect the phase conductors against lightning strokes and hence it is a protective conductor. However, the earth wire attracts strokes that would not normally terminate on the line. Similarly, phase-conductors themselves attract lightning strokes and it is hardly correct to talk of the **protective zone**. A more appropriate term is the **area of attraction**. Figure 3.10 shows the area of attraction of the transmission line and towers.

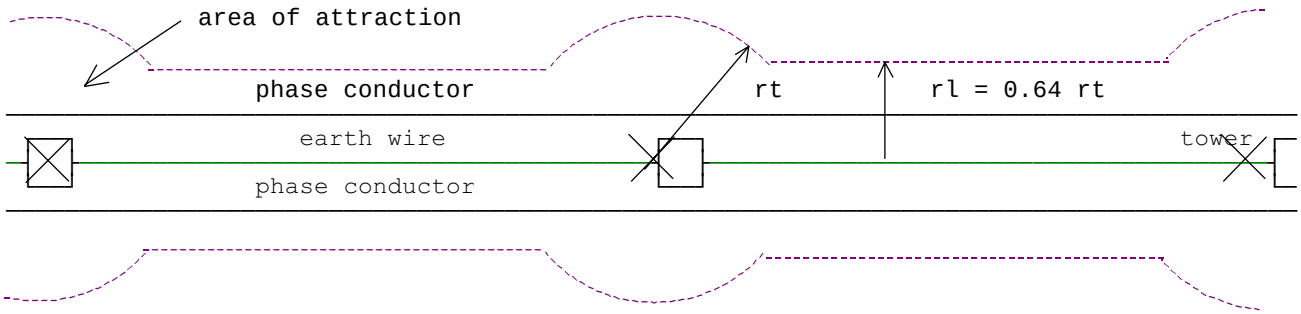

Figure 3.10 - Area of attraction of transmission line

Since the tower is like a lightning conductor, the area of attraction of the tower can be taken as equal to a circle with radius twice the tower height. An earth wire is more uniform that a transmission tower, in that it does not have a sharp point but a sharp line. It has been estimated that an area either side of the earth wire to a distance of 1.5 or 1.6 times the effective height of the earth wire multiplied by the length of the earth wire is a reasonable value to be taken. Further it must be noted that due to the sag of the earth wire, the effective height of the earth wire is itself only about 80% of the height at the tower. Thus a distance of 64% of the radius of attraction at the tower may be taken for the attraction distance of the earth wire. The phase conductor may be treated similarly, but with the height of the phase conductor being considered instead of that of the earth wire.

Thus if the line dimensions are known, it is possible to evaluate the total area of attraction that the line has to lightning strokes.

3.4 Effects of Lightning on a Transmission Line

Charged clouds induce charges on upstanding objects. These induced charges are distributed in such a way as to cause a concentration of potential at the upper end of the object, with the result that the electrostatic stress is very great. This causes the air in the immediate neighborhood to be ionised very rapidly, and charged particles are expelled from the pointed end. This produces a gradual lowering of the resistance of the discharge path between the cloud and the conductor until eventually the lightning discharge takes place.

3.4.1 Strokes to a Phase-conductor

The charged cloud could discharge directly onto the line. If the line is struck a long distance from a station or substation, the surge will flow along the line in both directions, shattering insulators and sometimes even wrecking poles until all the energy of the surge is spent. If it strikes the line immediately adjacent to a station, then the damage to plant is almost certain, since it is doubtful whether the ordinary lightning arrestor could divert to earth such a powerful discharge, without allowing a part to be transmitted to the terminal apparatus.

When lightning strikes an overhead phase-conductor, the magnitude of the current and the high frequency nature of the stroke causes voltage surges to be propagated in both directions from the point of the strike (Figure 3.11).

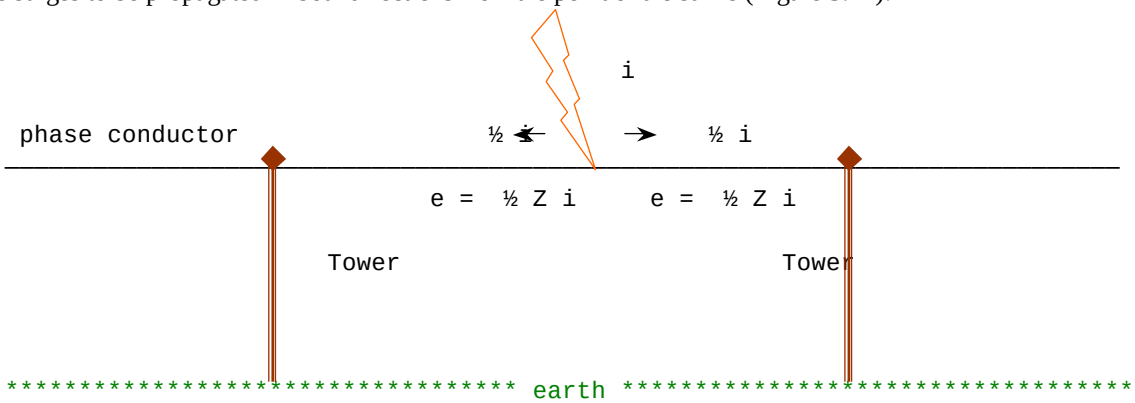

Figure 3.11 - Direct strike on phase conductor

The waveshape of these voltage surges is similar to that of the current in the lightning discharge. The discharge current splits itself equally on contact with the phase conductor, giving travelling waves of magnitude e.

$$e = \tfrac{1}{2} Z i (e^{-\alpha t} - e^{-\beta t})$$

where Z is the surge impedance of the phase conductor.

Using a typical value for the line surge impedance (say 300 Ω) and an **average lightning current** (20 kA), the voltage waves on the line would have a crest value of

$$E = \tfrac{1}{2} Z i = (300/2) \times 20 \times 10^3 = 3 \text{ MV}$$

3.4.2 Strokes to a tower with no earth wire

Fortunately, direct strokes to the line are infrequent in occurrence compared to side strokes, the effects of which are not so severe. If there is a direct stroke to the tower, a current would be discharged through the metal work of the tower and there would be a potential difference between the top and bottom of the tower.

Figure 3.12 shows a steel tower (inductance **L**) of a transmission line with no earth wire. If the earthing resistance of the tower is **R** (= 5 - 100 Ω), and it is struck by lightning, then the potential built up on the tower top would be

$$R i + L \frac{d i}{d t}$$

If $\mathbf{e_i}$ is the induced voltage on the conductor due to the lightning, then the potential difference built up across the tower and the conductor is given by

$$e = Ri + L\frac{di}{dt} + e_i$$

If the value of **e** exceeds the line insulation strength, then a flashover occurs from the tower to the line and this is termed a **backflashover**.

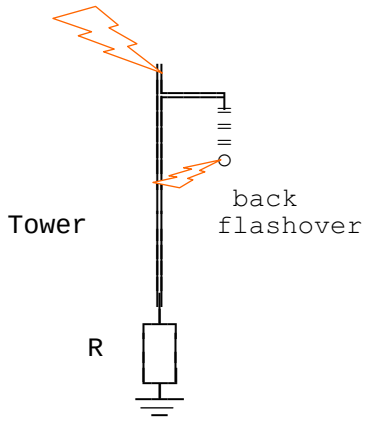

Figure 3.12 - Strokes to tower

3.4.3 Strokes to Earth Wire

When a lightning stroke terminates on the tower of a transmission line having an overrunning earth wire, or terminates on the earth wire of the transmission line, then the resulting current flow would be as shown in figure 3.13 (a) and (b).

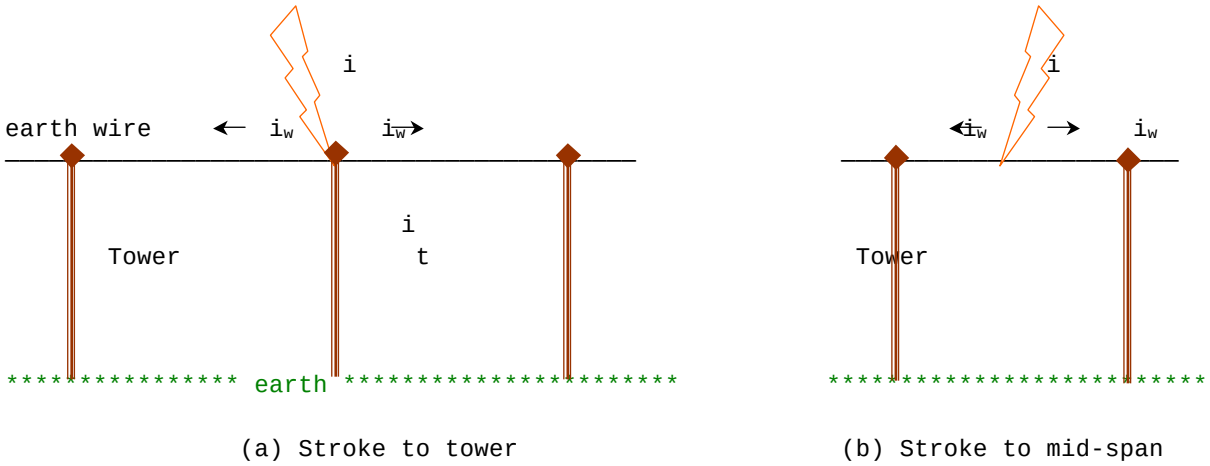

(a) Stroke to tower (b) Stroke to mid-span

Figure 3.13 - Stroke to earth wire

The voltage waves produced by the current i_w flowing along the earth wire will travel along the earth wire in both directions from the tower struck. On reaching the neighboring towers they will be partly reflected, and the reflected waves will arrive back at the tower after twice the transit time between the towers. Further reflections will take place as the waves travel further along the earth wire and reaches other towers. In calculation of the resulting voltage wave and hence the potential difference across the insulation it is useful to consider the **initial period**, **first reflection period**, **second reflection period** and so on and obtain separate equivalents.

For example, for the initial period and the first reflection period, the following equivalent circuits given in figures 3.14 and 3.15 may be used.

Initial period

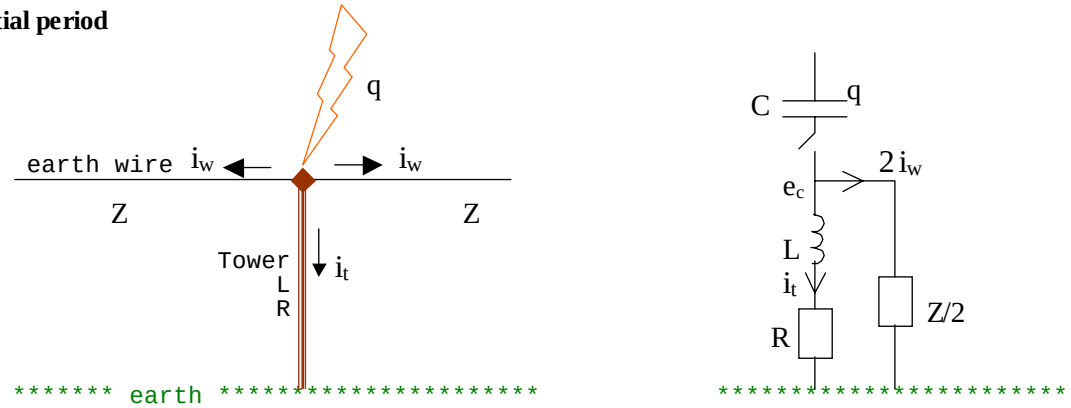

(a) Part of system (b) Equivalent circuit

Figure 3.14 - For initial period

In the figure 3.14, **L** is the effective inductance of the tower, **R** is the effective resistance of the tower and footing and **Z** is the surge impedance of the earth wire.

First Reflection period

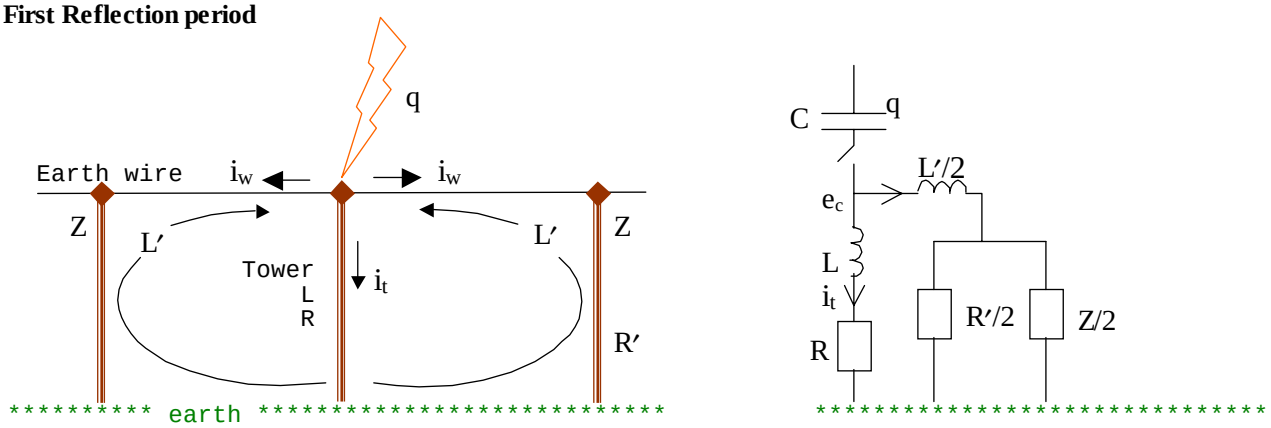

(a) Part of system (b) Equivalent circuit

Figure 3.15 - For first reflection period

where **L'** is the inductance of the first span loop and earth return.

If instead of the actual tower being struck, the earth wire is struck somewhere near mid-span, then this can be regarded as two towers in parallel being struck for the second reflection period, with the impedance of the span struck acting as an extension to the lightning channel.

For a given tower footing resistance **R**, strokes to the tower generally develop about one-and-half times the potential at the top of the tower as compared with the strokes to mid span. For a typical lightning current of 20 kA and a tower footing resistance of 20 Ω, those struck at the tower develop voltages of the order of 200 kV.

3.4.4 Strokes to nearby objects (Indirect Strokes)

In any lightning discharge, the charge on the down coming leader causes the conductors of the line to have a charge induced in them (figure 3.16).

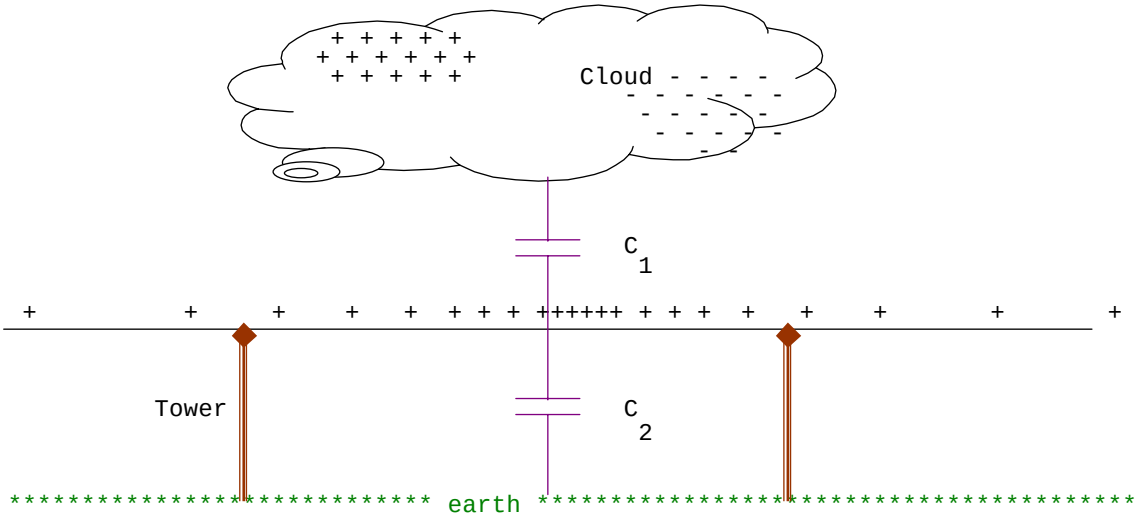

Figure 3.16 Induced charge on line

These charges are bound (held in that portion of the line nearest to the cloud) so long as the cloud remains near without discharging its electricity by a lightning stroke to an object. If however, the cloud is suddenly discharged, as it is when lightning strikes some object nearby, the induced charges are no longer bound, but travel with nearly the velocity of light, along the line to equalise the potential at all points of the line.

This bound charge collapse leads to a voltage wave to be generated on the line in either direction.
The value of this is given by

$$e_i = - E \cdot \frac{C_2}{C_1 + C_2} = \frac{q}{C}$$

where **q** = bound charge per unit length of line
C = capacitance per unit length of line

This potential will vary along the line depending upon the distance of each element of line from the lightning stroke.

The sequence of the travelling waves e_i propagating outwards is shown diagrammatically in figure 3.17

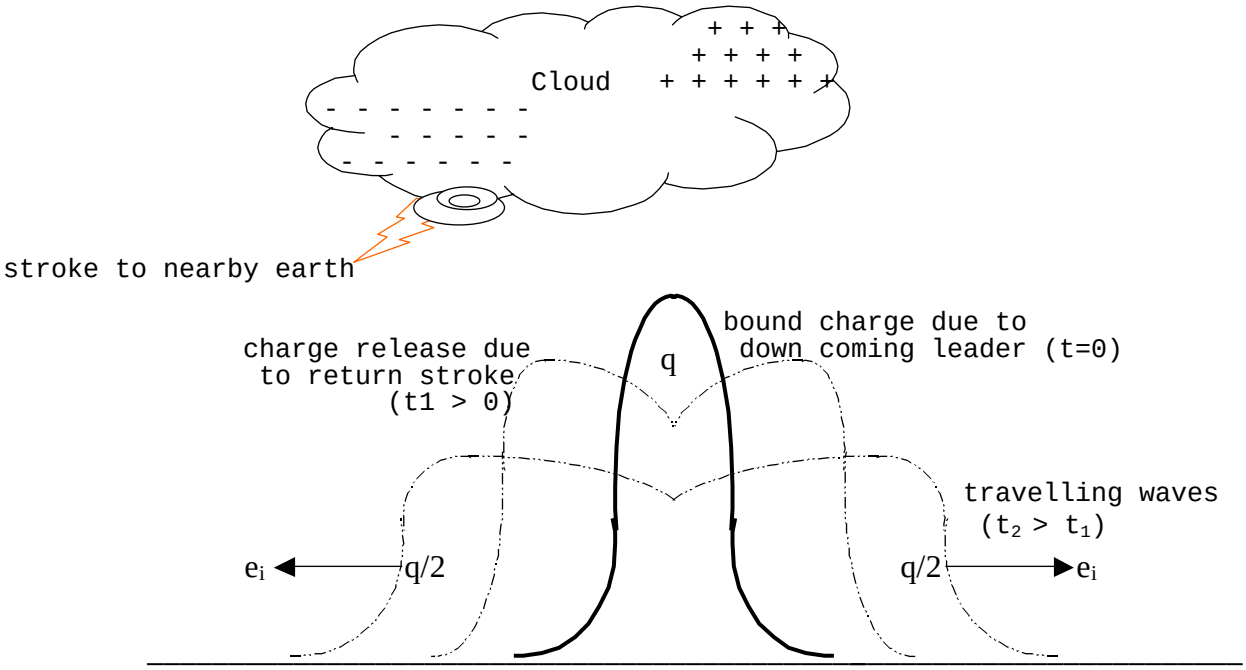

Figure 3.17 - Propagation of travelling waves

4

High Voltage Transient Analysis

4.1 Surges on Transmission Lines

Due to a variety of reasons, such as a direct stroke of lightning on the line, or by indirect strokes, or by switching operations or by faults, high voltage surges are induced on the transmission line. The surge can be shown to travel along the overhead line at approximately the speed of light. These waves, as they reach the end of the line or a junction of transmission lines, are partly reflected and partly transmitted. These can be analysed in the following manner.

Consider a small section of the transmission line, of length **dx**.

Let the voltage variation across this section at any instant of time be e to $e + \frac{\partial e}{\partial x}.dx$, and let the current vary similarly.

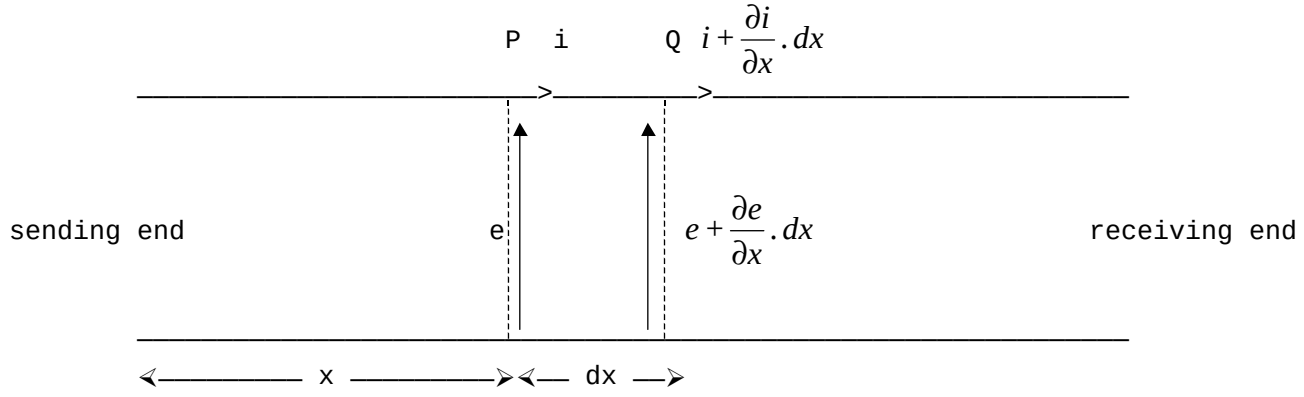

Figure 4.1 - Element of transmission line

Due to the surge, the voltage build-up in the line travels along the line and would cause damage to the transformer and other terminal equipment.

Let e = instantaneous voltage (varies with both distance and time)
i = instantaneous current (varies with both distance and time)
r = resistance of line per unit length
l = inductance of line per unit length
c = capacitance of line per unit length
g = conductance of line per unit length

The voltage drop across PQ and the corresponding current through it are given by the following equations.

$$v = -\frac{\partial e}{\partial x}.dx = r\,dx\,i + l\,dx\frac{\partial i}{\partial t}$$
$$i = -\frac{\partial i}{\partial x}.dx = g\,dx\,e + c\,dx\frac{\partial e}{\partial t}$$

Eliminating **dx** gives us the partial differential equations

$$-\frac{\partial e}{\partial x} = r\,i + l\frac{\partial i}{\partial t} \qquad (1)$$
$$-\frac{\partial i}{\partial x} = g\,e + c\frac{\partial e}{\partial t} \qquad (2)$$

Differentiating equation (1) with respect to x, and equation (2) with respect to t, and eliminating **i**, we have

$$\frac{\partial^2 e}{\partial x^2} = l.c\frac{\partial^2 e}{\partial t^2} + (c.r + l.g)\frac{\partial e}{\partial t} + g.r\,e$$

A very similar partial differential equation can be obtained for **i**.

In practical power lines, the resistance r is much less than the inductance l, and the conductance g is negligible. When these are neglected, the equation reduces to

$$\frac{\partial^2 e}{\partial x^2} = l.c\frac{\partial^2 e}{\partial t^2}$$

It is usual to substitute l.c = 1/a2, where a has the dimension of velocity. In this case the equation becomes

$$a^2\frac{\partial^2 e}{\partial x^2} = \frac{\partial^2 e}{\partial t^2}$$

The solution to this second order partial differential equation can be written in the form of two arbitrary functions.

Consider the function e = f(x - at) . For this

$$a^2\frac{\partial^2 e}{\partial x^2} = a^2\,f''(x - a\,t), \text{also}\ \frac{\partial^2 e}{\partial t^2} = f''(x - a\,t).(-a)^2$$

It is thus seen that this function satisfies the partial differential equation.

Similarly, consider the function e = F(x + at) . For this

$$a^2\frac{\partial^2 e}{\partial x^2} = a^2\,F''(x + a\,t), \text{also}\ \frac{\partial^2 e}{\partial t^2} = F''(x + a\,t).(a)^2$$

This too is seen to satisfy the partial differential equation.

Thus the general solution to the partial differential equation is

$$e = f(x - at) + F(x + at)$$

where **f** and **F** are two arbitrary functions of **(x-at)** and **(x+at)**. These two functions can be shown to be **forward** and **reverse** traveling, as follows.

Consider a point $\mathbf{x_1}$ at an instant $\mathbf{t_1}$ on a transmission line.

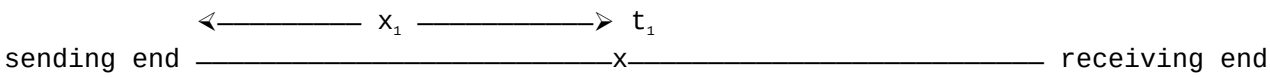

Figure 4.2 - Position (x_1, t_1) on transmission line

The value of the function **f(x-at)** at position $\mathbf{x_1}$ and time $\mathbf{t_1}$ would be

$$e_1 = f(x_1 - a\,t_1)$$

At any time **t** afterwards (i.e. at time $\mathbf{t+t_1}$), the value of this same function at the position **x** would be given by

$$e_2 = f[x - a\,(t+t_1)] = f(x-at + a\,t_1)$$

This latter voltage $\mathbf{e_2}$ would be equal to $\mathbf{e_1}$ at the position $\mathbf{x_1 = x - at}$.

Now **a.t** is the distance traveled by a wave traveling with velocity **a** in the forward direction in a time **t**. Thus it is seen that the voltage at a distance **a.t** in the forward direction is always equal to the value at the earlier position at the earlier time for any value of time. Thus the function **f(x-at)** represents a **forward wave**. Similarly, it can be seen that the function **F(x+at)** represents a **reverse wave.**

The effect of resistance and conductance, which have been neglected would be so as to modify the shape of the wave, and also to cause attenuation. These are generally quite small, and the wave travels with little modification. In fact this effect can be separately included in the analysis as will be shown later.

4.1.1 Surge Impedance and Velocity of Propagation

Consider the forward wave **e = f(x-at)**. The corresponding current wave **i** can be determined from equation (1) as follows.

$$l\frac{\partial e}{\partial t} = -\frac{\partial e}{\partial x} = -f'(x - a\,t)$$

$$\therefore i = \frac{1}{a\,l} f(x - at) = \frac{1}{a\,l}.e = \sqrt{\frac{c}{l}}.e$$

$$\text{i.e. } e = \sqrt{\frac{l}{c}}.i = Z_0.i \quad \text{where } Z_0 = \sqrt{\frac{l}{c}}$$

$\mathbf{Z_o}$ is known as the surge (or characteristic) impedance of the transmission line.

The surge current **i** traveling along the line is always accompanied by a surge voltage $\mathbf{e = Z_o\,i}$ traveling in the same direction. For a reverse wave, it can be similarly shown that the surge current **i** is associated with a surge voltage $\mathbf{e = -\,Z_o\,i}$.

For a transmission line, with conductors of radius **r** and conductor spacing **d**, it can be shown that the inductance per unit length of the line is given by

$$l = \frac{\mu_0}{2\pi}\left[\frac{\mu_r}{4} + \log_e\frac{d}{r}\right] \text{ H/m}$$

Since the internal flux linkage is small, if this is neglected

$$l = \frac{\mu_0}{2\pi} \log_e \frac{d}{r} \quad \text{H/m}$$

The capacitance **c** per unit length is given by

$$c = \frac{2\pi \varepsilon_0 \varepsilon_r}{\log_e \frac{d}{r}} \quad \text{F/m}$$

$$\text{for air} \quad \varepsilon_r = 1$$

$$\therefore \quad l.c = \mu_0 \varepsilon_0 = \frac{1}{a^2}$$

$$\text{but} \quad \frac{1}{\sqrt{\mu_0 \varepsilon_0}} = \text{velocity of light}$$

Therefore the velocity of propagation of the wave **a** is equal to the velocity of light. [Note: If the resistance of the line was not neglected, the velocity of propagation of the wave would be found to be slightly less than that of light (about 5 to 10%)].

For a cable, the dielectric material has a relative permittivity $\boldsymbol{\varepsilon_r}$ different from unity. In this case, the above derivation would give the velocity of propagation in a cable as

$$\text{velocity of propagation} = \text{velocity of light}/\sqrt{\varepsilon_r}$$

For commercial cables, ε_r lies between about 2.5 and 4.0, so that the velocity of propagation in a cable is about **half** to **two-third** that of light.

The surge impedance of a line can be calculated as follows.

$$Z_0 = \sqrt{\frac{l}{c}} = \sqrt{\frac{\mu_0}{\varepsilon_0}\left(\frac{\log_e d/r}{2}\right)^2}$$

Substituting the velocity of light as **3 x 10^8 m/s** and simplifying gives

$$Z_o = 60 \log_e (d/r) \qquad \Omega$$

For an overhead line, for practical values of conductor radius **r** and spacing **d**, the surge impedance $\mathbf{Z_o}$ is of the order of 300 to 600 Ω.

For a cable, the corresponding surge impedance would be given by the expression

$$Z_o = 60/\sqrt{\varepsilon_r} \,.\, \log_e (d/r) \qquad \Omega$$

which has values in the region of 50 to 60 Ω.

4.1.2 Energy stored in surge

The energy stored in a traveling wave is the sum of the energies stored in the voltage wave and in the current wave.

$$\text{Energy} = \tfrac{1}{2}\, c\, e^2 + \tfrac{1}{2}\, l\, i^2$$

$$e = \sqrt{\frac{l}{c}}\, i, \quad \text{i.e. } c\, e^2 = l\, i^2, \quad \text{i.e. } \tfrac{1}{2} c\, e^2 = \tfrac{1}{2} l\, i^2$$

$$\therefore \text{total energy} = c\, e^2$$

But for a surge, $\mathbf{e = Z_o\, i}$, so that we have

It is seen that half the energy of the surge is stored in the electrostatic field and half in the electromagnetic field.

4.2 Reflection of Traveling waves at a Junction

When a traveling wave on a transmission line reaches a junction with another line, or a termination, then part of the incident wave is reflected back, and a part of it is transmitted beyond the junction or termination.

The **incident wave**, the **reflected wave** and the **transmitted wave** are formed in accordance with Kirchhoff's laws. They must also satisfy the differential equation of the line.

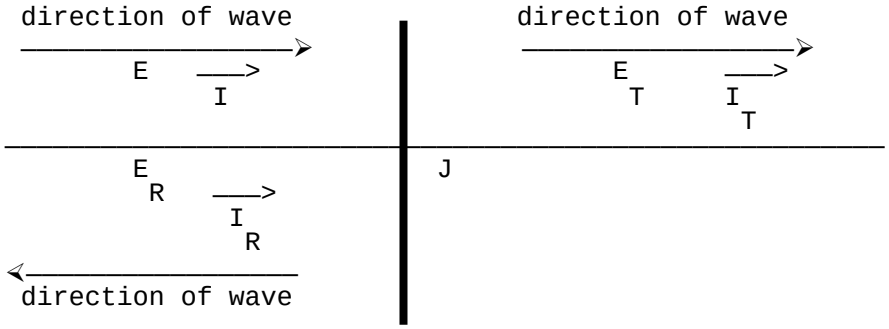

Figure 4.3 - Reflection at a junction

Consider a step-voltage wave of magnitude **E** incident at junction **J** between two lines of surge impedances $\mathbf{Z_1}$ and $\mathbf{Z_2}$. A portion $\mathbf{E_T}$ of this surge would be transmitted and a portion $\mathbf{E_R}$ would be reflected as shown in figure 4.3.

There is no discontinuity of potential at the junction J. Therefore

$$E + E_R = E_T$$

There is also no discontinuity of current at the junction. Therefore

$$I + I_R = I_T$$

Also, the incident surge voltage **E** is related to the incident surge current **I** by the surge impedance of the line $\mathbf{Z_1}$. Similarly the transmitted surge voltage $\mathbf{E_T}$ is related to the transmitted surge current $\mathbf{I_T}$ by the surge impedance of the line $\mathbf{Z_2}$ and the reflected surge voltage $\mathbf{E_R}$ is related to the reflected surge current $\mathbf{I_R}$ by the surge impedance of the line $\mathbf{Z_1}$.

However it is to be noted that the reflected wave is a reverse wave. Thus we can write

$$E = Z_1 I, \quad E_T = Z_2 I_T, \text{ and } E_R = -Z_1 I_R$$

Substituting these values gives

$$E/Z_1 - E_R/Z_1 = E_T/Z_2 = (E + E_R)/Z_2$$

This gives on simplification

$$E_R = \frac{Z_2 - Z_1}{Z_2 + Z_1} . E$$

Similarly, the transmitted surge may be written as

$$E_T = \frac{2 Z_2}{Z_2 + Z_1} . E$$

Thus we have obtained the transmitted wave E_T and the reflected wave E_R in terms of the incident surge E. Since both these surges are a definite fraction of the incident surge, a transmission factor **α** and a reflection factor **β** are defined as follows.

$$\alpha = \frac{2 Z_2}{Z_2 + Z_1}, \quad \beta = \frac{Z_2 - Z_1}{Z_2 + Z_1}$$

When the junction is matched (i.e. $Z_1 = Z_2$), then there is no reflection and the reflection factor can be seen to be zero.

When the line Z_1 is open circuited at the far end (i.e. $Z_2 = \infty$), then the full wave is reflected back and the reflection factor becomes 1.

When the line Z_1 is short circuited at the far end (i.e. $Z_2 = 0$), then no voltage can appear and the full wave is reflected back negated so as to cancel the incident wave and the reflection factor becomes - 1.

4.2.1 Open circuited line fed from a infinite source

For this case $Z_2 = \infty$ and $\beta = 1$.

When a voltage surge **E** arrives at the junction J, which is on open circuit, it is reflected without a change in sign (i.e. **E**).

Also, a current surge (**- I**) of opposite sign to the incident (**I**) is reflected so that the transmitted current is zero.

If the line is fed from a constant voltage source **E**, then as the reflected voltage surge (**E)** arrives at the generator end, since the generator maintains the voltage at its end at voltage **E**, it send a voltage surge of **-E** back to the line so as to keep its voltage at **E**.

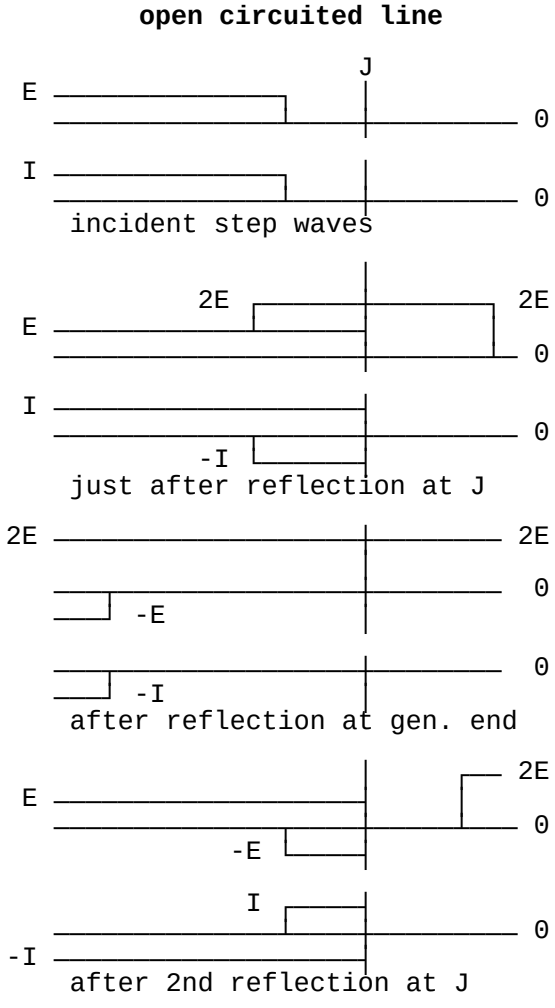

Figure 4.4 - Reflections under open circuit conditions

[This could also have been deduced by considering that a constant voltage source has a zero internal impedance, and the reflection coefficient can be calculated based on $Z_2 = 0$].

The voltage surge **- E** is accompanied by a current surge **- I**. The surge voltage **- E** as it reaches the open junction J, is reflected again without a change in sign, and accompanied by a current **+ I** so as to make the transmitted current again zero. Once these voltage and current waves reach the generator, the instantaneous voltage and current will be zero, and the line would once again be uncharged. The generator now sends a voltage surge **E** accompanied by a current surge **I**, and the who process described repeats again.

4.2.2 Short Circuit Line fed from an infinite source

For this case $Z_2 = 0$ and $\beta = -1$.

When a voltage surge **E** arrives at the junction J, which is on short circuit, it is reflected with a change in sign (**- E**), so as to cancel the incoming surge. Also, a current surge **I** of the same sign as the incident (**I)** is reflected so that the transmitted current is doubled (**2I**).

If the line is fed from a constant voltage source **E**, then as the reflected voltage surge (**- E**) arrives at the generator end, it send a voltage surge of **E** back to the line so as to keep its voltage at **E**.

The voltage surge **E** is again accompanied by a current surge **I** so that the transmitted current becomes **3I**. The surge voltage **E** as it reaches the junction J, is reflected again with a change in sign, and accompanied by a current **I** so as to make the transmitted current again increase by **I** to **4I**. At successive reflections, the current keeps on building. [This is to be expected as a short circuited line with zero line resistance and zero source resistance, fed from a constant voltage source will finally tend to zero.

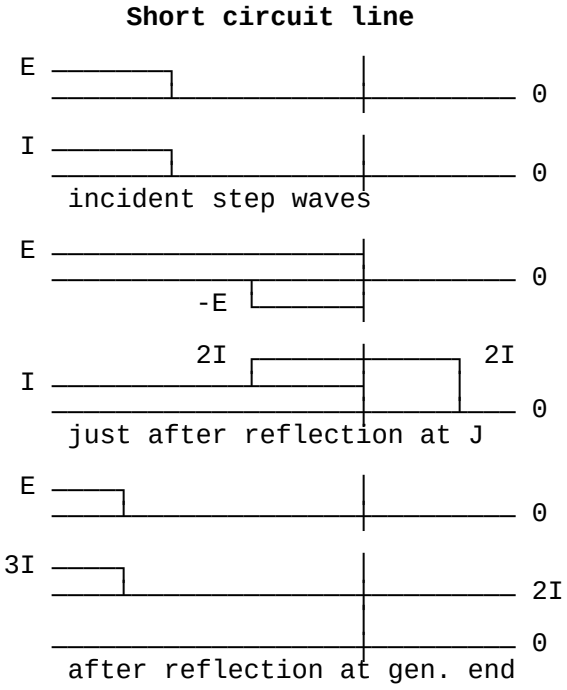

Figure 4.5
- Reflections under short circuit conditions

However the increase is in a step like manner rather than in a linear manner]. In practice, due to the resistance of the line, the current does not keep on building, but each successive current surge is lower than the earlier one due to attenuation. Thus the final current tends to a limiting value determined by the line resistance.

In the above transient, the voltage **E** has been assumed constant at the generator end. In practice, such an assumption is generally valid, owing to the fact that the very high velocity of propagation does not normally cause the system voltage to vary significantly during the period of interest for reflections.

Example: Consider a line 30 km long, operating at a frequency of 50 Hz.

Assuming the velocity of propagation to be $\mathbf{3 \times 10^8 m/s}$, the travel time for single transit of the line would be $\mathbf{30 \times 10^3 / 3 \times 10^8 s} = 100\ \mu s$.

During this time, the change in the phase angle of the 50 Hz voltage would be $\mathbf{\omega t = 2 \pi . 50 . 10^{-4} rad = 10^{-2} . 180^o = 1.8^o}$.

If we consider the peak value of the sinusoidal voltage as **1 pu**, then if we deviate from this position by **1.8°**, then the corresponding voltage would be **cos 91.8° = 0.9995 pu**. During this interval, it can be seen that the variation of the voltage is negligibly small and the step approximation can be considered valid. Even in other instances, the step analysis is useful because other waveforms can be considered as made up of step surges.

4.3 Bewley Lattice Diagram

This is a convenient diagram devised by Bewley, which shows at a glance the position and direction of motion of every incident, reflected, and transmitted wave on the system at every instant of time. The diagram overcomes the difficulty of otherwise keeping track of the multiplicity of successive reflections at the various junctions.

Consider a transmission line having a resistance **r**, an inductance **l**, a conductance **g** and a capacitance **c**, all per unit length.

If γ is the propagation constant of the transmission line, and
E is the magnitude of the voltage surge at the sending end,

then the magnitude and phase of the wave as it reaches any section distance **x** from the sending end is $\mathbf{E_x}$ given by.

$$E_x = E \,.\, e^{-\gamma x} = E \,.\, e^{-(\alpha + j\beta)x} = E\, e^{-\alpha x}\, e^{-j\beta x}$$

where

$\mathbf{e^{-\alpha x}}$ represents the attenuation in the length of line x
$\mathbf{e^{-j\beta x}}$ represents the phase angle change in the length of line x

Therefore,

α = attenuation constant of the line in neper/km
β = phase angle constant of the line in rad/km.

It is also common for an attenuation factor **k** to be defined corresponding to the length of a particular line. i.e. $\mathbf{k = e^{-\alpha l}}$ for a line of length **l**.

The propagation constant of a line γ of a line of series impedance **z** and shunt admittance **y** per unit length is given by

$$\gamma = \sqrt{z.y} = \sqrt{(r + j\,\omega\, l)(g + j\,\omega\, c)}$$

Similarly the surge impedance of the line (or characteristic impedance) $\mathbf{Z_0}$

$$Z_0 = \sqrt{\frac{z}{y}} = \sqrt{\frac{(r + j\,\omega\, l)}{(g + j\,\omega\, c)}}$$

When a voltage surge of magnitude **unity** reaches a junction between two sections with surge impedances $\mathbf{Z_1}$ and $\mathbf{Z_2}$, then a part $\boldsymbol{\alpha}$ is transmitted and a part $\boldsymbol{\beta}$ is reflected back. In traversing the second line, if the attenuation factor is **k**, then on reaching the termination at the end of the second line its amplitude would be reduced to $\mathbf{k.\alpha}$. The lattice diagram may now be constructed as follows. Set the ends of the lines at intervals equal to the time of transit of each line. If a suitable time scale is chosen, then the diagonals on the diagram show the passage of the waves.

In the Bewley lattice diagram, the following properties exist.

(1) All waves travel downhill, because time always increases.

(2) The position of any wave at any time can be deduced directly from the diagram.

(3) The total potential at any point, at any instant of time is the superposition of all the waves which have arrived at that point up until that instant of time, displaced in position from each other by intervals equal to the difference in their time of arrival.

(4) The history of the wave is easily traced. It is possible to find where it came from and just what other waves went into its composition.

(5) Attenuation is included, so that the wave arriving at the far end of a line corresponds to the value entering multiplied by the attenuation factor of the line.

4.3.1 Analysis of an open-circuit line fed from ideal source

Let τ is the time taken for a wave to travel from one end of the line to the other end of the line (i.e. single transit time) and **k** the corresponding attenuation factor.

Consider a step voltage wave of amplitude unity starting from the generator end at time **t = 0.** Along the line the wave is attenuated and a wave of amplitude **k** reaches the open end at time τ. At the open end, this wave is reflected without a loss of magnitude or a change of sign. The wave is again attenuated and at time 2τ reaches the generator end with amplitude $\mathbf{k}^2$. In order to keep the generator voltage unchanged, the surge is reflected with a change of sign ($-\mathbf{k}^2$), and after a time 3τ reaches the open end being attenuated to $-\mathbf{k}^3$. It is then reflected without a change of sign and reaches the generator end with amplitude $-\mathbf{k}^4$ and reflected with amplitude $+\mathbf{k}^4$. The whole process is now repeated for the wave of amplitude $\mathbf{k}^4$.

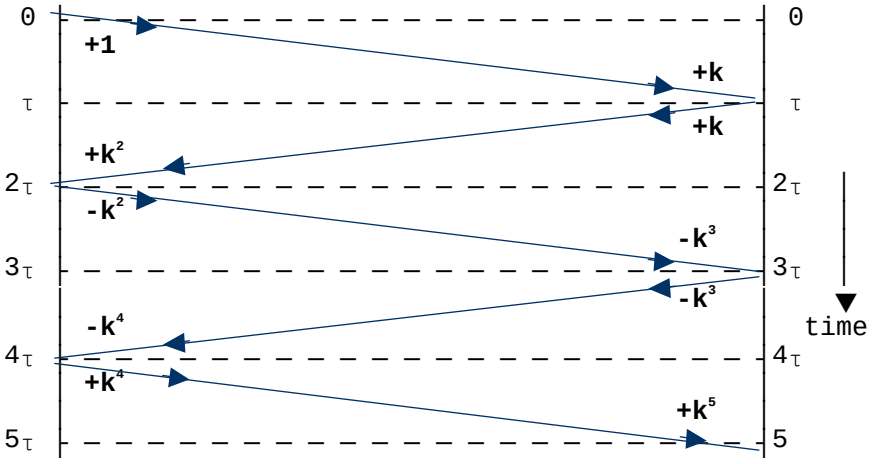

Figure 4.6 - Lattice diagram for an open-circuited line

The corresponding lattice diagram is shown in figure 4.6. At the receiving end of the line, the transmitted surge is twice the incident surge. [This can be obtained from either the transmission coefficient, or by adding the incident and reflected surges which make up the transmitted surge]. At any given instant, the voltage at this end is the summation of the surges arriving until that instant of time.

Thus the voltage at the open end after the $\mathbf{n}^{th}$ reflection is given by

$$V_r = 2\,(k - k^3 + k^5 - k^4 + ... k^{2n-1})$$

This is a geometric series which has the summation given by

$$V_r = 2k\,\frac{1-(-k^2)^n}{1-(-k^2)}$$

for the final value $t \to \infty$, $n \to \infty$

$$\therefore V_r = \frac{2k}{1+k^2}$$

$$\because (1-k)^2 > 0,\ 1+k^2 > 2k$$

$$\text{i.e.}\ \frac{2k}{1+k^2} < 1$$

It is thus seen that when attenuation is present, the receiving end voltage is less than the sending end voltage. The reason for this is that there is a voltage drop in the line due to the shunt capacitive currents flowing in the line even on open circuit. However, since **k is very close to** 1, the reduction is very very small. [For example, even for k = 0.90, the corresponding reduced value is $2x0.90/(1+0.90^2) = 0.9944$].

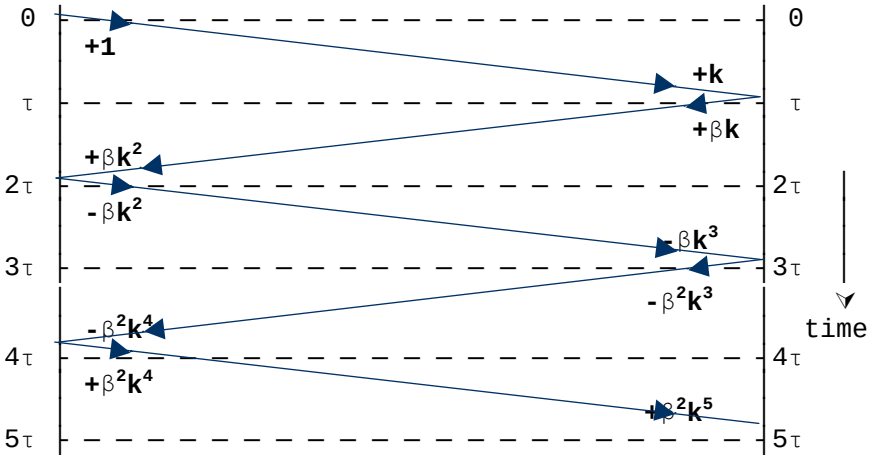

Figure 4.7 - Lattice diagram for a resistive termination

Let us now consider a line terminated through a resistance **R.** The corresponding reflection coefficient at the receiving end would be **$\beta = (R-Z_1)/(R+Z_1)$** and the reflection factor at the sending end would still be **-1.** Thus in addition to the attenuation occurring on the line, there is a non complete reflection occurring at the far end of the line. This would have a lattice diagram as shown in figure 4.7.

The final voltage attained at the resistive termination will now depend on both the attenuation and the reflection coefficient. From the lattice diagram it can be seen that this value can be calculated as follows.

$$V_r = k + \beta k - \beta k^3 - \beta^2 k^3 + \beta^2 k^5 + \beta^3 k^5 - .....$$

$$V_r = \frac{(1+\beta)k}{1+\beta k^2}$$

$$\because k<1,\ \beta k<1,\ (1-\beta k)(1-k)>0,$$

$$1+\beta k^2 - k - \beta k > 0$$

$$\text{i.e. } \frac{(1+\beta)\,k}{1+\beta\,k^2} < 1$$

Therefore, again, the receiving end voltage is less than the sending end voltage. However if there is no attenuation (k = 1), then the receiving end voltage tends to unity as shown in figure 4.8.

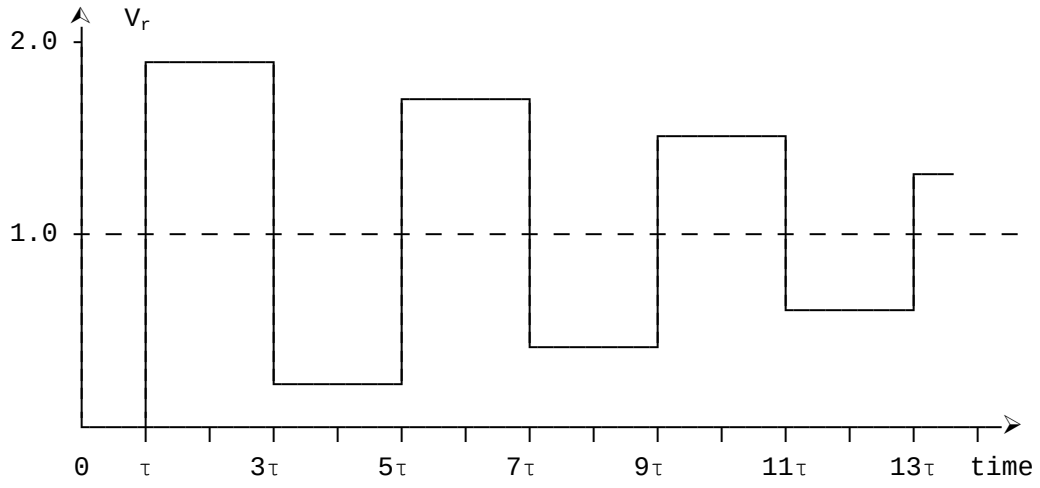

Figure 4.8 - Receiving end voltage with resistive termination

4.2.3 Reflections at 3 substation system

Consider 3 substations (1), (2) and (3) connected by lines Z_1, Z_2, Z_3 and Z_4, as shown in figure 4.9. Let α and α' be the transmission coefficients for a wave incident at the substation from the left hand side and the right hand side respectively, and let β and β' be the corresponding reflection factors.

In the Bewley lattice diagram, the junctions must be laid off at intervals equal to the time of transit of each section between junctions. (If all lines are overhead lines, then the velocity of propagation may be assumed to be the same and the junctions can be laid off proportional to the distance between them. Otherwise this is not possible).

The lattice diagram is shown together with the system diagram, and a unity magnitude surge is assumed to arrive from outside the on line 1.

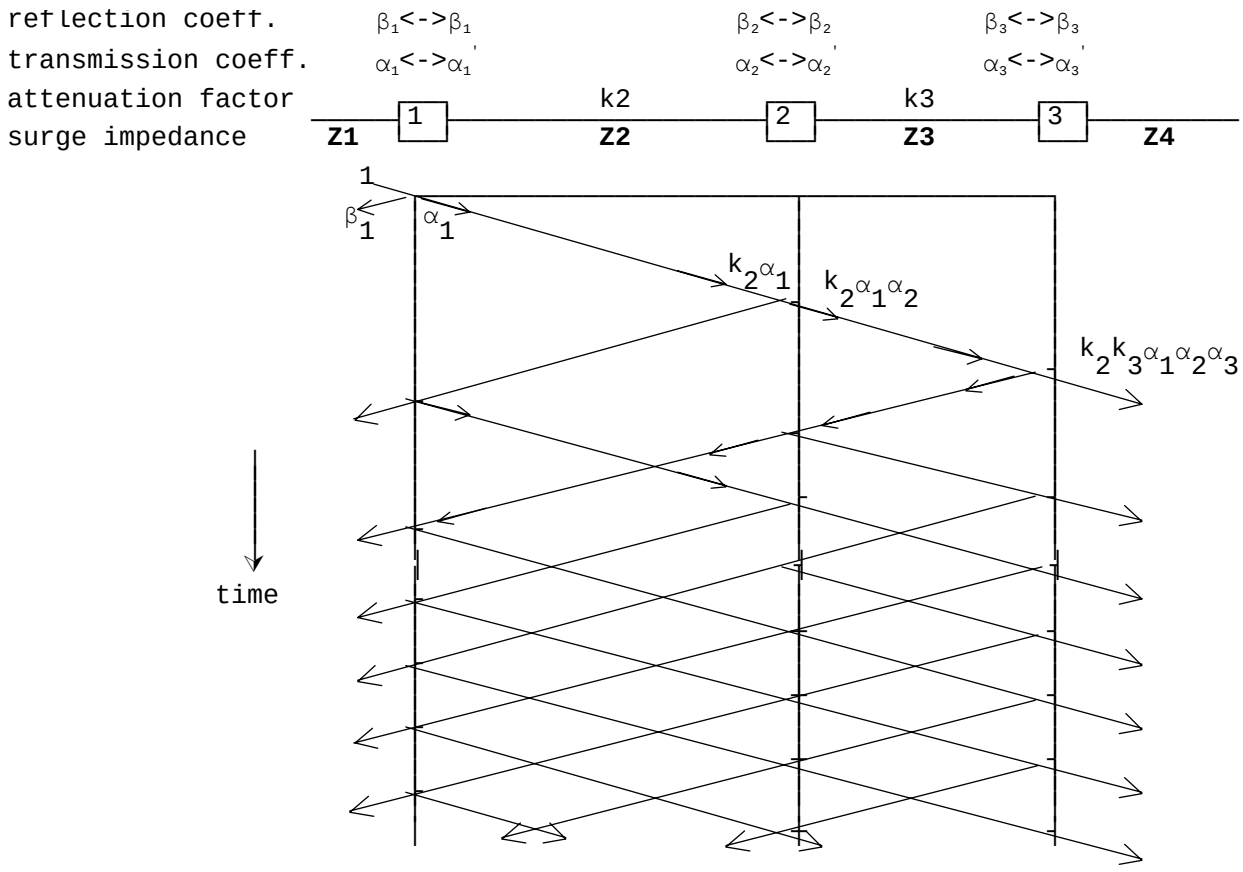

Figure 4.9 - Bewley Lattice Diagram

Example:

3 substations **A, B** and **C** are spaced 75 km apart as shown in figure 4.10. **B** and **C** are connected together by a cable (velocity of propagation 2 x 10^8 m/s), and the remaining connections are all overhead lines (velocity of propagation 3 x 10^8 m/s). The attenuation factors and the surge impedances of the lines are shown alongside the lines. The overhead lines beyond **A** and **C** on either side are extremely long and reflections need not be considered from their far ends. Determine using the Bewley lattice diagram the overvoltages at the 3 substations, at an instant **1_** ms after a voltage surge of magnitude unity and duration ¾ reaches the substation **A** from the outside.

The transmission and reflection coefficients can be calculated as follows.

At **A**,

$$\beta_1 = \frac{600 - 400}{600 + 400} = 0.2 \qquad \beta_{1'} = -0.2$$

$$\alpha_1 = \frac{2 \times 600}{1000} = 1.2 \qquad \alpha_{1'} = \frac{2x400}{1000} = 0.8$$

similarly, at **B**

$$\beta_2 = \frac{66\frac{2}{3} - 600}{66\frac{2}{3} + 600} = -0.8 \qquad \beta_{2'} = 0.8$$

$$\alpha_2 = \frac{2 \times 66\frac{2}{3}}{666\frac{2}{3}} = 0.2 \qquad \alpha_{2'} = \frac{2x600}{666\frac{2}{3}} = 1.8$$

similarly, at **C** it can be shown that

$\beta_3 = 0.8, \quad \beta_3' = -0.8, \quad \alpha_3 = 1.8,$ and $\alpha_3' = 0.2.$

The single transit times of the two lines connecting the substations are

$\tau_{AB} = 75 \times 10^3/3 \times 10^8 = ¼$ ms, $\quad \tau_{BC} = 75 \times 10^3/2 \times 10^8 =$ _ ms .

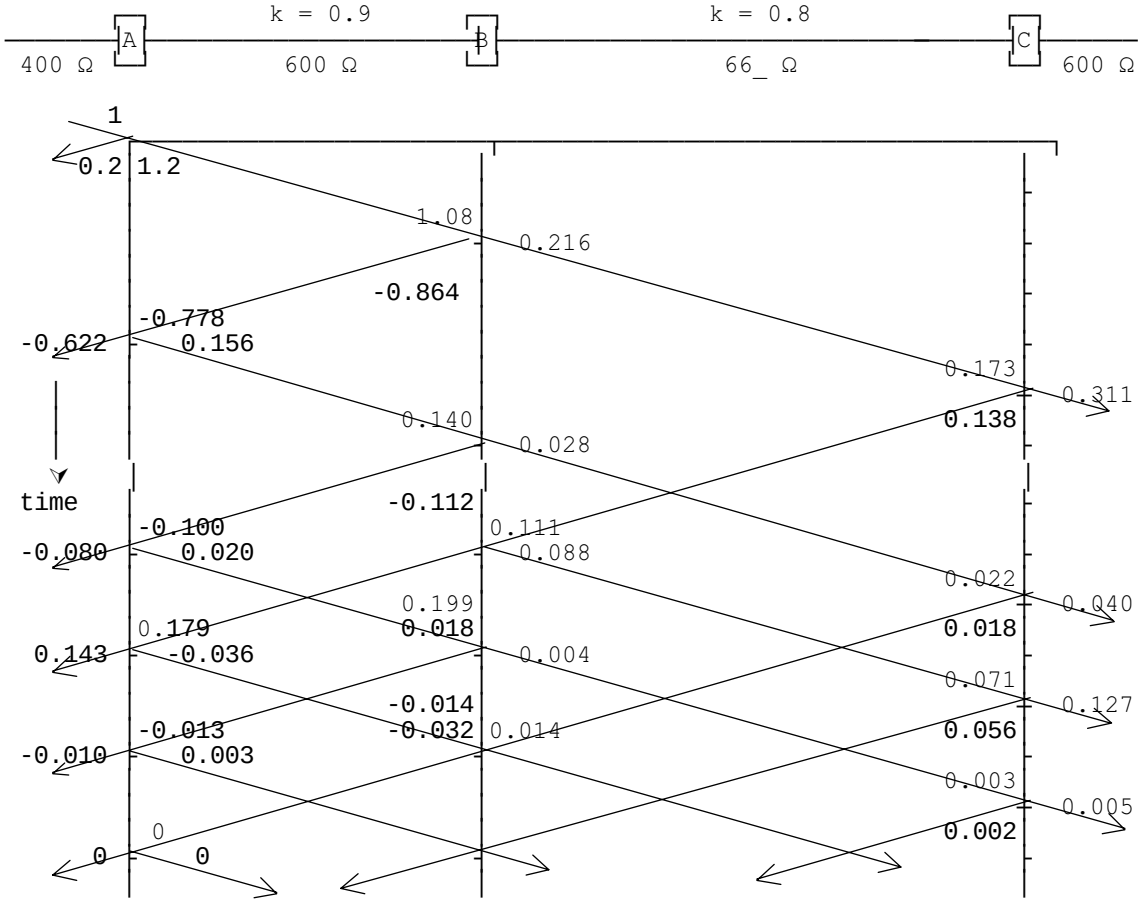

Figure 4.10 - Example of application of Bewley Lattice diagram

The lattice diagram must be set out, such that the intervals **AB** and **BC** are in the proportions to the times 1/4 ms and 3/8 ms respectively. These are shown in figure 4.10 .

Since the step voltage incident at substation **A** is of duration 3/4 ms, only reflections that have occurred after 3/4 ms prior to the present will be in existence.

at time **t = 1_** ms,

voltage at junction **A** = - 0.080 + 0.143 -0.010 = 0.053 pu
voltage at junction **B** = 0.199 + 0.004 + 0.032 + 0 = 0.235 pu

Since a surge arrives at junction **C** at the instant of interest, we can define values either just before or just after the time.

voltage at junction **C** at t^- = 0.040 + 0.127 = 0.167 pu
voltage at junction **C** at t^+ = 0.040 + 0.127 + 0.005 = 0.172 pu

4.4 Reflection and Transmission at a T-junction

When the intersection occurs between more than two lines, the analysis can be done as follows. Consider the connection shown in figure 4.11.

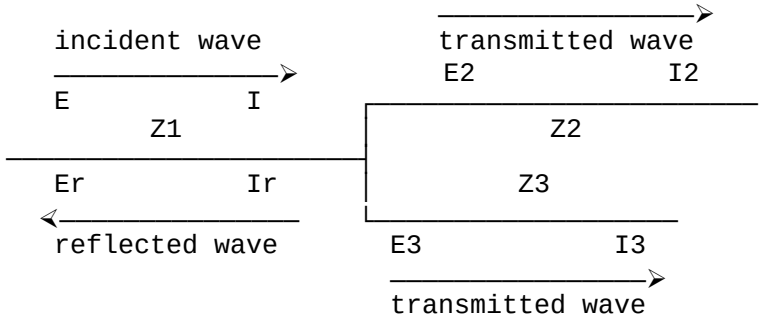

Figure 4.11 - Reflections and transmissions at T-junction

If a surge voltage of magnitude **E** is incident on the junction with two other lines (Z_2 and Z_3) from a line (Z_1), then the transmitted and reflected surges would be as shown. For these

$$E = Z_1 I,\ E_r = - Z_1 I_r,\ E_2 = Z_2 I_2 \text{ , and } E_3 = Z_3 I_3$$

Also, considering the fact that the total voltage and the current on either side of the junction must be the same,

$$E_2 = E_3 = E_T = E_r + E, \quad \text{and} \quad I_r + I = I_2 + I_3$$

These may be solved to give the following expressions for the transmitted and reflected surges.

$$\frac{2E}{Z_1} = E_T\left(\frac{1}{Z_1} + \frac{1}{Z_2} + \frac{1}{Z_3}\right)$$

$$\text{i.e. } E_T = \frac{\frac{2}{Z_1}}{\frac{1}{Z_1} + \frac{1}{Z_2} + \frac{1}{Z_3}} E\,, \quad \text{similarly } E_R = \frac{\frac{1}{Z_1} - \frac{1}{Z_2} - \frac{1}{Z_3}}{\frac{1}{Z_1} + \frac{1}{Z_2} + \frac{1}{Z_3}} E$$

The method can be extended to junctions with more than 3 lines. However, there is an easier method of analysis to obtain the same result.

For a surge, the voltage and the current are always related by the surge impedance, independent of the termination of the line at the far end. Thus for analysis purposes, the line behaves similar to a load of impedance $\mathbf{Z_0}$ connected between the start of the line and the earth. Thus when a single line ($\mathbf{Z_1}$) feeds two other lines (Z_2 and Z_3), the resultant reflections and transmissions could be obtained by considering both these lines as impedances connected from the junction to earth. That is, these two lines behave for surge purposes as if their surges impedances were connected in parallel.

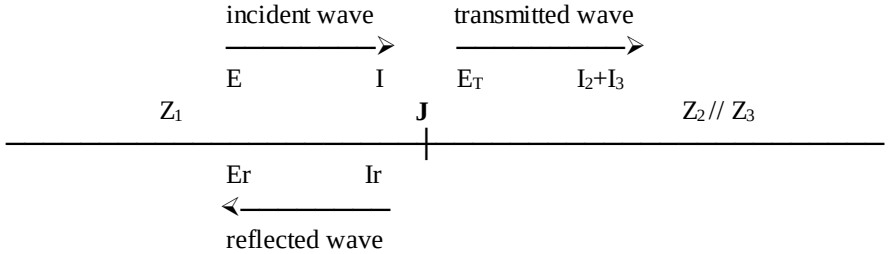

Figure 4.12 - Equivalent 2-branch connection

This gives the transmitted surge as

$$E_T = \frac{2(Z_2 // Z_3)}{Z_1 + (Z_2 // Z_3)} E$$

$$E_T = \frac{\frac{2 Z_2 Z_3}{Z_2 + Z_3}}{Z_1 + \frac{Z_2 Z_3}{Z_2 + Z_3}} E \quad = \frac{2 Z_2 Z_3}{Z_1 Z_2 + Z_1 Z_3 + Z_2 Z_3} E$$

which is basically the same expression as was obtained earlier. Extension of the latter method to a multiline junction is very much easier, as in this case only the parallel equivalent of a larger number of lines needs to be obtained. No new derivations are required.

Example:

An overhead line **A** with a surge impedance 450 Ω is connected to three other lines [overhead lines **B** and **C** with surge impedances of 600 Ω each, and a cable **D** with a surge impedance 60 Ω] at the junction **J**. A traveling wave of vertical front of magnitude 25 kV and very long tail travels on **A** towards the junction **J**. Calculate the magnitude of the voltage and current waves which are transmitted and reflected when the surge reaches the junction **J.** Attenuation in the lines can be neglected.

For an incident surge from **A**, lines **B, C** and **D** are effectively in parallel.

The parallel equivalent impedance is Z_T = 600 Ω//600 Ω//60 Ω = 50 Ω

$$E_T = 2 \times 50 \times 25 \ / (450 + 50) \ = \ 5 \text{ kV}$$

$$E_r = (50 - 450) \times 25 / (450 + 50) \ = - 20 \text{ kV}$$

$$I = 25 \times 10^3/450 = 55.56 \text{ A}, \ I_r = -(- 20 \times 10^3)/450 = 44.44 \text{ A},$$

$$I_B = 5 \times 10^3/600 = 8.33 \text{ A}, I_C = 5 \times 10^3/600 = 8.33 \text{ A}, \ I_D = 5 \times 10^3/60 = 83.33 \text{ A}$$

4.5 Bergeron's Method of Graphical Solution

The lattice diagram method of solution is not easily applied when the load impedance is a non-linear device. In such cases, the graphical method of Bergeron is suitable. This is also based on the partial differential equations

$$- \frac{\partial v}{\partial x} = l \frac{\partial i}{\partial t}, \quad - \frac{\partial i}{\partial x} = c \frac{\partial v}{\partial t}$$

which has the traveling wave solution

v = f(x-at) + F(x+at) where **a** is the wave velocity

The corresponding current can be obtained as follows.

$$-\frac{\partial i}{\partial x} = c\frac{\partial v}{\partial t} = c\,[\,-a\,f'(x-at) + a\,F'(x+at)]$$

$$\therefore\ i = a\,c\,[f\,(x-at) - F\,(x+at)],\quad \text{also}\ \ Z_0 = \sqrt{\frac{l}{c}} = \frac{1}{a\,c}$$

$$\text{i.e. } i\,Z_0 = f\,(x-at) - F\,(x+at)$$

$$\therefore\ v - i\,Z_0 = 2\,F\,(x+at),\qquad v + i\,Z_0 = 2\,f\,(x-at)$$

As was learnt earlier, **f(x-at) = constant** represents a **forward traveling wave**, and **F(x+at) = constant** represents a **backward traveling wave**.

From the expressions derived above, it can be seen that **$v + Z_0\,i$ = constant** represents a **forward wave** and **$v - Z_0\,i$ = constant** represents a **backward wave**. In either case the value of the constant is determined from the history of the wave up to that time.

The Bergeron's method is applied on a **voltage-current** diagram, and is illustrated by means of an example.

Example

A transmission line, surge impedance Z_0 is fed from a constant voltage supply **E** at one end and by a non-linear resistor whose V-I characteristic is known at the other end. Determine the waveform of the voltage at the load end when the initially open line is closed at end **A** at time zero.

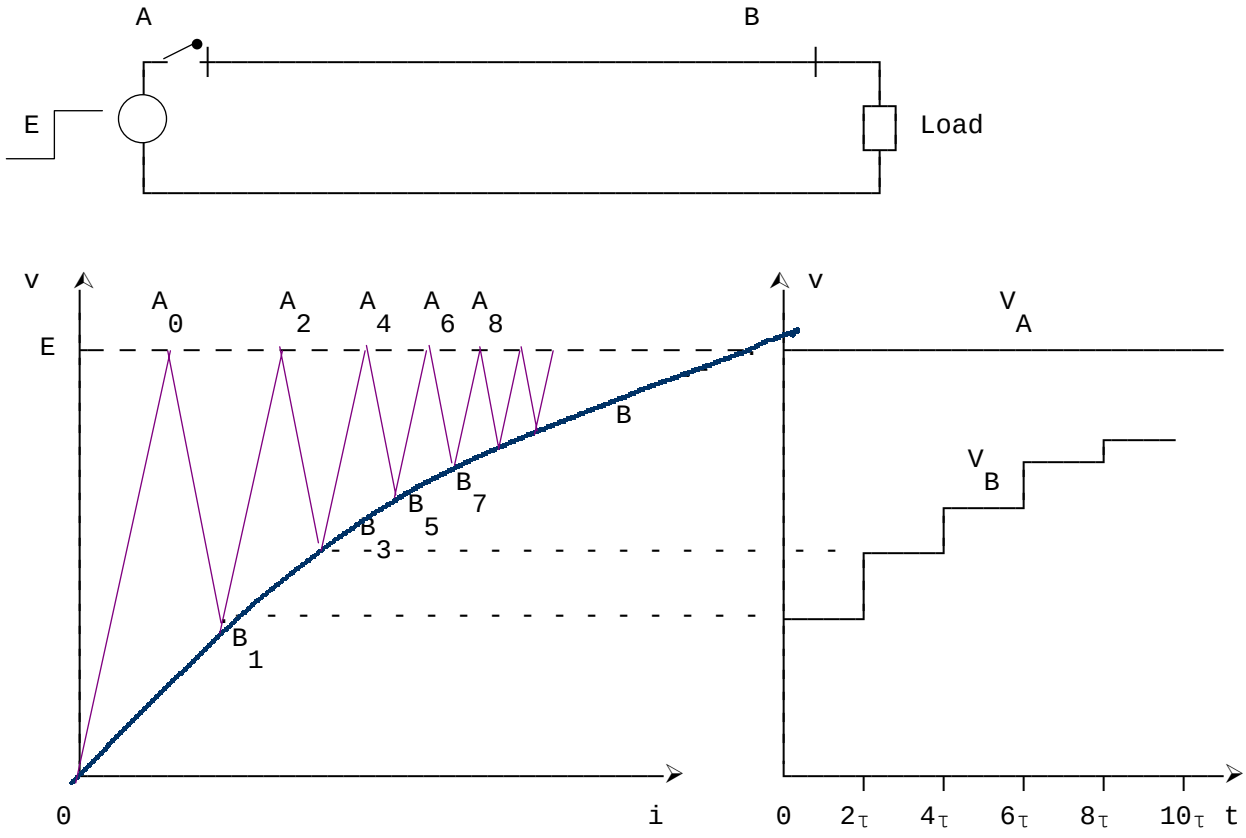

Figure 5.13 - Bergeron's method of solution

The method of constructing the diagram is as follows. The VI characteristic of the source (constant at E), and that of the load (non-linear) are drawn on the V-I diagram. If t = 0 is defined as the instant at which the surge initially reaches the load, then this surge leaves **A** at time t = -τ. This original surge must satisfy two conditions. Firstly, since it is leaving **A**, it must be a point on the source characteristic $\mathbf{A_{-1}}$. Secondly, this is a forward surge. Thus it must be of the form $\mathbf{v + Z_0 i = constant}$, or a line with slope $\mathbf{-Z_0}$.

Thus this surge is a line with slope $\mathbf{-Z_0}$ leaving $\mathbf{A_{-1}}$. This surge arrives at **B** at time **0**.
At this instant, it must also be a point on the load characteristic as well as on the surge line. Thus it must be the point $\mathbf{B_0}$. At **B** the surge is reflected back. This reflected surge must start from $\mathbf{B_0}$, and also have a slope $\mathbf{+Z_0}$ corresponding to $\mathbf{v - Z_0 i = constant}$. The surge reaches $\mathbf{A_1}$ at time **τ**. The process continues. From the diagram, we can determine the voltage at **A** at time **-τ, τ, 3τ, 5τ** etc, and the voltage at **B** at time **0, 2τ, 4τ, 6τ** etc. The voltage waveforms at both **A** and **B** are easily obtained by projecting the values as shown on the diagram on to the right hand side. Similarly, the current waveforms can be obtained by projecting the values below.

4.6 Representation of Lumped Elements in travelling wave techniques

In the Lattice diagram technique, basically only transmission lines can be represented. Since the surge impedance of transmission lines are purely resistive, resistances can also be represented with surge impedance equal to the resistance value, and no travel time.

Inductances and capacitances could be represented, by considering them as very short lines or stub lines. This is done by assuming that an inductance has a distributed capacitance of negligible value to earth, and that shunt capacitances have a negligible series inductance. These assumptions will make the lumped elements stub lines with negligible transmission times. It is usual to select the transmission times corresponding to the minimum time increment Δt.

For the lumped inductance connected in series

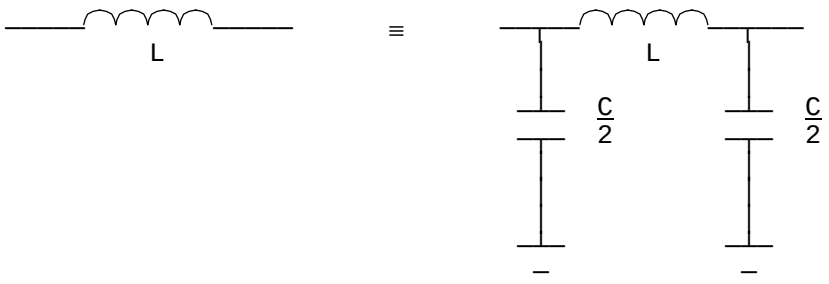

Figure 4.14 - Representation of Inductance

If the travel time of the line is selected corresponding to $\tau = \Delta t$

$$\tau = \sqrt{L\,C} \quad \text{so that} \quad C = \frac{\tau^2}{L} = \frac{(\Delta t)^2}{L}$$

$$Z_0 = \sqrt{\frac{L}{C}} = \frac{L}{\tau} = \frac{L}{\Delta t}$$

Thus a lumped inductance may be represented by a stub line of transit time **Δt** and surge impedance **L/Δt**.

For the lumped capacitance connected in shunt

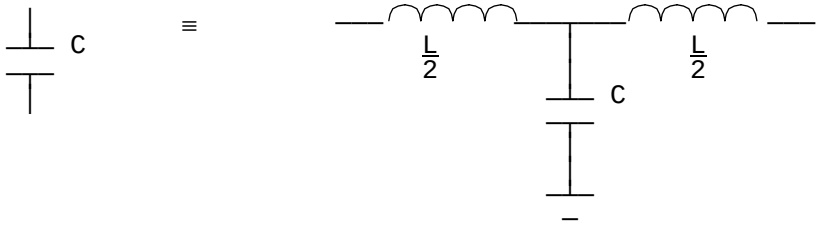

Figure 4.15 - Representation of Capacitance

$$\tau = \sqrt{L\,C} \quad \text{so that} \quad L = \frac{\tau^2}{C} = \frac{(\Delta t)^2}{C}$$

$$Z_0 = \sqrt{\frac{L}{C}} = \frac{\tau}{C} = \frac{\Delta t}{C}$$

Thus a lumped capacitance may be represented by a stub line of transit time **Δt** and surge impedance **Δt/C**.

Another method of analyzing in the presence of inductances and capacitances is to use the numerical form as indicated below.

$$v = L\frac{d\,i}{d\,t} \quad \text{for an inductance}$$

$$\frac{v_n + v_{n-1}}{2} = L\,\frac{i_n - i_{n-1}}{\Delta t}$$

$$\text{i.e.} \quad v_n = \frac{2L}{\Delta t}\,i_n - \left(v_{n-1} + \frac{2L}{\Delta t}\,i_{n-1}\right)$$

$$\text{also} \quad i_n = \frac{\Delta t}{2L}\,v_n + I_{eq,n-1}$$

$$\text{where} \quad I_{eq} = i + \frac{\Delta t}{2L}\,v$$

$$i = C\frac{d\,v}{d\,t} \quad \text{for an capacitance}$$

$$\frac{i_n + i_{n-1}}{2} = C\,\frac{v_n - v_{n-1}}{\Delta t}$$

$$\text{i.e.} \quad i_n = \frac{2C}{\Delta t}\,v_n - \left(i_{n-1} + \frac{2C}{\Delta t}\,v_{n-1}\right)$$

$$\text{i.e.} \quad i_n = \frac{2C}{\Delta t}\,v_n + I_{eq,n-1}$$

$$\text{where} \quad I_{eq} = -i - \frac{2C}{\Delta t}$$

4.7 Branch Time Table for digital computer implementation

The Bewley Lattice diagram cannot be implemented directly on the digital computer. When implemented on the computer, a physical diagram is not required to keep track of the travelling waves. The branch time table serves the purpose of the diagram, and keeps track of the voltage of each node, and the reflected and transmitted waves.

4.8 Transform Methods of solving Transients

Simple transient problems may be solved using the Laplace Transform. However, since its inverse transform is not evaluated for complicated transforms, the Fourier transform is preferred. Further, for digital computer application, what is used is the numerical form of the transform, which is obtained by approximating the integrals to summations.

$$F(\omega)=\int_0^{\infty} f(t)e^{-j\omega t}\,dt = \sum_0^{T} f(t)e^{-j\omega t}\Delta t$$

This is used with the transfer function **H(ω)** of a network to give the transform of the response.

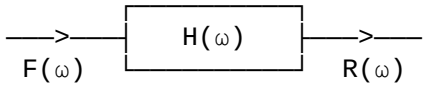

Figure 4.16 - Block diagram of system

$$R(\omega) = H(\omega) \,.\, F(\omega)$$

The response in the time domain is then obtained by inverse transformation.

$$r(t)=\frac{2}{\pi}\int_0^{\infty} R(\omega).e^{j\omega t}.d\,\omega$$

$$r(t)=\frac{2}{\pi}\sum_0^{\Omega} R(\omega).e^{j\omega t}.\Delta\omega$$

With the approximations introduced, the period of observation T and the maximum frequency Ω are limited to finite values.

The transmission line is usually represented by the frequency dependant two-port admittance parameters, for the determination of the transfer function.

$$\begin{bmatrix} I_S \\ I_R \end{bmatrix} = \begin{bmatrix} A & -B \\ -B & A \end{bmatrix} \begin{bmatrix} V_S \\ V_S \end{bmatrix}$$

where

$A = Y_0 \coth \gamma l$

$B = Y_0 \operatorname{cosech} \gamma l$

Y_0 = surge impedance matrix

γ = propagation matrix

5

High Voltage Cables

5.0 High Voltage Cables

High Voltage Cables are used when underground transmission is required. These cables are laid in ducts or may be buried in the ground. Unlike in overhead lines, air does not form part of the insulation, and the conductor must be completely insulated. Thus cables are much more costly than overhead lines. Also, unlike for overhead lines where tappings can easily given, cables must be connected through cable boxes which provide the necessary insulation for the joint.

Cables have a much lower inductance than overhead lines due to the lower spacing between conductor and earth, but have a correspondingly higher capacitance, and hence a much higher charging current. High voltage cables are generally single cored, and hence have their separate insulation and mechanical protection by sheaths. In the older paper insulated cables, the sheath was of extruded lead. Figure 5.1 shows three such cables, as usually laid out.

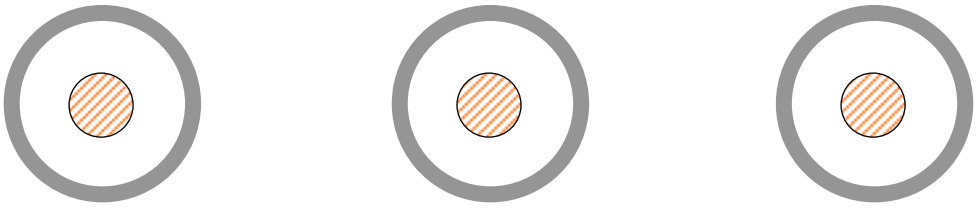

Figure 5.1 - Layout of three, single-core cables

The presence of the sheath introduces certain difficulties as currents are induced in the sheath as well. This is due to fact that the sheaths of the conductors cross the magnetic fields set up by the conductor currents. At all points along the cable, the magnetic field is not the same, Hence different voltages are induced at different points on the sheath. This causes eddy currents to flow in the sheaths. These eddy currents depend mainly on (a) the frequency of operation, (b) the distance between cables, (c) the mean radius of the sheath, and (d) the resistivity of the sheath material.

5.1 Power loss in the Cable

Power loss in the cable can occur due to a variety of reasons (Figure 5.2). They may be caused by the conductor current passing through the resistance of the conductor - **conductor loss** (also sometimes called the copper loss on account of the fact that conductors were mainly made out of copper), **dielectric losses** caused by the voltage across the insulation, **sheath losses** caused by the induced currents in the sheath, and **intersheath losses** caused by circulating currents in loops formed between sheaths of different phases. The dielectric loss is voltage dependant, while the rest is current dependant.

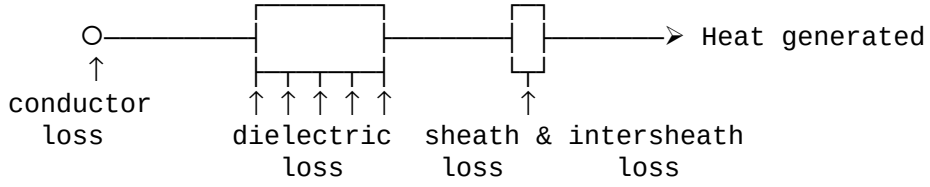

Figure 5.2 - Heat Transfer in a cable due to losses

5.1.1 Dielectric loss

For a perfect dielectric, the power factor is zero. Since the cable is not a perfect dielectric, the power factor is not zero. The current leads the voltage by an angle of less than 90^o, and hence there is a power loss (Figure 5.3).

If C is the capacitance of the cable, and E is the applied voltage, then

charging current $i = E\ C\ \omega$

power loss $P = E\ I \cos \varphi = E\ I \sin \delta$

$= E\ (i/\cos \delta) \sin \delta = E^2\ C\ \omega \tan \delta$

The power loss is proportional to E^2 and $\tan \delta$.

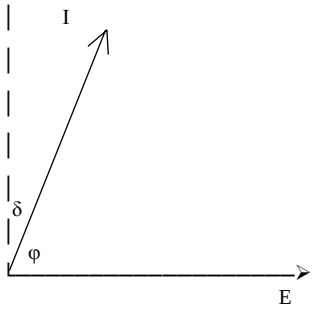

Figure 5.3 - Loss angle

5.1.2 Conductor loss

The conductor loss $\mathbf{P_c}$ is given by

$$P_c = I^2 R_c \quad \text{watt}$$

where $\mathbf{R_c}$ is the resistance of the conductor and **I** is the current in the cable.

5.1.3 Sheath loss

The losses occurring in the sheath of a cable is usually obtained by the empirical formula of Arnold. Arnold's formula for the sheath loss $\mathbf{P_{sh}}$ is given by

$$P_{sh} = 7.7 \times 10^{-3} \frac{I^2}{R_{sh}} \left(\frac{r_m}{d} \right)^2 \quad watt$$

where r_m = mean radius of sheath
d = distance between cables (centre to centre)
R_{sh} = resistance of full length of cable
I = current in cable

The sheath loss is usually about 2 to 5 % of the conductor loss.

5.1.4 Intersheath Loss

Intersheath losses are caused by the induced emf between the sheaths causing a circulating current.
This loss is thus present only when the sheaths of adjacent cables are connected together. The sheaths need to be connected together in practice, as otherwise sparking could occur causing damage to the sheaths. The intersheath loss $\mathbf{P_{ish}}$ can be calculated as follows.

The mutual inductance $\mathbf{M_{sh}}$ between a core of one cable and the sheath of an adjacent cable is given by

$$M_{sh} = \frac{\mu}{2\pi} \ln \left(\frac{d}{r} \right)$$

The voltage induced $\mathbf{E_{ish}}$ is given by

$$E_{ish} = I \,.\, \omega \,.\, M_{sh}$$

and the induced current $\mathbf{I_{ish}}$ is given by

$$I_{ish} = \frac{E_{ish}}{\left[R_{sh}^{\,2} + \omega^2 M_{sh}^{\,2}\right]^{\frac{1}{2}}} = \frac{i\,\omega\, M_{sh}}{\left[R_{sh}^{\,2} + \omega^2 M_{sh}^{\,2}\right]^{\frac{1}{2}}}$$

Therefore the intersheath loss $\mathbf{P_{ish}}$ is given by

$$P_{ish} = I_{ish}^{\,2} R_{sh} = \frac{I^2 \omega^2 M_{sh}^{\,2}}{R_{sh}^{\,2} + \omega^2 M_{sh}} \cdot R_{sh}$$

Generally, the sheath resistance $\mathbf{R_{sh}} >> \boldsymbol{\omega}\, \mathbf{M_{sh}}$ so that

$$P_{ish} = \frac{I^2 \omega^2 M_{sh}^{\,2}}{R_{sh}}$$

The intersheath loss is larger than the sheath loss and may range from 10% to 50% of the copper loss. Thus the total power loss (exclusive of the dielectric loss) is given as

$$\textbf{Total Power loss} = \mathbf{P_c + P_{sh} + P_{ish}}$$

$$P_{loss} = I^2 R + I^2 \frac{7.7 \times 10^{-3}}{R_{sh}} \left(\frac{r_m}{d}\right)^2 + \frac{I^2 \omega^2 M_{sh}^{\,2}}{R_{sh}}$$

Since the whole expression is dependant on $\mathbf{I^2}$, we may express the loss in terms of an effective resistance $\mathbf{R_{eff}}$. This gives the total power loss in terms of the effective resistance as

$$\mathbf{P_{total} = I^2\, R_{eff}}$$

$$R_{eff} = R_c + \frac{7.7 \times 10^{-3}}{R_{sh}} \left(\frac{r_m}{d}\right)^2 + \frac{\omega^2 M_{sh}^{\,2}}{R_{sh}}$$

Since the sheath loss is usually very small, the effective conductor resistance can be written as

$$R_{eff} = R_c + \frac{\omega^2 M_{sh}^{\,2}}{R_{sh}}$$

5.1.5 Cross-bonding of Cables

When three single phase cables are used in power transmission, currents are induced in the sheaths and lead to sheath circulating currents and power loss. These may be substantially reduced, and the current rating of the cable increased by cross bonding of the cables (Figure 5.4). Cross bonding of cables are done except for very short lengths of cable.

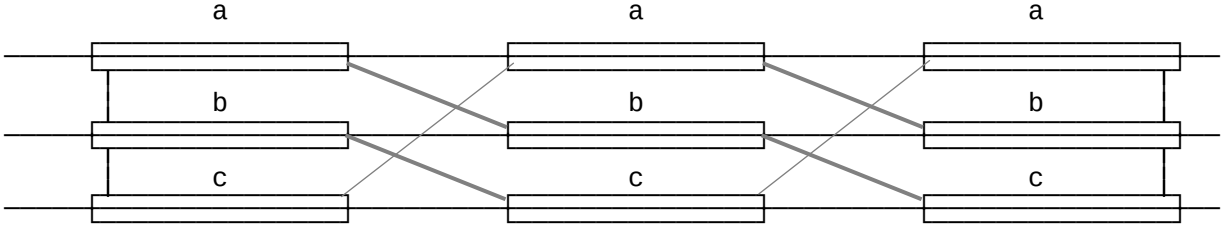

Figure 5.4 - Cross bonding of sheaths

The continuity of each cable sheath is broken at regular intervals; the cables between two adjacent discontinuities being a minor section. 3 minor sections make up a major section, where the sheaths are solidly bonded together and to earth. A residual sheath voltage exists, and the desired balance, giving negligible sheath voltage between the solid grounded positions is achieved by transposing the cables at each cross-bonded section. To prevent excessive voltage build up at the cross bonded points, especially during faults, these points are earthed through non-linear resistors which limit voltage build up. The cable is also transposed. (Figure 5.5)

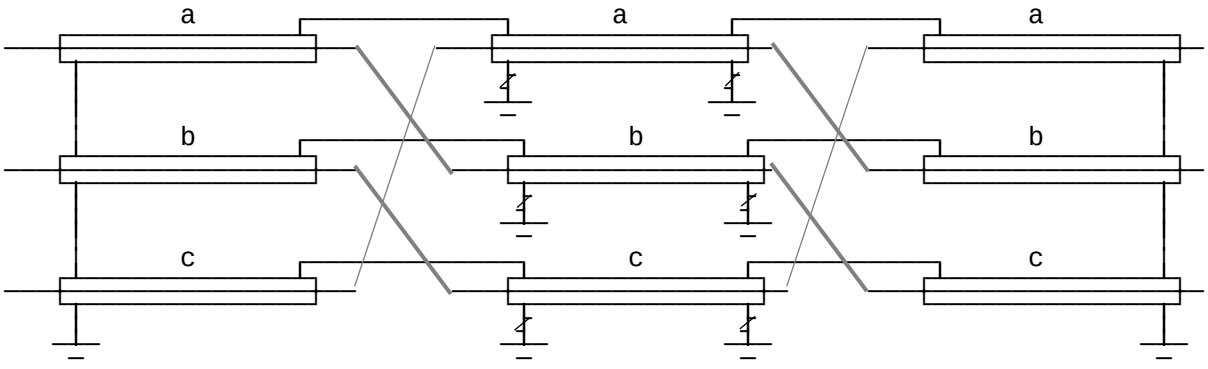

Figure 5.5 - Non-linear resistor earthing

5.2 Impregnated Paper Insulation

The insulation consists mainly of paper tape impregnated with compound. The paper must be free from ligneous fibres and from metallic or other conducting spots. The compound with which the paper is insulated should be of such a consistency that it is plastic at ordinary temperatures, and has no tendency to drain away from the cable.

The impregnating compound varies from manufacturer to manufacturer,but they all are based o paraffinic or naphthenic mineral oil, with resin frequently added to lower the viscosity and to improve its impregnating qualities. The paper is made from Manila fibre or wood pulp.

Impregnated paper can withstand an electric stress if about 5 to 10 times that which could be withstood by dry paper insulation. The dielectric strength of impregnated paper is about 200 to 300 kV/cm. Initially, they may be able to withstand about 400 to 600 kV/cm. The cause of breakdown is usually the non-homogeneity of the dielectric. When a test voltage is applied, the weakest part of the dielectric breakdown and deterioration starts getting more and more. This is accentuated by the fact that the cable is not carrying the same current all the time. The deterioration results in the formation of voids and gasses. When the voltage is raised, ionisation or glow discharge can occur in the voids and ionic bombardment of thee surface. Some of the oil suffers condensation and hydrogen and other gases are evolved. Thus the long term breakdown strength and the instantaneous break down strengths differ. This value may decrease with time due to deterioration to about 160 to 200 kV/cm. In the case of a badly impregnated dielectric, the breakdown stress will continue to decrease and ultimately leads to breakdown. With the use of a safety factor, not more than about 40 kV/cm is allowed in service (Figure 5.6).

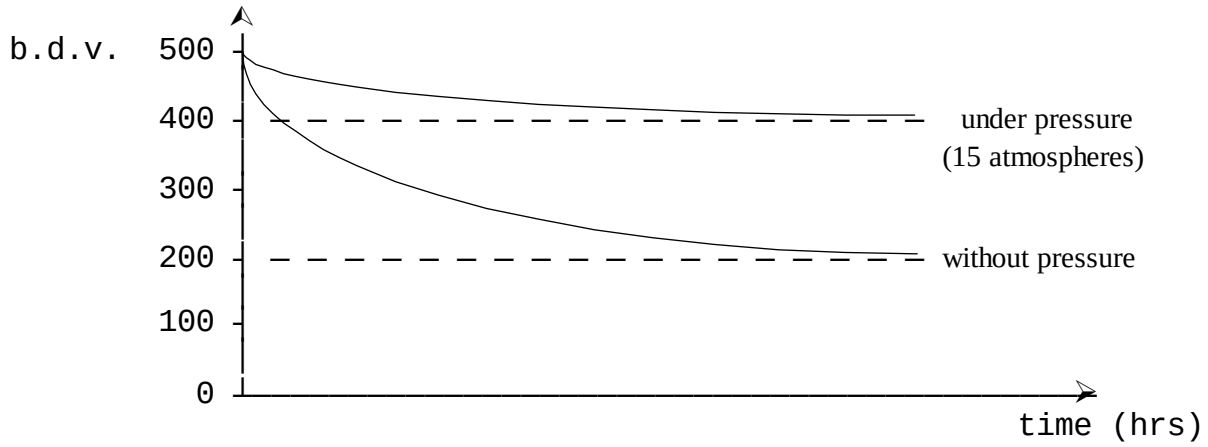

Figure 5.6 - Breakdown voltage characteristic of paper insulation

5.2.1 Properties required of cable insulation

Dielectrics used for cable insulation must have the following properties.

1. High Insulation resistance
2. High dielectric strength
3. Good mechanical strength
4. Immune to attack by acids and alkali in the range 0 - 100^{o} C
5. Should not be too costly
6. Should not be hygroscopic (tending to absorb water), or if hygroscopic should be enclosed in a water tight covering.

5.2.2 Principle underlying the design of high voltage cable insulation

By means of dielectric tests on cables, it has been observed that the long term breakdown stress is increased if the cable is subjected to pressure. This is due to the fact that the pressure discourages the formation of voids. Even for a badly impregnated cable, the application of pressure improves the power factor (or loss tangent) considerably. If the cable is subjected to a pressure of about 15 atmospheres, the long term dielectric strength improves to about 400 kV/cm and a working stress of about 150 kV/cm may be used (Figure 5.7).

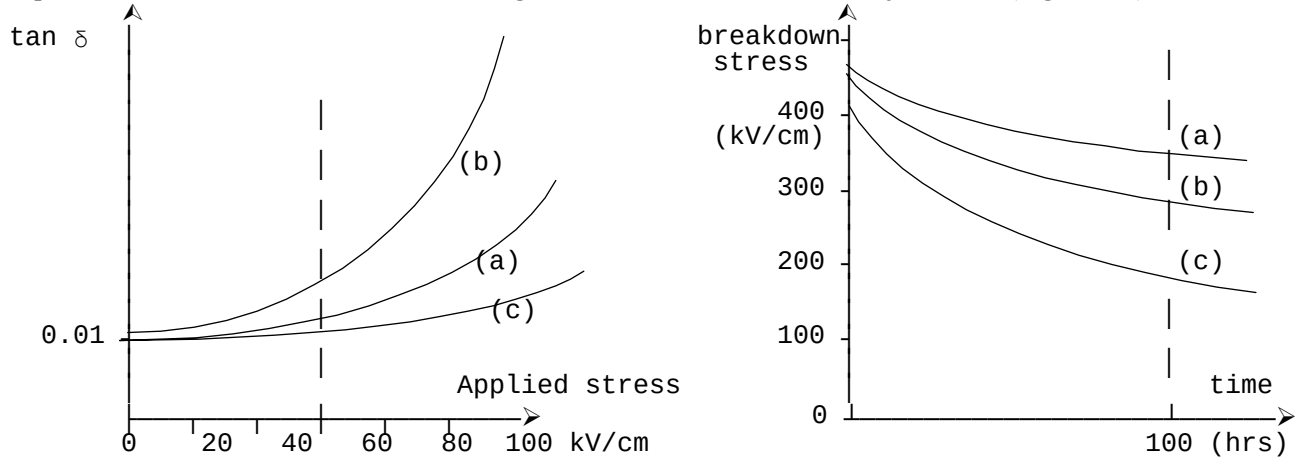

(a) impregnated (1 atmos)
(b) badly impregnated (1 atmos)
(c) badly impregnated (15 atmos)

(a) 15 atmospheres
(b) 8 atmospheres
(c) 1 atmosphere

Figure 5.7 - Variations with pressure

Comparison of the curves for (a) well impregnated cable at atmospheric pressure, (b) badly impregnated cable at atmospheric pressure, and (c) badly impregnated cable at a pressure of 15 atmospheres for about 47 hours, shows the advantages of the pressure on the reduction of power factor. Further the curves show how the long term breakdown stress is improved by pressure.

In modern high voltage cables, with the use of better materials, the power factor has been reduced from about (0.007 to 0.01) to about (0.002 to 0.003).

For high voltage cables, impregnated paper insulation is very commonly used. The paper is porous and contains in itself the impregnating compound. There are no voids present as the oil is present between the layers of the paper which forms the insulation.

5.2.3 Paper insulated power cables

The conductor of the cable is stranded, and this is lapped round with the paper tape. It is first heated to about 100^{oC} taking care not to burn it. A vacuum is then applied for 20 to 50 hours to get rid of any trapped air inside the cable, and while still under vacuum, impregnating compound is poured into the tank and thereafter a pressure of 50 p.s.i. (about 0.35 MN/m^2) is applied. Impregnating of the paper prevents void formation in the dielectric, as voids can easily lead to the breakdown of the dielectric. As paper is hygroscopic, a seamless lead sheath is extruded over the insulation so that no moisture will get in.

For high voltages, pressurised cables are used where the impregnated paper insulation is kept under pressure. A pressure of about 15 atmospheres is applied so that any potential voids would be instantaneously filled. The pressure may be applied by having either oil or gas under pressure. When the cable is pressurised, longitudinal reinforcement to prevent bulging and reinforcement to prevent hoop stress are used. With pressurised cables, the long term breakdown strength does not differ much from the short term strength, and as such using a safety factor, a working stress of about 100 to 120 kV/cm may be used.

5.2.4 Insulation Resistance

For a single core cable (figure 5.8), the insulation resistance between the conductor and the outer sheath is given by the following.

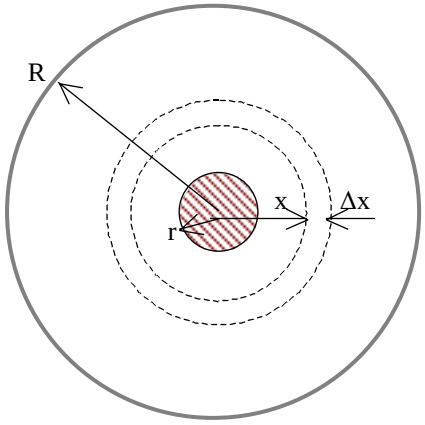

Figure 5.8 - Cable cross-section

$$\Delta Res = \frac{\rho \,.\, \Delta x}{2\pi x l}$$

$$\text{where } l = \text{length of cable (m)}$$

$$\therefore \text{Res} = \int \Delta \text{ Res} = \frac{\rho}{2\pi l}\int_r^R \frac{dx}{x} = \frac{\rho}{2\pi l}\ln(\frac{R}{r})$$

$$\text{i.e. Res} = \frac{3.665}{l'}\rho \log_{10}(\frac{R}{r}) \text{ x } 10^{-10} \text{ M}\Omega$$

$$\text{where } l' = \text{length of cable (km)}$$

5.2.5 Capacitance in a single-core cable

Consider a single core cable (figure 5.9) with the following data.

r = radius of core (m)
R = radius of earthed sheath (m)
q = charge/unit length of cable (C/m)
D = electric flux density = charge density (C/m^2)
ε_0 = permittivity of free space
= $1/(4\pi \times 9 \times 10^9)$ F/m

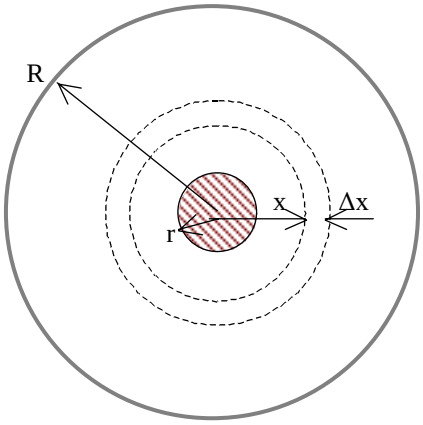

Figure 5.9 - Cable cross-section

Consider an elemental cylinder of radius **x** and thickness **dx**, and of length **unity** along the cable.

$$q = D \times 2\pi \times x1, \qquad \therefore\ D = \frac{q}{2\pi x}$$

$$\therefore \quad \text{electric stress } \xi = \frac{D}{\varepsilon} = \frac{q}{2\pi \varepsilon_0 \varepsilon_r x} = \frac{18 \times 10^9 \times q}{\varepsilon_r x}$$

$$\text{also,} \quad \xi = \frac{dv}{dx}, \quad \text{so that } V = \int_r^R \xi \, dx = \int_r^R \frac{18 \times 10^9 \times q}{\varepsilon_r x} dx$$

$$\text{i.e. } V = \frac{18 \times 10^9}{\varepsilon_r} q \log_e(R/r) = \frac{q}{2\pi\varepsilon} \log_e(R/r)$$

$$\therefore \text{ capacitnace} = \frac{q}{V} = \frac{\varepsilon_r}{18 \times 10^9 \log_e(R/r)} \text{ F/m}$$

$$\therefore \ C = \frac{0.0383\,\varepsilon_r}{\log_{10}(R/r)}\ \mu\text{F/mile} = \frac{0.024\,\varepsilon_r}{\log_{10}(R/r)}\ \mu\text{F/km}$$

(For impregnated paper insulation, $\varepsilon_r = 3.5$)

5.2.6 Three-core Cables

When three phase power is being transmitted, either three single-core cables or a single three-core cable may be used. In the case of the single core cables, the stress is radial, and its magnitude alternates with time.

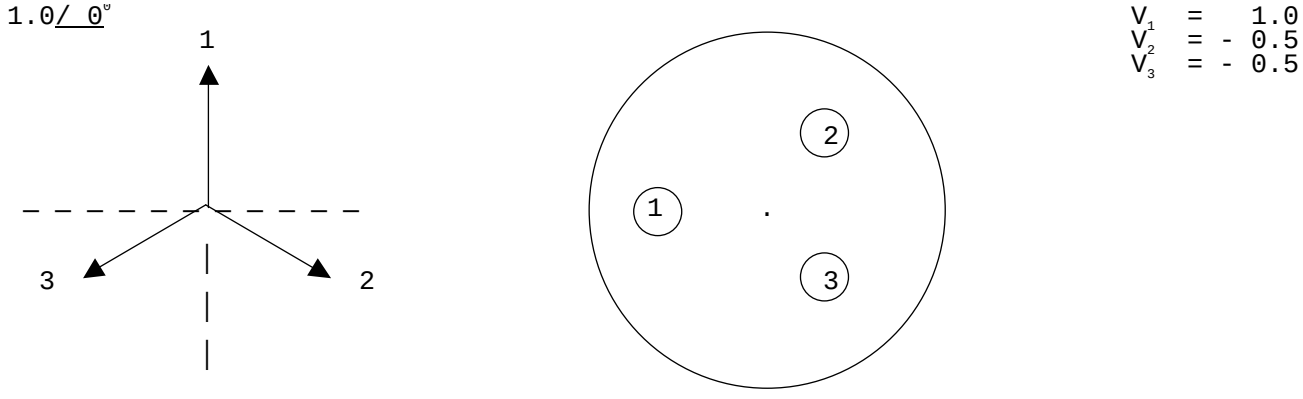

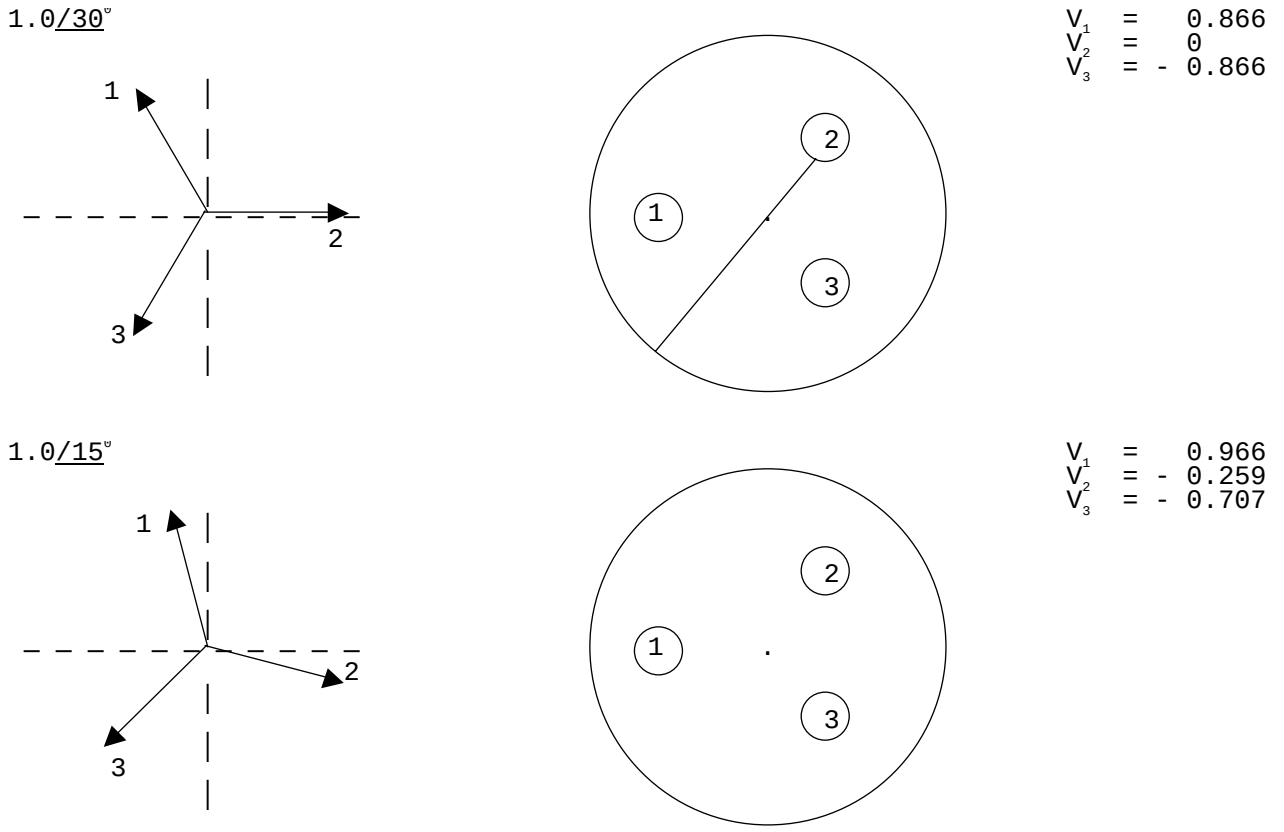

Figure 5.10 - Equipotential lines in three-core cables

In the case of the 3-core cable, since the centres of the cores lie in a circle, the electrostatic field is a somewhat rotating field and not a pulsating one. Typical variations of the equipotential surfaces, for a few points of the cycle are illustrated in figure 5.10.

From these it will be seen that the field lines, which are perpendicular to the equipotential lines, are not radial to the individual cores. Consequently, the electric stress is not radial, and tangential components of stress exist. If paper insulation is used around each cores, then tangential stresses will be applied along the surface of the paper rather than just across it. The electrical properties of paper varies in different directions. The effective dielectric stress of paper insulation is much greater across the layers than along it. Thus the presence of tangential stress in paper insulation leads to greater risk of breakdown.

5.2.7 Three-core belted type Cables

In the case of a 3-core cable, the 3-cores are individually insulated with paper insulation. The filler spaces between the core insulation is also filled up with insulation, but depriving these of voids is much more difficult. Belt insulation is used on top of all three core insulations, and the lead sheath is extruded over this. Over the lead sheath, there is generally bitumen to prevent damage.

In buried cables, additional protection is necessary to prevent damage. There are two types of armouring used for these cables.

(i) Steel tape armouring - the steel tape is usually wound in two layers with opposite directions of lay

(ii) Steel wire armouring - the steel wires are laid in one or two layers.

Capacitance of 3-core belted type

The capacitance between the conductor to neutral of 3-core belted cables (Figure 5.11) cannot be obtained by a simple derivation as for the single core cable. Simon's expression can be used to obtain this value.

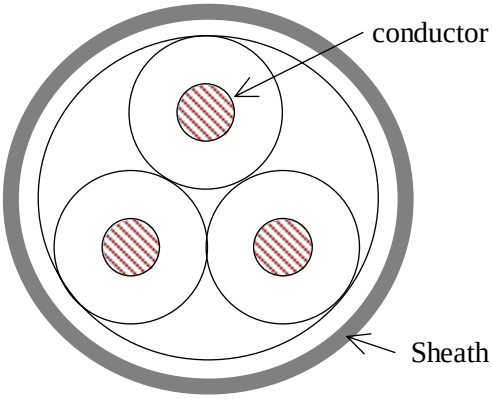

Figure 5.11 - 3 core belted cable

The capacitance per unit length to neutral is given by

If t = thickness of belt insulation
T = thickness of conductor insulation
d = diameter of conductor
ε_r = dielectric constant

$$C_0 = \frac{0.03\,\varepsilon_r}{\log_{10}\left[\left(0.52\left(\frac{t}{T}\right)^2 - 1.7\left(\frac{t}{T}\right) + 3.84\right)\left(\frac{T+t}{d}\right) + 1\right]}\ \mu\text{F/km}$$

Measurement of capacitance of 3-core cables

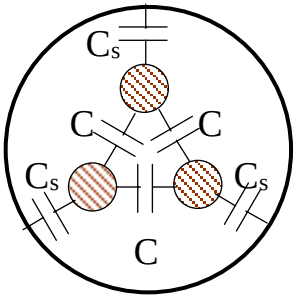

Figure 5.12 - Cable Capacitances

In three-core cables, capacitance does not have a single value, but can be lumped as shown in figure 5.12.

Capacitance between each core and sheath = C_s

Capacitance between cores = C

These can be separated from measurements as described in the following section.

(a) Strap the 3 cores together and measure the capacitance between this bundle and the sheath as shown in figure 5.13.

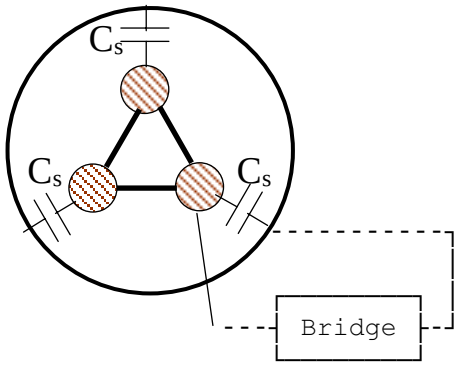

Figure 5.13 - Capacitance measurement

Measured value = $C_{m1} = 3\ C_s$

This gives the capacitance to the sheath as $C_s = C_{m1}/3$

(b) Connect 2 of the cores to the sheath and measure between the remaining core and the sheath (Figure 5.14).

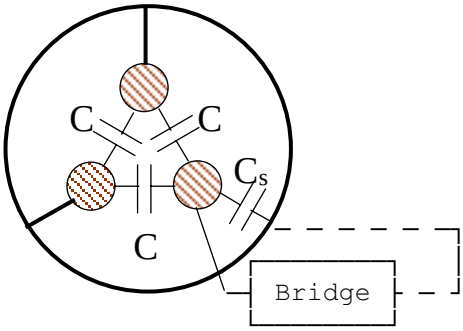

Figure 5.14 - Capacitance measurement

Measured value $C_{m2} = 2\ C + C_s$

i.e. $C = (C_{m2} - C_s)/2 = (3\ C_{m2} - C_{m1})/6$

which gives the capacitance between the conductors.

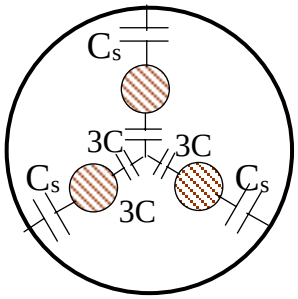

Figure 5.15 - Calculation of C_o

The effective capacitance to neutral C_o of any of the cores may be obtained by considering the star equivalent (Figure 5.15). This gives

$$C_0 = C_s + 3C = \frac{1}{3}C_m 1 + 3\frac{3C_m 2 - C_m 1}{6}$$

$$C_0 = \frac{3}{2}C_m 2 - \frac{1}{6}C_m 1$$

In the breakdown of actual 3-core belted cables, it is generally observed that charring occurs at those places where the stress is tangential to the layers of paper. Thus for the insulation to be effective, the tangential stresses in paper insulation should be preferably avoided. This can usually be accomplished only screening each core separately (or by having individual lead sheaths for each of the cores), so that the cable in effect becomes 3 individual cables laid within the same protective covering.

5.2.8 Hochstadter or "H" type Cable

In this type of cable (Figure 5.16), there is no belt insulation. The screening of individual cores is generally thin and flexible so that there is not much power dissipation in them. All the individual screens are earthed so that the potential at these sheaths are all zero and thus the stress lines between the cores and screens would be now radial.

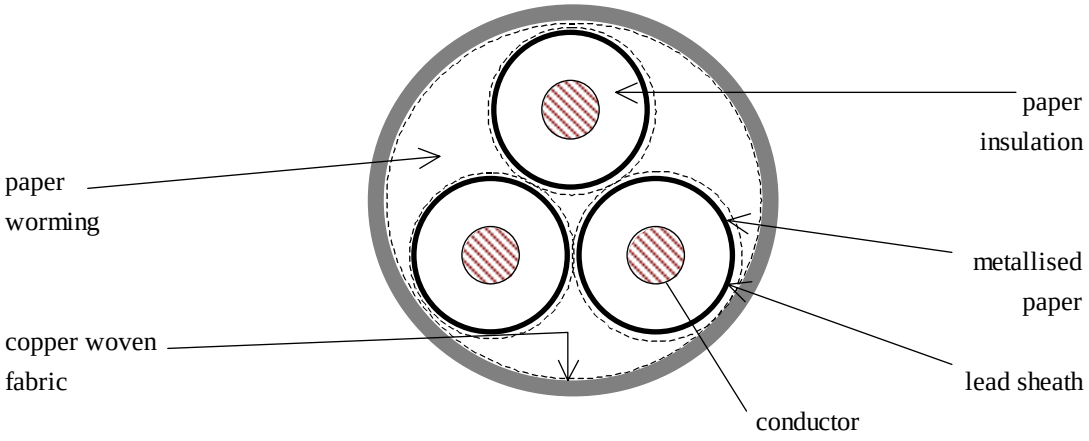

Figure 5.16 - H-type cable

The screens are thin so that there is hardly any current induced. The sheaths surrounding the insulation of the cores consist of metallised perforated paper. These are wrapped round with copper woven fabric (cotton tape into which are woven copper wire). This outer screen is in contact with the inner screens and is earthed. The cable has the additional advantage that the separation of the cores by thermal expansion or mechanical displacement cannot introduce stresses in the dielectric. The metallised screens help to dissipate the heat. These are used upto 66 kV. In the H-type cable, the individual cores contain no lead covering. The three cores are laid up with fillers in the ordinary way. If the cable is to be buried, then the cable is armoured with steel wire and tape. The wormings of the H-type cable are full of oil.

5.2.9 S.L. type Cable

Another development of the screening principle is the SL type cable (Figure 5.17). In this, each core is screened and then individually sheathed with lead or aluminium. These do not have an overall lead sheath.

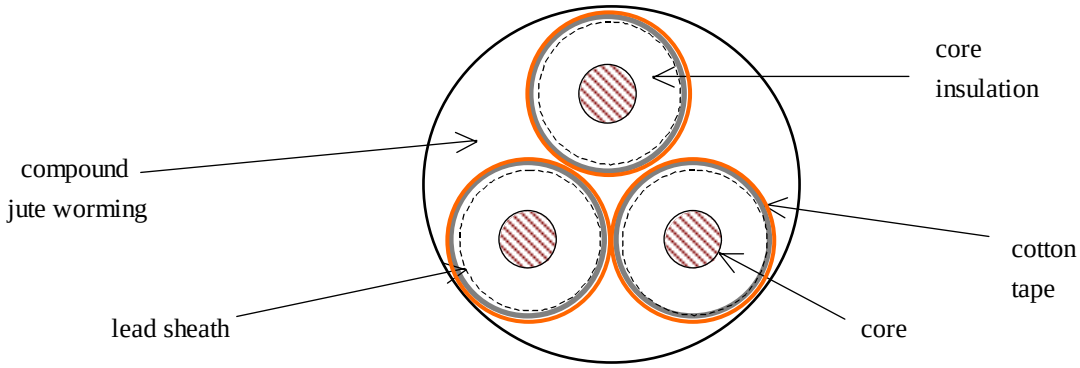

Figure 5.17 - S L type cable

The electric field in the insulation surrounding each core is naturally radial and the function of the screens in this case is to eliminate the possibility of any stress across the clearance space between core and sheath. The wormings of the filler spaces in the S.L. type cables do not contain much oil as do not get any electric stress.

The three metal sheathed cores, after being lapped with paper and cotton tapes are laid with tarred jute yarn to get a circular formation and then wrapped with hessian tapes to form a bedding for the armouring. The electrical and thermal advantages of H-type cables are also enjoyed by the S.L. type cables. These cables are suitable for hilly routes, as the absence of oil in the filler spaces lessens the risk of oil drainage. Also, the S.L. type construction is useful on short runs because the terminating equipment is simplified. Also the void formation in the filler spaces are of no consequence. The separate lead sheaths in the S.L. cable are the seats of induced currents, but the resulting losses are small, and appear to be of no practical significance.

5.2.10 Copper Space Factor

Unlike in overhead lines, insulation in cables occupies a greater portion of the cable space. Thus higher installation costs are involved. Ideally we would like the insulation to occupy the minimum possible thickness. Thus we define a **space factor** to indicate the utilisation of the space. The copper space factor is defined as

$$\text{copper space factor} = \frac{\text{cross-section area of conductor}}{\text{cross-section area of whole cable}}$$

For a single core cable, the best space factor is obtained with a concentric arrangement (Figure 5.18), as this gives the minimum conductor perimeter for the greatest conductor area and given insulation thickness. Thus

$$\text{Space factor} = r^2/R^2$$

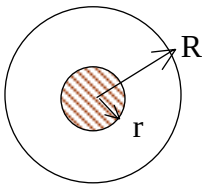

Figure 5.18

For the 3-core cable (Figure 5.19), consisting of circular conductors within a circular sheath,

$$\text{Space factor} = 3\,r^2/R^2$$

where T = thickness of core insulation, t = thickness of belt insulation

and $R_1 = r + T$

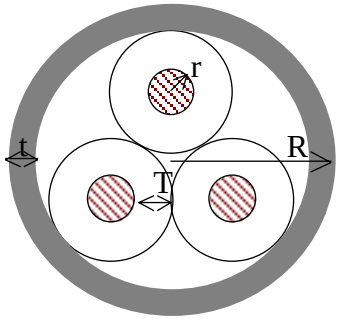

Figure 5.19 - three-core cable

However, for the 3-core cable the circular cross-section is not the best shape for the conductors.

Other shapes which gives better space factors are the elliptical shaped conductors and the sector shaped conductors (Figure 5.20).

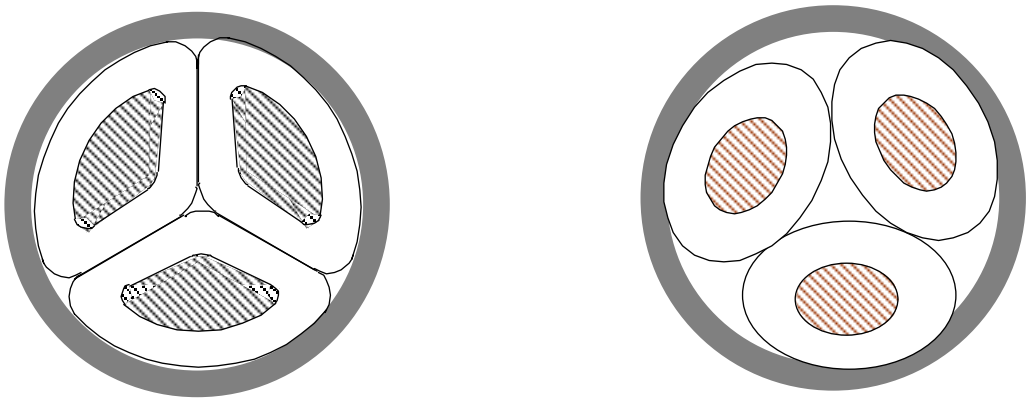

Figure 5.20 - Special shapes of conductors to give better space factors

5.3 Dielectric Stress in a Single Core Cable

The voltage difference across the conductor and the sheath of a single core cable is given by

$$v = \frac{q}{2\pi\varepsilon}\log_e\frac{R}{r}, \quad \text{also,} \quad \xi_x = \frac{q}{2\pi\varepsilon x}$$

$$\text{so that } \xi_x = \frac{V}{x\log_e\frac{R}{r}}$$

It is seen that since **x** is the only variable, the maximum stress in the dielectric occurs at the minimum value of the radius **x** (i.e. x = r).

$$\text{i.e. } \xi_{max} = \frac{V}{r\log_e\frac{R}{r}}$$

Since it is required that this maximum stress in the dielectric should be as low as possible, differentiating with respect to r for minimum ξ_{max} gives

$$\frac{d\,\xi_{max}}{d\,r} = 0$$

$$\text{i.e. } \left[\frac{V}{r\log_e R/r}\right]^2 . \left[\log_e\frac{R}{r} + r.\left(-\frac{1}{r}\right)\right] = 0$$

$$\text{i.e. } \frac{R}{r} = e = 2.718$$

Thus if the overall diameter of the cable is kept fixed, then **R/r = e** is the condition for minimum ξ_{max}. This value of radius of conductor will generally be larger than would be required for current carrying capacity.

Since **R/r = e**, the minimum value of ξ_{max} is given by

$$\xi_{max} = \frac{V}{r \log_e R/r} = \frac{V}{r}$$

Since the radius of the conductor that would be given from the above expression is larger than is necessary for current carrying capacity, this value of radius may be achieved by using Aluminium or hollow conductors.

As can be seen (Figure 5.21), the dielectric is not equally stressed at all radii, in a cable of homogeneous insulation. The insulation is fully stressed only at the conductor, and further away near the sheath the insulation is unnecessarily strong and thus needlessly expensive.

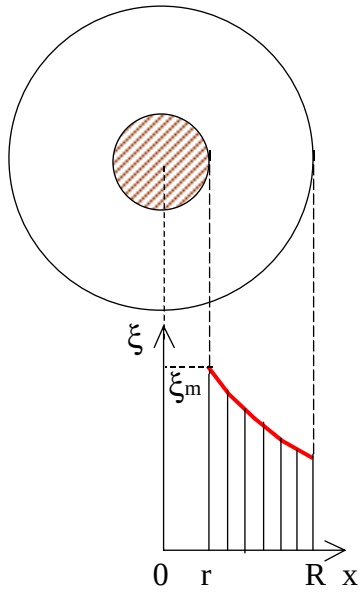

Figure 5.21 - Stress Distribution

5.3.1 Cable Grading for Uniform Stress Distribution

The electric stress in the dielectric may be more equally distributed by one of the two following methods.

(i) Capacitance grading
(ii) Intersheath grading

5.3.2 Capacitance Grading

In this method of grading, the insulation material consists of various layers having different permittivities.

Consider a cable graded by means of 3 layers of insulation, as shown in Figure 5.22, having permittivities ε_1, ε_2, ε_3, respectively. Let the outer radii of these layers by **r_1, r_2 and r_3 = R** respectively, an the conductor radius **r**.

In order to secure the same value of maximum stress in each layer, the maximum stresses in the layers are equated.

Let the voltage across the inner-most layer of insulation be V_1. Then

$$\frac{q}{2\pi\varepsilon_0\varepsilon_1 r} = \frac{q}{2\pi\varepsilon_0\varepsilon_2 r_1} = \frac{q}{2\pi\varepsilon_0\varepsilon_3 r_2}$$

$$\therefore \quad \varepsilon_1 r = \varepsilon_2 r_1 = \varepsilon_3 r_2$$

$$V_1 = \xi_{max}\, r \log_e \frac{r_1}{r}$$

similarly V_2, V_3 can be determined

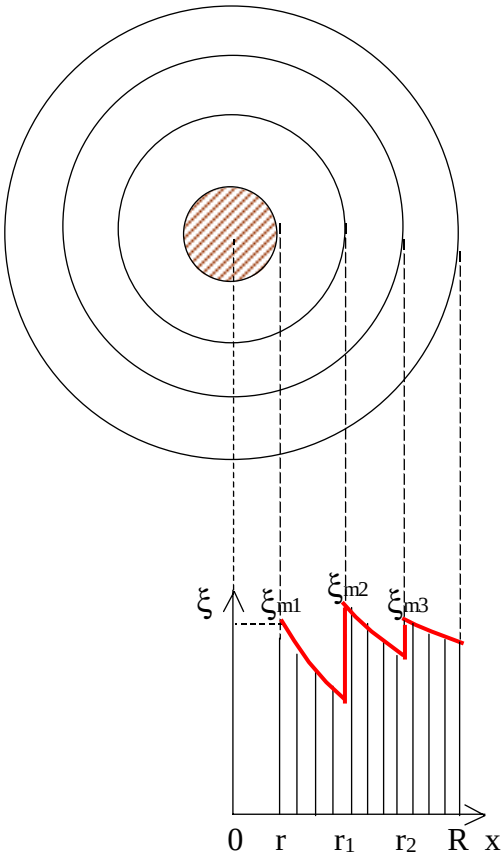

Figure 5.22 - Capacitance Grading

Therefore the total voltage across the dielectric can be obtained as follows.

$$V = \xi_{max}\left(r \ln\frac{r_1}{r} + r_1 \ln\frac{r_2}{r_1} + r_2 \ln\frac{r_3}{r_2} \right)$$

$$= \xi_{max}\left(r \ln\frac{r_1}{r} + r \ln\frac{r_2}{r_1} + r \ln\frac{R}{r_2} + (r_1 - r)\ln\frac{r_2}{r_1} + (r_2 - r)\ln\frac{R}{r_2} \right)$$

$$= \xi_{max}\left(r \ln\frac{R}{r} + (r_1 - r)\ln\frac{r_2}{r_1} + (r_2 - r)\ln\frac{R}{r_2} \right)$$

$$> \xi_{max}\, r \log_e\frac{R}{r}, \qquad \text{since } r_1 > r,\ r_2 > r$$

Hence by grading the insulation, without increasing the overall diameter of the cable, the operating voltage can be raised. A difficulty with this method is that we cannot obtain a wide range of permittivities in practice, as paper insulation has permittivities limited to the range 2.8 to 4.0.

In the above analysis, it has been assumed that the maximum permissible stress is the same for all three dielectrics used. If the maximum stress in the three sections are different, and are ξ_1, ξ_2, ξ_3 respectively, then the maximum stresses should be reached at the same time for the most economical operation of the insulation. This condition gives us the result

$$\xi_1 \varepsilon_1 r = \xi_2 \varepsilon_2 r_1 = \xi_3 \varepsilon_3 r_2$$

5.3.3 Intersheath Grading

In this method of grading, the same insulating material is used throughout the cable, but is divided into two or more layers by means of cylindrical screens or intersheaths (Figure 5.23). These intersheaths are connected to tappings from the supply transformer, and the potentials are maintained at such values that each layer of insulation takes its proper share of the total voltage. The intersheaths are relatively flimsy, and are meant to carry only the charging current.

Since there is a definite potential difference between the inner and outer radii of each sheath, we can treat each section separately as a single core cable.

If $\mathbf{V_1, V_2, V_3, \ldots}$ are the potential differences across the sections of insulation, then

$$\xi_{max} = \frac{V_1}{r \log_e\frac{r_1}{r}} = \frac{V_2}{r \log_e\frac{r_2}{r_1}} = \ldots\ldots$$

Since the cable insulation now consists of a number of capacitors in series, formed by the respective intersheaths, all potential differences $\mathbf{V_1, V_2, V_3, \ldots}$ are in phase. Thus, if $\mathbf{V}$ is the phase to neutral voltage, we can also write

$$V = V_1 + V_2 + V_3 + \ldots\ldots\ldots + V_n$$

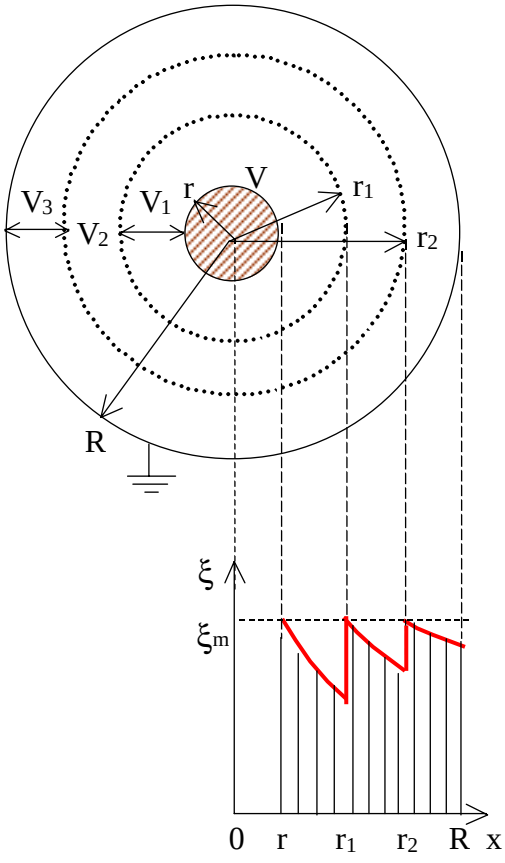

Figure 5.23 - Intersheath Grading

In the particular case that all the **n** layers have the same thickness **d**, and if **r** is the conductor radius,

$$r_1 = r + d;\ r_2 = r + 2d;\ r_3 = r + 3d;\ \ldots\ldots\ r_n = r + n\,d$$

$$\xi_{max} = \frac{V_1}{r \log_e \frac{r+d}{r}} = \frac{V_2}{(r+d)\log_e \frac{r+2d}{r+d}} = \ldots\ldots = \frac{V}{M}$$

$$\text{where}\quad M = \sum_{m=1}^{n} \left(r + (m-1)\,d\right) \log_e \frac{r + m\,d}{r + (m-1)\,d}$$

The voltage across the $\mathbf{m^{th}}$ section is given by

$$V_m = \frac{V}{M}\left[r + (m-1)\,d\right] \log_e \frac{r + m\,d}{r + (m-1)\,d}$$

Hence substituting for the different values of **m**, we can obtain the voltage across the various layers that have to be maintained to give equal maximum stress in each section.

In practice, there is a considerable difficulty in arranging for many intersheaths, this difficulty being mainly associated with the provision of the different voltages for the intersheaths, and as a result it is usual to design a cable of this type with only one intersheath.

This simplifies the design calculations, and the expression for the maximum stress then given by

$$\xi_{max} = \frac{V}{r_1 \log_e \frac{R}{r_1} + r \log_e \frac{r_1}{r}}$$

For the purpose of comparison with the ungraded cable, let us first take the optimally designed ungraded cable (i.e. with **R/r = e**), and introduce an intersheath at a radius $\mathbf{r_1}$. Since **R** and **r** are both kept fixed, $\mathbf{r_1}$ is the only variable, and the expression for stress must be differentiated with respect to $\mathbf{r_1}$ to obtain the condition for the minimum value of the maximum stress.

$$\text{i.e.}\ -1 + \log_e \frac{R}{r_1} + \frac{r}{r_1} = 0$$

$$\text{considering}\quad \frac{R}{r} = e,\ \text{also}\ \log_e e = 1$$

$$\therefore\ \frac{r_1}{r} \log_e \frac{r_1}{r} = 1$$

$$\frac{\partial \xi_{max}}{\partial r_1} = 0 \quad \text{so that}\quad r_1 . \frac{r_1}{R} . \left(\frac{-R}{r_1^{\,2}}\right) + \log_e \frac{R}{r_1} + r . \frac{r}{r_1} . \frac{1}{r} = 0$$

This gives the solution $\mathbf{r_1 = 1.76\ r}$.

$$\therefore \xi_{max} = \frac{V}{1.76\, r \log_e\left(\frac{e\, r}{1.76\, r}\right) + r \log_e\left(\frac{1.76\, r}{r}\right)} = \frac{V}{1.33\, r}$$

However, for the cable without intersheath, we have $\xi'_{max} = V/r$. Hence, the addition of the intersheath raises the maximum applicable voltage by **33%**.

Now let us consider the case of only the overall diameter of the cable **R** being fixed, and both **r** and r_1 being variable. Then for minimum value of the maximum stress we have

$$\frac{\partial \xi_{max}}{\partial r} = 0, \quad \frac{\partial \xi_{max}}{\partial r_1} = 0$$

$$\text{i.e. } \log_e \frac{r_1}{r} - 1 = 0, \text{ also } -1 + \log_e \frac{R}{r_1} + \frac{r}{r_1} = 0$$

$$\text{i.e. } \frac{r_1}{r} = e, \quad -1 + \log_e \frac{R}{r_1} + \frac{1}{e} = 0$$

$$\text{This gives } \log_e \frac{R}{r_1} = 1 - \frac{1}{e} \text{ giving } \frac{R}{r_1} = 1.881$$

$$\xi_{max} = \frac{V}{e\, r \log_e \frac{R}{r_1} + r \log_e e} = \frac{V}{e\, r\left(1 - \frac{1}{e}\right) + r} = \frac{V}{e\, r}$$

$$\text{i.e. } \xi_{max} = \frac{V}{2.718\, r}$$

5.4 Pressurised High Voltage Cables

In high voltage paper insulated cables, the application of pressure (about 13 atmospheres) increases the maximum allowable working stress (after applying a suitable safety factor) from about 50 kV/cm to about 150 kV/cm.

In super voltage cables, the void control is effected by pressurising the oil-impregnated paper tape insulation by (a) pressurising the oil, and (b) applying gas pressure.

5.4.1 Oil-pressure cables

In oil filled cables, the oil must be free to flow inorder to transmit the pressure. The maximum pressure of oil utilised is about 0.35 MN/m^2 (3.5 atmospheres or 50 p.s.i.). Due to the pressure of oil, the sheath tends to bulge out and therefore reinforcement of the sheathing is necessary. A reservoir maintains the required pressure. The cable can now operate at a maximum working stress of 150 kV/cm.

In normal, solid type of cable, the drying and impregnating are done before sheathing, while in oil-filled cables they can be done after sheathing by circulating hot oil. The oil filled construction permits a great reduction in size of the cable.

There are 3 main types of oil filled cables. These are (a) single-core, conductor channel; (b) single-core, sheath channel; and (c) three-core, filler-space channels.

(a) Single-core conductor channel

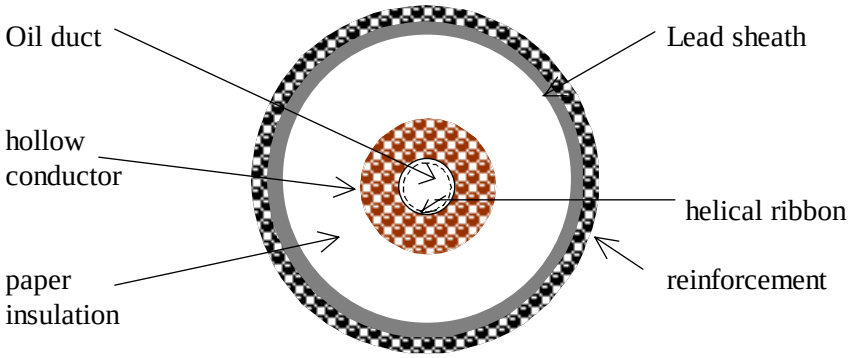

Figure 5.24 - Single core conductor channel cable

This type of cable shown in figure 5.24 has a hollow conductor which acts as an oil channel, and is the simplest from the point of view of the cable itself. A disadvantage of this arrangement is that the oil is at high voltage with respect to earth being at the voltage of the conductor. The copper strands of which the conductor is made are laid over a helical metal ribber, so that oil can reach the insulation.

(b) Single-core sheath channel

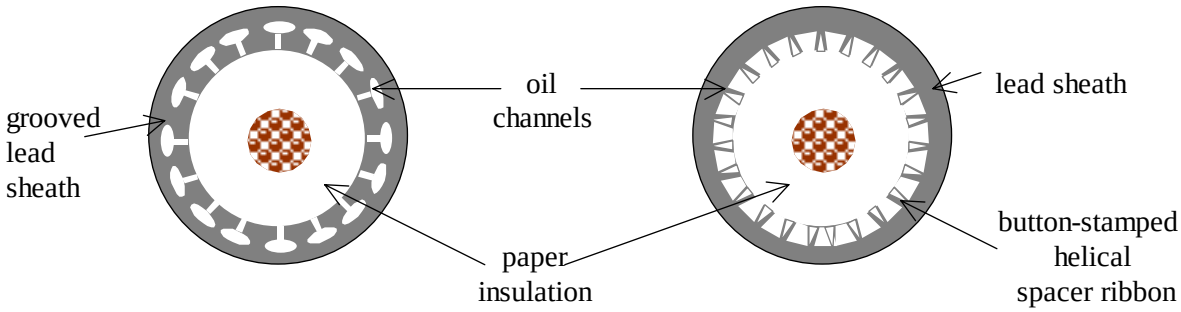

Figure 5.25 - Single core sheath channel cable

In this type (Figure 5.25), the oil channels are produced either by grooving the sheath or by arranging spacers between sheath and insulation. The resistance to oil flow in this type is 6 to 8 times that of type (a), so that more feeding points are necessary to maintain the pressure. An advantage is that the channels are at earth potential so that joints and installation are simpler.

(c) Three-core, filler space channels

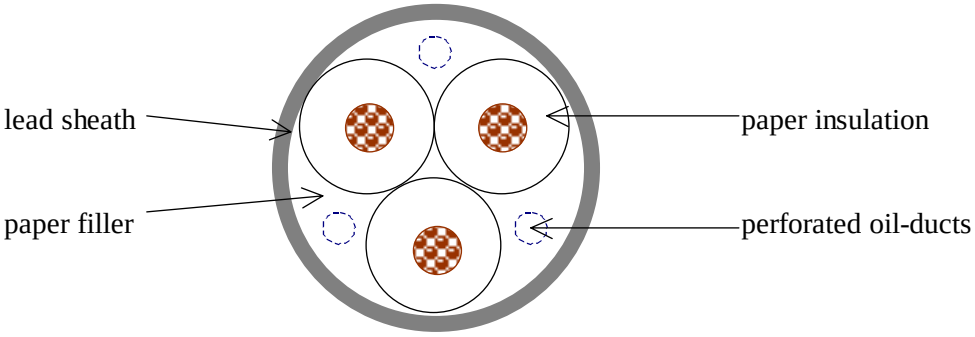

Figure 5.26 - Three core filler space channel cable

In this type (Figure 5.26), the oil channels are located in the filler spacers. These channels are composed of perforated metal-ribbon tubing and are at earth potential.

5.4.2 Gas-pressure cables

In Gas pressure cables, a pressure of about 1.4 MN/m^2 (14 atmospheres or 200 p.s.i.) is used. Figure 5.27 shows the different types of gas pressure cables.

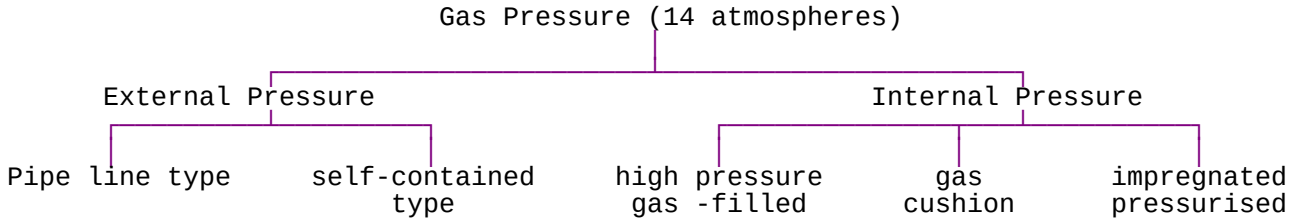

Figure 5.27 - Types of gas pressure cables

5.4.3 External Pressure Cables

Pipe line type

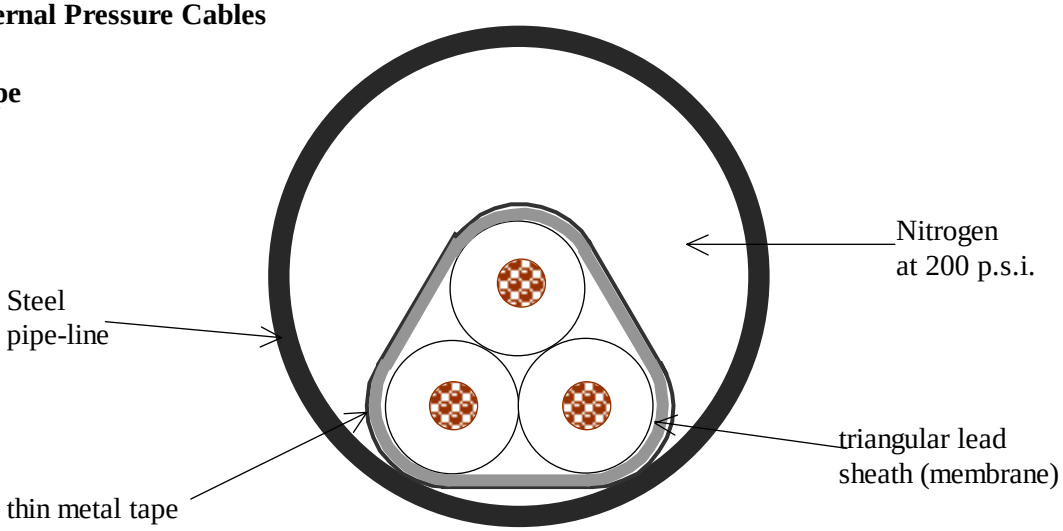

Figure 5.28 - Pipe line type cable

The cable, shown in Figure 5.28, is manufactured in the usual way and the outside is made triangular, and covered by a diaphragm lead sheath. The pipe is filled with Nitrogen subjected to a pressure of 200 p.s.i. which is transmitted to the insulation through the diaphragm.

The steel pipe is laid first, and the cable is drawn in afterwards. Nitrogen under pressure is then introduced into the pipe. The pressure is transmitted to the membrane through the membrane.

In the **Self-contained type**, an additional reinforced lead sheath is used, but otherwise the principle is the same as that of the pipe line type.

5.4.4 Internal Pressure Cables

In the internal pressure cables, the gas is in contact with the dielectric.

(a) Gas filled cables

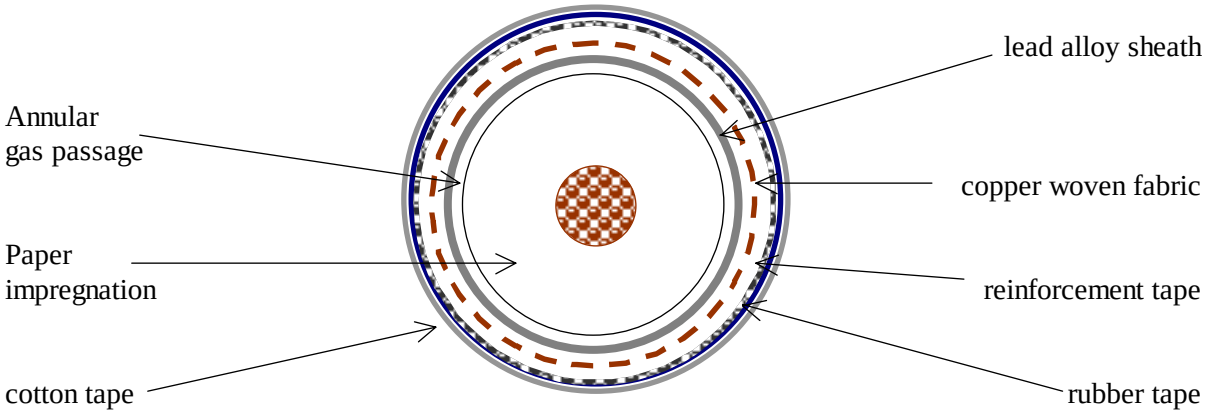

Figure 5.29 - Gas filled cable

In these cables (Figure 5.29), spaces are left between the convolutions so that the gas is between them. The presence of Nitrogen prevents the formation of voids. The method of manufacture is such that the gas can move freely inside packets, but cannot diffuse outside the insulation.

(b) Gas cushion type

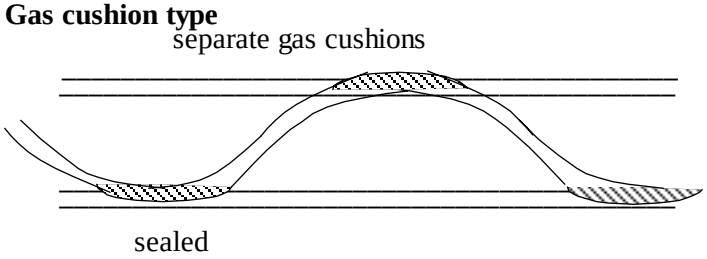

Figure 5.30 - Gas Cushion Type cable

(This type shown in Figure 5.30 is not of much practical use but only of academic use). In this type, a screened space is provided between the lead sheath and the dielectric, this space providing accommodation at all points along the length of the cable for the storage of inert gas under pressure.
This storage is maintained by the subdivision of the screened space into a series of gas cushions by means of barriers, with the result that the cable may be cut for joining without losing gas from more than a short length.

(c) Impregnated pressurised cable

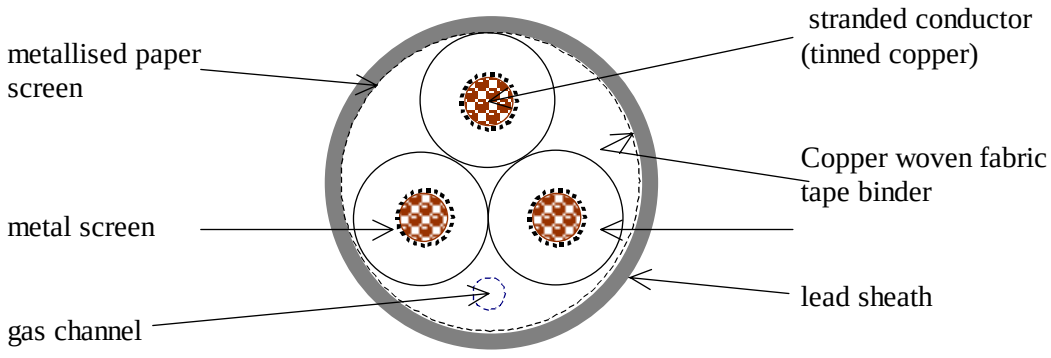

Figure 5.31 - Impregnated Pressurized cable

In the manufacture of this type of cable (Figure 5.31), provision is made for longitudinal gas flow, and the impregnating compounds used are suitable for the higher dielectric stresses necessary for high voltage cables. The cable has a mass impregnated paper dielectric and the impregnating oil is maintained under a pressure of 200 p.s.i. by means of nitrogen. Special reinforcement is provided to cater for the large hoop and longitudinal stresses set up.

The core is stranded and is covered with a metallised paper screen so as to obtain a completely uniform stress. The gas channel is in one of the filler spaces.

5.5 Thermal Design of Cables

Underground cables are installed in trenches of rectangular cross-section. After excavation of the trench, a layer of sand is placed in it to serve as a bedding, as shown in Figure 5.32.

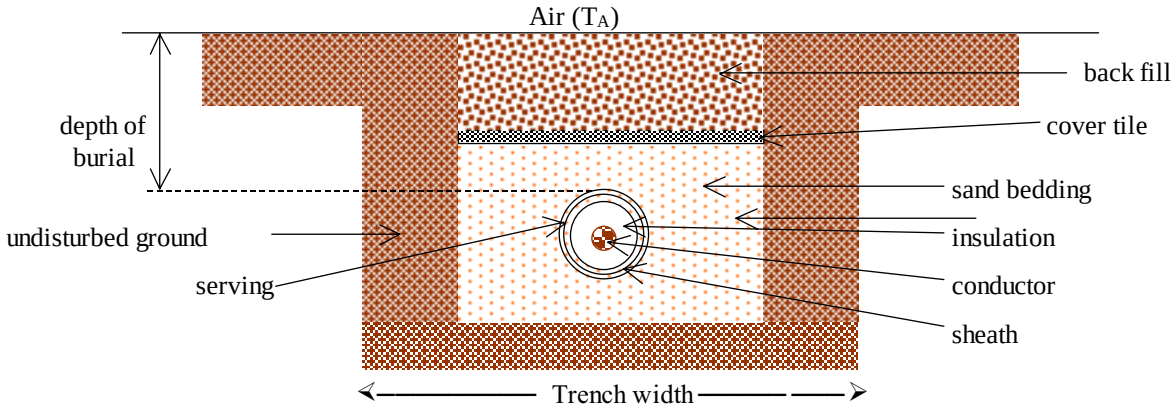

Figure 5.32 - Cross-section of Trench and buried cable

The length of cable is pulled in along the trench and covered with a further layer of sand. Sand free from flints and stone is employed to avoid damage to the cable serving during pulling and initial back filling. Above the cable and sand bedding are placed cover tiles to protect the cable from mechanical damage from subsequent excavation activities. The excavated material is replaced in the trench and stamped to consolidate it. The minimum trench width that can be conveniently excavated is about 700 mm (27 inches), and for safety reasons, the minimum depth of burial in normal circumstances is 900 mm (36 inches).

An underground cable carrying current will have in addition to the conductor loss, dielectric loss and losses in the sheath. These produce heat which are conducted away from the cable to the surface, producing a temperature gradient.

When more than one single core cable is laid together (as is required for three phase systems exceeding 150 kV), the heat produced by one conductor affects the other and the heat factors need to be modified. When the spacing between the cables is increased, the heat produced by the circulating currents between the cables will increase whereas the eddy current losses decrease. Thus there is an optimum spacing for cables and various alternatives may have to be evaluated before the economic arrangement is finally selected.

5.5.1 Current rating of Cables

In a cable, the factor which ultimately limits the current carrying capacity is the maximum operating temperature which may be sustained by the cable throughout its life without risk of damage or deterioration. As was discussed in an earlier section, the heat generated in the cable is due to (a) ohmic loss in the conductor, (b) the dielectric loss in the insulating medium and (c) the sheath and intersheath losses.
The heat so generated is radiated to the surroundings. The current that can be carried depends on the conductivity of the surrounding medium as well, so that the same cable would have different ratings depending on whether the cable is buried or not.

5.5.2 Thermal Resistance

Since the flow of heat can be considered analogous to the flow of charge or current in the insulation, the thermal resistance of the cable and surroundings is measured in terms of the **thermal ohm**.

Thermal Ohm: The thermal ohm is the resistance of a path through which a temperature difference of 1 ^{0}C produces a heat flow of 1 watt.

Thermal Resistivity: The thermal resistivity is the temperature drop in degree centigrade produced by the flow of 1 watt between the opposite faces of a metre cube of the material.

Consider a cable buried under the surface of the earth.

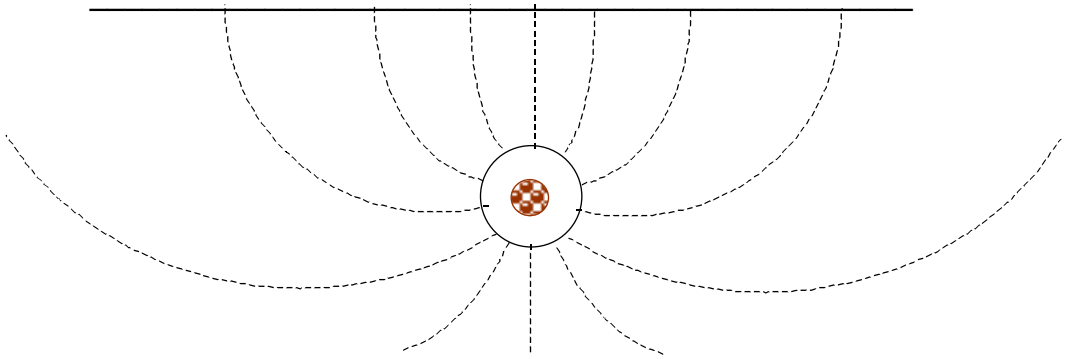

Figure 5.33 - Heat flow lines from buried cable

Let	θ	=	maximum allowable difference in temperature between the core and surroundings (^{o}C)
	R_θ	=	Effective Resistance of conductor (including effects of sheath loss)
	I	=	Current carried by conductor
	H	=	Heat produced in the core (W)
	S'	=	Thermal resistance of dielectric
	S''	=	Thermal resistance of cable outside dielectric
	S	=	S' + S'' = Total thermal resistance of cable
	G	=	Thermal resistance of ground from cable to surroundings

From the definition, the total temperature rise between the conductor and the surroundings is given by

$$\theta = H\,(S + G)$$

Total power loss = dielectric loss (W_d) + ohmic loss ($I^2 R_\theta$)

At equilibrium, the total power loss must equal to the heat produced.

$$\therefore \quad H = \frac{\theta}{S+G} = W_d + I^2 R_\theta$$

$$\text{i.e.} \quad \theta = (W_d + I^2 R_\theta)(S + G)$$

This gives the current rating of the cable as

$$I = \sqrt{\frac{\theta - W_d (S+G)}{R_\theta (S+G)}}$$

In calculating the flow if heat it is useful to to remember the following analogies.

Heat	Electricity	Electrostatic	Electromagnetic
Temperature Difference θ	Potential difference	Potential difference	magnetomotive force (mmf)
Heat Flow H	Current I	Electric charge Q	Magnetic flux φ
Thermal resistance S	Resistance	1/Capacitance	Reluctance

If a method exists to study any of the above phenomena, the analogous quantity can also be studied by comparison.

5.5.3 Thermal Resistance of single-core cable

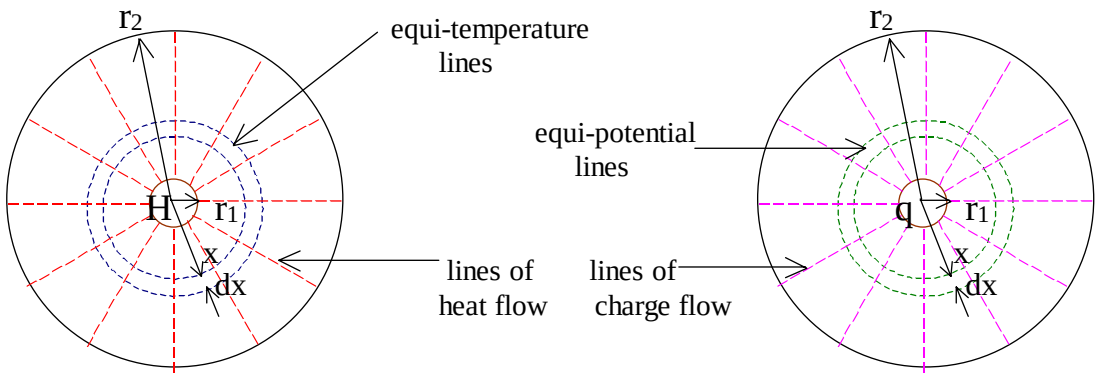

Figure 5.34 - Analogous heat-flow and charge-flow lines

The analysis of this problem is similar to the analysis of the analogous electrostatic case. Figure 5.34 shows these two cases.

In the heat problem, H is the amount of heat generated per unit length of cable, and in the corresponding electrostatic case, q is the electric flux flowing out per unit length.

For the electrostatic case, consider a gaussian cylinder of radius **x** and thickness **dx**.

$$D \cdot 2\pi x \cdot 1 = q, \text{ so that } D = q/(2\pi x)$$

$$\therefore \xi = \frac{q}{\varepsilon 2\pi x}, \text{ where } \varepsilon = \varepsilon_0 \varepsilon_r$$

$$\therefore V = \int_{r_2}^{r_1} \frac{q}{2\pi\varepsilon} \cdot \frac{1}{x} \cdot dx = \frac{q}{2\pi\varepsilon} \log_e \frac{r_1}{r_2}$$

Considering the analogous heat flow case,

Let $d\theta$ = drop in temperature across dx
k = thermal resistivity

$$\text{then} \quad d\theta = \frac{k \,.\, H \,.\, dx}{2\pi x}$$

$$\text{integration gives} \quad \theta = \frac{k\,H}{2\pi} \log_e \frac{r_1}{r_2}$$

Thermal resistance is θ/H, so that

$$\therefore \text{ thermal resistance } S = \frac{k}{2\pi} \log_e \frac{r_1}{r_2}$$

5.5.4 Thermal resistance of three-core cables

For three-core cables, the following two quip expressions are used.

$$(i)\ S = \frac{k}{6\pi}\left(0.85 + \frac{0.2\,t}{T}\right)\ln\left[\left(4.15 + \frac{1.1\,t}{T}\right)\left(\frac{T+t}{r}\right) + 1\right] \ \Omega/\text{km}$$

where

t = thickness of belt insulation

T = thickness of conductor insulation

r = radius of conductor

$$(ii)\ S = \frac{k}{6\pi} \ln\left[\frac{r_2^{\,6} - a^6}{3\,r_2^{\,3}\,a^2\,r}\right]$$

where

r = radius of conductor

a = radius at which the centres of each conductor lies

r_2 = outer radius of dielectric

5.5.5 Thermal resistance of protective coverings

Since the protective covering of the cable is in the form of a cylinder, the expression is of the same form as that for a single core cable.

$$S = \frac{k}{2\pi} \ln \frac{r_3 - A/2}{r_2 + A/2}$$

where

r_3	=	radius of outer covering of cable
r_2	=	radius of lead sheath
A	=	thickness of armouring
k	=	thermal resistivity

5.5.6 Thermal resistance of ground around cable

Inside the cable constant temperature lines would all be concentric cylinders since the outer lead sheath is a conductor of heat. The flow of heat would consequently be radial.

However, outside the cable, the equi-temperature lines would no longer be concentric and the heat flow would go radially outwards from the surface of the cable and ending up at the surface of the ground normally (assuming that the surface of the earth is at a constant temperature).

Here again, let us analyse using the analogy of the infinitely long conductor carrying a charge **q** per unit length, placed at a distance **h** above the earth surface (Figure 5.35).

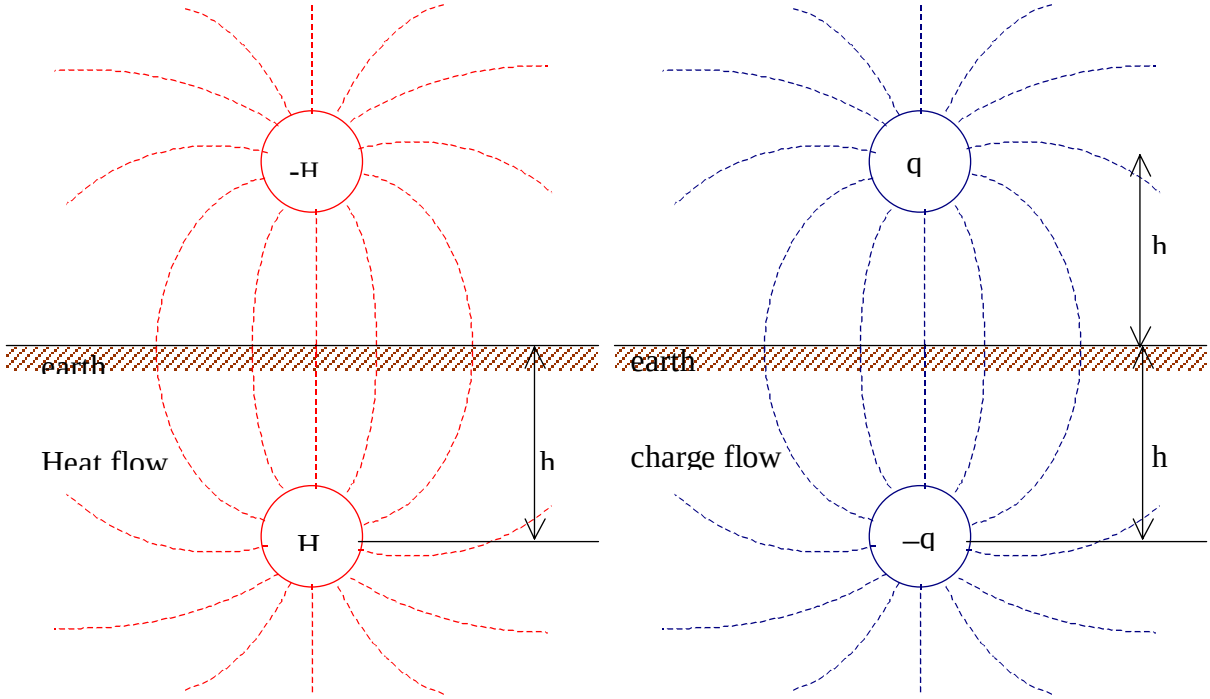

Figure 5.35 - Effect of Earth Surface

This has the same effect as having a charge of -q at the same distance beneath the earth.

The effect of the earth can be replaced by an equal and opposite charge on the opposite side of the surface at the same distance from the surface.

The effects of the charge +q and -q can now be separately considered, and the results superimposed. Each charge considered separately will give rise to radial flux lines.

The potential difference between the charges caused by one of the charges is given by

$$V = \frac{q}{2\pi\varepsilon}\log_e\frac{2h}{r}$$

The total potential difference caused between the charges is twice that of the individual charge. This is equal to

$$V = \frac{q-(-q)}{2\pi\varepsilon}\log_e\frac{2h}{r} = \frac{2q}{2\pi\varepsilon}\log_e\frac{2h}{r}$$

Thus the potential difference to the neutral of each conductor is given as

$$V = \frac{q}{2\pi\varepsilon}\log_e\frac{2h}{r}$$

Analogy: The temperature difference from the heat source to earth is given by

$$\theta = \frac{kH}{2\pi}\log_e\frac{2h}{r}$$

Thus the thermal resistance of the ground is given by

$$\text{thermal resistance} = \frac{\theta}{H} = \frac{k\,H}{2\pi}\log_e\frac{2\,h}{r}$$

When applied to the practical case, it is found that the theoretical thermal resistance a found above has to be multiplied by a factor of 2/3. This is because we have assumed the earth to be a plane of perfect conductivity (or constant temperature). Thus the modified thermal resistance **G** of the ground for practical application is given by

$$G = \frac{k\,H}{3\pi}\log_e\frac{2\,h}{r}$$

A representative value of the thermal resistivity **k** of the soil of average moisture content is 180.

5.5.7 Cables exposed to air

The heat dissipation of a cable exposed to the air depends on the radiation. For a surface in direct contact with the air, with unrestricted ventilation, the heat dissipation is given by

$$H = 2\pi r_2(\theta_s - \theta_a)^{1.25} \quad \text{watt/cm of length}$$

where

r_2 = exernal radius of cable, usually of lead sheath,

θ_s = temperature of cable surface,

θ_a = ambient temperature,

k = emissivity constant whose value varies with r_2

5.6 High Voltage Bushings

Bushings are insulators which are used to take high voltage conductors through earthed barriers such as walls, floors, metal, tanks etc. The bushings have to provide electrical insulation of the conductor for the working voltage and for various over-voltages which may occur in service and also have to provide mechanical support against various mechanical forces.

5.6.1 Simple cylindrical bushing

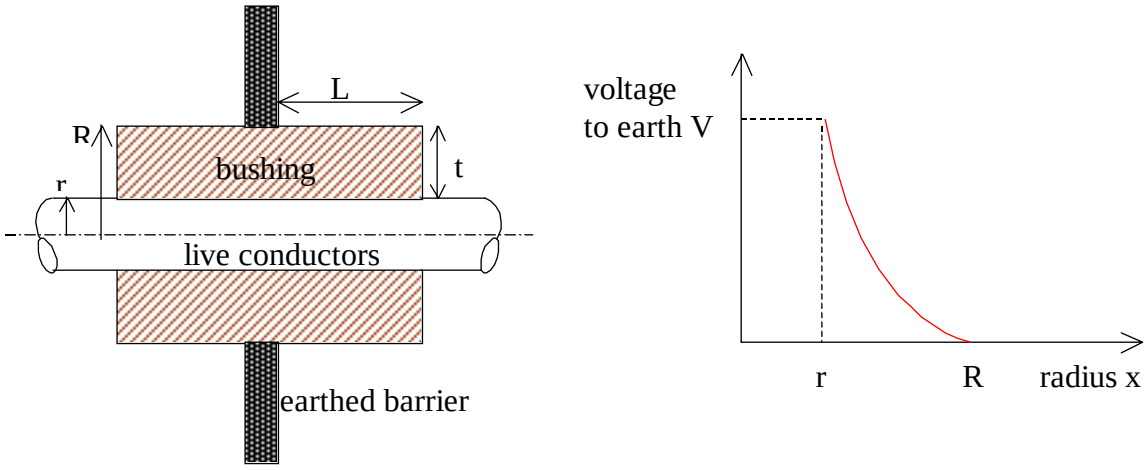

Figure 5.36 - Simple cylindrical bushing

The simplest form of bushing is a cylinder of insulating material around the conductor (Figure 5.36), with radial clearance **t = (R - r)** and axial length **L** to suit electrical strengths of the insulating material and surrounding media.

In this case, the voltage distribution with radius x is not linear so that the material is not equally stressed.

The expressions for stress ξ and voltage to earth $\mathbf{V_x}$ at radius **x** is given by

$$\xi = \frac{V}{x \ln \frac{R}{r}}, \quad V_x = \frac{V \ln \frac{R}{x}}{x \ln \frac{R}{r}}$$

The maximum stress in the bushing occurs at the conductor surface (i.e. at x = r), so that

$$\xi_{max} = \frac{V}{r \log_e \frac{r+t}{r}}$$

so that the thickness **t** required for the bushing is given by

$$t = r\left[\exp\left(\frac{V}{r\,\xi_{max}}\right) - 1\right]$$

$$t = \frac{V}{\xi_{max}} + \frac{V^2}{2\,r\,\xi_{max}^{\,2}} + ...$$

Thus as the voltage increases, the dimensions required become very large, so much so that for very high voltages, simple cylindrical bushings of this form are not satisfactory. Upto about 66 kV, porcelain bushings (with or without oil) may be used.

5.6.2 Condenser bushing

The difficulty of the dimensions increasing rapidly is overcome by the condenser bushing. In this case, the busing is divided into a number of capacitors by concentric cylinders of metallic foil or metallic coated paper. By proper choice of lengths of these cylinders, it is possible to obtain a nearly uniform voltage distribution with radius (Figure 5.37).

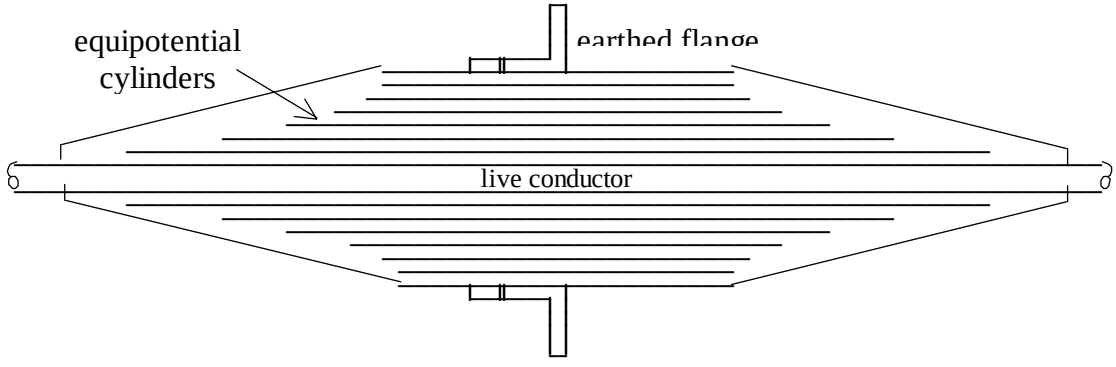

Figure 5.37 - Condenser Bushing

Since the stress is now made uniform, it must be equal to the ratio of the applied voltage **V** to the thickness **t'** of the insulation.

$$\xi_{max} = \frac{V}{t'}, \quad \text{so that} \quad t' = \frac{V}{\xi_{max}}$$

As can be seen when comparing with the simple bushing, the thickness **t'** required now is much less than **t**.

Example

A condenser bushing for an r.m.s. voltage of 30 kV to earth is designed to have a uniform radial voltage gradient (Figure 5.38). The insulating material used has a maximum permissible working voltage stress of 10 kV/cm (peak). Assuming a uniform and very small thickness of insulation between each successive foil, determine the radial thickness t' of the bushing.

If the length of the bushing at the outermost radius is 10 cm, determine the length at the surface of the conductor (radius 2 cm).

Estimate also the thickness t for the bushing without foils, if it is to have the same maximum radial stress.

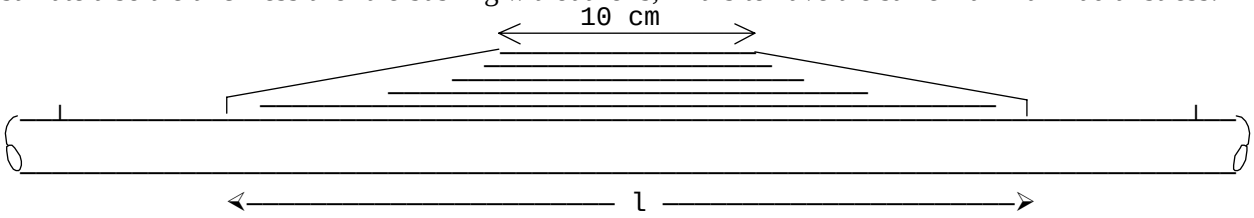

Figure 5.38 - Length of Condenser Bushing

Since stress is uniform,

$$t' = \frac{V}{\xi_{max}} = \frac{30\sqrt{2}}{10} = 4.24 \text{ cm}$$

The profile of the bushing has the equation **y = a/x**,

at x = t' + 2, y = 10 cm, so that a = 10(t' + 2) = 10(4.24 + 2)

therefore, x.y = a = 62.4

at x = r = 2, y = l

therefore, l = 62.4/x = 62.4/2 = **31.2 cm**

In the absence of foils,

$$\xi_{max} = \frac{V}{r \log_e \frac{r+t}{r}} \quad \therefore \quad 10 = \frac{30\sqrt{2}}{2 \log_e \frac{t+2}{2}}$$

$$\therefore \quad \log_e (1 + \tfrac{1}{2} t) = 1.5\sqrt{2} = 2.121$$

$$\text{i.e.} \quad 1 + \tfrac{1}{2} t = 8.342 \quad \therefore \quad t = 2 \text{ x } 7.342 = 14.68 \text{ cm}$$

Thus in the absence of grading, it is seen that a much greater thickness of insulation is required (**14.68 cm** as compared to **4.24 cm**).

In addition to the simple cylinder bushing, and the condenser type bushing, there are other types of bushings, which may consist of more than one material.

Measurement of High Voltage

6.0 High Voltage Measurement

High voltages can be measured in a variety of ways. Direct measurement of high voltages is possible up to about 200 kV, and several forms of voltmeters have been devised which can be connected directly across the test circuit. High Voltages are also measured by stepping down the voltage by using transformers and potential dividers. The sparkover of sphere gaps and other gaps are also used, especially in the calibration of meters in high voltage measurements. Transient voltages may be recorded through potential dividers and oscilloscopes. Lightning surges may be recorded using the Klydonograph.

6.1 Direct Measurement of High Voltages

6.1.1 Electrostatic Voltmeters

One of the direct methods of measuring high voltages is by means of electro-static voltmeters. For voltages above 10 kV, generally the attracted disc type of electrostatic voltmeter is used.
When two parallel conducting plates (cross section area **A** and spacing **x**) are charged **q** and have a potential difference **V**, then the energy stored in the is given by

$$\text{Energy stored } W = \tfrac{1}{2} C V^2 \text{ so that change } dW = \tfrac{1}{2} V^2 dC = F\,dx$$

$$\therefore \text{ Force } F = \tfrac{1}{2} V^2 \frac{dC}{dx} \text{ N}$$

$$\text{for uniform field Capacitance } C = \frac{A\varepsilon}{x} \text{ so that } \frac{dC}{dx} = -\frac{A\varepsilon}{x^2}$$

$$\therefore F = -\tfrac{1}{2} A\varepsilon \frac{V^2}{x^2} \text{ N}$$

It is thus seen that the force of attraction is proportional to the square of the potential difference applied, so that the meter reads the square value (or can be marked to read the rms value).

Electrostatic voltmeters of the attracted disc type may be connected across the high voltage circuit directly to measure up to about 200 kV, without the use of any potential divider or other reduction method. [The force in these electrostatic instruments can be used to measure both a.c. and d.c. voltages].

Abraham Voltmeter

The Abraham voltmeter is the most commonly used electrostatic meter in high voltage testing equipment. In this instrument, there are two mushroom shaped hollow metal discs.

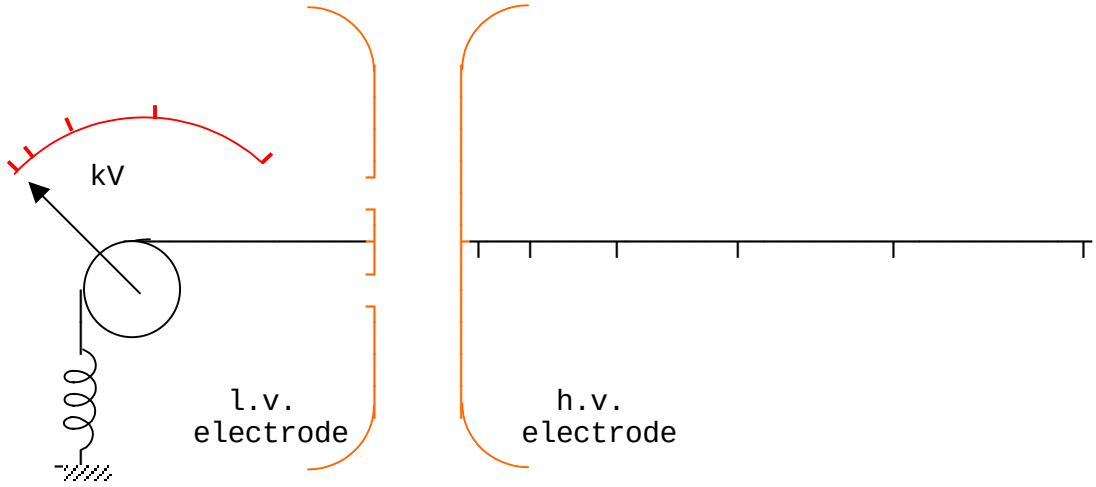

Figure 6.1 - Abraham electrostatic voltmeter

As shown in figure 6.1 the right hand electrode forms the high voltage plate, while the centre portion of the left hand disc is cut away and encloses a small disc which is movable and is geared to the pointer of the instrument. The range of the instrument can be altered by setting the right hand disc at pre-marked distances. The two large discs form adequate protection for the working parts of the instrument against external electrostatic disturbances. These instruments are made to cover ranges from 3 kV to 500 kV. Owing to the difficulty of designing electrostatic voltmeters for the measurement of extra high voltages which will be free from errors due to corona effects, within the instrument, and to the external electrostatic fields, a number of special methods have been devised for the purpose.

6.1.2 Sphere gaps

The sphere gap method of measuring high voltage is the most reliable and is used as the standard for calibration purposes.

The breakdown strength of a gas depends on the ionisation of the gas molecules, and on the density of the gas. As such, the breakdown voltage varies with the gap spacing; and for a uniform field gap, a high consistency could be obtained, so that the sphere gap is very useful as a measuring device.

By precise experiments, the breakdown voltage variation with gap spacing, for different diameters and distances, have been calculated and represented in charts.

In the measuring device, two metal spheres are used, separated by a gas-gap. The potential difference between the spheres is raised until a spark passes between them. The breakdown strength of a gas depends on the size of the spheres, their distance apart and a number of other factors. A spark gap may be used for the determination of the peak value of a voltage wave, and for the checking and calibrating of voltmeters and other voltage measuring devices.

The density of the gas (generally air) affects the spark-over voltage for a given gap setting. Thus the correction for any air density change must be made. The air density correction factor δ must be used.

$$\delta = \frac{P}{760} x \frac{273+20}{273+t} = 0.386\left[\frac{P}{273+t}\right]$$

The spark over voltage for a given gap setting under the standard conditions (760 torr pressure and at 20°C) must be multiplied by the correction factor to obtain the actual spark-over voltage.

The breakdown voltage of the sphere gap (figure 6.2) is almost independent of humidity of the atmosphere, but the presence of dew on the surface lowers the breakdown voltage and hence invalidates the calibrations.

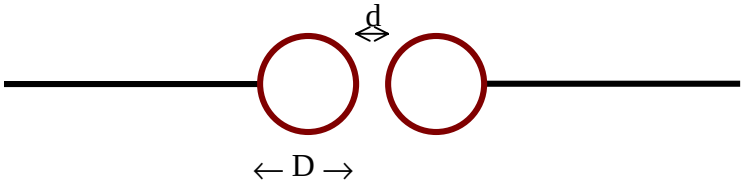

where d = gap spacing, D = sphere diameter

Figure 6.2 - Measuring spheres

The breakdown voltage characteristic (figure 6.3) has been determined for similar pairs of spheres (diameters 62.5 mm, 125 mm, 250 mm, 500 mm, 1 m and 2 m)

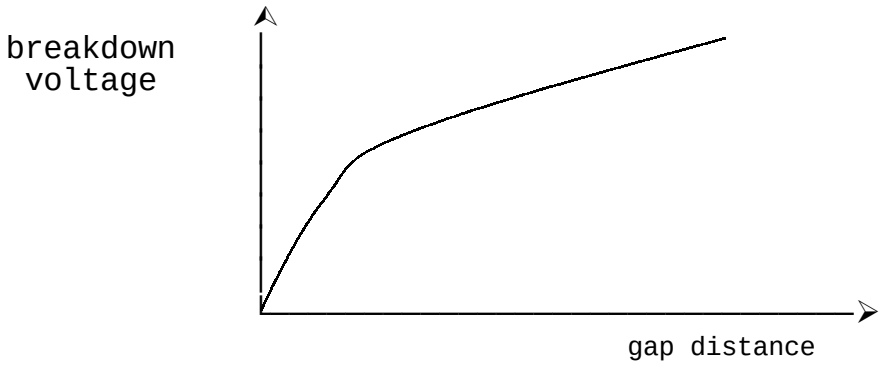

Figure 6.3 - Breakdown voltage characteristic of sphere gaps

When the gap distance is increased, the uniform field between the spheres becomes distorted, and accuracy falls. The limits of accuracy are dependant on the ratio of the spacing **d** to the sphere diameter **D**, as follows.

d	< 0.5 D,	accuracy = ± 3 %
0.75 D > d	> 0.5 D,	accuracy = ± 5 %

For accurate measurement purposes, gap distances in excess of 0.75D are not used.

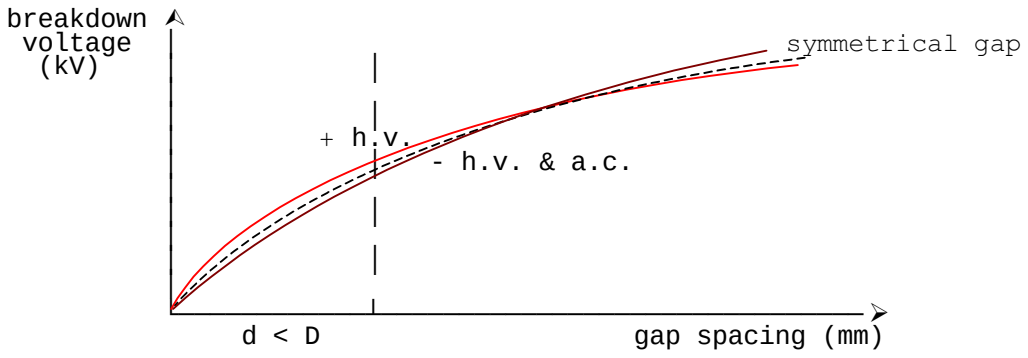

Figure 6.4 - Breakdown voltage characteristics

The breakdown voltage characteristic is also dependant on the polarity of the high voltage sphere in the case of asymmetrical gaps (i.e. gaps where one electrode is at high voltage and the other at a low voltage or earth potential). If both electrodes are at equal high voltage of opposite polarity (i.e. + ½ V and - ½ V), as in a symmetrical gap, then the polarity has no effect. Figure 6.4 shows these breakdown voltage variations.

In the case of the asymmetrical gap, there are two breakdown characteristics; one for the positive high voltage and the other for the negative high voltage. Since the breakdown is caused by the flow of electrons, when the high voltage electrode is positive, a higher voltage is generally necessary for breakdown than when the high voltage electrode is negative. However, when the gaps are very far apart, then the positive and the negative characteristics cross over due to various space charge effects. But this occurs well beyond the useful operating region. Under alternating voltage conditions, breakdown will occur corresponding to the lower curve (i.e. in the negative half cycle under normal gap spacings). Thus under normal conditions, the a.c. characteristic is the same as the negative characteristic.

In sphere gaps used in measurement, to obtain high accuracy, the minimum clearance to be maintained between the spheres and the neighbouring bodies and the diameter of shafts are also specified, since these also affect the accuracy (figure 6.5). There is also a tolerance specified for the radius of curvature of the spheres.

"The length of any diameter shall not differ from the correct value by more than 1% for spheres of diameter up to 100 cm or more than 2% for larger spheres".

Peak values of voltages may be measured from 2 kV up to about 2500 kV by means of spheres. One sphere may be earthed with the other being the high voltage electrode, or both may be supplied with equal positive and negative voltages with respect to earth (symmetrical gap).

When spark gaps are to be calibrated using a standard sphere gap, the two gaps should not be connected in parallel. Equivalent spacing should be determined by comparing each gap in turn with a suitable indicating instrument.

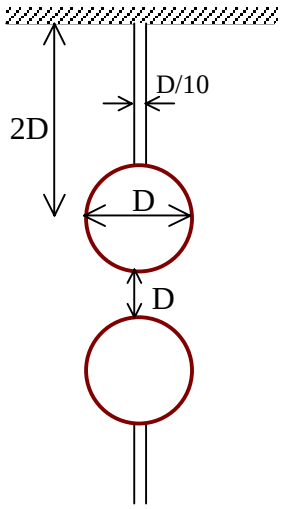

Figure 6.5 - sphere gap

Needle gaps may also be used in the measurement of voltages up to about 50 kV, but errors are caused by the variation of the sharpness of the needle gaps, and by the corona forming at the points before the gap actually sparks over. Also the effect ~~of~~ the variation of the humidity of the atmosphere on such gaps is much greater.

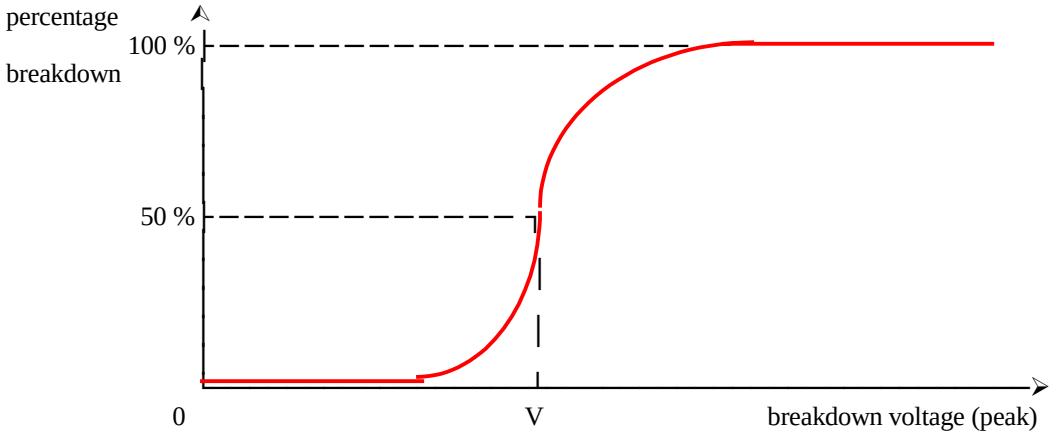

Figure 6.6 - Breakdown voltage characteristic for impulses

Usually, a resistance is used in series with the sphere gap, of about 1 Ω/V so as to limit the current under sparkover conditions to about a maximum of 1 A.

However for impulse measurements, a series resistance must not be used since this causes a large drop across the resistance. In measuring impulse voltages, since the breakdown does not occur at exactly the same value of voltage each time, what is generally specified is the 50 % breakdown value. A number of impulses of the same value is applied and a record is kept of the number of times breakdown occurs, and a histogram is plotted with the peak value of the impulse voltage and the percentage of breakdown (figure 6.6).

6.2 Transformer and potential divider methods of measurement

6.2.1 Transformer ratio method

The use of the primary voltage to estimate the secondary voltage is a fairly rough method of measurement, but is satisfactory enough for most ac tests. In this method (figure 6.7), the voltage on the low voltage side of the high-tension transformer is measured. The actual voltage across the load is not measured.

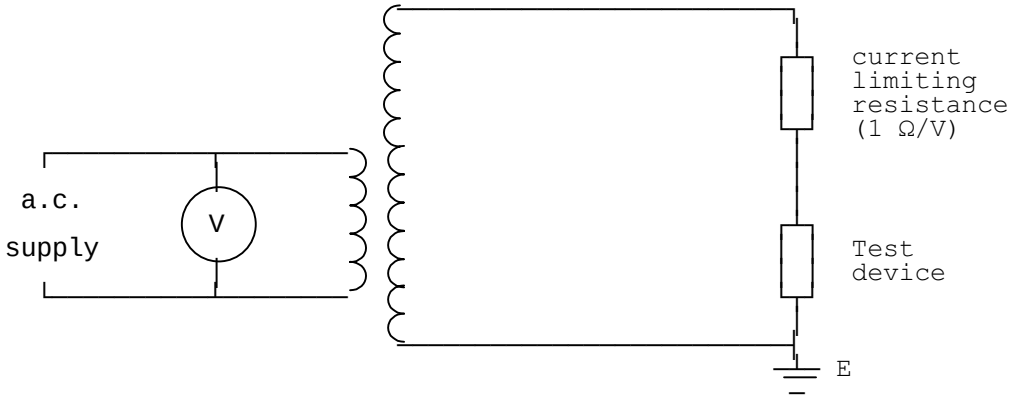

Figure 6.7 - transformer ratio method

Since the current taken by the device under test is usually very small, currents such as due to corona may cause considerable error in the measured voltage. This method measures the rms voltage. In order to determine the peak value it is necessary to determine the wave form of the secondary voltage.

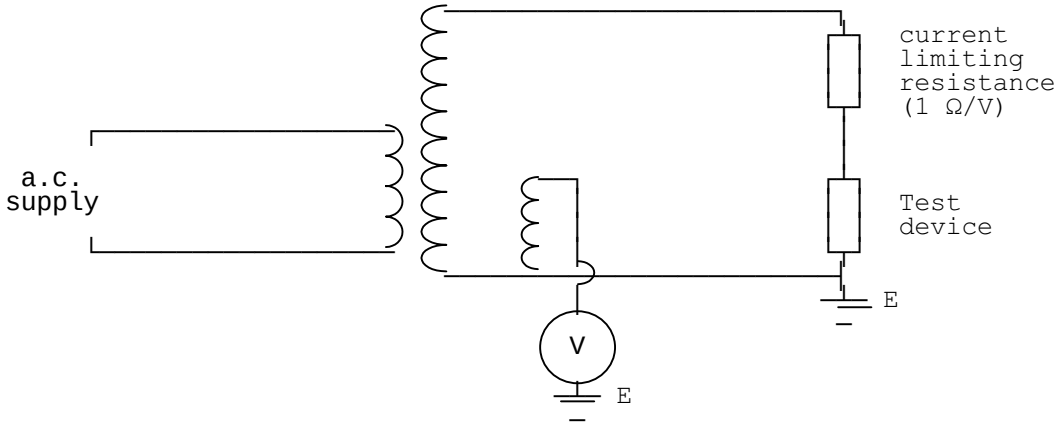

Figure 6.8 - with additional potential winding

Some high voltage transformers (figure 6.8) carry a separate voltmeter-coil having a number of turns which is a definite fraction of the secondary turns. This method cannot be used with the cascade arrangement of the transformers.

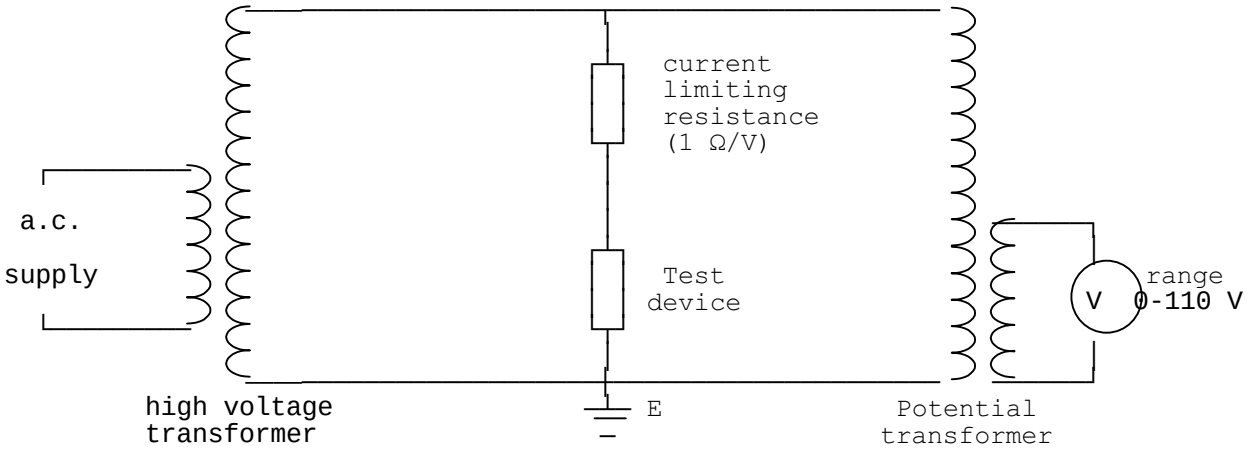

Figure 6.9 - with potential transformer

It may also be possible to have a potential transformer connected across the test device and the voltage measured, however this is an expensive arrangement.

Even this method may not be very satisfactory under very high voltage conditions and the series resistance method of measurement may be used.

Series resistance method of measurement

In the series resistance method a high series resistance (specially designed to withstand high voltage) and resistance of 20 kΩ/V, is used with micro-ammeter (having a 50 μA movement). This method is applicable for both ac and dc. A number of resistances would be necessary in series, and to prevent leakage current, we would have to have the whole system in a insulated container, which is earthed for shielding purposes. As a safety measure, a safety gap or neon lamp is connected across the micro-ammeter. If we use a stable supply (of accuracy 0.10%) we would finally end up with an accuracy of 1%.

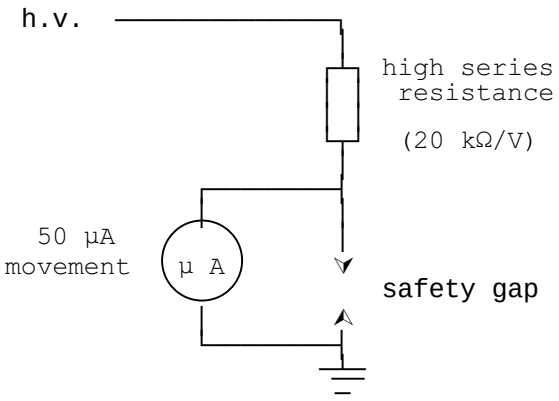

Figure 6.10 - Series resistor microammeter

When the above method is used for alternating voltages, there would be the effect of the distributed capacitances as well. The capacitive effects can be reduced by providing a suitable screen, or by balancing the capacitance.

6.2.2 Resistive potential divider method

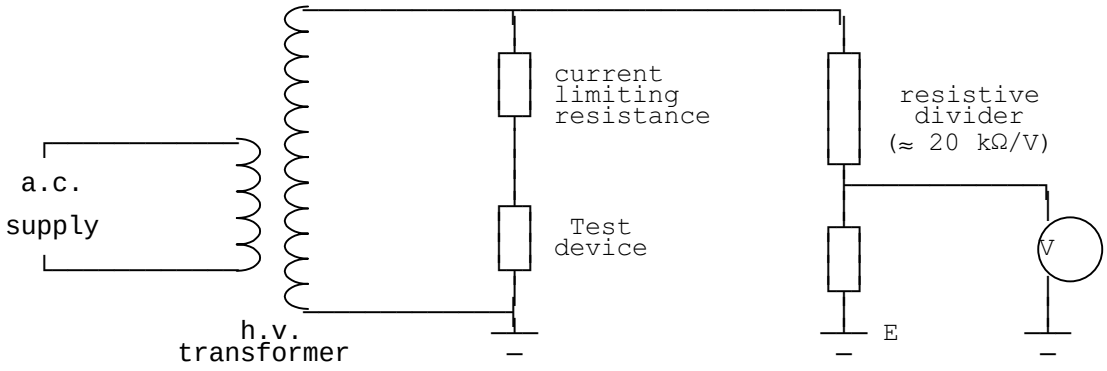

Figure 6.11 - Resistive potential divider method

In this method, a high resistance potential divider is connected across the high-voltage winding, and a definite fraction of the total voltage is measured by means of a low voltage voltmeter.

Under alternating conditions there would be distributed capacitances. One method of eliminating this would be to have a distributed screen of many sections and using an auxiliary potential divider to give fixed potential to the screens.

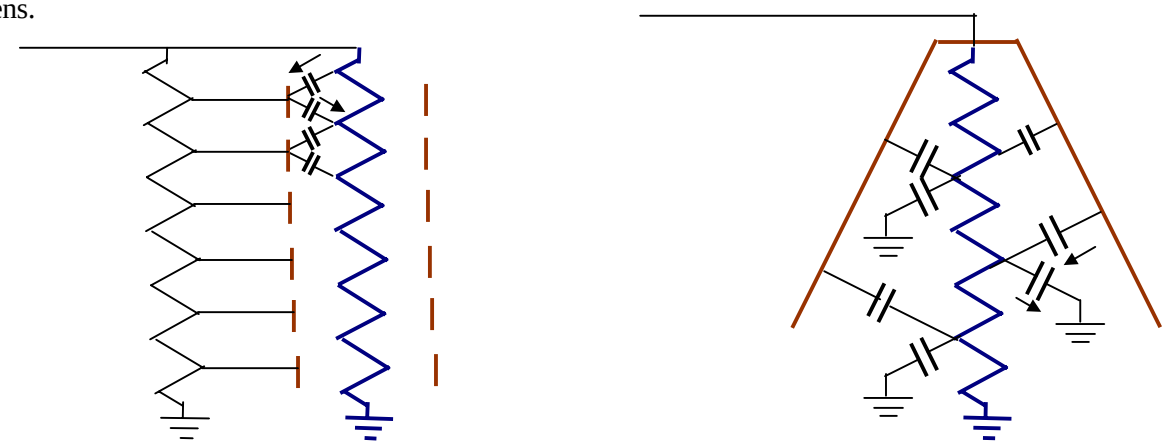

Figure 6.12 - Screening of resistive dividers

The currents flowing in the capacitances would be opposite in directions at each half of the screen so that there would be no net capacitive current (Figure 6.12 (a)).

It also possible to have a metal conical screen (Figure 6.12 (b)). The design has to be done by trial and error. There would be capacitances to the conical screen as well as capacitances to earth, so that if at any point the capacitive current from conical screen to the point is equal to that from the point to the earth, then the capacitances would have no net effect.

6.2.3 Capacitive potential divider method

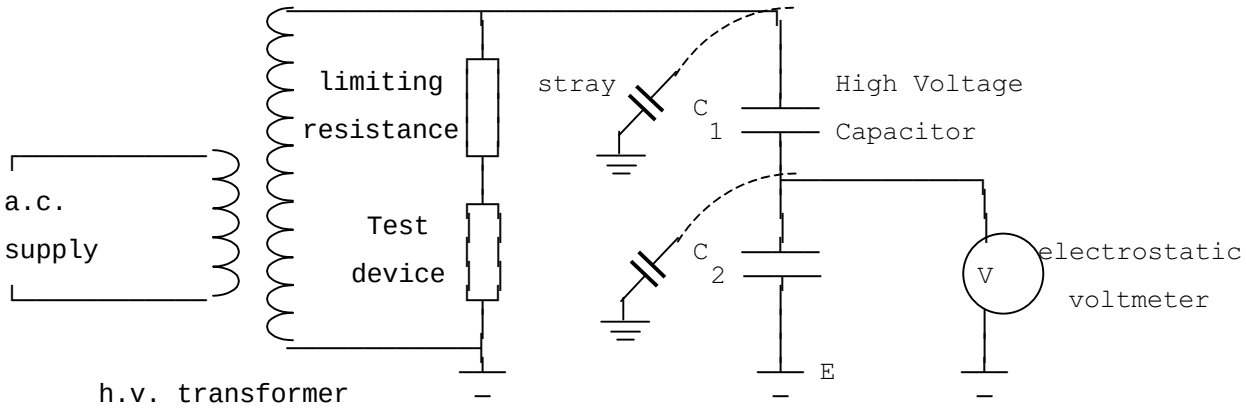

Figure 6.13 - Capacitive potential divider method

For alternating work, instead of using a resistive potential divider, we could use a capacitive potential divider. In this two capacitances C_1 and C_2 are used in series, the electrostatic voltmeter being connected across the lower capacitor.

If the system is kept at a fixed position, we can make corrections for the fixed stray capacitances. Or if screens are used, the capacitance to the screen would be a constant,and we could lump them up with the capacitances of the arms.

Neglecting the capacitance of the voltmeter (or lumping the electrostatic voltmeter capacitance with C_2) the effective capacitance of C_1 and C_2 in series is $C_1C_2/(C_1+C_2)$, and since the charge is the same,

$$\text{Voltage across } C_2 = \frac{1/C_2}{(C_1 + C_2)/C_1 C_2}.V = \frac{C_1}{C_1 + C_2}.V$$

The capacitance of h.v. standard capacitor must be accurately known, and the capacitance must be free from dielectric losses.For this reason, air capacitances are always used for this purpose.This method also measures the r.m.s. value.

It is sometimes more useful to have a measure of the peak value of the alternating voltage rather than the r.m.s. value,since it is the peak value of the applied voltage which produces the actual breakdown stress in the material under test.

If the shape of the voltage waveform is known, the peak voltage may be obtained from the r.m.s. voltage.It is often more satisfactory however, to use some method of voltage measurement which gives the peak value of the voltage directly.

6.2.4 Matching of Potential dividers

When waveforms are observed on the oscilloscope, through a potential divider, a cable is necessary to connect the test waveform to the oscilloscope, and also to cause a small delay between the arrival of the trigger pulse and the waveform (Figure 6.14).

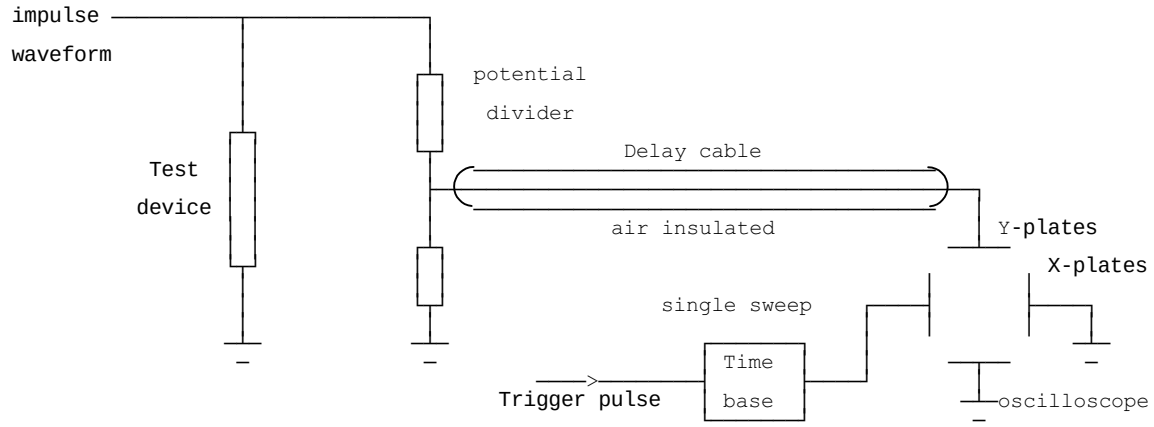

Figure 6.14 - Observation of impulse waveform through potential divider

If the delay cable is lossless , then it may be represented by purely inductances and capacitors, so that the surge impedance of cable or delay network = Zo = $[z/y]^{1/2}$. In a lossless cable , Zo is purely resistive.

$$\text{Velocity of the wave in cable} = \frac{1}{\sqrt{L\,C}} \approx \frac{1}{\sqrt{\mu_0 \varepsilon}} = \frac{3 \times 10^8}{\sqrt{\varepsilon_r}}$$

The oscilloscope can display a maximum of about 50 V to 100 V and thus the impulse voltage must be reduced by a suitable potential divider. The requirement of the potential divider used are that it reduces the applied voltage without producing any distortion (i.e: the ratio of the potential divider does not vary with time or frequency). The potential divider can be of two types.

(i) Resistive
and (ii)Capacitive.

In practice , neither case is obtained in the pure form, but a mixture of both.The capacitive effect in the resistive divider is much more than the resistive effect on the capacitive divider.

In the case of the resistive divider , the lower arm of the divider has its resistance fixed by the surge impedance of the cable used (for matching) and by the wave-tail requirements of the impulse generator circuit (if any impulse generator is used).The ratio of the divider is determined by the sensitivity of the C.R.O and the voltage.

The capacitive divider is generally bulkier than the resistive divider , but has several advantages. It can be used as part of the wavefront forming circuit. The self capacitance of the cable connecting the device to the C.R.O adds to the capacitance of the cable connecting the divider to the oscilloscope adds to the capacitance of the lower arm.

When the initial part of the surge enters the cable, it acts as a transmission line and presents its surge impedance to the surge, but when the line becomes charged, it behaves as a capacitor.

When using potential dividers, it is necessary to suitably terminate the cable at the two ends so as to have perfect matching of the cables at two ends.

Resistive potential dividers

There are three ways in which they may be matched to delay cables.

(1) Matching at potential divider end only:

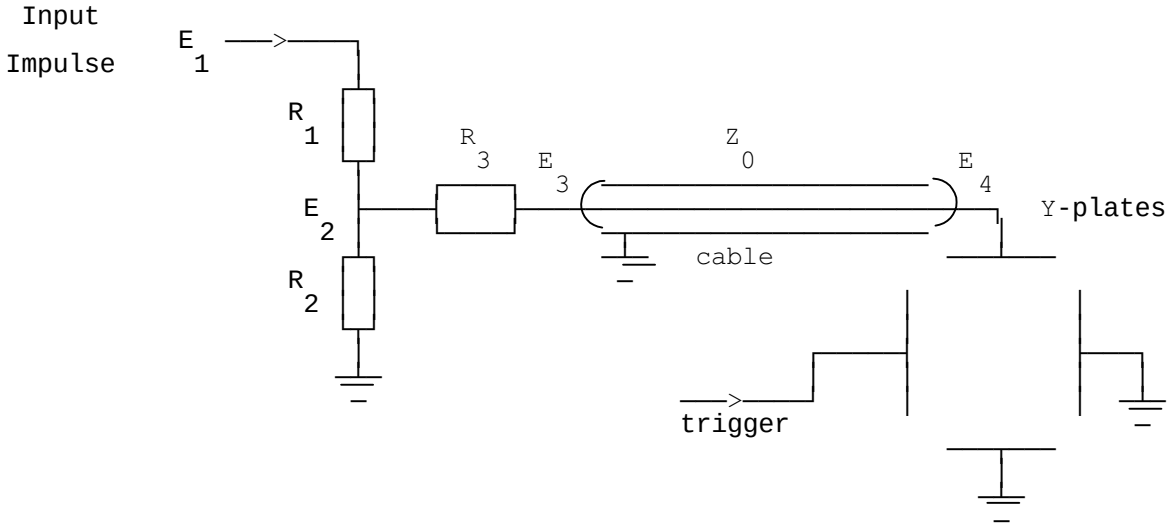

Figure 6.15 - Matching of resistive divider at sending end only

In this arrangement, the receiving (ie: the end connected across the CRO Y-plates) is kept on open circuit, and we try to obtain perfect matching at the sending end, so that there is no reflection, and perfect reflection at the receiving end.

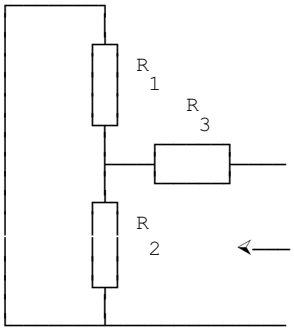

Figure 6.16

For perfect matching at the sending end, the equivalent impedance of the section before the cable must be Z_O

Impedance $= R_3 + R_1//R_2$

$= R_3 + R_1.R_2/(R_1 + R_2)$

$= Z_O$ for perfect matching at s.e

If $R_1 >> R_2$ as usually is, then we have $R1//R2 \approx R2$, $\therefore Z_O = R_2 + R_3$

At the junction of the divider **E_2**, the equivalent impedance to earth Z_1 is given by

$$Z_1 = R_2 // (R_3 + Z_0) = \frac{R_2(R_3 + Z_0)}{(R_2 + R_3 + Z_0)} = \frac{R_2(R_3 + Z_0)}{2Z_0}, \because Z_0 = R_2 + R_3$$

$$\therefore \text{ voltage at junction } E_2 = \frac{Z_1}{Z_1 + R_1} \cdot E_1 = \frac{R_2(R_3 + Z_0)}{2Z_0(Z_1 + R_1)} \cdot E_1$$

$$\text{so that } E_3 = \frac{Z_0}{R_3 + Z_0} \cdot E_2 = \frac{Z_0}{(R_3 + Z_0)} \cdot \frac{R_2(R_3 + Z_0)}{2Z_0(Z_1 + R_1)} \cdot E_1 = \frac{R_2}{2(Z_1 + R_1)} \cdot E_1$$

This voltage waveform E_3 travels towards the receiving end and is reflected at the open end without change of sign, so that the voltage transmitted to the CRO is 2 E_3.

$$\therefore E_r = E_4 = \frac{R_2}{Z_1 + R_1} \cdot E_1, \quad \text{where } Z_1 = \frac{R_2(R_3 + Z_0)}{2Z_0}$$

OR If the lower arm itself is balanced, that is $R_2 = Z_0$, then $R_3 = 0$ and the voltage transmitted to the oscilloscope is given by

$$E_r = \frac{Z_0}{R_1 + \frac{1}{2}Z_0} \cdot E_1$$

(2) Matching the cable at the oscilloscope end only:

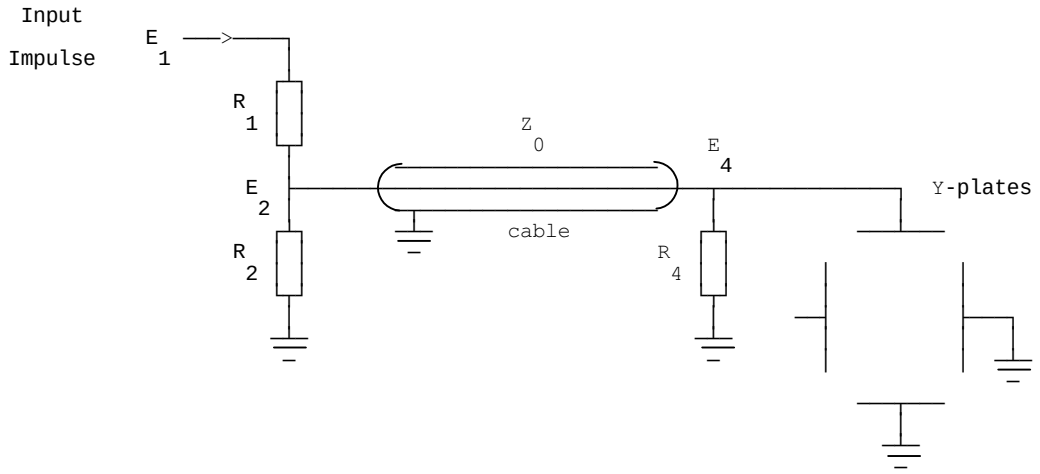

Figure 6.17 - Matching of resistive divider at receiving end only

In this arrangement, the cable is matched only at the receiving end so that there will no reflection at this end.

$$\text{Equivalent impedance at E 2} = Z_1 = R_2 // Z_0 = \frac{R_2 Z_0}{R_2 + Z_0}$$

$$\therefore E_2 = \frac{Z_1}{Z_1 + R_1} \cdot E_1$$

Since the cable is properly matched at the receiving end, $R_4 = Z_0$

The voltage wave E_2 travels along the cable , and since there is proper matching at the receiving end, it is transmitted with out any reflection.

$$\therefore E_4 = E_2 = \frac{Z_1}{Z_1 + R_1} \cdot E_1 = \frac{R_2 Z_0}{R_2 Z_0 + + (R_2 + Z_0) R_1} \cdot E_1 = \frac{R_2 Z_0}{(R_1 + R_2) Z_0 + R_1 R_2} \cdot E_1$$

For given values of R_1, R_2 and E_1 this arrangement gives smaller voltages at the C.R.O than when only the divider end is matched.

If the point E_2 is not connected to earth through the resistance R_2, (ie. if $R_2 = \infty$), then we have

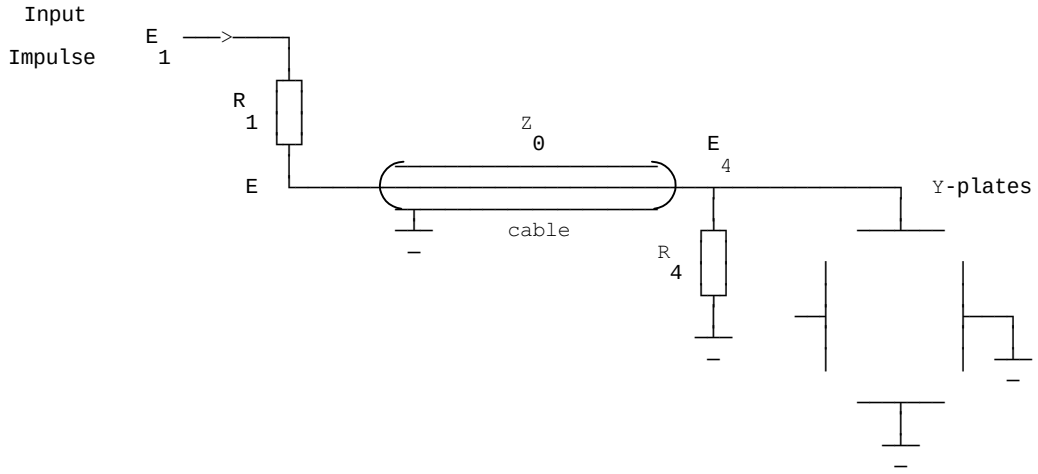

Figure 6.18 - Matching of resistive divider at receiving end (with $R_2 = \infty$)

For this case the voltage at the oscilloscope is given by

$$E_4 = \underset{R_2 \to \infty}{Lt} \frac{R_2 Z_0}{(R_1 + R_2) Z_0 + R_1 R_2} \cdot E_1 = \frac{Z_0}{Z_0 + R_1} \cdot E_1$$

(3) Matching at both ends of the cable :

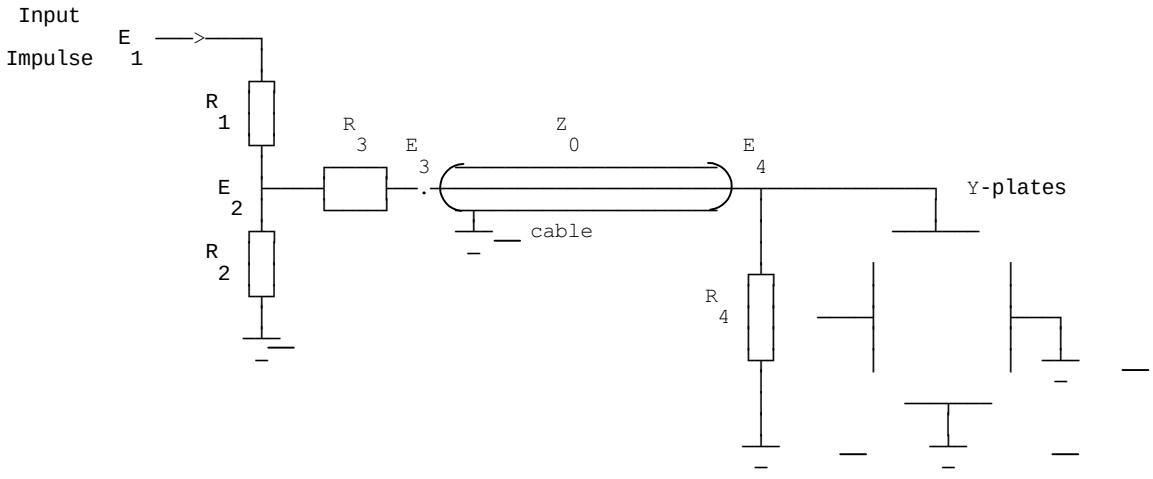

Figure 6.19 - Matching of resistive divider at both ends

In this case, the cable is matched at both ends . With this termination there is no reflection at either end. This arrangement is used when it is necessary to reduce to a minimum the irregularities produced in the delay cable circuit.

As before, for perfect matching at receiving end, $R_4 = Z_0$
and for perfect matching at sending end, $R_2 + R_3 = Z_0$.

Also, at E_2, the equivalent impedance Z_1 to earth is given by

$$Z_1 = R_2 // (R_3 + Z_0) = \frac{R_2(R_3 + Z_0)}{(R_2 + R_3 + Z_0)} = \frac{R_2(R_3 + Z_0)}{2Z_0}, \because Z_0 = R_2 + R_3$$

$$\therefore \text{ voltage at junction } E_2 = \frac{Z_1}{Z_1 + R_1} \cdot E_1 = \frac{R_2(R_3 + Z_0)}{2Z_0(Z_1 + R_1)} \cdot E_1$$

$$\text{so that } E_3 = \frac{Z_0}{R_3 + Z_0} \cdot E_2 = \frac{Z_0}{(R_3 + Z_0)} \cdot \frac{R_2(R_3 + Z_0)}{2Z_0(Z_1 + R_1)} \cdot E_1 = \frac{R_2}{2(Z_1 + R_1)} \cdot E_1$$

Due to perfect matching at the receiving end, this is transmitted without any reflections.

$$\therefore E_4 = E_3 = \frac{R_2}{2(R_1 + Z_1)} \cdot E_1$$

The stray capacitances present between the turns of the resistances would make the current distribution along the resistance non-uniform. When the rate of change of voltage is high, then the errors due to the capacitances are large (especially in waves such as chopped waves).

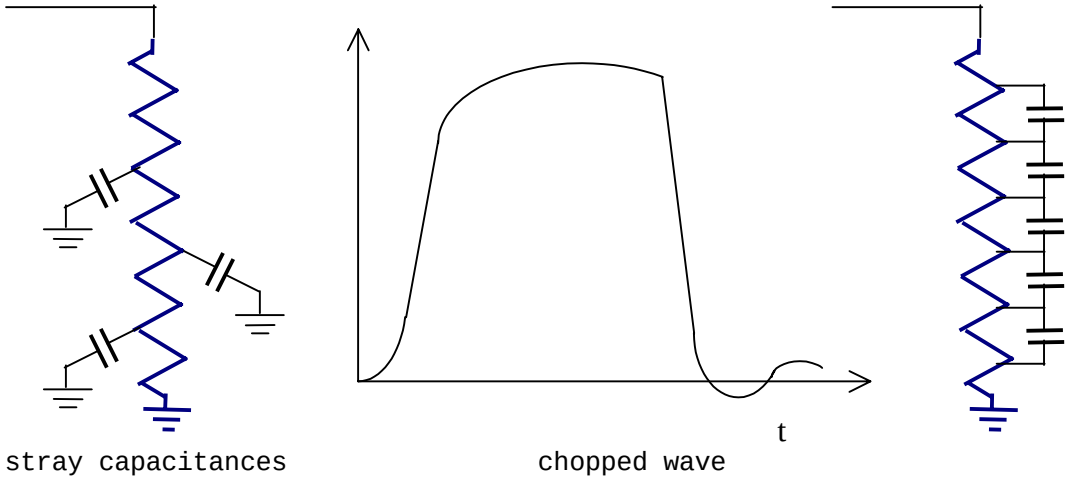

Figure 6.20 - Stray capacitances and chopped wave

By having a distributed capacitance along the resistance which are larger than the stray capacitances, the effect of the stray capacitance may be eliminated.

An easier way to compensate for the stray capacitances is by having capacitive potential divider instead of the resistive divider.

Capacitive potential dividers

The effect of stray capacitance may be made constant, in a capacitive divider, by shielding the potential, divider; and hence make an allowance for it. The disadvantage of the capacitive potential divider is that proper termination cannot be done.

There are two methods used to couple capacitive dividers to delay cables.

(1) Simple capacitor connection

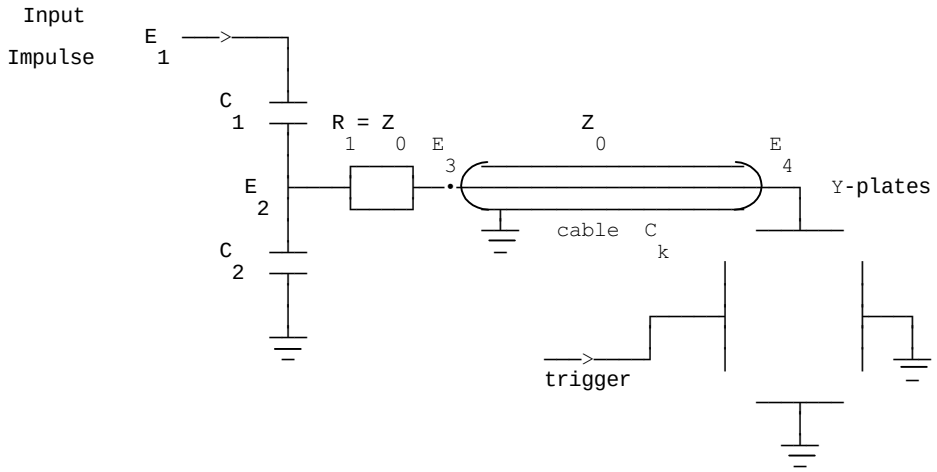

Figure 6.21 - Matching of capacitive divider (simple capacitor connection)

In the simple capacitor connection, we attempt to prevent reflections at sending end.

The sending end is terminated with a resistance $R_1 = Z_o$ in series with the cable. Initially the cable capacitance would not have charged up, and only C_1 and C_2 would be present.

Initially,

$$E_2 = E_1 . \frac{C_1}{C_1 + C_2}$$

$$E_3 = E_2 . \frac{Z_0}{Z_0 + R_1} = \tfrac{1}{2} E_2, \ \because \textit{for matching} \ R_1 = Z_0$$

Due to perfect reflection at the receiving end, E_3 travelling towards it would be reflected and hence the voltage transmitted to the CRO would be doubled.

$$\text{i.e. } E_r = 2 E_3 = 2 \times \tfrac{1}{2} E_2 = E_2 = E_1 . \frac{C_1}{C_1 + C_2}$$

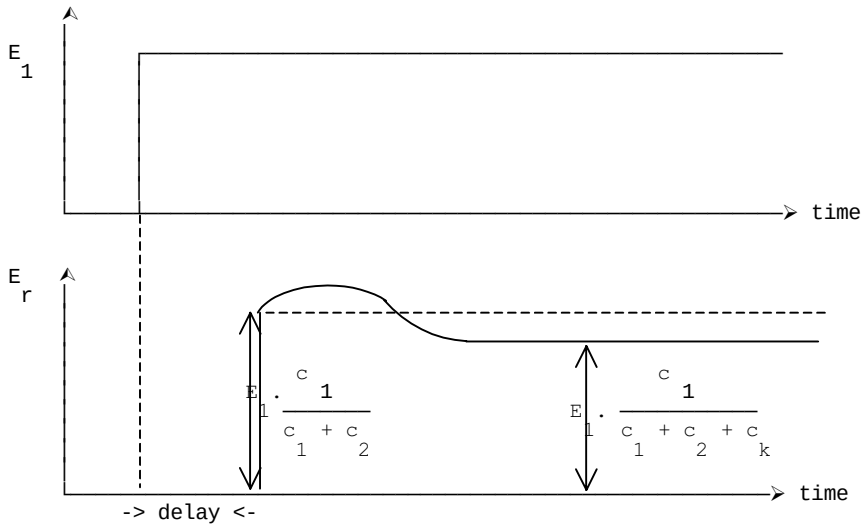

Figure 6.22 - Waveforms for simple capacitor connection

This gives the amplitude of the voltage wave as it reaches the Y-plates. As time goes on, the cable capacitance charges up and behaves as a capacitance in parallel with the lower arm.

Therefore, after infinite time, voltage at Y-plates would be given by

$$E_r = E_1 . \frac{C_1}{C_1 + C_2 + C_k}$$

Thus the ratio of the input voltage to the output voltage of the capacitive divider varies with time and we get a distorted output waveform displayed on the oscilloscope. Thus the capacitive potential divider introduces distortion. The difference between the initial and final ratios will be appreciable unless C_2 is at least 10 times that of the cable capacitance C_k, in which case the error would be about 10%.

This error can be reduced by transferring part of the low voltage capacitor to the C.R.O. end of the delay cable and connecting it in series with a resistance equal to the cable surge impedance Z_0 (resistive if cable is lossless).

(2) Split capacitor connection

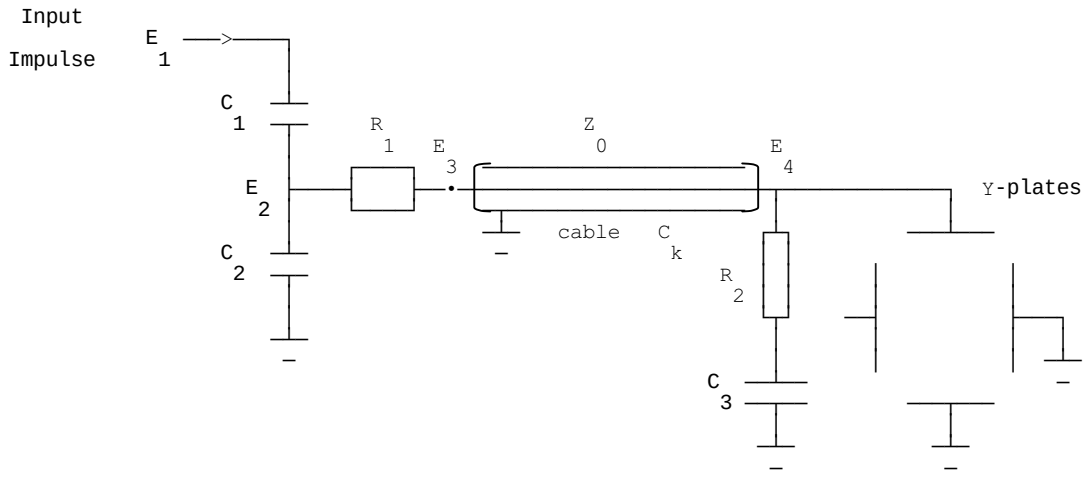

Figure 6.23 - Matching of capacitive divider (simple capacitor connection)

In this connection, in addition to matching the cable at the sending end ($R_1 = Z_0$), it is also matched at the oscilloscope end ($R_2 = Z_0$). Further to ensure that the long term ratio remains the same as the initial ratio, the lower end capacitor is split into C_2 and C_3.

Initially the capacitances C_k and C_3 would not have charged, and only the capacitances C_1 and C_2 would be effective in the voltage ratio.

$$\text{Initially} \quad E_2 = E_1 . \frac{C_1}{C_1 + C_2}$$

$$\text{also} \quad E_3 = E_2 . \frac{Z_0}{R_1 + Z_0} = \tfrac{1}{2} E_2, \quad \because R_1 = Z_0 \text{ for matching}$$

Due to perfect matching at the receiving end, the voltage wave is transmitted without any reflection. Therefore the observed voltage is given by

$$\therefore \quad E_r = E_3 = \tfrac{1}{2} E_2 = \frac{E_1}{2} . \frac{C_1}{C_1 + C_2}$$

After infinite time, the capacitances C_k and C_3 would have completely charged up, and the receiving end in effect would be on open circuit, since C_3 would no longer be conducting.

Since all the capacitors C_2, C_3 and C_k are in parallel,

$$E_2 = E_1 \cdot \frac{C_1}{C_1 + C_2 + C_3 + C_k}$$

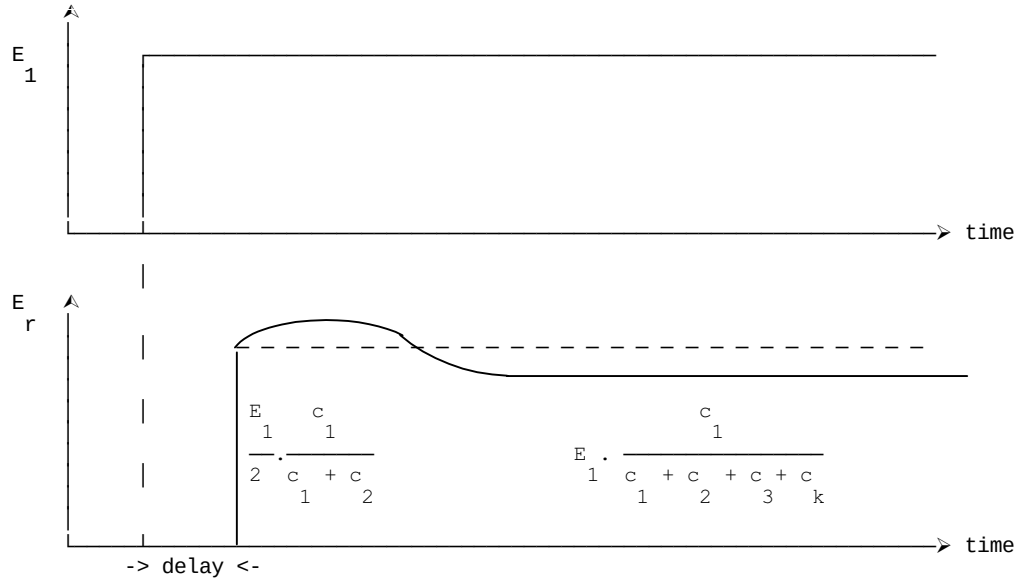

Figure 6.24 - Waveforms for split capacitor connection

If the initial and the final values of the ratio are made equal, then the distortion is reduced to a great degree.

$$\frac{E_1}{2} \cdot \frac{C_1}{C_1 + C_2} = E_1 \cdot \frac{C_1}{C_1 + C_2 + C_3 + C_k}$$

$$\text{i.e. } C_1 + C_2 = C_3 + C_k$$

If this condition is satisfied, then the distortion is low and near faithful reproduction can be expected as shown in figure 6.25.

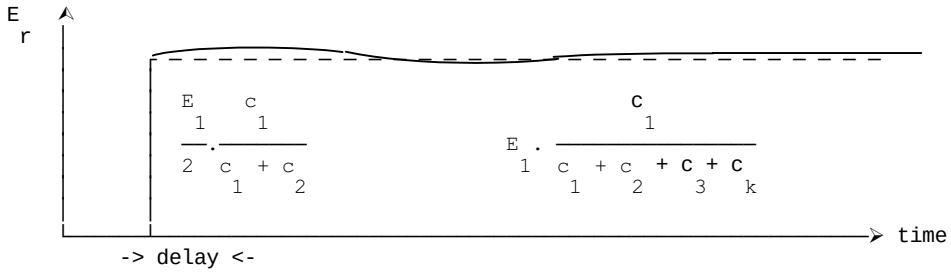

Figure 6.25 - Waveforms for split capacitor connection (low distortion)

6.3 Measurement of Surges

6.3.1 Klydonograph

Lightning is probably the most spectacular of the high voltage phenomena. Very little is known about lightning, as it is not possible to create lightning or to obtain a lightning strike when and where we please. Also very little is known of its effects and the voltages of the surges that appear in the transmission lines due to it.

The phenomena of the lightning could be studied to a certain extent by the surges it produces on the transmission lines. The frequency of occurrence of surge voltages and the magnitude of the surge it produces on the transmission lines could be studied using Litchenberg patterns obtained by using a Klydonograph.

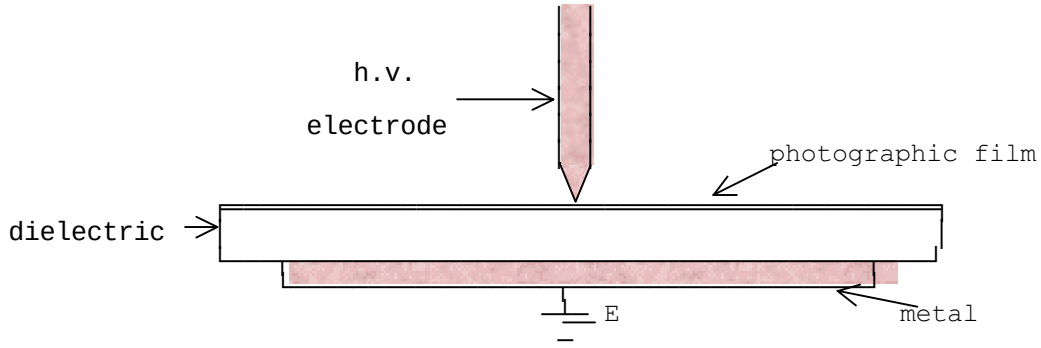

Figure 6.26 - Klydonograph

The Klydonograph (Figure 6.26) has a dielectric sheet, on the surface of which is placed a photographic film. The insulator material separates a plane electrode on one side, and a pointed electrode which is just in contact with the photographic film. The high voltage is applied to the pointed electrode and the other electrode is generally earthed. The photographic film can be made to rotate continuously by a clockwork mechanism. The apparatus is enclosed in a blackened box so as not to expose the photographic film. When an impulse voltage is applied to the high voltage electrode, the resultant photograph shows the growth of filamentary streamers which develop outwards from the electrode.

This imprint on the photographic plate is not due to normal photographic action, and occurs even through there is no visible discharge between the electrodes. If flashover of the insulator or a visible discharge occurs, then the film would become exposed and no patterns would be obtained. These patterns obtained on the photographic film are known as Litchenberg patterns. When a positive high voltage is applied to the upper electrode, clearly defined steamers which lie almost within a definite circle is obtained. If the voltage applied is negative, then the observed pattern is blurred and the radius of the pattern is much smaller. For both types of surges, the radius of the pattern obtained increases with increase in voltage.

For a given apparatus with a fixed thickness of dielectric, the radius of the pattern obtained (Figure 6.27a) is a definite function of the voltage applied, and thus by calibrating the Klydonograph using a high voltage oscilloscope and known surge voltages, it is possible to use this apparatus to record surges that occur. If the positive voltage applied is increased beyond a certain value, branching may occur along the branches coming out from the electrode. The maximum voltage that can be measured using a Klydonograph is dependant on the thickness of the dielectric material. Thus to measure voltages beyond this value,such as occuring in transmission lines, an insulator string potential divider is used. (Figure 6.27b)

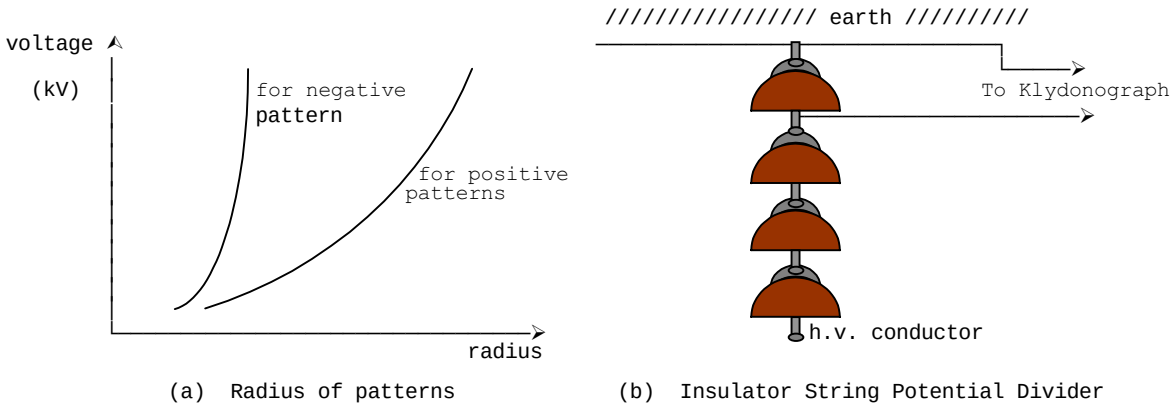

Figure 6.27 - Klydonograph

For a fixed apparatus, for a positive high voltage applied as the top electrode, the variation of the applied voltage with radius of the pattern obtained is quite definite and the radius is quite large. In the case of the negative high voltages, the characteristics is much more variable and the radius is much smaller.

Thus usually it is preferable to use the positive pattern for the measurement of high voltage surges. The applied voltage versus radius of pattern characteristics of the Litchenberg pattern is shown in figure 6.28.

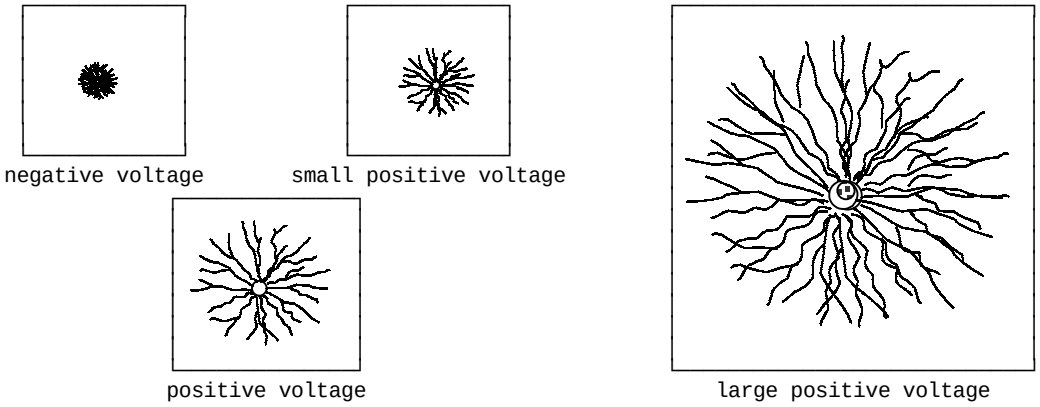

Figure 6.28 - Litchenberg patterns

Since the surges due to lightning may be either positive or negative, and since it is preferable to observe the positive pattern in either case, we make a modification to the apparatus.

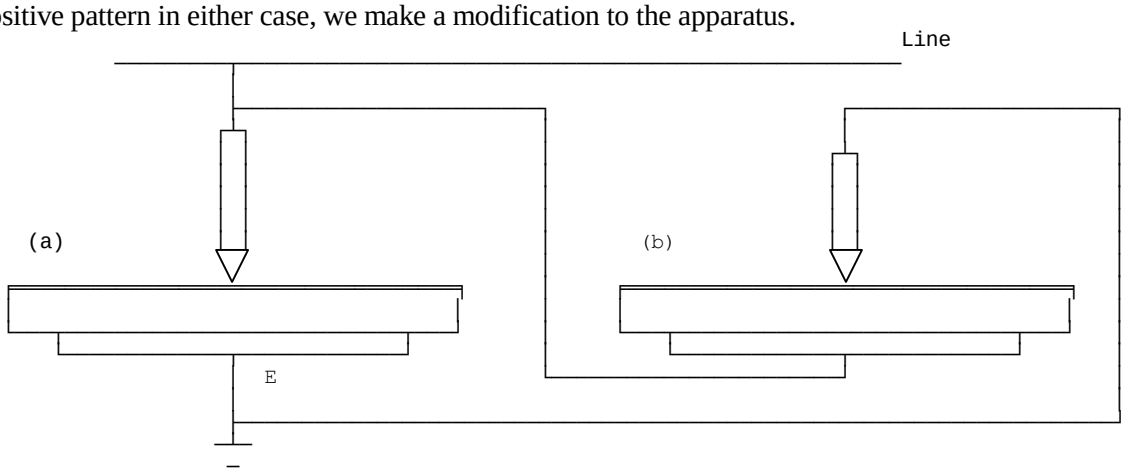

Figure 6.29 - Klydonograph for measurement of both polarities

In the modification shown in figure 6.29, there are two such instruments, with the electrode connections made in opposite directions. Thus in the modification, if a positive surge comes, then a positive pattern would be recorded in (a) and a negative pattern in (b), of which the pattern on (b) can be used for the measurement of the positive surge.

In the case of a negative surge, the opposite would happen, and the pattern on (b) could be used for the measurement. Thus the magnitude of the surge as well as the polarity could be determined from the Litchenberg patterns on (a) and (b). Since the photographic film is continuously moving, it is possible in some elaborate apparatus to record the date and time occurrence of the surge as well.

6.4 General measurements

6.4.1 Peak reading voltmeters

(i) Capacitor charging method

In the positive half cycle, the capacitor charges up to the peak value, and when the voltage falls it discharges (very slightly) through the milliammeter, and so that the voltage across the capacitor is very nearly a constant at the peak value and the current is thus proportional to the peak value. (The time constant RC of the above circuit must be very high in comparison to the period of the applied voltage).

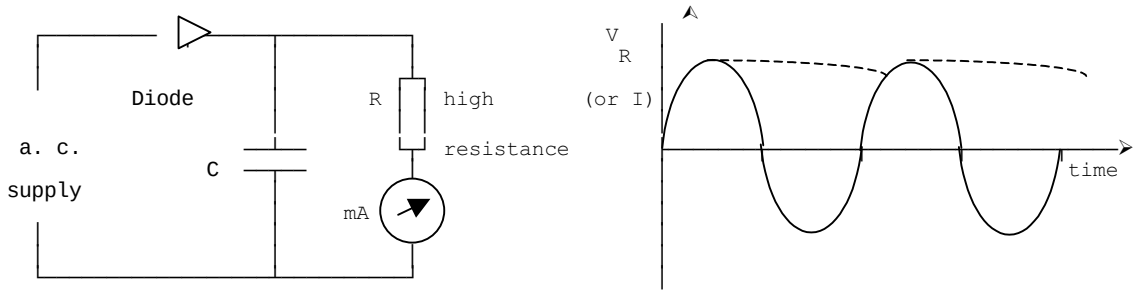

Figure 6.30 - Capacitor charging method

(ii) Using neon lamp

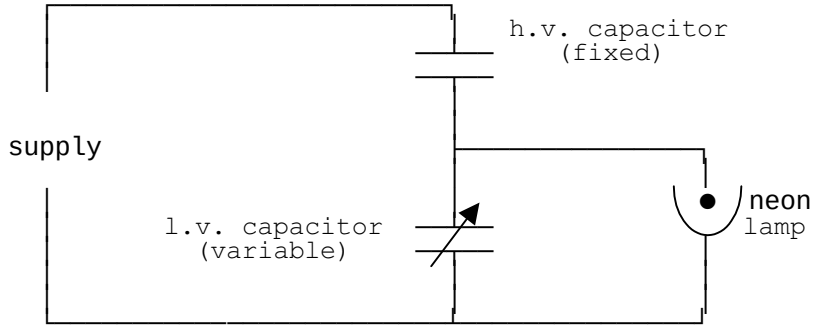

Figure 6.31 - Using neon lamp

A neon tube (if the voltage at which the lamp strikes is known) can be used with a capacitive potential divider to obtain the peak value of an applied voltage waveform. The low voltage variable capacitor is varied until the neon lamp strikes.

From the ratio of the capacitances, the supply voltage can be calculated. Since the extinction voltage is more constant than the striking voltage, the extinction voltage could be used as the standard. An accuracy of ± ½ % could be obtained with the striking voltage and an accuracy of ± ¼ % could be obtained with extinction voltage.

(iii) Rectifier-Capacitor current method

The best known and the most usual method of measuring the peak value is the rectified capacitor current method. A high voltage capacitor is connected to the hv supply with a rectifier ammeter in the earth connection. The indicated value will correspond to the peak value of the positive or negative half cycle. The diode used in series with the milliammeter should have a low forward resistance and a high reverse resistance a ratio of $1:10^5$ is desirable. Silicon diodes provide an ideal rectifier for the purpose.

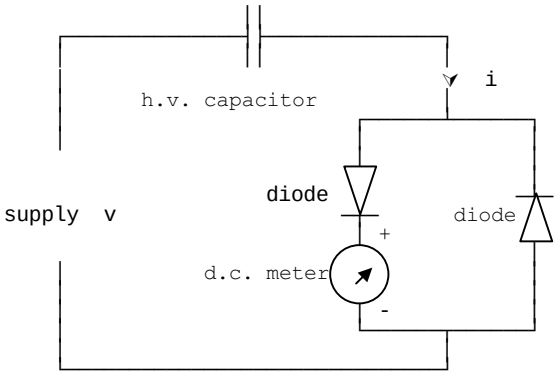

Figure 6.32 - Rectifier-capacitor current method

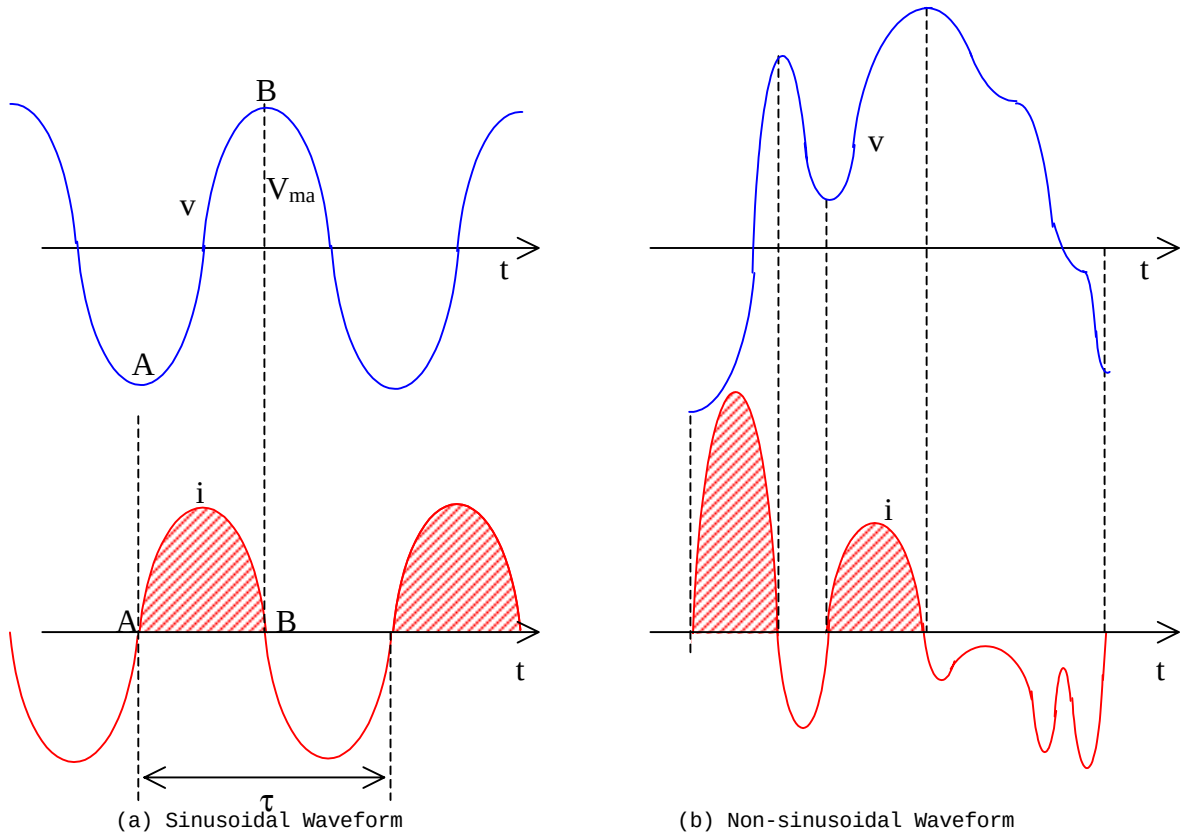

Figure 6.33 - Waveforms for peak measurement

For the circuit shown in figure 6.32, and the corresponding waveforms in figure 6.33 (a),

$$i = C\frac{dv}{dt}, \text{ so that } \int_A^B i.dt = \int_A^B C.dV$$

$$\therefore I_{av}.\tau = C.2V_{max}, \quad \text{giving } V_{max} = \frac{\tau.I_{av}}{2C} = \frac{I_{av}}{2Cf}$$

Since a d.c meter is used it would read I_{av}, and hence would correspond to the maximum value of voltage, independent of the waveform, except in the case when there is more than one maxima and minima per cycle. In such a case the meter reading would no longer corresponds to the actual maxima (Figure 6.33(b)), but an addition of successive peak-to-peaks.

Instead of using a half wave rectifying unit as in figure 6.32, we could also used a full wave rectifying unit as shown in figure 6.34.

In this case, the reading of the meter would effectively be double giving the result

$$V_{max} = \frac{I_{av}}{4Cf}$$

Thus using either half wave or full wave rectifying units, we can obtain the peak value of the voltage independent of the wave form, if the capacitance and frequency are known from the reading of the d.c meter.

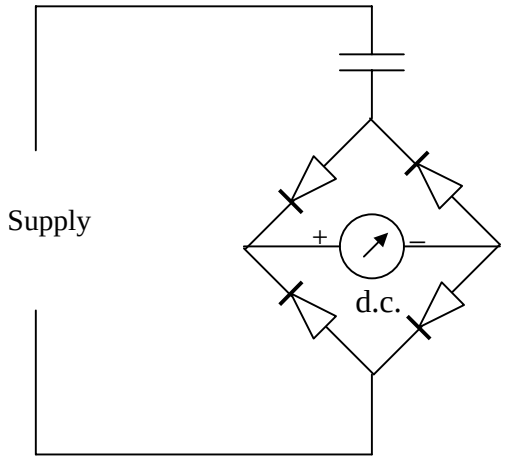

Figure 6.34 - Full wave circuit

6.4.2 Oscilloscope for measurement of fast transients

High voltage oscilloscopes are used for the study of fast transient phenomena, particularly in the work on high-voltage and on spark breakdown in small gaps.These have a high sweep speed. Since the speed is high, the intensity is lowered and hence a higher intensity is required. In these the beam should not come on till the transient comes in because;

(a) if it is stationary, the spot of high intensity would fog the photograph before the transient comes on, and

(b) if it is moving, the beam may have swept before the transient comes.

Thus the beam should be brought on just before the transient comes on, by being triggered by the transient. The transient should come on the Y-plate only shortly after the beam, so that the whole transient is clearly seen. For this a delay cable is used.

The delay cable ensures that the transient appears slightly after the beam comes on.

Such a scope can have a maximum of 50 V to 100 V applied across Y plate so that we would have to use a potential divider. For high writing speed,the anode - cathode voltage should be high (50 - 100 kV). The sweep generator should produce a single sweep (not repetitive) , as transients are not repetitive, and triggered by the signal. The delay cable causes the signal to appear at the Y-plates a fraction of a micro second after the sweep generator is triggered (100m length of cable may cause a delay of about 0.3 μs.

6.5 Measurements of capacitance and loss tangent

6.5.1 High Voltage Schering Bridge

The high voltage Schering bridge is the method most widely used for measuring capacitance and loss tangent (or

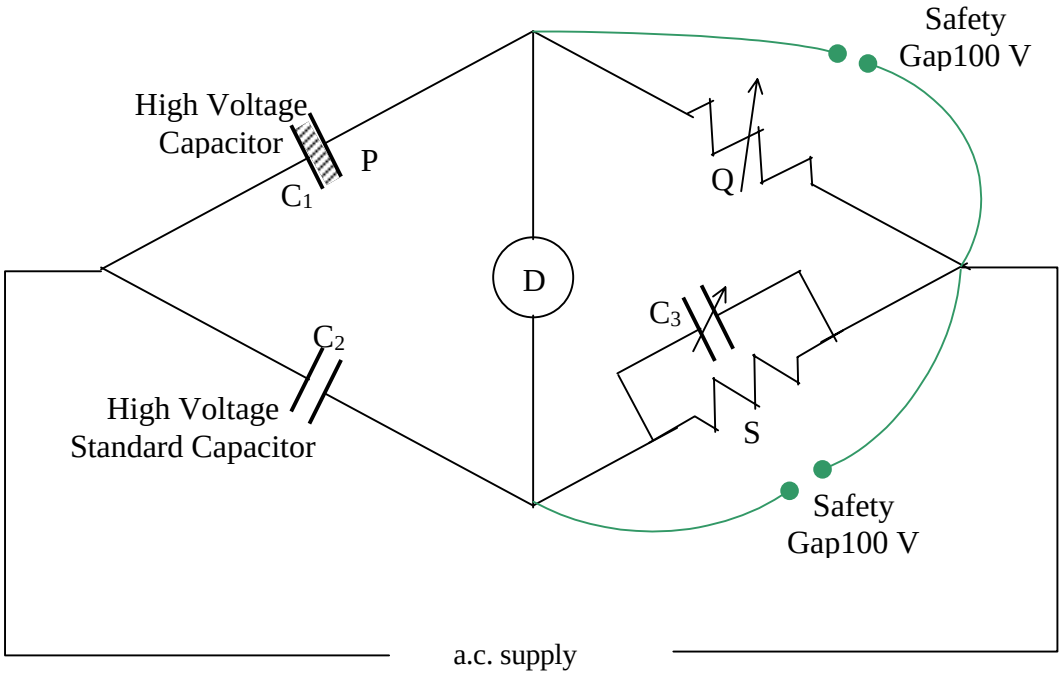

Figure 6.35 - High Voltage Schering Bridge

power factor) in dielectrics. Figure 6.35 shows the arrangement.

One arm of the bridge is the high voltage test capacitor (assumed to be represented by a series combination of capacitance C_1 and resistance P). The other three arms are a standard high voltage capacitor C_2 (generally a loss free air capacitor of value 100 to 500 pF) a variable low resistance Q, and a parallel combination of a standard low resistance S and a variable capacitance C_3.

The high voltage supply for the bridge is obtained through a high voltage transformer. For reasons of safety, only the high voltage test capacitor and the high voltage standard capacitor will be at high voltage. The other components are at low voltage and are not allowed to have voltages greater than about 100 V applied across them by means of safety gaps connected across them (The safety gaps are either gas discharge gaps or paper gaps). The impedance of these arms must thus necessarily be of values much less than that of the high voltage capacitors. For measurements at power frequencies, the detector used is a vibration galvanometer, usually of the moving magnet type (If the moving coil type is used, it has to be tuned). The arms Q and C_3 are varied to obtain balance.

It can be shown that this bridge is frequency independent, and that at balance

$$\frac{C_2}{C_1} = \frac{Q}{S}, \quad \text{also} \quad \frac{P}{Q} = \frac{C_3}{C_2}$$

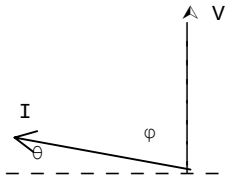

Figure 6.36

power factor angle = φ, loss angle = $\pi/2 - \varphi = \theta$

$$\theta \approx \tan\theta = \omega P C_1 = \omega C_3 S$$

The low voltage end of the bridge is usually earthed, and since the voltages across Q and S are limited to about 100 V, the detector would also be near earth potential. Thus all the variable arms and the detector can be safely handled by the operator.

It should be noted that the bridge is an unequal arm bridge, so that the relative sensitivity will be small. However, since the applied voltage is high, this is not a practical disadvantage and a reasonable variation can be obtained across the detector.

Since the value of the standard capacitor must be accurately known, there should be no distortion of the field in it. Thus a high voltage guard is provided in it design. This guard is earthed directly (which causes a small error), or kept at the same potential as the main electrode without a direct connection as shown in figure 6.37.

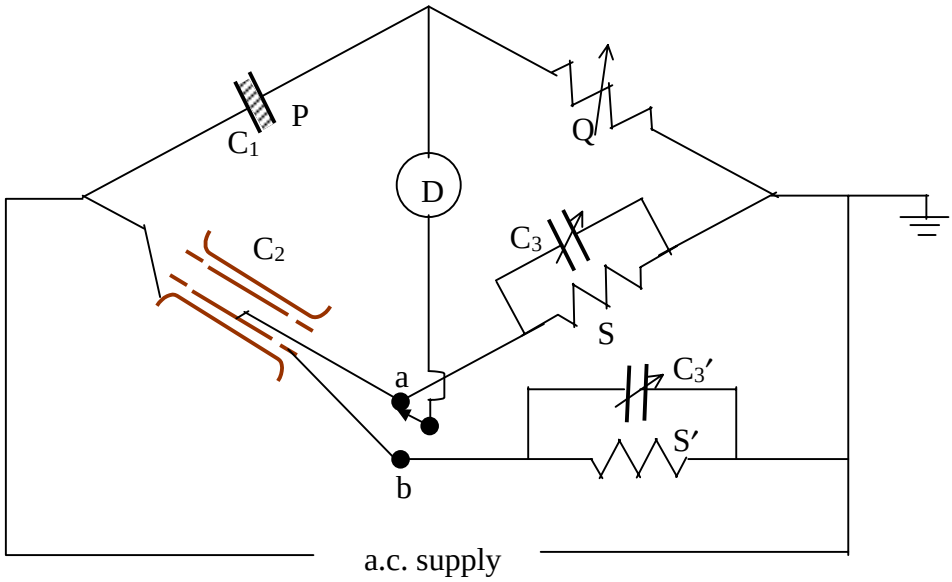

Figure 6.37 - Bridge with guarded standard capacitor

The following procedure is used to have the guard electrode at the same potential as the main electrode. The bridge is adjusted for balance with the switch in position (a) - the normal Schering Bridge. Then with the switch in position (b) the bridge is again balanced using only S' and C_3'. This ensures that finally **a** and **b** are at the same potential (same potential as the other end of the detector). Successive balance is carried out in positions **a** and **b** alternately until final balance is obtained. This connection can be used for capacitances up to 2000 pF.

When it is required to obtain higher value unknown capacitances (such as in the case of a very long cable), the circuit is modified in the following manner so that high current variable resistance standards would not be required. In this case we have a high current fixed value resistor shunted by a low current variable high resistance which acts similar to a potential divider. The expression at balance is obtained by converting the mesh consisting of r, p and Q into star form, thus obtaining the normal schering bridge arrangement.

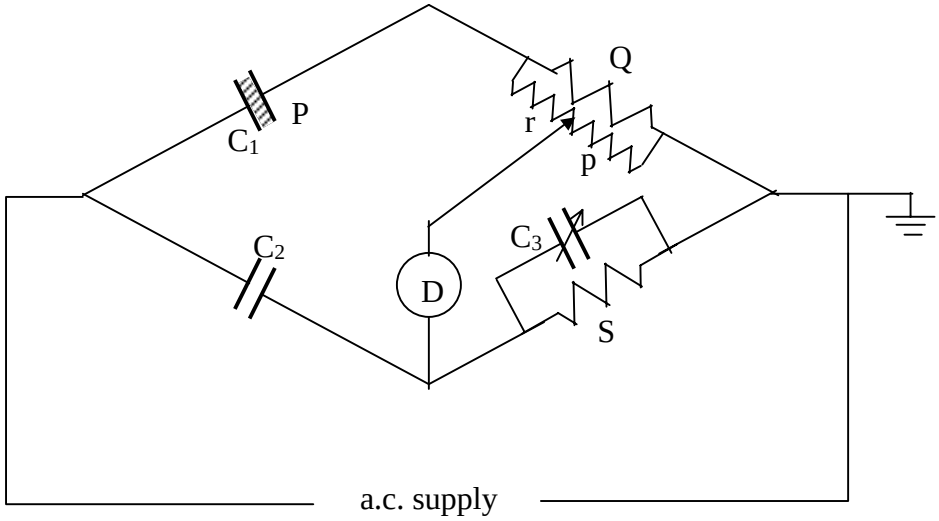

Figure 6.38 - Schering Bridge for high capacitances

At balance, it can be shown that

$$C_1 = C_2 \frac{S}{Q} \frac{Q + r + p}{p}, \quad \text{also} \quad P =$$

$$\text{so that} \quad \tan\theta = \omega C_3 S \left[1 - \frac{C_2 r}{C_3 p} \right]$$

In the case of a cable already buried or earthed, then we would have to earth the end of the source near the test capacitor. Then all the equipment, and hence the operator would have to be at a high voltage to earth. The operator can either operate the instruments using long insulated rods, or get into a Faraday cage (A cage which is raised to the same potential as the high voltage electrode so that there is no difference in potential). The earthing of the test capacitor near the detector end instead of the source end would bring the instruments near earth potential, but is not used due to the introduction of stray capacitances by this means which would cause measuring errors.

6.5.2 Dielectric loss measurement using Oscilloscope

In an oscilloscope, if two alternating voltages of the same frequency are applied to the x and y plates, the resulting figure will be an ellipse. When the two voltages are in phase, the figure will be a straight line with an enclosed area of zero. As the phase angle increases, the area increases and reaches a maximum when the phase angle difference is 90^o.

This property is made use of in dielectric loss measurements. A potential difference proportional to the applied voltage is applied to one pair of plates and a potential difference proportional to the integral of the current through the dielectric is applied to the other pair. Since the loss is to be measured in a dielectric sample, a lossless large capacitor is connected in series with the sample.

The voltages across the capacitor and across the sample are applied across the two plates. The area of the ellipse thus formed is proportional to the power loss in the dielectric. If the power loss in the dielectric is zero, the figure traced out on the oscilloscope would be a straight line.

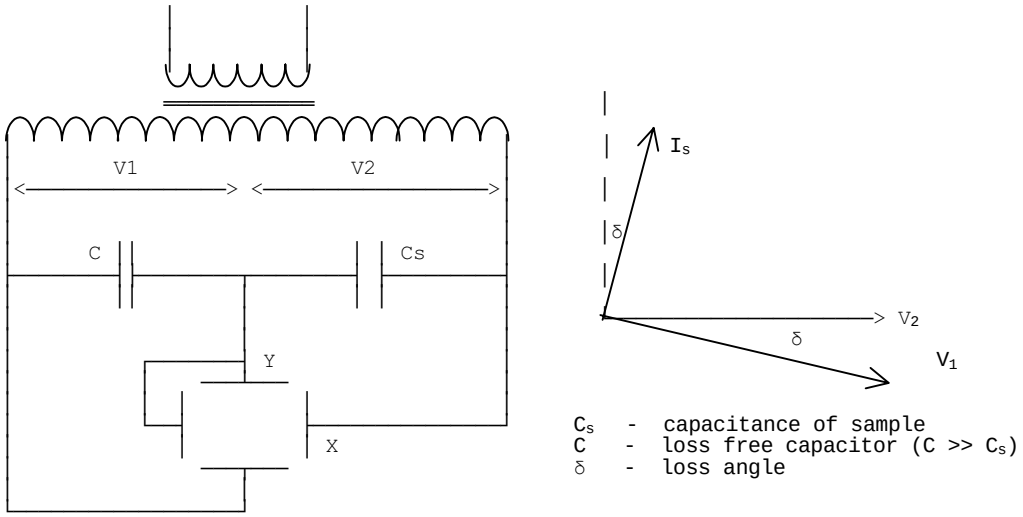

Figure 6.39 - Dielectric loss measurement using oscilloscope

The use of the standard capacitor C ensures that the voltage across it is 90^o out of phase with the current. Hence the angle on which the area of the ellipse depends is not the power factor angle but the loss angle.

$$\text{Power loss in } C_s = V_2 I_s \sin\delta$$

The **y**-deflection on the oscilloscope is proportion to $\mathbf{v_1 = V_{1m} \sin(\omega t - \delta)}$ and the **x**-deflection is proportional to $\mathbf{v_2 = V_{2m} \sin \omega t}$ which is taken as the reference.

i.e. $$y = a \,.\, V_{1m} \sin(\omega t - \delta) = a \,.\, (I_{sm}/\omega C) \sin(\omega t - \delta)$$

and $$x = b \,.\, V_{2m} \sin \omega t$$

where a, b are constants.

The area of the ellipse traced out on the oscilloscope screen is given by

$$A = \int y \,.\, dx = \int_0^T a \,.\, \frac{I_{sm}}{\omega C} \,.\, \sin(\omega t - \delta) \,.\, b \,.\, V_{2m} \,.\, \omega \,.\, \cos\omega t \,.\, dt$$

$$= \frac{a \,.\, b}{C} \,.\, \frac{2\pi}{\omega} \,.\, I_s V_2 \sin\delta$$

It is thus seen that the area of the ellipse is proportional to the power loss.

6.5.3 Detection of internal discharges

Detection of internal discharges can be carried out by various methods. It can be done by (a) visual methods - in transparent insulation the sparks can be detected by either direct observation or by using a photo-electric cell; (b) audible methods - the audible clicks given out by the discharges may be detected by using a microphone, an ultrasonic detector or other transducer; and (c) electrical methods - these will be detailed out in the following sections.

Electrical Methods of discharge detection

(a) Using a corona detector

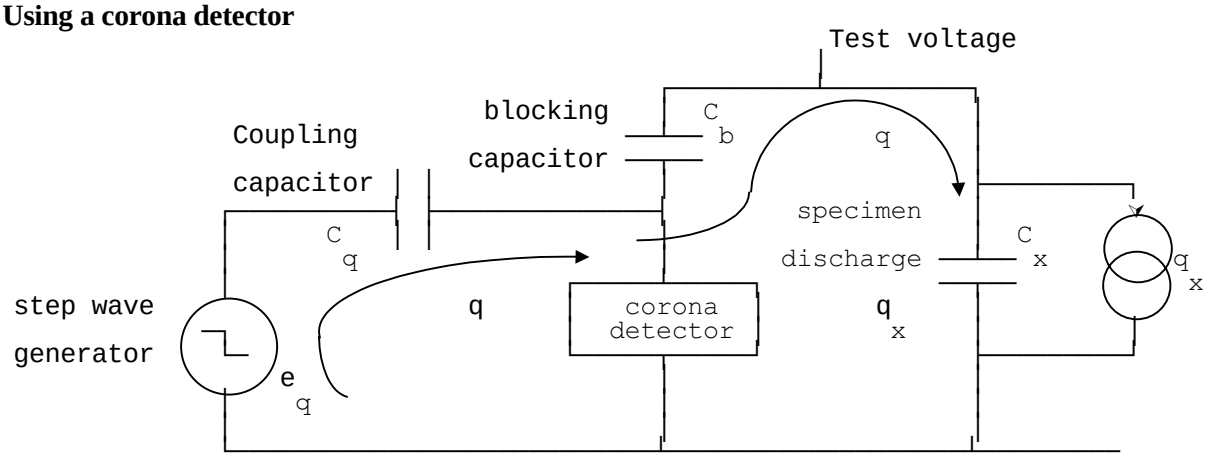

Figure 6.40 - Discharge detection using corona detector

The discharge detector shown in the figure 6.40, is basically a wide band amplifier with a gain of 10^6 and a bandwidth of 10 kHz to 150 kHz. The lossy dielectric sample may be represented by a capacitance C_x in parallel with its discharge q_x. For the charge flow, it may be assumed that the high voltage supply circuit provides almost infinite impedance, and that the step wave generator has a negligible internal impedance. Thus the discharge flow path is as shown on the diagram. When the corona detector shows no discharge across it, the voltage drop caused by the coupling capacitor C_q must equal the voltage produced by the step wave generator, and the voltage across the blocking capacitor C_b and by the specimen must must be zero. Since the specimen has its own discharge in the opposite direction to **q**, the total discharge through the specimen in the direction of **q**, must be $\mathbf{q - q_x}$.

Since no drop occurs across the detector at balance,

$$e_q - \frac{q}{C_q} = 0, \quad \text{i.e. } q = e_q C_q$$

$$\text{also } \frac{q}{C_b} + (q - q_x)/C_x = 0$$

$$\text{i.e. } q\left(\frac{1}{C_b} + \frac{1}{C_x}\right) = \frac{q_x}{C_x}$$

$$q_x = e_q C_q \left(1 + \frac{C_x}{C_b}\right)$$

Substituting for **q**, we have
The energy dissipated in the void is given by

$$w = \tfrac{1}{2} q_x V_0$$

where V_0 = peak voltage across specimen at inception voltage

(b) Using the oscilloscope with filtration and amplification

Internal discharges occurring within dielectric samples can be observed by measuring the electrical pulses in the circuit where such discharges occur.

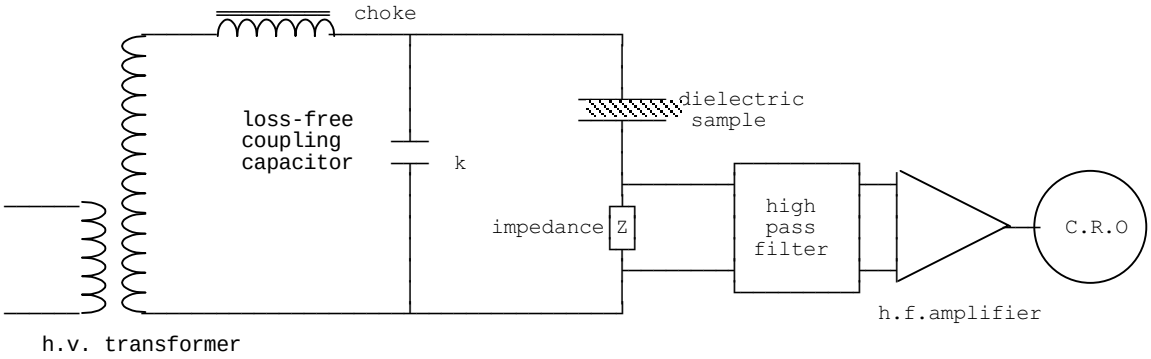

Figure 6.41 - Circuit for discharge detection

The apparatus used in the observation (namely the coupling capacitor and the impedance) should be discharge tree, so that all the discharges caused is due to the sample. However, discharges occurring in the transformer and the choke are short circuited through the coupling capacitor and do not affect the measurement. The discharge pulses caused in the sample are of high frequency, so that we bypass the low frequency and amplify the high frequency in the measurement circuit.

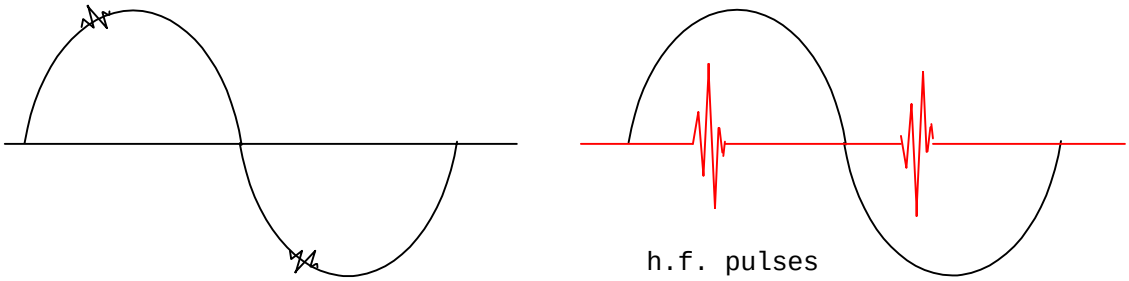

low amplitude high frequency pulses superposed on sine wave (power freq)

Figure 6.42 - Output waveforms

The coupling capacitor k is provided so that the high frequency components would be provided with a low impedance path. In the absence of this low impedance path, the path is highly inductive so that these would act as high impedance to the high frequency.

(c) Using oscilloscope with elliptical time base

In many instances, the detector cannot be used close to equipment, and matching units are employed which permit the use of about 30 m of co-axial lead between detector and the source of discharge. Calibration is done by injection of a known step voltage into the system. This gives direct calibration of discharge amplitude and takes into account the response of the amplifier. The discharge detector input circuit is shown in figure 6.43. The output of the amplifier is displayed on a oscilloscope having an elliptical time base. The time base is produced from a phase shifting R-C network. It is possible to distinguish between several types of discharges from the nature of the output displayed on the oscilloscope.

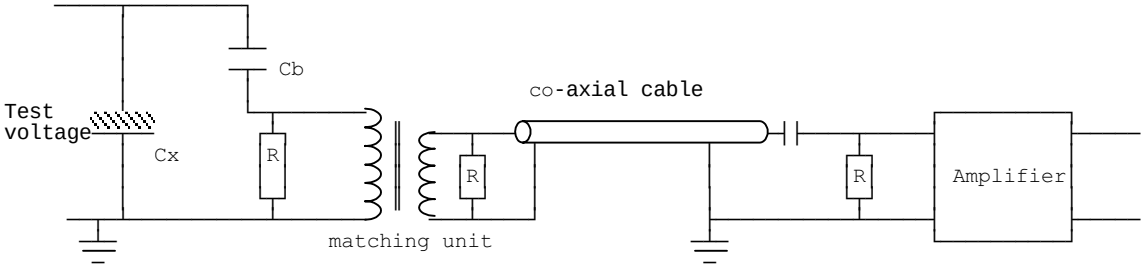

Figure 6.43 - Discharge detector input circuit

Displays on the oscilloscope for some typical discharges are shown in figure 6. together with corresponding waveforms arising out of external discharges as well as from contact noise.

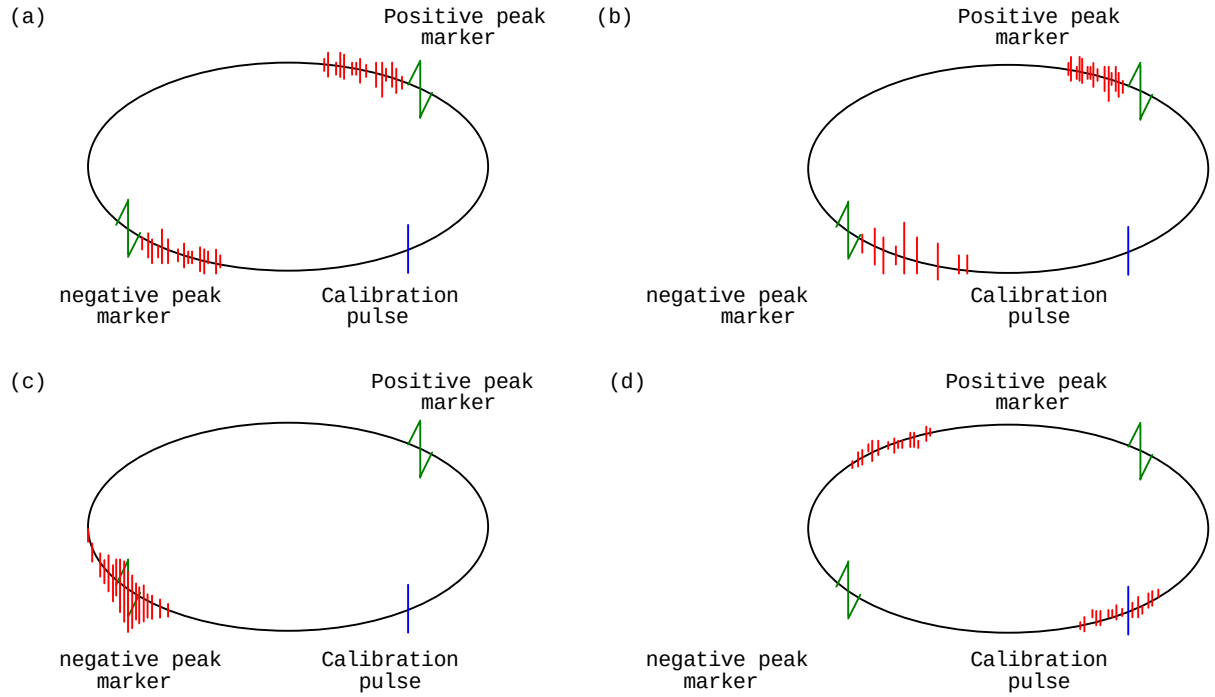

Figure 6.44 - Displays for typical discharges

(a) For a typical oil-impregnated paper capacitor: The discharges are approximately equal in magnitude and number in the two half cycles, but have opposite polarity.

(b) For a polythene insulated cable: The discharges show the asymmetry typical of discharges between a conductor and the solid insulation for a polythene insulated cable.

(c) External discharges: Corona produces a very symmetrical display about the negative voltage peak and as the voltage increases the discharges spread over a larger part of the ellipse but remain symmetrical.

(d) Contact noise: Bad contacts in the system produce many small discharges at the current peaks.

Oscilloscope connections for elliptical time base

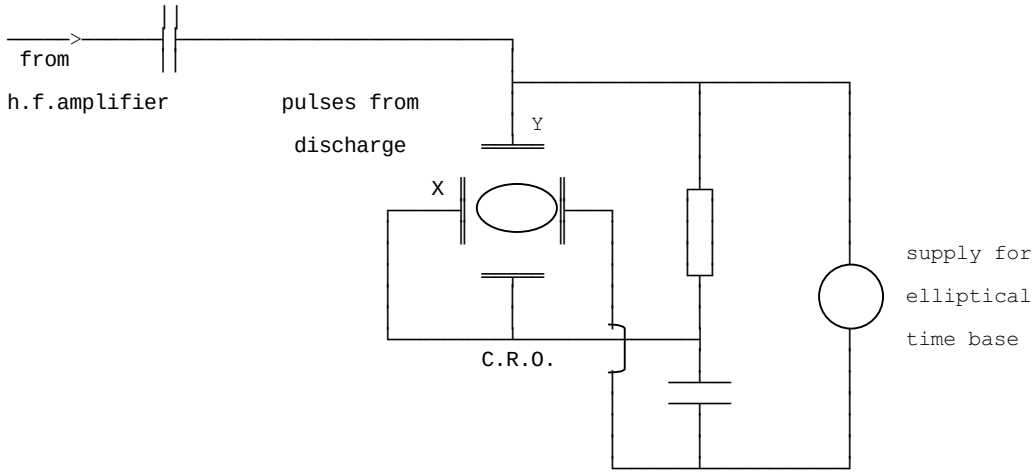

Figure 6.45 - Generation of elliptical time base

The oscilloscope X and Y plates are supplied from a separate source so as to form an ellipse on the screen. By applying the output from the high frequency amplifier to the Y-plates, we can obtain the high frequency pulse superposed on the ellipse. The height of the pulse can be measured.

Knowing the voltage sensitivity of the scope, we can find the magnitude. Knowing the characteristics of the amplifier we can calculate the output from the circuit. Then deriving a relation between the discharge from the sample and the output across the impedance we can know the discharge from the sample.

Calculation of internal discharge from measurements

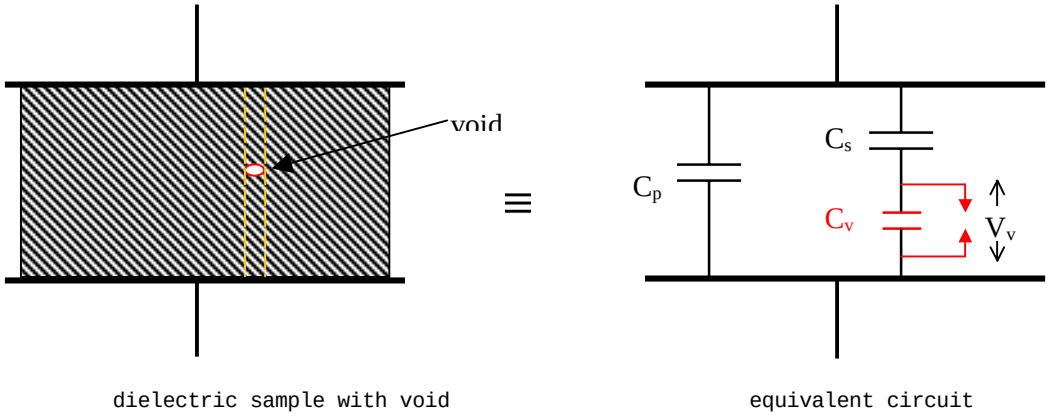

Figure 6.46 - Equivalent circuit of dielectric with void

The internal discharges can be analysed by considering a single flaw in the dielectric as shown in figure 6.46.

The dielectric can be considered as being composed of a number of capacitances. Between the two electrodes (other than in the strip containing the flaw), the material is homogeneous and can be represented by a single capacitance between the electrodes. The strip containing the flaw can also be considered as made up of three capacitances in series; one representing the capacitance of the flaw and the other two representing the capacitance on either side of the flaw.

The series capacitance on either side can be combined together to form a single capacitance as shown in figure 6.47.

a - capacity of rest of dielectric
b - capacity of section of dielectric in series with cavity
c - capacity of cavity

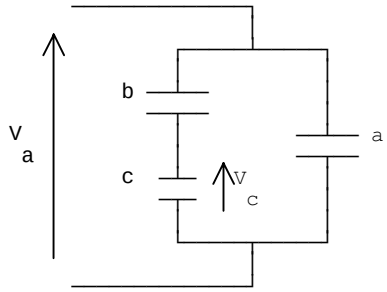

Figure 6.47 - Equivalent circuit

If the voltage across the cavity is greater than a certain critical value, then the cavity would breakdown, the cavity capacitor discharges instantly, and the voltage across the cavity would fall to zero.

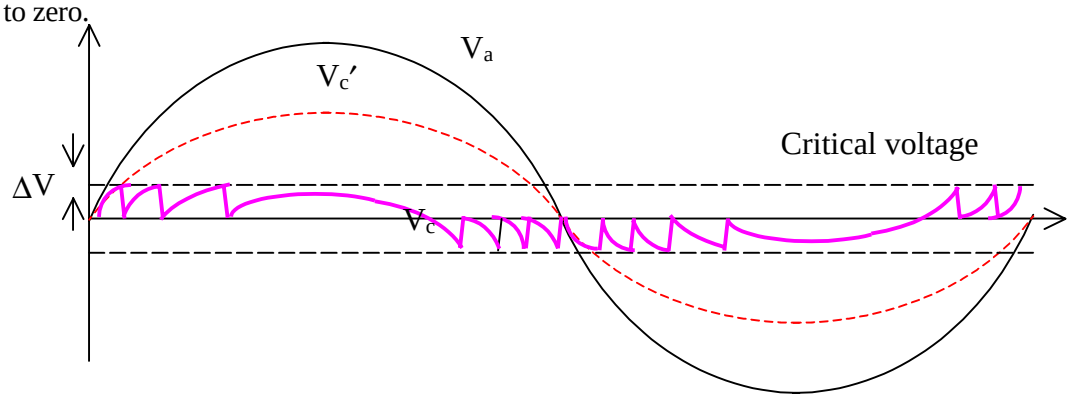

Figure 6.48 - Discharge waveforms across void

The cavity capacity again charges up within a very short period, and again collapses discharging the charge.

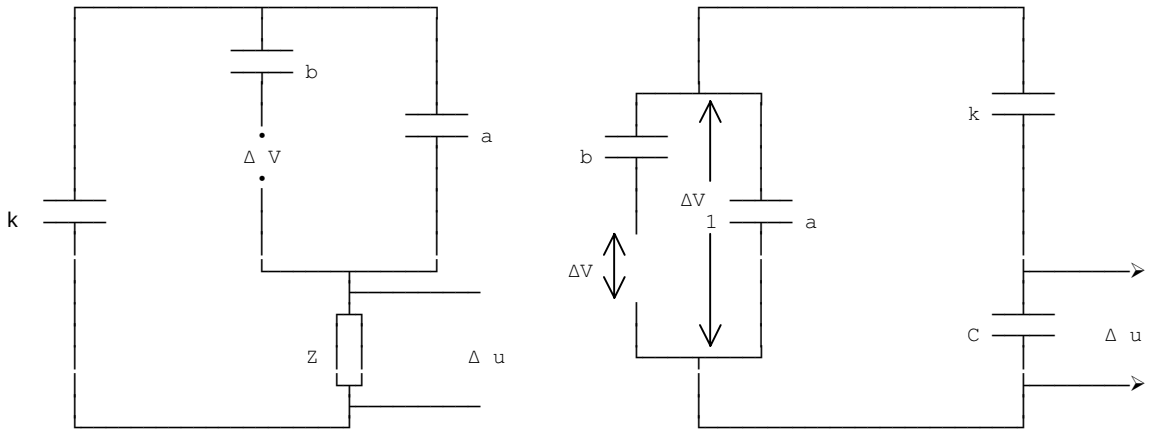

where Δu - measured voltage across impedance Z

ΔV - critical voltage across cavity

ΔV_1 - Voltage across sample

Figure 6.49 - Circuit for analysis

This process repeats itself until the voltage across the cavity falls below the critical value. This gives rise to a series of high frequency pulses (each of duration of the order of 100 ns). Figure 6.49 shows the actual circuit with the sample replaced by its equivalent circuit.

Consider the case of the impedance Z being a capacitor C. The voltage ΔV_1 would also be the voltage across the series combination of C and k.

Thus

$$\frac{\Delta V_1}{\Delta V} = \frac{b}{b + a + \dfrac{C\,k}{C + k}}, \quad \text{so that} \quad \frac{\Delta u}{\Delta V_1} = \frac{k}{k + C}$$

$$\therefore \ \Delta u = \frac{\Delta V \,.\, b}{b + a + \dfrac{C\,k}{k + C}} \cdot \frac{k}{k + C}$$

$$= \frac{b \,.\, \Delta V}{(b + a)\,(1 + C/k) + C}$$

In this expression **b.ΔV** is the charge dissipated in the discharge. Also, since the cavity is small, its capacity has negligible effect on the total capacitance.

$$\Delta u = \frac{q}{(\text{apparatus capacitance})\,(1 + C / k) + C}$$

If the impedance across which the voltage is measured is a parallel combination of a capacitance C and a resistance R, then the above calculated value of voltage would correspond to the value before the capacitor C discharges through the resistance R exponentially, and the actual expression would be

$$\Delta u = \frac{q \,.\, e^{-\frac{t}{CR}}}{(\text{apparatus capacitance})\,(1 + C / k) + C}$$

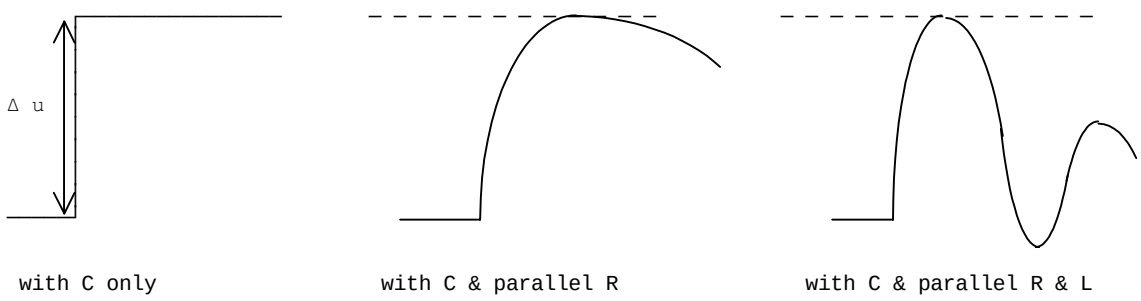

Figure 6.50 - Output waveform

All the apparatus other than the sample should be as discharge free as possible. If there are external discharges other than from the sample, the value of Δu would be due to the total discharge and the calculations would be in error. A method of avoiding external discharges is by having a bridge type of circuit as shown in figure 6.51.

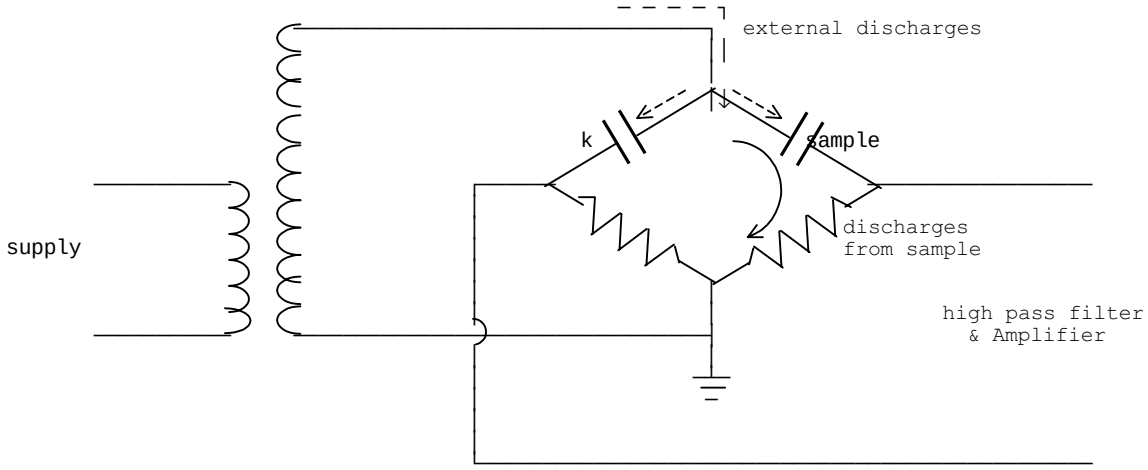

Figure 6.51 - Circuit to avoid effects of external discharges

In this circuit, external discharges would affect both the resistances equally, so that if the detection is done across the two resistances, it would measure only the discharges due to the internal flaws in the sample.

6.5.4 Measurement of dielectric constant and dissipation factor of a liquid dielectric at high frequencies using a resonance method

The test cell used in the measurement consists of a brass cell inside which is suspended a brass electrode from a perspex cover. The outer cell is the earthed electrode, and there is a gap of 3 mm all round between this and the inner brass electrode. Since the electrodes are near each other, we have to take into account the stray capacitance as well.

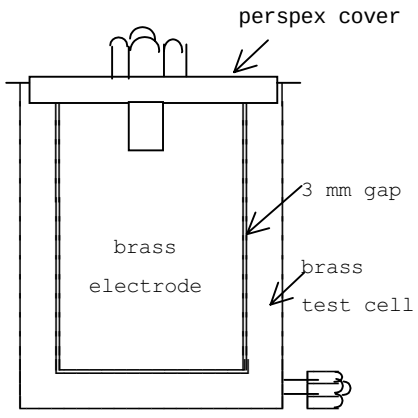

Figure 6.52 - Test Cell

The test cell is connected in parallel with a variable capacitor and made part of a resonant circuit as shown in figure 6. . In the circuit, R is a high series resistance used to keep the total current in the circuit very nearly constant. The stray capacitance C_0 of the test cell can be obtained by removing the inner electrode of the test cell and with the empty cell resonance obtained.

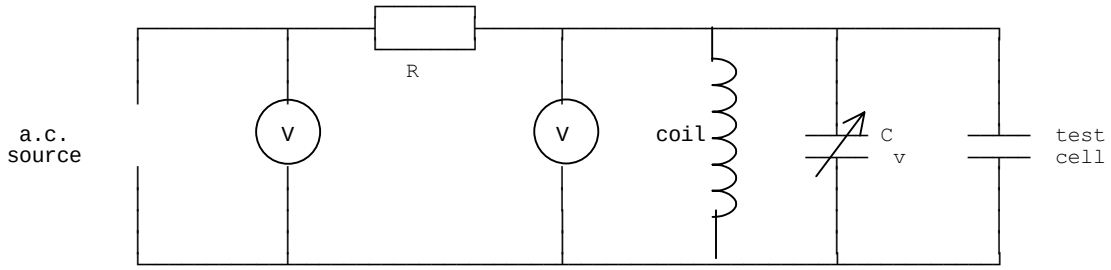

Figure 6.53 - Test Circuit

If C_v is the value of the variable capacitor at resonance, at the angular frequency ω, then

$$\omega^2 L(C_v + C_0) = 1$$

The above calculation is required only if the stray capacitance value is actually required. Otherwise the stray capacitance can be eliminated using the following procedure at the selected frequency (say 1 MHz).

(i) With the outer cell and with only the brass screw and the perspex cover of the inner cell in position, the variable capacitor C_{v0} is varied until resonance is obtained. Under this condition, only the stray capacitance C_0 is present, and the total capacitance will be at resonance with the coil inductance L. The effective capacitance, in this case, is $C_{v0} + C_0$.

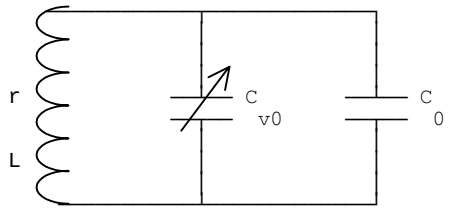

Figure 6.54 - Equivalent circuit for case (i)

The Q-factor of the circuit will be dependant on the resistance r of the coil. The Q-factor can be determined from the half-power points. The variable capacitance is varied in either direction from resonance until the half-power points (voltage corresponding to $1/\sqrt{2}$) are reached. If C_+ and C_- are the values at the half power points,

$$Q = \frac{C_+ + C_-}{C_+ - C_-} = \frac{2C + (\Delta C_+ - \Delta C_-)}{\Delta C_+ + \Delta C_-}$$

where ΔC_+, ΔC_- are the variations at the half-power points

then it can be shown that the Q factor is given by
If Q is high,

$$\Delta C_+ = \Delta C_- = \Delta C, \text{ so that } Q = \frac{C}{\Delta C}$$

(ii) The inner electrode is now screwed in, and the circuit is again adjusted for resonance at the same frequency.

If C_a is the capacitance of the active portion of the test cell with air as dielectric, and R_a is the equivalent shunt resistance of the circuit with air as dielectric, then the total value of the capacitance required must remain the same. This is true for all cases.
Thus we have

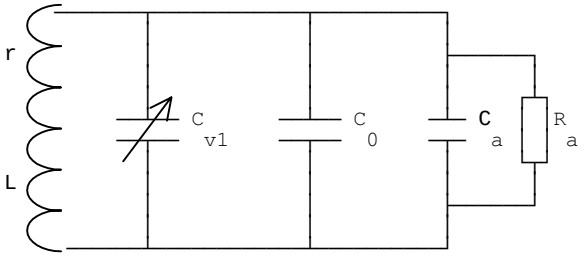

Figure 6.55 - Equivalent circuit for case (ii)

$$C_{v0} + C_0 = C_{v1} + C_0 + C_a$$
$$\therefore C_a = C_{v0} - C_{v1}$$

The Q-factor of the circuit however will be different from the earlier value, due to the additional parallel resistance. If the parallel equivalent resistance of the inductor is considered, then it is seen that the overall Q factor Q_a is given as the parallel equivalent of the Q-factors of the coil resistance and the resistance R_a. The Q-factor corresponding to the resistance R_a is $\omega C R_a$, so that

$$\frac{1}{Q_a} = \frac{1}{Q_L} + \frac{1}{\omega C R_a}$$

(iii) The liquid is now introduced into the test cell. [The liquid level should be slightly below the perspex cover, so that the surface condition of the perspex is not changed.] If R_k is the equivalent shunt resistance of the liquid, and k is the relative permittivity of the liquid dielectric, then the capacitance of the active portion of the test cell with the liquid would be kC_a.

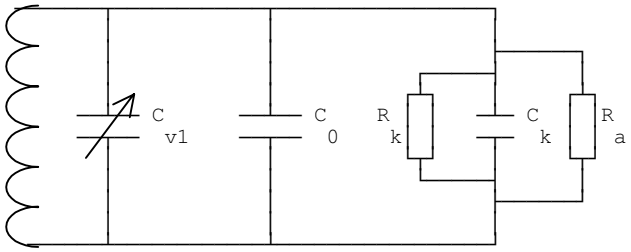

Figure 6.56 - Equivalent circuit for case (iii)

If C_{v2} is the value of the variable capacitor at resonance, then

$$C_{v0} + C_0 = C_{v2} + C_0 + k C_a$$

$$\text{giving } k C_a = C_{v0} - C_{v2}$$

$$\therefore k = \frac{C_{v0} - C_{v2}}{C_{v0} - C_{v1}}$$

Also we have the equivalent Q factor Q_k equivalent to the parallel equivalent. Thus

$$\frac{1}{Q_k} = \frac{1}{Q_L} + \frac{1}{\omega C R_a} + \frac{1}{\omega C R_k}$$

Thus the inverse of $\omega C R_k$ can be determined from

$$\frac{1}{\omega C R_k} = \frac{1}{Q_k} - \frac{1}{Q_a}$$

$$\frac{1}{Q_k}, \frac{1}{Q_a} \text{ can be calculated using } \frac{1}{Q_k} = \frac{(\Delta C)_k}{C}, \frac{1}{Q_a} = \frac{(\Delta C)_a}{C}$$

$$\text{loss factor} = \frac{1}{\omega C_k R_k} = \frac{1}{\omega C R_k} \cdot \frac{C}{C_k}$$

$$= \frac{C}{k C_a} \cdot \left[\frac{1}{Q_k} - \frac{1}{Q_a}\right] = \frac{C}{k C_a} \cdot \frac{[\Delta C_k - \Delta C_a]}{C}$$

$$= \frac{1}{k C_a} \cdot [\Delta C_k - \Delta C_a]$$

The loss factor of the dielectric is given by

$$\text{i.e. loss factor} = \frac{\Delta C_k - \Delta C_a}{C_{v0} - C_{v2}}$$

Note: in making connections it is essential that care is taken to minimise stray capacitances by using short leads, and the components should not be disturbed during the experiment.

6.5.5 Ionic Wind Voltmeter

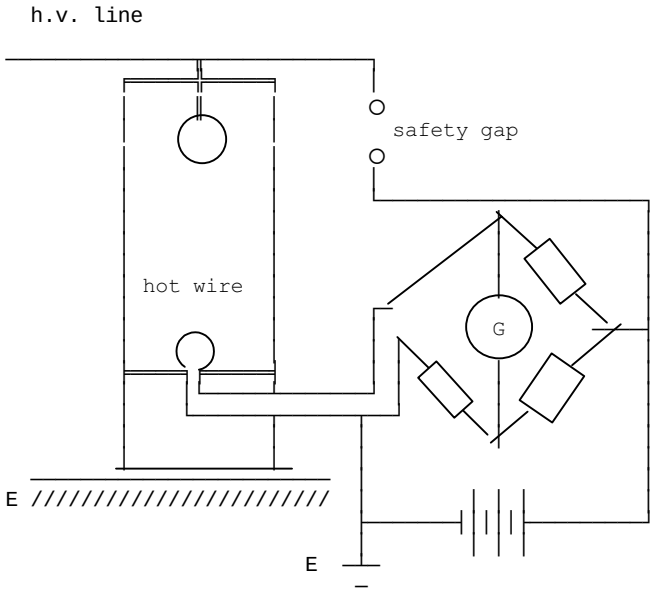

Figure 6.57 - Ionic Wind Voltmeter

When a highly charged point is situated in air or other gas, a movement of the air around the point is observed. This is referred to as the electric wind and is brought about by the repulsion of ions from the surface of the point by the intense electro-static field. These ions colliding with uncharged molecules of air carry them with it setting up the electric wind. A similar wind is observed also at the earth electrode. In the ionic wind voltmeter, a hot wire, of platinum-gold alloy, included in one arm of a Wheatstone bridge network is used as the earthed electrode of high-tension gap. Before the high voltage is applied, the bridge is balanced. When the voltage of the gap exceeds the "threshold voltage" (voltage required before the potential gradient is sufficient for ionization to commence), the electric wind cools the hot wire and hence reduces the resistance. This reduction causes an appreciable out-of-balance voltage in the bridge. The voltage waveform influences the instrument reading, and the instrument is calibrated for a sine wave.

The voltmeter can be used to determine either the peak value or the r.m.s. value of alternating voltages and direct voltages. The principle advantages are that the h.v. may be measured by an observer at some distance from the charged conductors, and the robust construction and freedom from disturbances by temperature and weather conditions which make it suitable for outdoor use.

6.5.6 Dumb-bell Voltmeter

A rather specialized way of measuring r.m.s. voltage was developed by F.M.Bruce in which the period of oscillation of a conducting spheroid in an electro-static field was determined. This enabled the voltage to be determined in terms of length and time, with an accuracy of 0.05%.

The instrument is shown on figure 6.58.

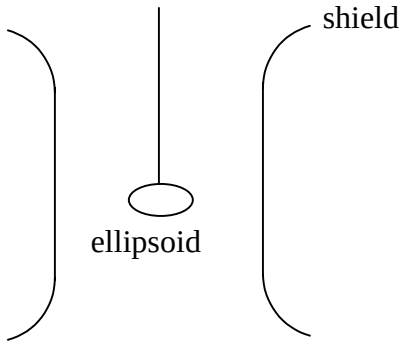

Figure 6.58 - Dumb-bell voltmeter

7

High Voltage Generators for Testing

7.0 Generation of High Voltages

The power systems engineers is interested in high voltages primarily for power transmission, and secondly for testing of his equipment used in power transmission. In this chapter we are interested in generating high voltages for testing of insulation. Thus generation has to be carried out in the testing laboratory. In many testing laboratories, the primary source of power is at low voltage (400 V three phase or 230 V single phase, at 50 Hz). Thus we need to be able to obtain the high voltage from this. Since insulation is usually being tested, the impedances involved are extremely high (order of MΩ) and the currents small (less than an ampere). Therefore high voltage testing does not usually require high power. Thus special methods may be used which are not applicable when generating high voltage in high power applications.

7.1 Generation of High Alternating Voltages

Single transformer test units are made for high alternating voltages up to about 200 kV.
However, for high voltages to reduce the cost (insulation cost increases rapidly with voltage) and make transportation easier, a cascade arrangement of several transformers is used.

7.1.1 Cascade arrangement of transformers

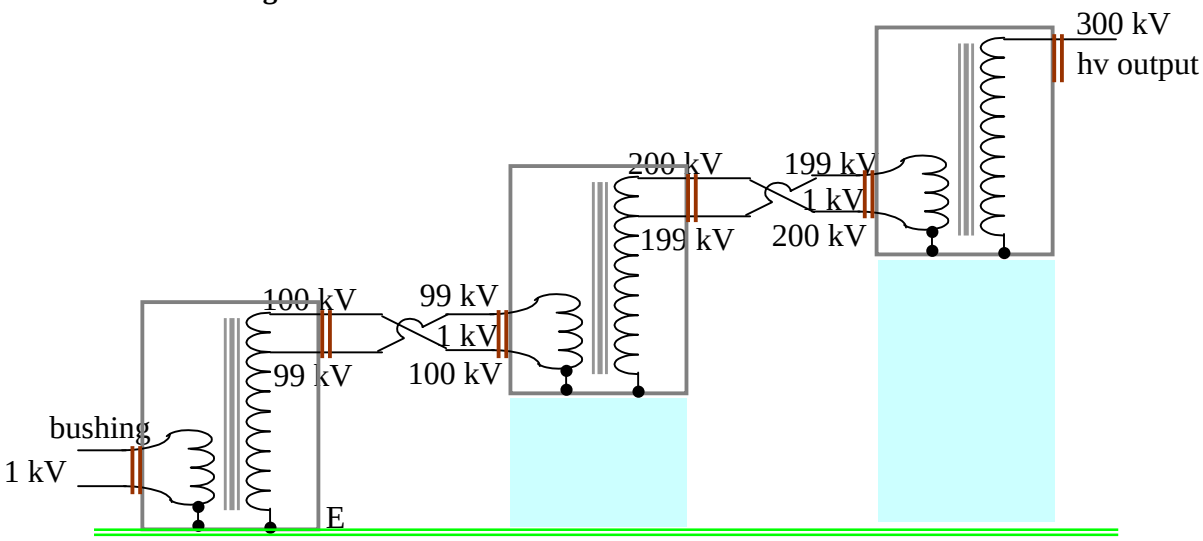

Figure 7.1 - Cascade arrangement of transformers

Figure 7.1 shows a typical cascade arrangement of transformers used to obtain up to 300 kV from three units each rated at 100 kV insulation. The low voltage winding is connected to the primary of the first transformer, and this is connected to the transformer tank which is earthed. One end of the high voltage winding is also earthed through the tank. The high voltage end and a tapping near this end is taken out at the top of the transformer through a bushing, and forms the primary of the second transformer. One end of this winding is connected to the tank of the second transformer to maintain the tank at high voltage. The secondary of this transformer too has one end connected to the tank and at the other end the next cascaded transformer is fed.
This cascade arrangement can be continued further if a still higher voltage is required.

In the cascade arrangement shown, each transformer needs only to be insulated for 100 kV, and hence the transformer can be relatively small. If a 300 kV transformer had to be used instead, the size would be massive. High voltage transformers for testing purposes are designed purposely to have a poor regulation. This is to ensure that when the secondary of the transformer is short circuited (as will commonly happen in flash-over tests of insulation), the current would not increase to too high a value and to reduce the cost. In practice, an additional series resistance (commonly a water resistance) is also used in such cases to limit the current and prevent possible damage to the transformer.

What is shown in the cascade transformer arrangement is the basic principle involved. The actual arrangement could be different for practical reasons.

7.1.2 Resonant Transformers

The resonance principle of a series tuned **L-C** circuit can be made use of to obtain a higher voltage with a given transformer.

Let **R** represent the equivalent parallel resistance across the coil and the device under test. The current **i** would be given by

$$i = \frac{E}{\frac{1}{j\omega C} + \frac{j\omega L R}{R + j\omega L}}$$

$$\text{so that} \quad v = i . \frac{j\omega L R}{R + j\omega L}$$

$$\text{i.e.} \quad v = \frac{-\omega^2 L C R . E}{R + j\omega L - \omega^2 L C R} = -\frac{E . R}{j\omega L} \quad \text{at resonance}$$

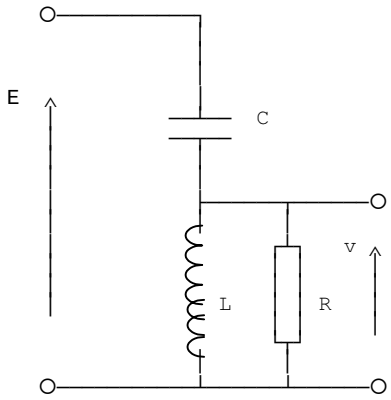

Figure 7.2 - Resonance circuit

Since **R** is usually very large, the **Q** factor of the circuit ($Q = R/L\omega$) would be very large, and the output voltage would be given by

$$|v| = E . \frac{R}{L\omega} = E . Q$$

It can thus be seen that a much larger value that the input can be obtained across the device under test in the resonant principle.

$$\text{at resonance} \quad \omega = 2\pi f = \frac{1}{\sqrt{L C}}$$

Figure 7.3 shows the application of the resonance principle at power frequency.

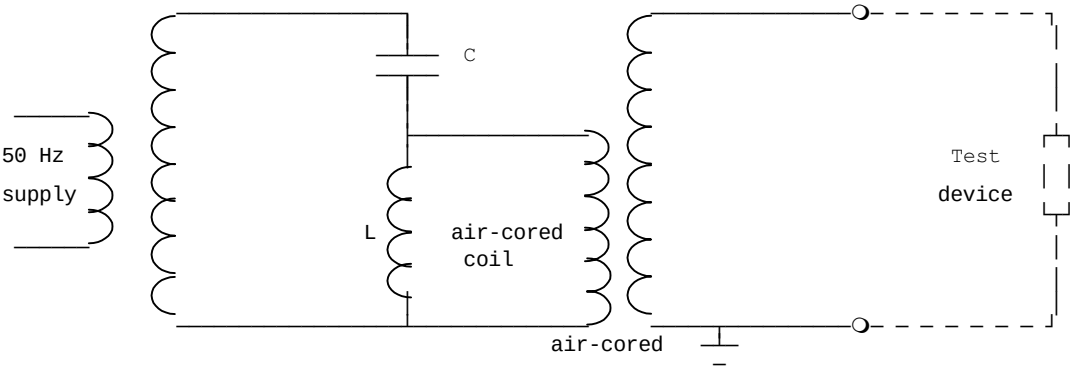

Figure 7.3 - resonant transformer

For certain applications, particularly when the final requirement is a direct voltage, it is an advantage to select a frequency higher than power frequency (50 Hz). This would result in a smaller transformer having fewer turns, and also simplifies the smoothing after rectification. High voltage high frequency voltages are not readily available, and the following is sometimes used to obtain a supply at three times power frequency. It makes use of the fact that the magnetising current of a transformer has a high third harmonic component. Thus if an open delta secondary is used, no power frequency voltage would remain and only the third harmonic component would be present. Figure 7.4 shows the circuit arrangement.

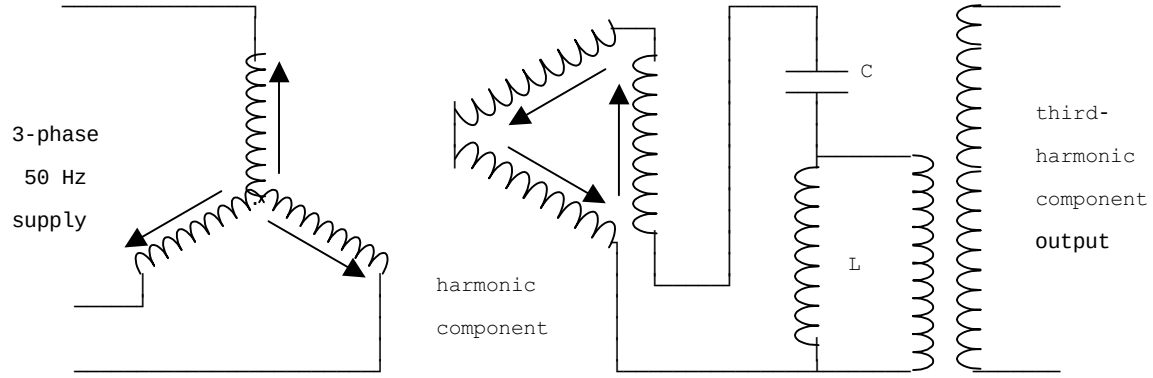

Figure 7.4 - Resonant transformer with third harmonic

Air-cored coils are used to simplify the construction and the insulation.

7.1.3 High frequency high voltages

High frequency (few kHz to Mhz) high voltages are required in testing apparatus for behaviour with switching surges, insulation flashover etc. The importance of testing with high frequency is that high frequency oscillations cause failure of insulator at comparatively low voltage due to high dielectric los and consequent heating. Thus it is necessary to produce damped high frequency voltages.

The damped oscillations are obtained by the use of a Tesla coil, together with a circuit containing a quenched spark gap. The tesla coil constitutes the high voltage transformer. It consists of two air-cored coils which are placed concentrically. The high voltage secondary coil has a large number of turns, and is wound on a frame of insulating material, the insulation between turns being air, or in some cases, oil. The primary winding has only a few turns wound on an insulating frame.

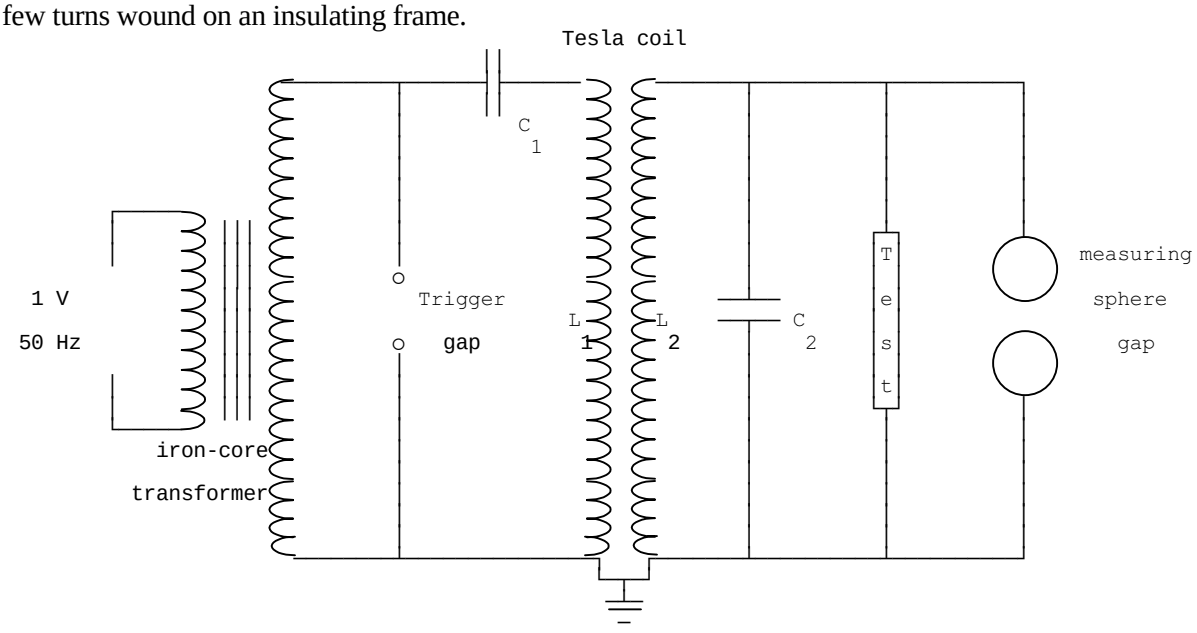

Figure 7.5 - Tesla coil circuit for high frequency generation

The supply is usually 50 Hz to the primary of the high voltage testing transformer. [In the circuit shown, C_2 includes the capacitance of the sphere gap used for measurement.] The primary circuit of the tesla transformer also contains a trigger spark gap. Since the supply to the primary of the tesla transformer is alternating, the capacitor C_1 is charged up to some maximum voltage, which depends upon the secondary side of the supply transformer, and upon the setting of the trigger gap.
At this voltage, the trigger gap breaks down, the capacitor C_1 discharges, and a train of damped oscillations of high frequency is produced in the circuit containing C_1, the spark gap and the primary winding of the tesla transformer. During the time taken for this train of oscillations to die away, the spark gap is conducting, due to the formation of an arc across it. This charge and discharge of capacitor C_1 takes place twice in one voltage cycle. Thus there will be a hundred of these trains of damped oscillations per second. The frequency of oscillations themselves is very high (about 100 kHz usually), its actual value depending upon the inductance and capacitance of the oscillatory circuit.

The circuit parameters are generally such that the resonant frequencies of the two sides are the same.

$$C_1 L_1 = C_2 L_2 \approx \frac{1}{\omega^2}$$

The expression for the voltage variation being obtained as the solution to a fourth order differential equation.

$$v = A e^{-\alpha_1 t} + B e^{-\alpha_2 t} + C e^{-\alpha_3 t} + D e^{-\alpha_4 t}, \quad \text{where } \alpha \text{ is complex}$$

The solution to the differential equation will generally be in conjugate pairs.

$$\alpha_1 = a + j\omega, \quad \alpha_2 = a - j\omega; \quad ....etc$$

Thus the solution can be written in the form

$$v = A_1 e^{-a_1 t} \sin(\omega_1 t + \phi_1) + A_2 e^{-a_2 t} \sin(\omega_2 t + \phi_2)$$

$$\text{where } a_1, a_2, A_1, A_2, \omega_1, \omega_2, \phi_1, \phi_2 \text{ are constants}$$

If the two undamped frequencies are equal (corresponding to $L_1C_1 = L_1C_1$), then the damped resonant frequencies are nearly equal ($\omega_1 \approx \omega_2$).

The exponential decays of the components of the voltage depends on the resistance values.

If amplitudes A_1 and A_2 are equal, and the decays also equal, then the summation in **v** would have the form

$$\sin(\omega_1 t + \phi_1) + \sin(\omega_2 t + \phi_2) = 2 \sin\frac{(\overline{\omega_1 + \omega_2}.t + \phi_1 + \phi_2)}{2} . \cos\frac{(\overline{\omega_1 - \omega_2}.t + \phi_1 - \phi_2)}{2}$$

If $\omega_1 \approx \omega_2$, then $(\omega_1 + \omega_2)/2 \approx \omega$, so that the sum of the two sine terms represents a product of terms, one of which is of very nearly the resonant frequency, and the other with a frequency equal to the difference frequency between the primary and the secondary resonance frequencies. If the magnitudes and decays were not considered equal, the above result will be modified by the constants A_1 and A_2, and the exponential decays $e^{-a1\,t}$ and $e^{-a2\,t}$.

The energy tends to get transferred from primary to the secondary and vice versa, so that the voltage of primary is minimum when the secondary voltage is maximum and vice versa. Oscillation would occur which would be damped out due to the resistance in the circuit.

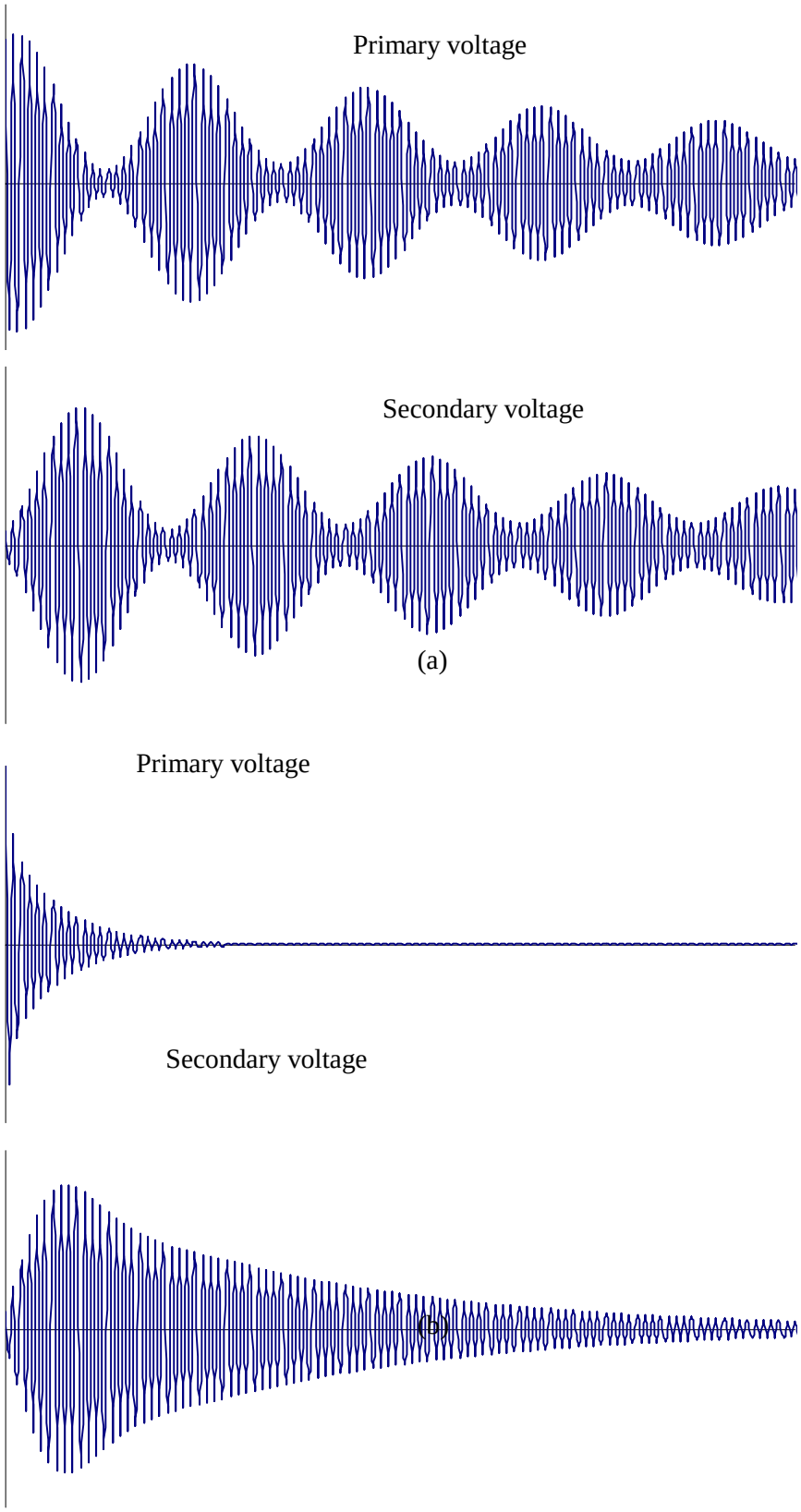

Figure 7.6 - Voltage waveforms across tesla transformer

What we require is a single series of short duration pulses. This can be done by preventing the energy from travelling backwards and forwards in the tesla transformer by quenching the trigger gap by air blast cooling. When the primary voltage is zero, the blast of air removes the spark in the primary gap so that the energy is confined to the secondary. Figure 7.6 (a) shows the primary and secondary voltage waveforms without quenching and figure 7.6 (b) shows the corresponding waveforms with quenching.

7.2 Generation of High Direct Voltages

Generation of high direct voltages are required in the testing of high voltage direct current apparatus as well as in testing the insulation of cables and capacitors where the use of alternating voltage test sets become impractical due to the steady high charging currents. Impulse generator charging units also require high direct voltages as their input.

7.2.1 Rectifier circuits

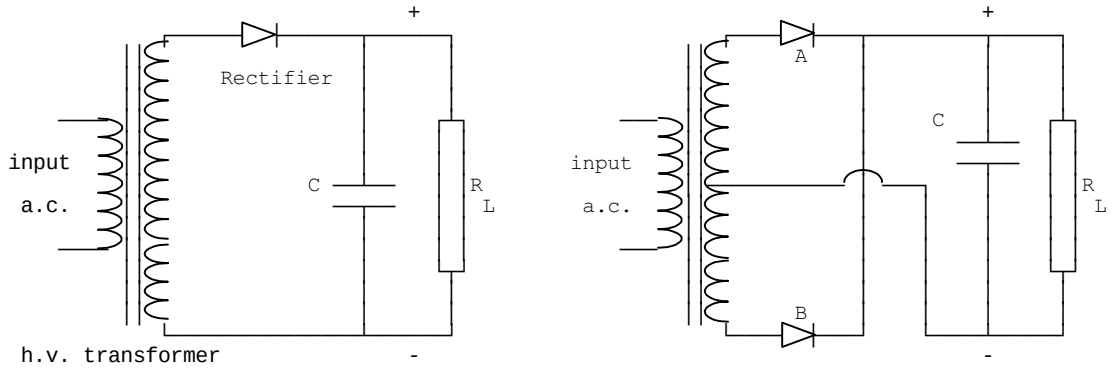

(a) half-wave rectifier (b) full-wave rectifier

Figure 7.7 - Half-wave and full-wave rectifier circuits

One of the simplest methods of producing high direct voltages for testing is to use either a half-wave for full-wave rectifier circuit with a high alternating voltage source. The rectifiers used must be high voltage rectifiers with a peak inverse voltage of at least twice the peak value of the alternating voltage supply. In theory, a low pass filter may be used to smooth the output, however when the test device is highly capacitive no smoothing is required. Even otherwise only a capacitance may be used across the test device for smoothing. Figure 7.7 shows the half-wave and the full wave arrangements.

In testing with high voltage direct current care must be taken to discharge any capacitors that may be present before changing connections. In certain test sets, automatic discharging is provided which discharges the capacitors to earth.

7.2.2 Voltage Multiplier Circuits

Both full-wave as well as half-wave circuits can produce a maximum direct voltage corresponding to the peak value of the alternating voltage. When higher voltages are required voltage multiplier circuits are used. The common circuits are the voltage double circuit and the Cockroft-Walton Circuit.

Voltage Doubler Circuit

The voltage doubler circuit makes use of the positive and the negative half cycles to charge two different capacitors. These are then connected in series aiding to obtain double the direct voltage output. Figure 7.8 shows a voltage doubler circuit.

In this case, the transformer will be of small rating that for the same direct voltage rating with only simple rectification. Further for the same direct voltage output the peak inverse voltage of the diodes will be halved.

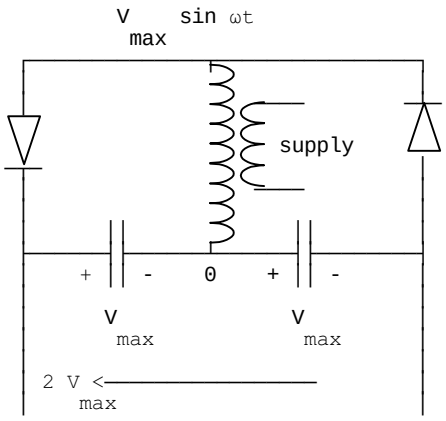

Figure 7.8 - Voltage doubler circuit

Cockroft-Walton Circuit

When more than doubling of the voltage is required, the Cockroft-Walton voltage multiplier circuit is commonly used. The circuit is shown in figure 7.9.

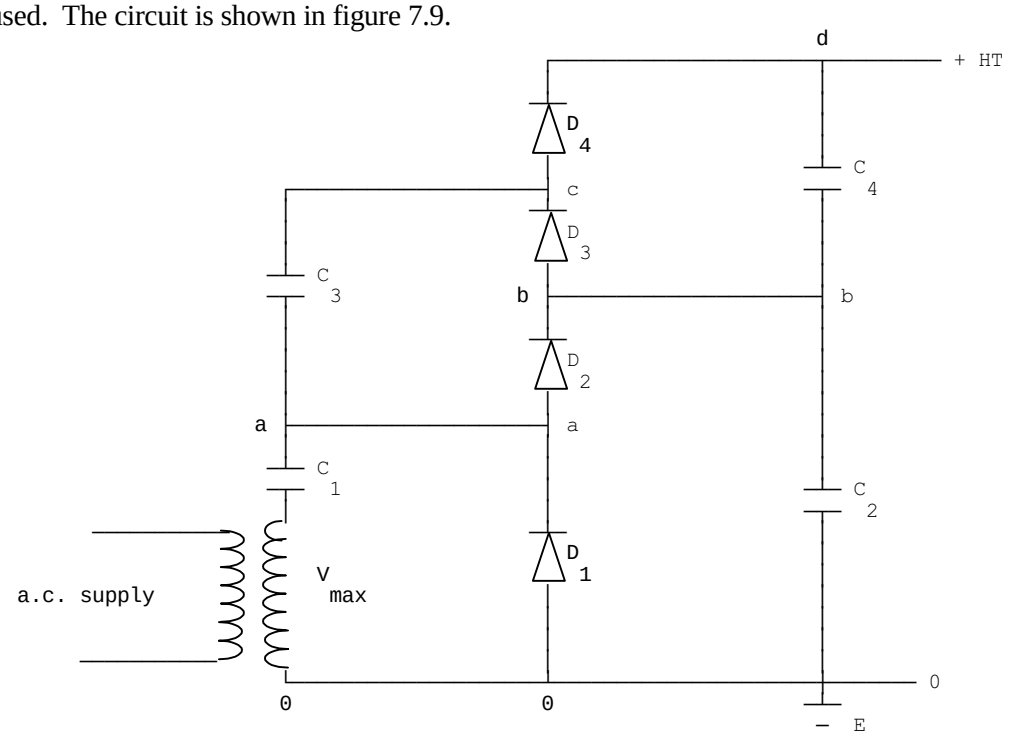

Figure 7.9 - Cockroft-Walton Circuit

Let $\mathbf{V_{max}}$ be the peak value of the secondary voltage of the high voltage transformer. To analyze the behaviour, let us consider that charging of capacitors actually takes place stage by stage rather than somewhat simultaneously. This assumption will not invalidate the result but will make analysis easier to follow. Consider the first part of the circuit containing the diode $\mathbf{D_1}$, the capacitor $\mathbf{C_1}$, and the secondary winding. During the first negative half cycle of the applied voltage, the capacitor $\mathbf{C_1}$ charge up to voltage $\mathbf{V_{max}}$. Since during the positive half cycle which follows, the diode $\mathbf{D_1}$ is reverse biassed, the capacitor $\mathbf{C_1}$ will not discharge (or will not charge up in the other direction) and the peak of this half cycle, the point **a** will be at $\mathbf{2\ V_{max}}$. During the following cycles, the potential at **a** will vary between **0** and $\mathbf{2\ V_{max}}$, depending on whether the secondary voltage and the capacitor voltage are opposing or assisting.

Initially, capacitor C_2 would be uncharged, and the voltage at **b** would be zero. Thus as the voltage at **a** varies between 0 and 2 V_{max}, the diode D_2 is forward biassed, and the capacitor C_2 would charge to 2 V_{max}. Once the voltage at **b** has reached 2 V_{max}, the voltage at **a** would be less than or equal to the voltage at **b**. Thus once C_2 has charged up, this diode too would be reverse biassed and the capacitor C_2 would not discharge. The voltage at **b** would now remain constant at 2 V_{max}. C_3 is also initially assumed uncharged. Since the voltage at **a** varies between 0 and 2 V_{max}, the diode D_3 would initially be forward biassed for almost the whole cycle. Thus the capacitor C_3 charges until it reaches 2 V_{max} when **b** is 2 V_{max} and **a** is 0. As the voltage at **a** again increases to 2 V_{max}, the voltage at **c** increases, and thus the diode D_3 is reverse biassed and C_3 would not discharge. Now as **a** reaches 2 V_{max} the voltage at **c** rises to 4 V_{max}, as C_3 has not discharged.

Thus after charging up has taken place, the voltage at **c** varies between 2 V_{max} and 4 V_{max}. Assuming C_4 also to be initially uncharged, since the voltage at **b** is a constant at 2 V_{max} and the voltage at **c** varies between 2 V_{max} and 4 V_{max} initially, during most of the cycle, the diode D_4 is forward biassed and C_4 charges up to the maximum difference between **d** and **b** (i.e. to 2 V_{max}). This occurs when the voltage at **c** is 4 V_{max} and the voltage at **d** would now be 4 V_{max}. As the voltage at **c** falls from 4 V_{max} to 2 V_{max}, since the capacitor C_4 has charged up it would not discharge, since there is no discharge path. Thus once the capacitors are charged up the voltage at **d** remains constant at 4 V_{max}.

This sequence of voltages gained is shown in Table 7.1.

Cycle Location	0 -	T/2 +	T -	3T/2 +	2T -	5T/2 +	3T -	7T/2 +	4T -
a	0	2 Vm	0	2 Vm	0	2 Vm	0	2 Vm	0
b	0	2 Vm	2 Vm	2 Vm	2 Vm	2 Vm	2 Vm	2 Vm	2 Vm
c	0	0	2 Vm	4 Vm	2 Vm	4 Vm	2 Vm	4 Vm	2 Vm
d	0	0	0	4 Vm	4 Vm	4 Vm	4 Vm	4 Vm	4 Vm

Table 1

When the generator is used for a test, or when it is loaded, a current is drawn from the generator, and the capacitors lose some of their charge to the load, and the voltage falls slightly depending on the load. As the voltage across any of the capacitors drops, then at some point in the applied alternating voltage cycle, the corresponding diode would become forward biassed and charging up of the capacitor would once again result. Thus when a load is connected, there would be a small ripple in the output voltage.

7.2.3 Electrostatic generators

Electrostatic generators using the principle of charge transfer can give very high direct voltages. The basic principle involved is that the charge is placed on a carrier, either insulating or an isolated conductor, and raised to the required potential by being mechanically moved through the electrostatic field.

Van de Graeff generator

The Van de Graeff generator is one of the methods used to obtain very high voltages. However they cannot supply much currents and the power output is restricted to a few kilowatt, and their use is restricted to low current applications.

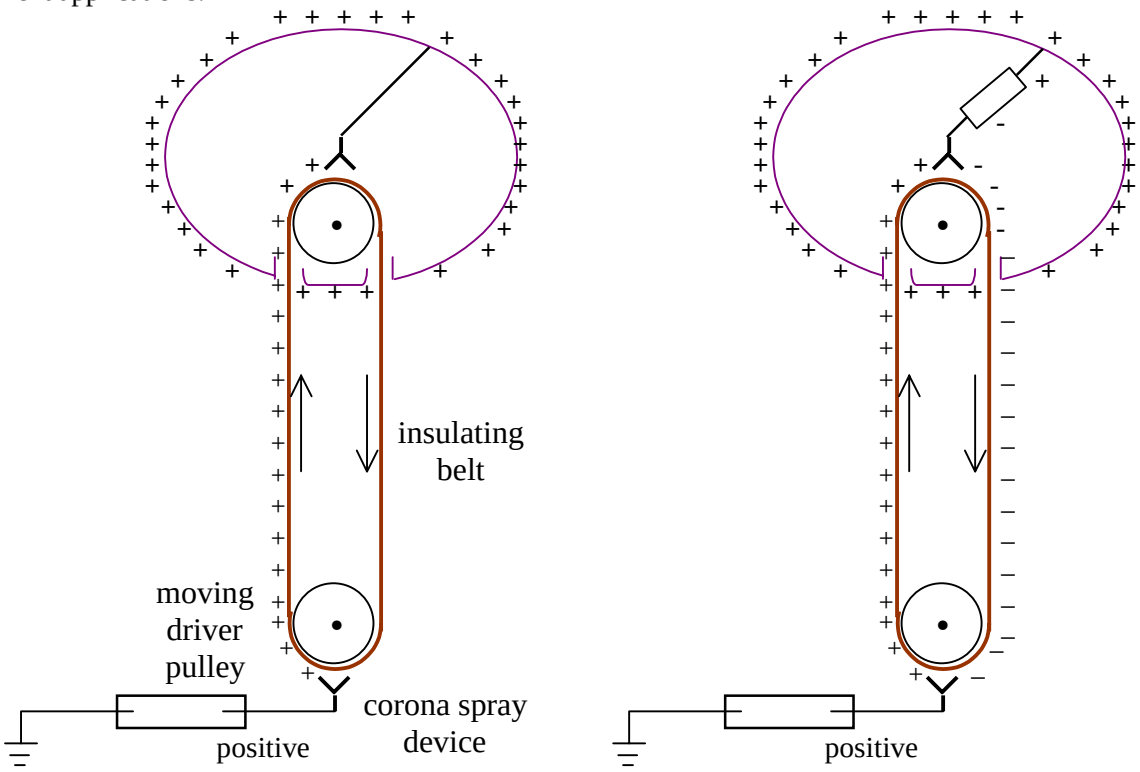

Figure 7.10 - Van de Graeff Generator

The Van de Graeff generator uses an insulating belt as the carrier of charge. The generator consists of a low direct voltage source, with corona discharge taking place at the positive end of the source. The corona formation (spray) is caused by a core like structure with sharp points (corona spray device). Charge is sprayed onto the belt at the bottom by corona discharges at a potential of 10 to 100 kV above earth and carried to the top of the column and deposited at a collector. The upper electrode at which the charge is collected has a high radius of curvature and the edges should be curved so as to have no loss. The generator is usually enclosed in an earthed metallic cylindrical vessel and is operated under pressure or in vacuum.

The higher voltage of the upper electrode arises from the fact that for the same charge, a smaller capacitance gives a larger voltage. The upper electrode has a smaller capacitance to earth on account of the larger spacing involved.

$$V = \frac{Q}{C}$$

The potential of the high voltage electrode rises at a rate of

$$\frac{dV}{dt} = \frac{1}{C}\frac{dQ}{dt} = \frac{I}{C}$$

where I is the net charging current

A steady potential will be reached by the high voltage electrode when the leakage currents na the load current are equal to the charging current. The edges of the upper electrode are so rounded as to avoid corona and other local discharges.

With a single source at the lower end, the belt moves upwards with a positive charge and returns uncharged. Charging can be made more effective by having an additional charge of opposite polarity sprayed onto the belt by a self inducing arrangement (negative corona spray). using an ingenious method. this arrangement effectively doubles the charging rate.

Sames Generator

This is a more recent form of the electrostatic generator. In this the charge is carried on the surface of an insulating cylinder. A two pole of this kind is shown in figure 7.11, but other number of poles are also possible. In this the power output will depend on the size of rotor. The number of poles will determine the current and the voltage. For example, a four pole rotor will produce twice the current at half the voltage of that of a two pole machine of the same size.

In the Sames generator, the rotor is a hollow cylinder made of an insulating material. Electric charges are deposited on the surface of the rotor which is driven by an electric motor to effect the transfer of charges in the field. The whole unit is sealed in a pressure unit and insulated ith hydrogen at a pressure of 10 to 25 atmospheres.

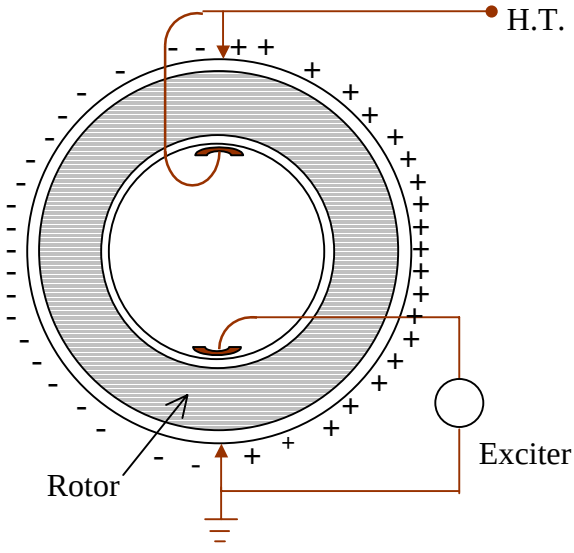

Figure 7.11 - Sames Generator

High Voltage Surge Generators

8.0 High Voltage Impulse Generators

In order that equipment designed to be used on high voltage lines, and others, be able to withstand surges caused in them during operation, it is necessary to test these equipment with voltages of the form likely to be met in service.

The apparatus which produces the required voltages is the impulse generator. In high voltage engineering, an impulse voltage is normally a unidirectional voltage which rises quickly without appreciable oscillations, to a peak value and then falls less rapidly to zero. A full impulse wave is one which develops its complete waveshape without flashover or puncture, whereas a chopped wave is one in which flash-over occurs causing the voltage to fall extremely rapidly. The rapid fall may have a very severe effect on power system equipment.

The lightning waveform, is a unidirectional impulse of nearly double exponential in shape. That is, it can be represented by the difference of two equal magnitude exponentially decaying waveforms. In generating such waveforms experimentally, small oscillations are tolerated. Figure 8.1 shows the graphical construction of the double exponential waveform

$$v(t) = V\left(e^{-\alpha t} - e^{-\beta t}\right)$$

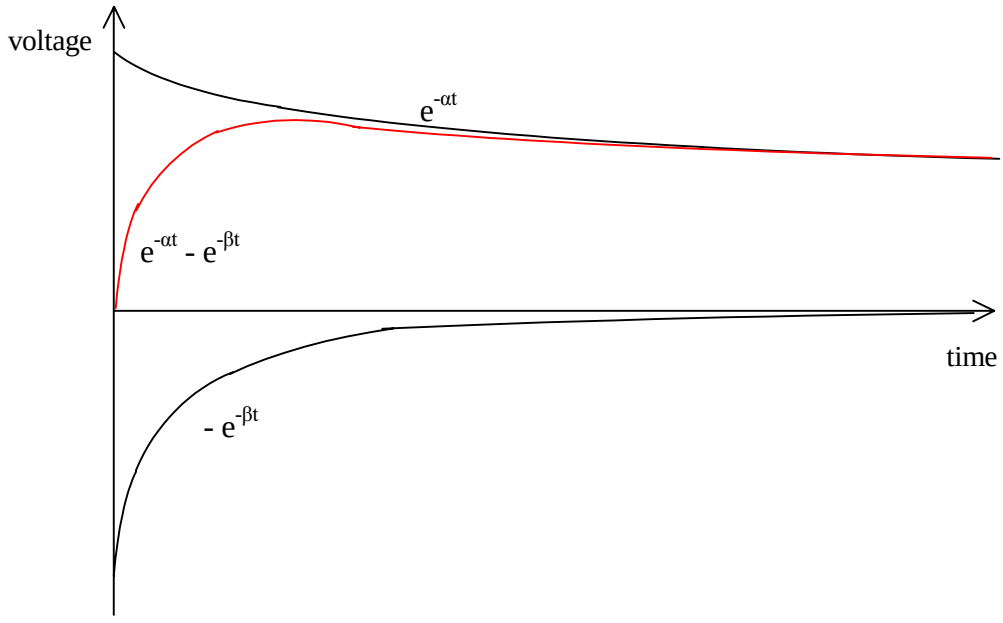

Figure 8.1 - Double exponential waveform

In most impulse generators, certain capacitors are charged in parallel through high series resistances, and then discharged through a combination of resistors and capacitors, giving rise to the required surge waveform across the test device.

8.1 Impulse Waveform

8.1.1 Single exponential waveform

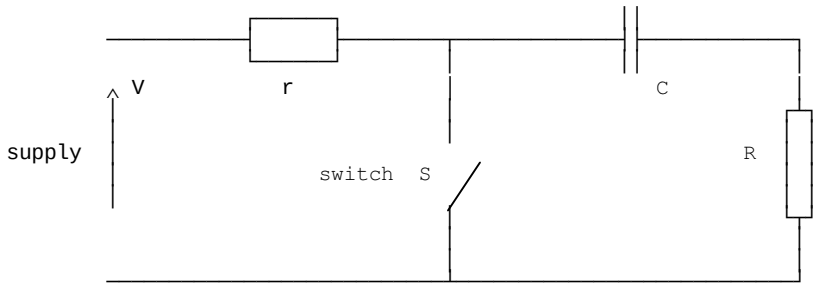

Figure 8.2 - Circuit to produce single exponential waveform

Consider the circuit shown in figure 8.1, The capacitor C is charged through the high series resistor r so that the capacitor gradually charges up to the supply voltage V. During the charging process there will be a small voltage across the load R, which falls to zero as the capacitor charges up. If the switch S is now closed, the charge on the capacitor discharges through the resistance R so that instantaneously the voltage across R rises to V and will then decay exponentially according to the equation $v = V e^{-t/CR}$, where CR is the time constant of the discharging circuit.

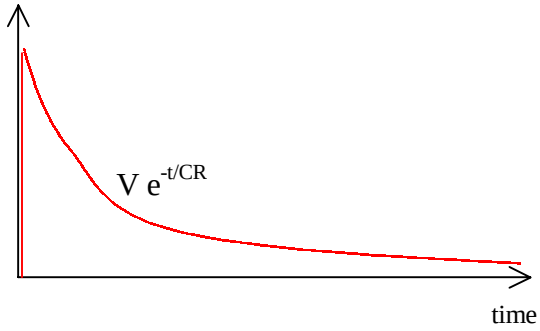

Figure 8.3 - Single exponential waveform

For this waveform, the rise time (wavefront time) is zero, and the time to fall to half maximum (wavetail time) corresponds to CR $\log_e 2$.

8.1.2 Double exponential waveform

The simple RC circuit to obtain the single exponential voltage waveform can be modified to generate a double exponential waveform by the addition of another capacitor to the circuit. Figure 8.4 shows the circuit used, with the capacitor C_1 being initially charged from an outside circuit.

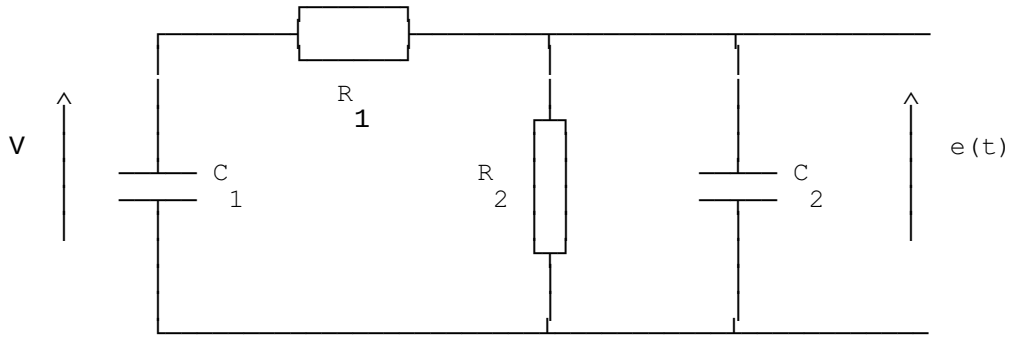

Figure 8.4 - Circuit to produce double exponential waveform

This circuit can be analysed using the Laplace transform equivalent circuit shown in figure 8.5.

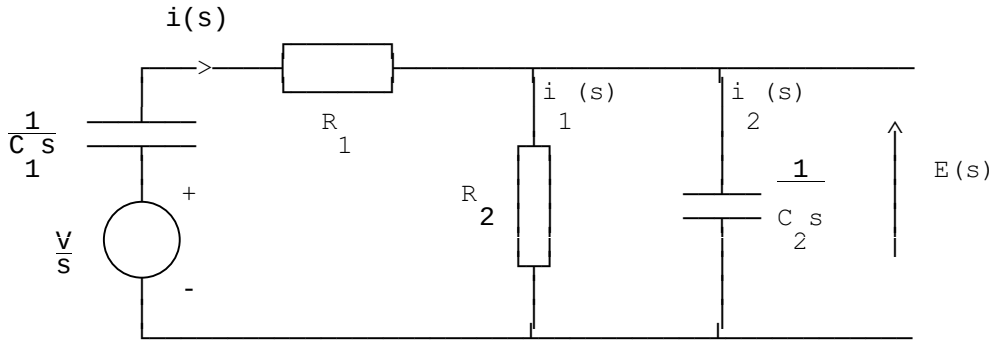

Figure 8.5 - Laplace equivalent circuit for double exponential

This circuit can be analysed in the following manner.

$$\frac{V}{s} = i(s).\frac{1}{C_1 s} + i(s).R_1 + i_1(s).R_2$$

$$E(s) = i_1(s).R_2 = i_2(s).\frac{1}{C_2 s}, \quad \text{also} \quad i(s) = i_1(s) + i_2(s)$$

$$\therefore \; i_1(s).(R_2 + R_1 + \frac{1}{C_1 s}) + i_2(s).(R_1 + \frac{1}{C_1 s}) = \frac{V}{s}$$

$$\text{Also} \quad i_2(s) = C_2 R_2 s.i_1(s)$$

$$\therefore \; i_1(s).(R_2 + R_1 + \frac{1}{C_1 s} + R_1 C_2 R_2 s + \frac{R_2 C_2}{C}) = \frac{V}{s}$$

$$\text{substitution gives} \quad E(s) = i_1(s).R_2 = \frac{V C_1 R_2}{R_1 R_2 C_1 C_2 s^2 + (C_1 R_2 + C_1 R_1 + C_2 R_2) s + 1}$$

If α and β are the solutions of the equation

$$R_1 R_2 C_1 C_2 s^2 + (C_1 R_1 + C_1 R_2 + C_2 R_2) s + 1 = 0$$

then the Laplace transform expression can be simplified as follows.

$$E(s) = \frac{V}{R_1 C_2}.\frac{1}{(s+\alpha)(s+\beta)} = \frac{V}{R_1 C_2}.\frac{1}{\beta - \alpha}.\left[\frac{1}{s+\alpha} - \frac{1}{s+\beta}\right]$$

$$\text{This gives} \quad e(t) = \frac{V}{C_2 R_1}.\frac{1}{\beta - \alpha}(e^{-\alpha t} - e^{-\beta t})$$

It is seen that the output waveform is of the double exponential form required.

For a 1/50 μs waveform, it can be shown that $\alpha \approx 0.0139$, and $\beta \approx 6.1$ when t is in μs. Also for the standard 1.2/50 μs IEC waveform, $\alpha \approx 0.0143$ and $\beta \approx 4.87$.

The alternate form of the circuit shown in figure 8.6 can also be used to obtain the double exponential waveform. The analysis of this circuit is also very similar.

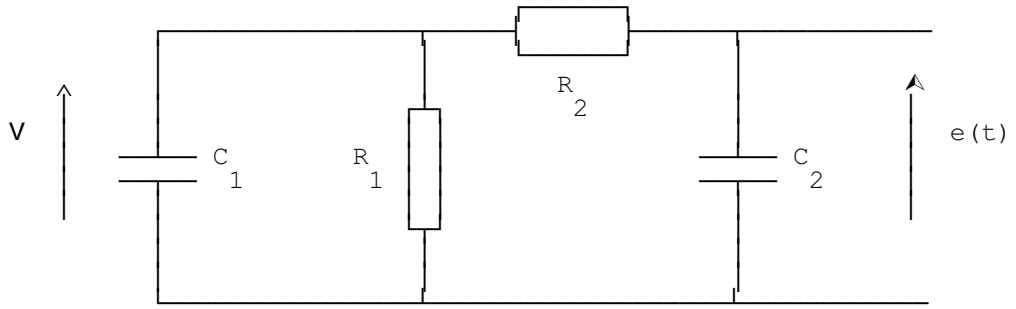

Figure 8.6 - Alternate Circuit to produce double exponential waveform

In practice, in addition to the main capacitors and inductors shown in the impulse generator circuit considered, stray capacitances will also be present. These will cause the order of the Laplace transform equation to become much higher and more complicated. Thus the actual waveform generated would be different and would contain superimposed fluctuations on the impulse waveform as shown in figure 8.7.

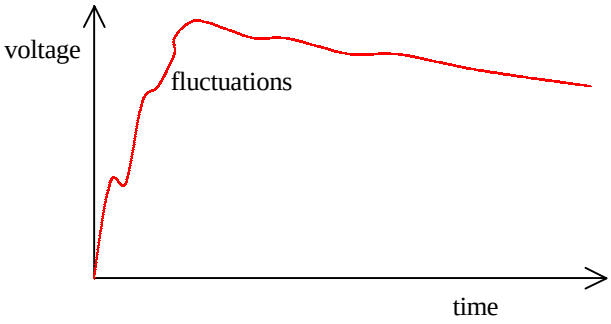

Figure 8.7 - Waveform with fluctuations

8.1.3 Calculation of α and β from resistance and capacitance values

Consider again the expression for the surge voltage

$$e(t) = \frac{V}{C_2 R_1} \cdot \frac{1}{\beta - \alpha} \cdot (e^{-\alpha t} - e^{-\beta t})$$

The peak value of this voltage occurs when its derivative becomes zero.

$$\frac{d\, e(t)}{d\, t} = 0, \quad \text{giving} \quad \alpha e^{-\alpha t} = \beta e^{-\beta t}$$

$$\because \ \beta >> \alpha, \qquad e^{(\beta - \alpha) t_1} = \frac{\beta}{\alpha} \approx e^{\beta t} \quad \text{------(1)}$$

$$\text{maximum value of voltage is} \quad E_{max} = \frac{V}{C_2 R_1} \cdot \frac{1}{\beta - \alpha} \left(1 - \alpha - \frac{\alpha}{\beta}\right) \approx \frac{V}{\beta C_2 R_1}$$

After reaching the peak, the voltage falls to half maximum in time t_2 given by

$$\frac{V}{2 \beta R_1 C_2} \approx \frac{V}{\beta C_2 R_1} \cdot e^{-\alpha t_2}, \ \because \ e^{-\beta t_2} << e^{-\alpha t_2}$$

$$\therefore \quad e^{-\alpha t_2} \approx \tfrac{1}{2} \quad \text{------(2)}$$

From equations (1) and (2) it is seen that the wavefront time t_1 is determined predominantly by β, and the wavetail time predominantly by α.

α and β are the solutions of the following quadratic equation in s.

$$R_1 R_2 C_1 C_2 s^2 + [(C_1 + C_2) R_2 + R_1 C_1] . s + 1 = 0$$

$$\text{so that} \quad \alpha . \beta = \frac{1}{R_1 R_2 C_1 C_2},$$

$$\text{also} \quad \alpha + \beta = \frac{(C_1 + C_2) R_2 + R_1 C_1}{R_1 R_2 C_1 C_2} \approx \beta \quad \because \beta \ll \alpha$$

$$\therefore \ \alpha \approx \frac{1}{(c_1 + C_2) R_2 + C_1 R_1}$$

$$\text{generally} \quad R_1 << R_2, \quad \text{so that}$$

$$\beta \approx \frac{C_1 + C_2}{R_1 C_1 C_2} \qquad \text{-----(3)}$$

$$\alpha \approx \frac{1}{(C_1 + C_2) R_2} \qquad \text{-----(4)}$$

Since β is a function of R_1, and α is a function of R_2, the effect of R_1 will be to determine the rate of rise of voltage across the load, and thus the wavefront time. It is thus known as the wavefront control resistance.

The maximum voltage available at the output is given by

$$E_{max} = \frac{V}{\beta C_2 R_1} = \frac{V R_1 C_1 C_2}{(C_1 + C_2) C_2 R_1} \approx V . \frac{C_1}{C_1 + C_2}$$

Thus the maximum (peak) voltage available at the output will depend on the ratio of C_2 to C_1, and on the charging voltage. If C_2 is low compared to C_1, then we can have a higher voltage peak. The voltage efficiency of the impulse generator can be approximately be estimated as $C_1/(C_1 + C_2)$ multiplied by a factor of about 0.95 (to account for approximations made in the analysis).

The wavefront control resistance can be connected either outside or within the impulse generator, or partly within and partly outside.

8.1.4 Definition of Wavefront and Wavetail times of practical waveforms

In practical impulse waveforms, the initial region and near the peak in the voltage are not very well defined. Also, near zero and near the peak, the rate of change is quite often much less than in the rest of the wavefront. Hence the wavefront time is not well defined. It is thus usual to define the wavefront by extrapolation based on a rise time for a specific change (say 10% to 90% or in even from 30% to 90% when the initial region is not clear). Figure 8.8 shows how the measurement of this rise time is made.

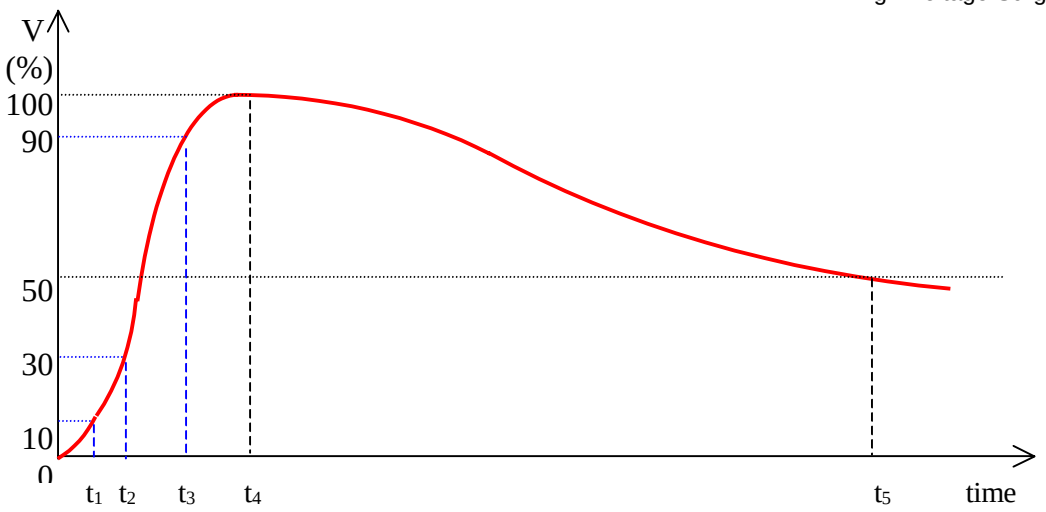

Figure 8.8 - Definition of wavefront

The wavefront time is given as $(t_3 - t_1)/(0.9 - 0.1)$ or $1.25\ (t_3 - t_1)$ for the 10% to 90% measurement and as $(t_3 - t_2)/(0.9 - 0.3)$ or $1.67\ (t_3 - t_2)$ for the 30% to 90% measurement.

The wavetail time is defined as the time from the initial point of the waveform to falling to 50 % of peak. In the case where the initial point is not well defined, the initial point may be extrapolated from the wavefront.

8.1.5 A valid approximate analysis of double exponential impulse generator circuit

The properties that in practical impulse waveforms the wavefront time is usually very much smaller than the wavetail time ($t_f << t_t$ and $\alpha << \beta$), and that impulse generators are designed for a high voltage efficiency may be made use of in making approximations to the solution.

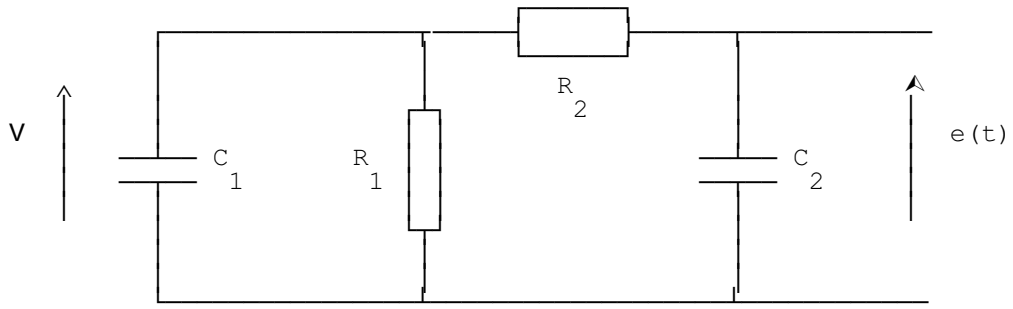

Figure 8.9 - Circuit to produce double exponential waveform

Consider the circuit shown in figure 8.9. Also, to obtain a small wavefront time and a long wavetail time, the series resistance R_2 must be small and the shunt resistance R_1 must be comparatively much larger.

Thus to analyse the wavefront, it is permissible to open circuit the resistor R_1 and redraw the approximate circuit as shown in figure 8.10.

During the wavefront, the charging rate was seen from figure 8.1 to be dependant mainly on the inverse time constant β. This should thus correspond to the inverse of the time constant of the approximate circuit.

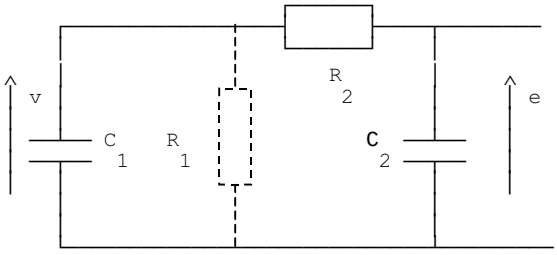

Figure 8.10 - Circuit to analyse wavefront

Thus

$$\beta \approx \frac{1}{R_2 C_{eq}} = \frac{C_1 + C_2}{R_2 C_1 C_2}$$

where $C_{eq} = \dfrac{C_1 C_2}{C_1 + C_2}$, $\because C_1, C_2$ are series

which is the same expression obtained using the normal method of analysis. The approximate voltage efficiency of the impulse generator can also be determined from this circuit. The maximum possible value of the output voltage **e** that can be obtained can be determined by potential divider action. Thus

$$e = \frac{C_1}{C_1 + C_2}.v \quad \text{neglecting resistance } R_2$$

$$\therefore \text{ efficiency } \eta = \frac{e}{v} = \frac{C_1}{C_1 + C_2}$$

which also corresponds to the simple expression obtained earlier.

To obtain a high voltage efficiency, a large proportion of the energy from the initially charged capacitor C_1 must be retained in the capacitor C_1, so that $C_1 > C_2$.

Similarly, since both capacitors discharge through the resistor R_1, and since $R_1 >> R_2$, to analyse the wavetail, it is permissible to short circuit the resistor R_2 and redraw the approximate circuit as shown in figure 8.11.

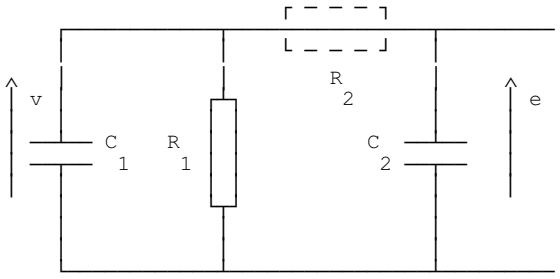

Figure 8.11 - Circuit to analyse wavetail

During the wavetail, the discharging rate was seen from figure 8.1 to be dependant mainly on the inverse time constant α. This should thus correspond to the inverse of the time constant of the approximate circuit. Thus

$$\alpha \approx \frac{1}{R_1 C_{eq}} = \frac{1}{R_1 (C_1 + C_2)}$$

where $C_{eq} = C_1 + C_2$, $\because C_1, C_2$ are paralleled

which is the same expression obtained using the normal method of analysis.

8.1.6 Wavefront and Wavetail Control

In a practical impulse generator circuit, the nominal voltage is defined by the peak theoretical voltage and the nominal energy is defined by the maximum stored energy. The capacitance values in the impulse generator circuit are not variable except for the capacitance contribution of the test object. Thus waveshape control is achieved by varying the resistance values.

As has already been derived

$$\alpha = \frac{1}{R_1 (C_1 + C_2)}, \quad \beta = \frac{C_1 + C_2}{R_2 C_1 C_2}, \quad \eta = \frac{C_1}{C_1 + C_2}$$

$$\text{giving } \frac{1}{\alpha} = \frac{R_1 C_1}{\eta}, \quad \frac{1}{\beta} = \eta R_2 C_2$$

The wavefront time $\mathbf{t_f}$ and the wavetail time $\mathbf{t_t}$ may be evaluated as follows.

Defining the wavefront from 10 % to 90 % and considering only that β determines the wavefront,

$$t_f = \frac{(t_b - t_a)}{0.9 - 0.1} = 1.25(t_b - t_a)$$

$$1 - 0.1 = e^{-\beta t_a}, \quad 1 - 0.9 = e^{-\beta t_b}$$

$$\text{so that } t_a = -\frac{1}{\beta}\log_e(0.9) = \frac{0.1054}{\beta}, \quad t_b = -\frac{1}{\beta}\log_e(0.1) = \frac{2.3026}{\beta}$$

$$\text{i.e. } t_f = 1.25(t_b - t_a) = \frac{1.25 \times 2.197}{\beta} = \frac{2.75}{\beta}$$

$$\text{i.e. } t_f = 2.75\eta R_2 C_2$$

It can also be shown that if the wavefront is considered from 30 % to 90 %, the corresponding expression becomes

$$t_f = 3.243\eta R_2 C_2$$

Similarly, defining the wavetail time as the time to decay to 50 % of peak, and considering only that α determines the wavetail,

$$0.5 = e^{-\alpha t_t}, \text{ so that } \alpha = -\frac{\log_e 0.5}{t_t}, \text{ giving } t_t = \frac{0.693}{\alpha}$$

$$\text{Thus } t_t = \frac{0.693 R_1 C_1}{\eta}$$

8.2 Operation of Impulse Generator

8.2.1 Uncontrolled operation

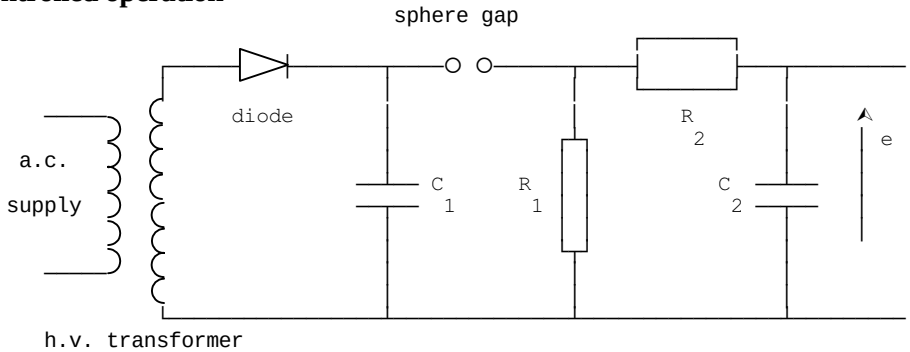

Figure 8.12 - Circuit for uncontrolled operation

In the simplest form of the single stage impulse generator, shown in figure 8.12, the high direct voltage required is obtained from a high voltage transformer through a high voltage rectifier. The direct voltage need not be smooth as it only has to charge the first capacitor to peak value. A sphere gap is used as the switch, and as the charge on the capacitor builds up, so does the voltage across the sphere gap.

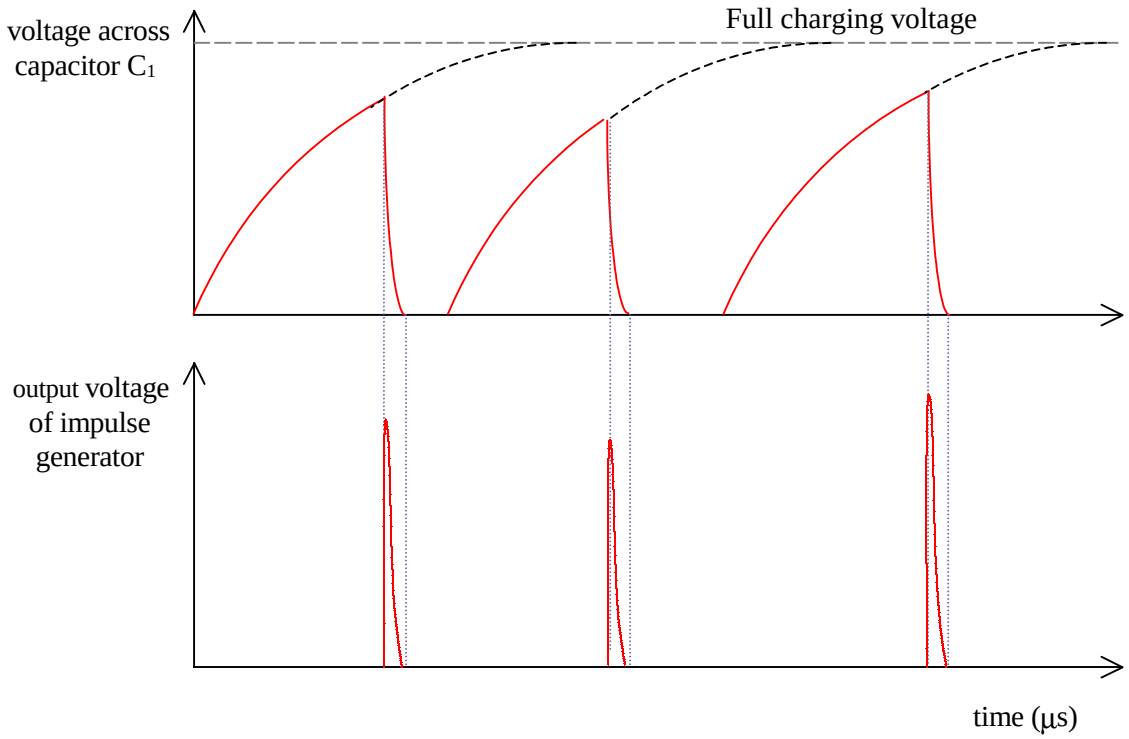

Figure 8.13 - Impulse generator waveforms for uncontrolled operation

In the uncontrolled operation, the break down voltage of the sphere gap is less than the peak value of the supply, so that it effectively closes when the voltage across the gap builds up above its breakdown value. The capacitor would then discharge through the impulse generator circuit producing an impulse waveform. The impedance of the impulse generator charging circuit is much higher than that of the impulse generator circuit so that during the impulse the rectifier and other related components can be disregarded. Subsequently, the capacitor would charge up again and the process would be repetitive. However, as the breakdown of a sphere gap is not exactly a constant but statistical, the time of occurrence of the impulse nor the exact magnitude are controllable. The waveforms of the voltage of the charging capacitor and of the impulse generator output are shown in figure 8.13.

8.2.2 Controlled operation

In the controlled mode of operation, the same basic circuit is used, but the capacitor is allowed to reach the full charging voltage without the sphere gap breaking down. The spark over voltage is set at slightly higher than the charging voltage. In this case, at the sphere gap we need a special arrangement, such as a third sphere between the other two, to be able to initiate breakdown of the gap. The modified circuit is shown in figure 8.14.

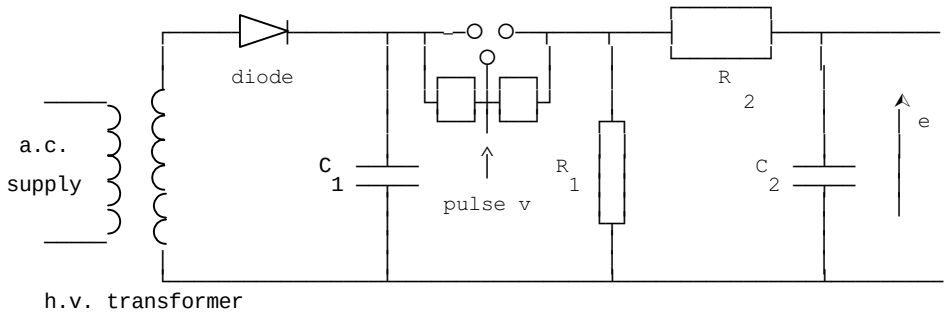

Figure 8.14 - Circuit for controlled operation

The potential across the main gap is divided into two by means of 2 equal resistors R, each of about 100 MΩ. By this means, half the applied voltage V appears across each of the two auxiliary gaps.

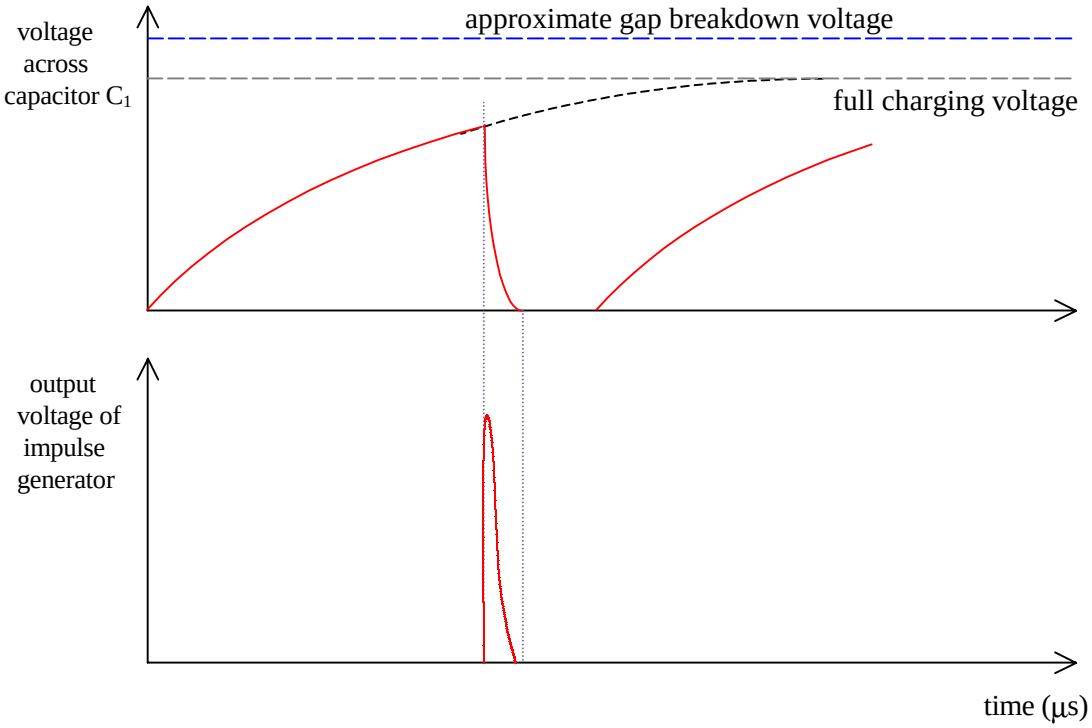

Figure 8.15 - Impulse generator waveforms for controlled operation

Once the capacitor C_1 has charged up to the full value, a small pulse voltage **v** is applied (about 20 %) at the third electrode (also known as the trigger electrode). This pulse raises the voltage across one of the auxiliary gaps to more than half the charging voltage (½ V + v) so that it would be just sufficient to breakdown the gap. As this auxiliary gap breaks down, the full voltage would be applied across the remaining auxiliary gap causing it also to breakdown.

Once both auxiliary gaps have broken down, the ionisation present in the region would cause the main gap also to breakdown almost simultaneously and thus the impulse voltage would be applied. The waveforms for the controlled operation are shown in figure 8.15.

8.2.3 Trigatron gap

The third sphere arrangement described for the trigger arrangement is not very sensitive. A better arrangement is to have an asymmetrical gap arrangement. The trigatron gap is such an arrangement which is in general use.

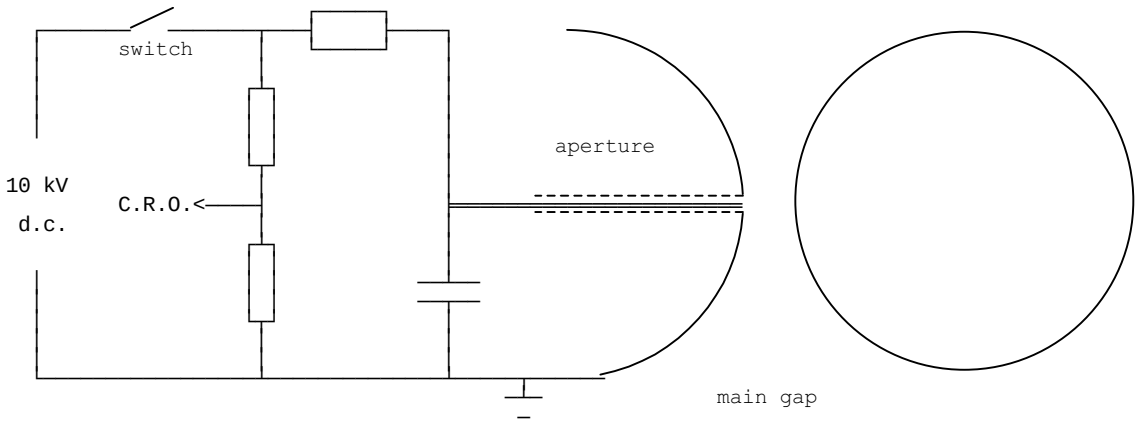

Figure 8.16 - Trigatron gap arrangement

The main gap has one of its spherical electrodes earthed, and as a cup with a hole at the centre. A pin protrudes through it, and is insulated from the electrode with solid insulation. The pin has an auxiliary circuit which can supply high voltage of about 10 kV to it. Since the pin is sharp, corona is produced at a relatively low voltage causing it to spark over to the earthed electrode.

Thus when the generator needs to be energised, a pulse is applied to the pin. Breakdown of the pin gap simultaneously causes the main gap and hence the impulse generator to operate. A delay is usually provided between the auxiliary d.c. source and the pin so that the oscilloscope time base can be started just prior to the impulse being initiated. When the polarity of the generator is changed, it is necessary to change the polarity of the auxiliary supply as well. Since the pilot gap is much smaller than the main gap, we need to apply only a proportionately lower pulse for initiation. Also the performance with the trigatron gap is much more consistent than with the third sphere arrangement.

8.3 Multi-stage Impulse Generators

To obtain large impulse voltages, a multistage impulse generator is used so that the relative size of the high voltage transformer can be kept small, and the costs small. The basic idea is to charge a number of capacitors in parallel through a rectifier from a high voltage transformer and then to discharge them in series, giving the nominal output voltage equal to the charging voltage multiplied by the number of stages in the impulse generator.

In the practical circuit, the capacitors are not all charged to the same voltage, due to the resistances that come in series during charging being not negligible compared to the leakage resistances of the capacitors (especially when the number of stages are large). In theory, the number of gaps and the capacitors may be increased to give almost any desired multiple of the charging voltage and it has been found feasible in practice to operate a 50 stage impulse generator. The number which can be used successfully is limited to some extent, however, by the fact that the high resistance between the supply and the distant capacitors reduce the impulse voltage obtainable.

Two of the commonly used impulse generator circuits are shown. However, as the principles involved are similar only one will be described.

8.3.1 Marx Impulse Generator Circuit

Marx was the first to propose that multistage impulse generators can be obtained by charging the capacitors in parallel and then connecting them in series for discharging.

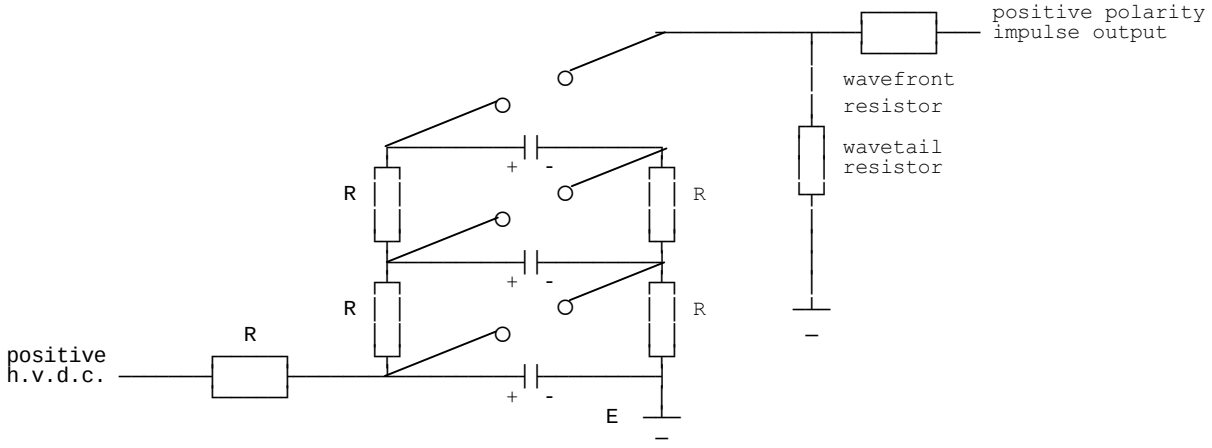

Figure 8.17 - Marx Impulse generator circuit

In the circuit shown in figure 8.17, the resistances R are the charging resistors which are very high in value, and selected such that charging of all capacitors occurs in about 1 minute. The waveshaping circuit is external to the capacitor stages shown. The waveform of the surge generated depends on the resistance, inductance and capacitance of the testing circuit connected. In the modified Marx circuit is more common use, the part of the charging resistors are made use of for waveshape control.

8.3.2 Goodlet Impulse Generator Circuit

The Goodlet impulse generator circuit is very similar to the Marx impulse generator circuit except that the Goodlet circuit gives a negative polarity output for a positive polarity input while the Marx circuit gives the same polarity output.

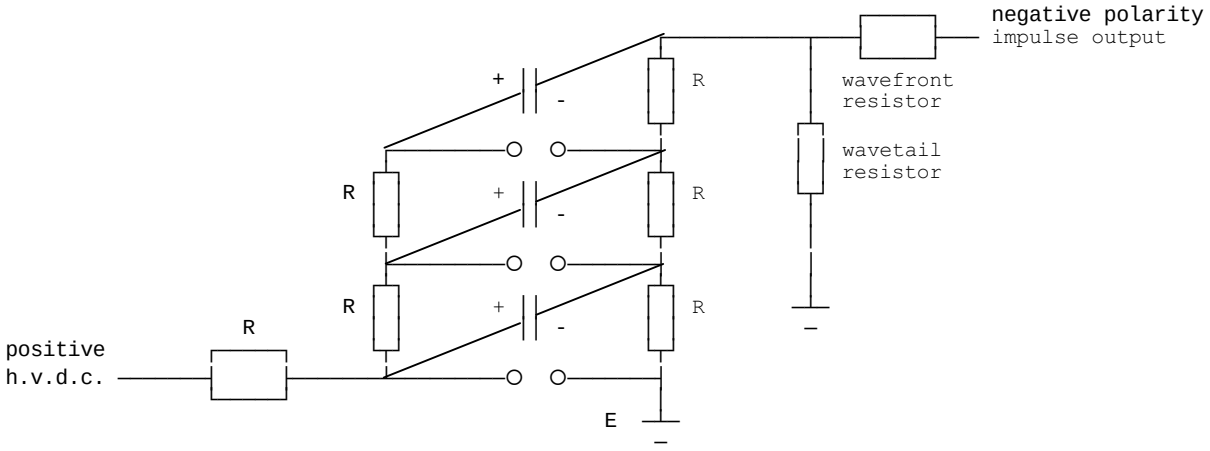

Figure 8.18 - Goodlet Impulse generator circuit

Since all the gaps in the impulse generator should be of almost the same spacing, if they are to breakdown in succession, the spheres of the gaps are fixed along an insulating rod which can be rotated so that the gaps simultaneously increase or decrease as required.

In the case of a controlled impulse generator, the magnitude of the impulse voltage is not directly dependant on the gap spacing as in the case of uncontrolled generators. In this case, a certain range of impulse voltages are available for the same gap spacing. This range is determined by the conditions that (a) uncontrolled operation should not occur, (i.e. the spark over voltage of the gaps must be greater than the applied direct voltage), and (b) the spark over voltage must not be very much larger than the applied voltage (in which case breakdown cannot be initiated even with the pulse).

8.3.3 Simultaneous breakdown of successive sphere gaps

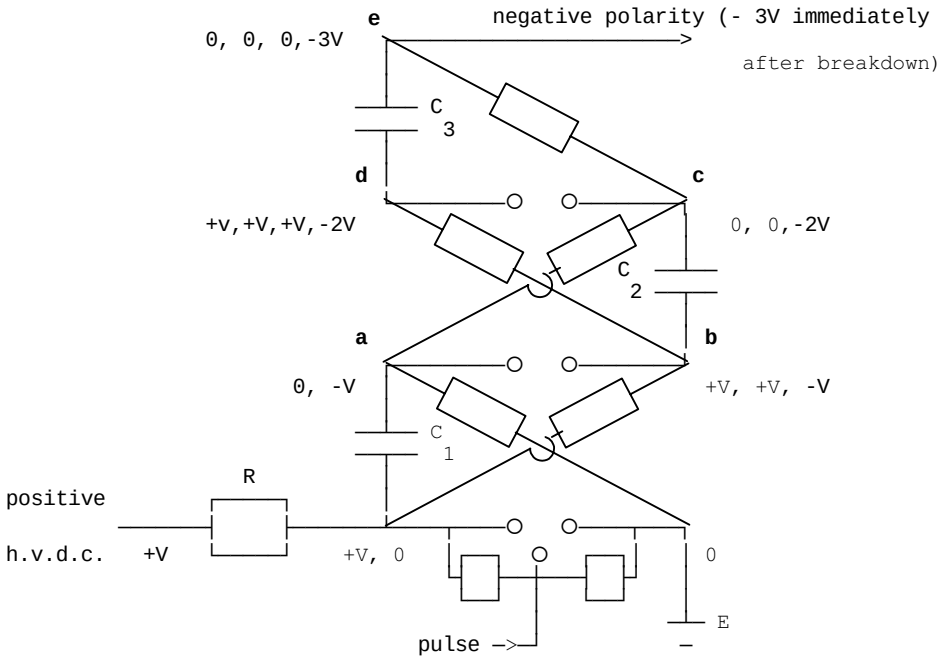

Figure 8.19 - Physical arrangement of the Goodlet Impulse generator circuit

The resistance and capacitance units are arranged so that the sphere gaps are placed one above the other. The capacitors are placed in either two or 4 parallel columns, and the resistances are arranged in a diagonal manner, as shown. The capacitors are mounted vertically above each other with layers of insulation separating them. This arrangement is shown in figure 8.19, without the waveshape control elements.

Once the initial pulse breaks down the first gap, the breakdown of the successive gaps occurs in the following manner.

If the supply voltage is **+V**, under steady charged condition and before the breakdown of the gaps, the voltage across each capacitor will be **V**, assuming the leakage across the capacitors is negligible.

When the trigger pulse is applied, the breakdown of the trigger electrode and hence of the first gap occurs, and the voltage across it falls to zero (disregarding the arc voltage drop). As the voltage across the capacitor C_1 cannot change instantly, the voltage at **a** must fall to **-V** from **0**. Due to the initial voltage **+V** at **b**, which also occurs across the stray capacitance to earth at **b**, and since this stray capacitance too cannot discharge suddenly, the voltage at **b** must remain at **+V**. Thus a voltage of **+2V** must appear across the second gap **ab**. This voltage is sufficient to breakdown the gap (as the settings of the gaps are so arranged), and thus the gap breaks down. This breakdown causes the voltage at **b** to change to that at **a** (i.e. to **-V**). Since C_2 does not discharge suddenly, the voltage at **c** falls to **-2V.** The voltage at **d** would remain at **+V** which value it would have reached when **b** became **+V**. Thus the voltage of **3V** across the third gap breaks it down. Similarly, any other gaps present would breakdown in succession.

Effect of sphere gap capacitances on the successive breakdown

In the above analysis, the sphere gaps are assumed to be large and the stray capacitances across the gaps have been neglected. However, when the voltage of the impulse generator is increased, the gaps further. In this case we must also take the gap capacitance into account. Figure 8.20 shows the impulse generator circuit with the stray capacitances also indicated, and with $C_1 = C_2 = C_3 = C$.

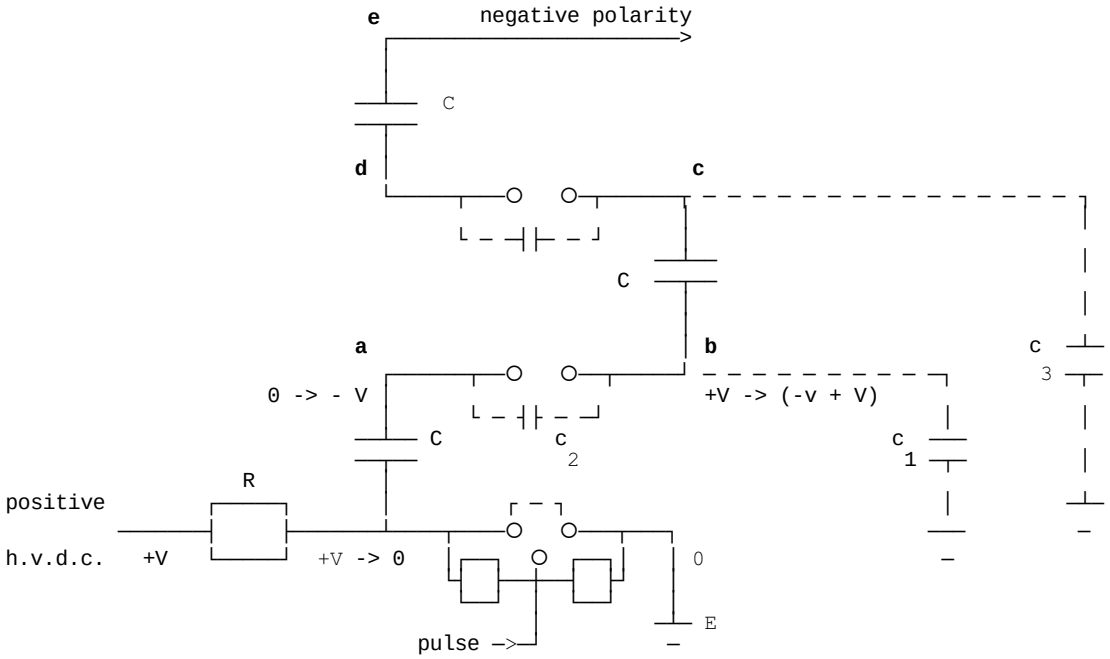

c_1, c_2 and c_3 are stray capacitances

[Some of the resistors have been left out of the figure for clarity of presentation]

Figure 8.20 - Stray Capacitances of the Goodlet Impulse generator circuit

When the first gap breaks down due to the trigger pulse, since one end of the gap is at each potential, the other end will also come to earth potential. Since the voltage across the first capacitor cannot change suddenly, the voltage at **a** falls to **- V**. This change of **-V** would cause, by potential divider action, a change of

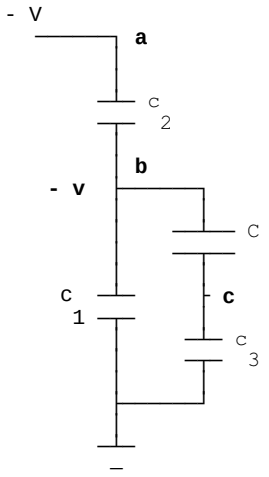

Figure 8.21

$$\frac{v}{V} = \frac{c_2}{c_2 + c_1 + \dfrac{c_3 C}{c_3 + C}}$$

voltage of **- v** at **b**, so that the voltage at **b** just after the breakdown of the first gap is (**- v + V**). From figure 8.21

Being stray capacitance, $c_3 << C$, so that $\dfrac{c_3 C}{c_3 + C} \approx c_3$

$$\therefore \frac{v}{V} = \frac{c_2}{c_1 + c_2 + c_3}$$

Therefore the potential at **b** after the breakdown of the first gap is given by

$$v_b = -v + V = V\left[1 - \frac{c_2}{c_1 + c_2 + c_3}\right]$$

At this instant, the potential at **a** has fallen from **0** to **- V**. Therefore the potential difference across **ab** after breakdown of the gap is given by

$$v_{ab} = -v - V\left[1 - \frac{c_2}{c_1 + c_2 + c_3}\right]$$

$$= V\left[2 - \frac{c_2}{c_1 + c_2 + c_3}\right] = V\left[1 + \frac{c_1 + c_3}{c_1 + c_2 + c_3}\right]$$

If the gap is large, $c_2 = 0$, and the voltage across the second sphere gap is **2V**, which is the ideal case, since this ensures the breakdown of successive gaps.

On the other hand, if $c_1 + c_3$ is small compared to c_2, then the voltage across the second sphere gap is approximately equal to **V**, so that the breakdown of successive gaps would not occur. Therefore, for good operating conditions, $c_1 + c_3$ must be large, and c_2 small, so that the upper gaps would breakdown simultaneously.

Generally, for a small impulse generator, since the sphere gap is small, c_2 is high and $c_1 + c_3$ small, so that the conditions for the breakdown of successive gaps is poor. In this case, c_1 can be deliberately increased to improve breakdown conditions. In the case of large impulse generators, c_2 is small, so that the conditions are favourable for the breakdown of the upper gaps.

Effect of illumination on the breakdown of gaps

In general the voltage appearing across an upper gap, on the breakdown of the gap immediately below it, must be sufficient to initiate the breakdown of the gap. Since breakdown must be almost instantaneous, there should be some amount of initial electrons present in the gap. The presence of ultra-violet illumination aids breakdown due to photo-ionisation. To make use of this phenomena, the sphere gaps in the impulse generator are arranged one above the other so that the illumination caused by the breakdown of one gap illuminates the next.

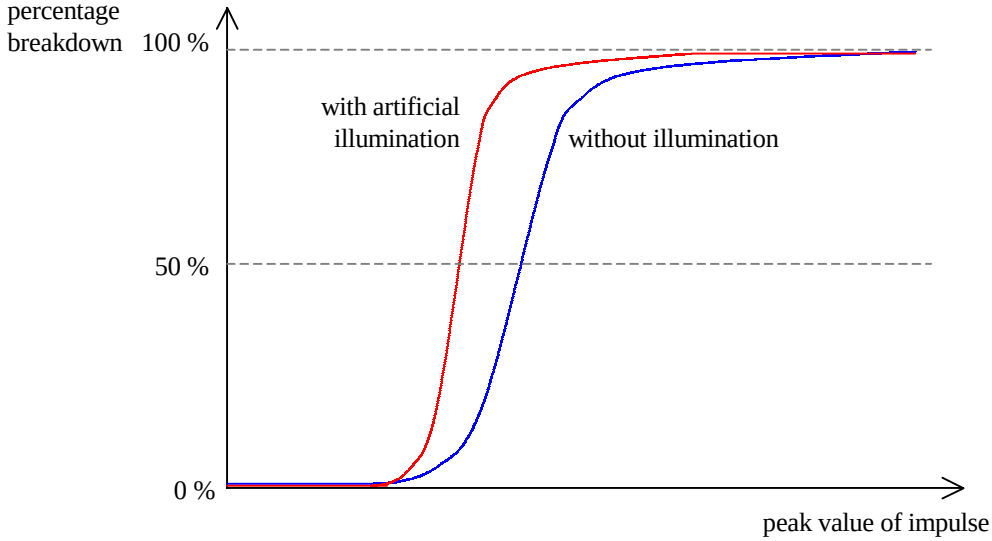

Figure 8.22 - Statistical breakdown characteristic

The breakdown of a sphere gap is subject to statistical variations. The peak value of the impulse necessary for the breakdown of a gap may vary over a small range, as shown in figure 8.22. If artificial illumination is provided at the gap (as with the ultra violet radiation from the breakdown of the previous gap), the uncertainty of the breakdown for a particular gap setting is reduced. This is due to the fact that a certain amount of electrons/second are created by phot-ionisation in the gap, and the breakdown is more constant.

Due to the presence of stray capacitances etc, the order of the differential equation governing the impulse waveform is increased, and the practical circuit will have exponential terms to the order of the number of storage elements.

Modified Goodlet impulse generator circuit

To obtain a good impulse voltage waveform, it is necessary to damp out the oscillations caused. This is done using waveshape control resistances distributed throughout the multi-stage impulse generator, as shown in figure 8.23.

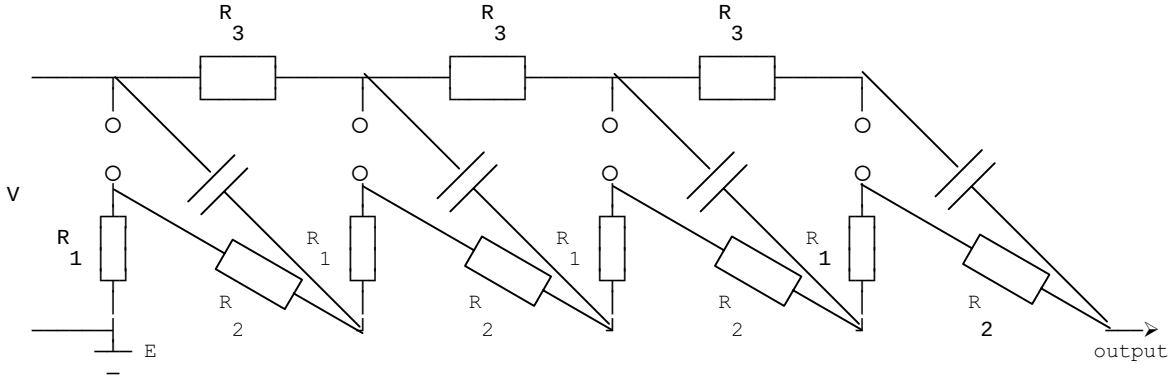

Figure 8.23 - Multi-stage impulse generator with distributed waveshape control elements

In the figure shown, the wavefront control resistances R_1 is distributed between the different stages. The wavetail control resistors R_2 are also distributed to the stages. The resistance R_3 is required only for the purpose of charging the capacitances in parallel, and is not part of the actual impulse generating circuit. Thus R_3 is selected large compared to R_1 and R_2. By proper selection of R_1 and R_2 the desired wavefront and wavetail can be obtained.

8.3.4 Generation of chopped impulse waveforms

The basic impulse generator circuit is for the generation of the full impulse waveform. Sometimes it is necessary to obtain a chopped wave (to represent the lightning waveform appearing when a gap flashes over). The chopping action can be accomplished by having a gap across the load at the last stage of the impulse generator as shown in figure 8.24.

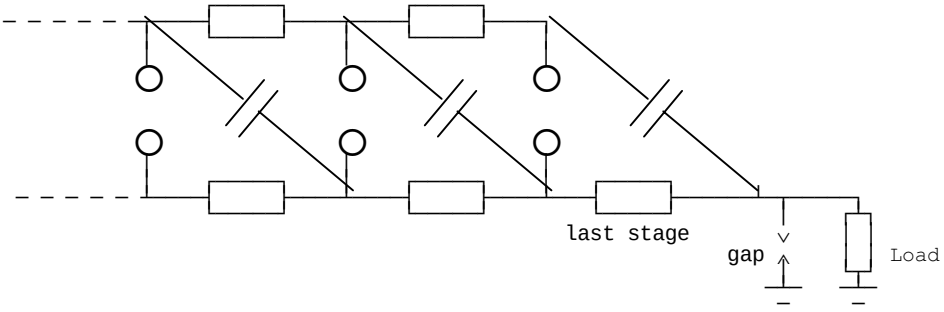

Figure 8.24 - Multi-stage impulse generator to obtain chopped waveform

The exact point of flashover on the surge waveform depends on the breakdown voltage against time characteristic of the gap. For an uncontrolled gap, this is rather uncertain, so that the instant of application of the collapse is not controllable. This is not satisfactory.

The problem can be overcome by having a triggered gap or a trigatron gap after the last stage. A pulse is applied to the pilot gap at the instant the waveform is required to be chopped, so that the point of chopping is well defined. [The instant of application of the pulse for this is in fact synchronised with the initiation of the impulse, but with an intended delay introduced.] Figure 8.25 show the chopped wave obtained, and the arrangement to obtain the chopped wave using a trigatron type gap.

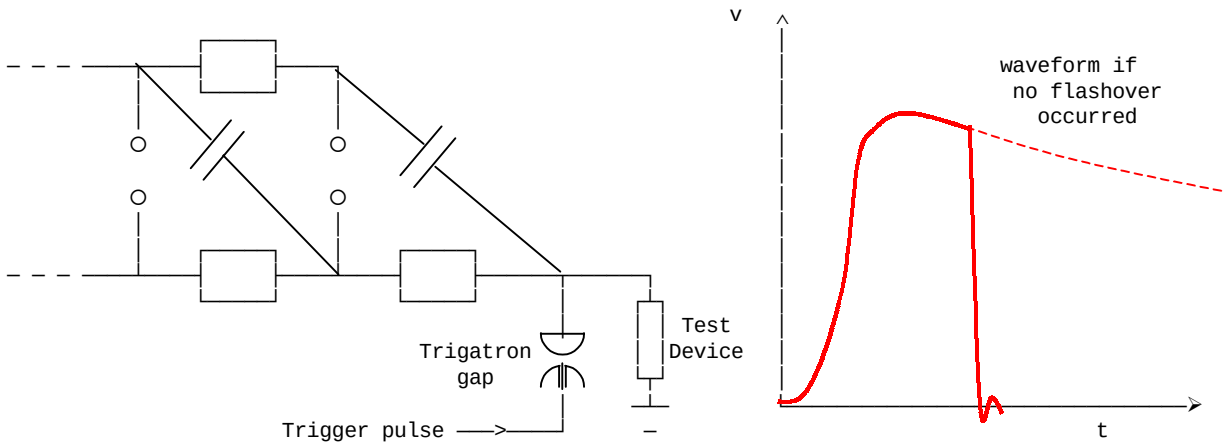

Figure 8.25 - Chopped waveform & Circuit to obtain chopped waveform

High Voltage Testing

9.0 High Voltage Testing Procedure

Electrical equipment must be capable of withstanding overvoltages during operation. Thus by suitable testing procedure we must ensure that this is done.

High voltage testing can be broadly classified into testing of insulating materials (samples of dielectrics) and tests on completed equipment.

The tests carried out on samples of dielectric consist generally of the measurement of permittivity, dielectric loss per unit volume, and the dielectric strength of the material. The first two can be measured using the High Voltage Schering Bridge.

The tests carried out on completed equipment are the measurement of capacitance, the power factor or the total dielectric loss, the ultimate breakdown voltage and the flash-over voltage. The breakdown voltage tests on completed equipment is only done on a few samples since it permanently damages and destroys the equipment from further use. However since all equipment have to stand up to a certain voltage without damage under operating conditions, all equipment are subjected to withstand tests on which the voltage applied is about twice the normal voltage, but which is less than the breakdown voltage.

9.1 General tests carried out on High voltage equipment

9.1.1 Sustained low-frequency tests

Sustained low frequency tests are done at power frequency (50 Hz), and are the commonest of all tests. These tests are made upon specimens of insulation materials for the determination of dielectric strength and dielectric loss, for routine testing of supply mains, and for work tests on high voltage transformers, porcelain insulators and other apparatus.

Since the dielectric loss is sensitive to electric stress, the tests are carried out at the highest ultimate stress possible. For testing of porcelain insulators and in high tension cables, voltages as high as 2000 kV may be used.

High voltage a.c. tests at 50 Hz are carried out as Routine tests on low voltage (230 or 400 V) equipment. Each one of these devices are subjected to a high voltage of 1 kV + 2 $\times$ (working voltage). A 230 V piece of equipment may thus be subjected to about 1.5 to 2 kV. These tests are generally carried out after manufacture before installation.

The high voltage is applied across the device under test by means of a transformer. The transformer need not have a high power rating. If a very high voltage is required, the transformer is usually build up in stages by cascading. By means of cascading, the size of the transformer and the insulation bushing necessary may be reduced in size. The transformers are usually designed to have poor regulation so that if the device under test is faulty and breakdown occurs, the terminal voltage would drop due to the high current caused. A resistance of about 1 ohm/volt is used in series with the transformer so as to limit the current in the event of a breakdown to about 1 A. The resistance used could be of electrolyte type (which would be far from constant, but would be a simple device) such as a tube filled with water.

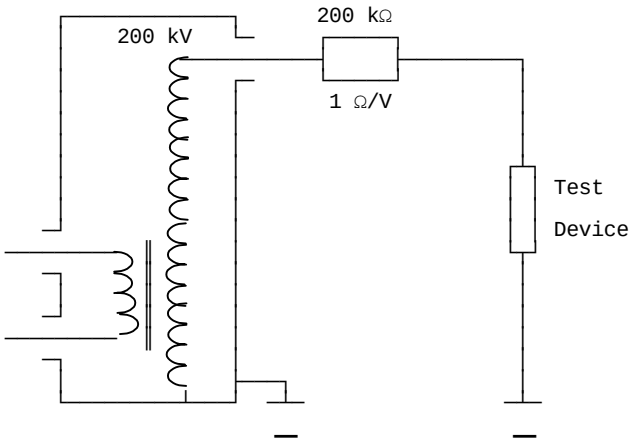

Figure 9.1 - a.c. generation test circuit

In all high voltage tests, safety precautions are taken so as to ensure that there is no access to the testing area when the high voltage is on. There would be switches that would automatically be operated when the door to the area is opened etc..

9.1.2 High Voltage direct current tests

These tests are done on apparatus expected to operate under direct voltage conditions, and also where, due to the inconvenience of the use of high capacity transformers required for extra high tension alternating voltage tests and due to transport difficulties, alternating voltage tests cannot be performed after installation.

A special feature of importance of the d.c. test is the testing of cables which are expected to operate under a.c. conditions. If the tests are done under a.c. conditions, a high charging current would be drawn and the transformer used would have to have a current rating. It is thus normal to subject the cable (soon after laying it, but before energising it) to carry out a high voltage test under d.c. conditions. The test voltage would be about 2 (working voltage) and the voltage is maintained from 15 min to 1.5 hrs. This d.c test is not complete equivalent to the corresponding a.c. conditions , it is the leakage resistance which would determine the voltage distribution, while in the a.c. conditions, it is the layers of different dielectrics that determine the voltage distribution in the cable. Although the electric field differs in the 2 cases, it is likely that the cable will stand up to the required a.c. voltage.

The methods used to generate these high d.c. voltages have already been described.

9.1.3 High-frequency tests

High frequency tests at frequencies varying from several kHz are important where there is a possibility of high voltage in the lines etc., and in insulators which are expected to carry high frequency such as radio transmitting stations. Also in the case of porcelain insulators, breakdown or flashover occurs in most cases as a result of high frequency disturbances in the line, these being due to either switching operations or external causes. It is also found that high frequency oscillations cause failure of insulation at a comparatively low voltage due to high dielectric loss and heating.

High voltage tests at high frequency are made at the manufacturing works so as to obtain a design of insulator which will satisfactorily withstand all conditions of service.

In the case of power line suspension insulators, it is possible that breakdown or flash over would occur due to high frequency over voltages produced by faults or switching operations in the line. Sudden interruptions in the line would give rise to resonant effects in the line which would give rise to voltage waves in the line of high frequency. These might cause flashover of the insulators.

The behaviour of insulating materials at high frequencies are quite different to that at ordinary power frequency. The dielectric loss per cycle is very nearly constant so that at high frequencies the dielectric loss is much higher and the higher loss causes heating effects.The movements of charge carriers would be different.

At high frequency the polarity of electrodes might have changed before the charge carriers have travelled from one electrode to the other, so that they may go about half-way and turn back (figure 9.2).

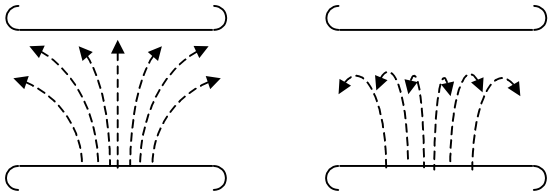

Figure 9.2 Movement of charge carriers

There are two kind of high frequency tests carried out. These are

(a) Tests with apparatus which produces undamped high-frequency oscillations.

Undamped oscillations do not occur in power systems, but are useful for insulation testing purposes especially for insulation to be in radio work.

(b) Tests with apparatus producing damped high-frequency oscillations.

When faults to earth or sudden switching of transmission lines occur, high frequency transients occur whose frequency depends on the capacitance and inductance of the line and will be about 50 kHZ to about 200 kHZ. These are damped out with time.

9.1.4 Surge or impulse tests

These tests are carried out in order to investigate the influence of surges in transmission lines, breakdown of insulators and of the end turns of transformer connections to line. In impulse testing, to represent surges generated due to lightning, the IEC Standard impulse wave of 1.2/50 μs wave is generally used. By the use of spark gaps, conditions occurring on the flash over to line are simulated. The total duration of a single lightning strike os about 100 μs, although the total duration of the lightning stroke may be a few seconds.

Overvoltages of much higher duration also arise due to line faults, switching operations etc, for which impulse waves such as 100/5000 μs duration may be used.

In surge tests it is required to apply to the circuit or apparatus under test, a high direct voltage whose value rises from zero to maximum in a very short time and dies away again comparatively slowly . Methods of generating such voltages have already been discussed earlier.

While impulse and high frequency tests are carried out by manufacturers , in order to ensure that their finished products will give satisfactory performance in service , the most general tests upon insulating materials are carried out at power frequencies .

Flash-over Tests

Porcelain insulators are designed so that spark over occurs at a lower voltage than puncture, thus safeguarding the insulator, in service against destruction in the case of line disturbances. Flash-over tests are very importance in this case .

The flash-over is due to a breakdown of air at the insulator surface, and is independent of the material of the insulator. As the flash-over under wet conditions and dry conditions differ , tests such as the one minute dry flash-over test and the one minute wet flash-over test are performance.

(i) 50 percent dry impulse flash-over test, using an impulse generator delivering a positive 1/50 μs impulse wave.

The voltage shall be increased to the 50 percent impulse flash-over voltage (the voltage at which approximately half of the impulses applied cause flash-over of the insulator)

(ii) Dry flash-over and dry one-minute test

In this the test voltage (given in the B.S.S.) is applied . The voltage is raised to this value in approximately 10 seconds and shall be maintained for one minute. The voltage shall then be increased gradually until flash- over occurs .

(iii) Wet flash-over and one minute rain test

In this the insulator is sprayed throughout the test with artificial rain drawn from source of supply at a temperature within 10 degrees of centigrade of the ambient temperature in the neighborhood of the insulator. The resistivity of the water is to be between 9,000 and 11,000 ohm cm.

In the case of the testing of insulating materials , it is not the voltage which produces spark-over breakdown which is important , but rather the voltage for puncture of a given thickness (ie. dielectric strength) . The measurements made on insulating materials are usually , therefore , those of dielectric strength and of dielectric loss and power factor , the latter been intimately connected with the dielectric strength of the material.

It is found that the dielectric strength of a given material depends , apart from chemical and physical properties of the material itself, upon many factors including,

(a) thickness of the sample tested
(b) shape of the sample
(c) previous electrical and thermal treatment of the sample
(d) shape , size , material and arrangement of the electrodes
(e) nature of the contact which the electrodes make with the sample
(f) waveform and frequency of the applied voltage (if alternating)
(g) rate of application of the testing voltage and the time during which it is maintained at a constant value .
(h) temperature and humidity when the test is carried out
(i) moisture content of the sample.

9.2 Testing of solid dielectric materials

9.2.1 Nature of dielectric breakdown

Dielectric losses occur in insulating materials, when an electrostatic field is applied to them. These losses result in the formation of heat within the material. Most insulating materials are bad thermal conductors,so that, even though the heat so produced is small, it is not rapidly carried away by the material. Now, the conductivity of such materials increases considerably with increase of temperature, and the dielectric losses, therefore, rise and produce more heat, the temperature thus building up from the small initial temperature rise. If the rate of increase of heat dissipated, with rise of temperature, is greater than the rate of increase of dielectric loss with temperature rise, a stable condition (thermal balance) will be reached. If, however, the latter rate of increase is greater than the former, the insulation will breakdown owing to the excessive heat production, which burns the material.

Now, the dielectric losses per cubic centimetre in a given material and at a given temperature, are directly proportional to the frequency of the electric field and to the square of the field strength. Hence the decrease in breakdown voltage with increasing time of application and increasing temperature and also the dependence of this voltage upon the shape, size, and material of the electrodes and upon the form the electric field.

The measurement of dielectric loss in insulating materials are very important, as they give a fair indication as to comparative dielectric strengths of such materials. In the case of cable, dielectric loss measurements are now generally recognized as the most reliable guide to the quality and condition of the cable.

9.2.2 Determination of dielectric strength of solid dielectrics

A sheet or disc of the material of not less than 10cm in diameter, is taken and recessed on both sides so as to accommodate the spherical electrodes (2.5 cm in diameter) with a wall or partition of the material between them 0.5mm thick. The electrical stress is applied to the specimen by means of the two spheres fitting into the recesses without leaving any clearance, especially at the centre. The applied voltage is of approximately sine waveform at 50Hz. This voltage is commenced at about 1/3 the full value and increased rapidly to the full testing voltage.

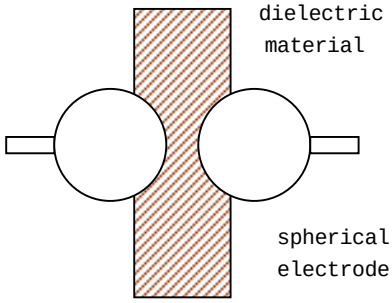

Figure 9.3 - solid sample

Sometimes insulators after manufacture are found to contain flaws in the form of voids or air spots.These spots (due to non-homogeneity) have a lower breakdown strength than the material itself, and if present would gradually deteriorate and cause ultimate breakdown after a number of years.

High degree ionisations caused in these spots would give rise to high energy electrons which would bombard the rest of the material, causing physical decomposition. In plastic type of materials,there might be carbonizations, polymerisations, chemical decomposition etc.,which would gradually diffuse into the material the by-products, causing chemical destruction.

The useful life of a component using such material will depend on the weak spots and the applied voltage. If the applied voltage is small, the life of the component is longer. From design considerations the voltage to be applied if a particular life span is required can be calculated.
The schering bridge type of measurement gives an average type of measurement,where the p.f. and the power loss indicates the value over the whole of the length.Thus small flaws if present would not cause much of a variation in the overall p.f. Thus in the schering bridge type of measurement such flaws would not be brought out.

The loss factor of a material does not vary much for low voltages, but as the voltage is increased at a certain value it starts increasing at a faster rate. This is the long time safe working voltage, since beyond this, the specimen would keep on deteriorating.

If the apparatus need be used only for a short period, the applied voltage can be higher than this safe value.

In a long length of cable, the greater part of the cable would be in good conditions but with a few weak spots here and there.

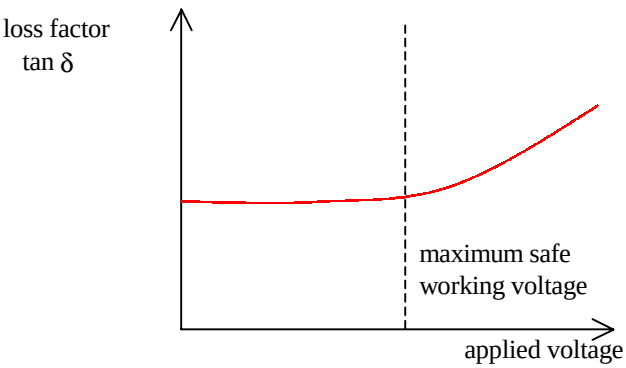

Figure 9.4 - variation of loss factor

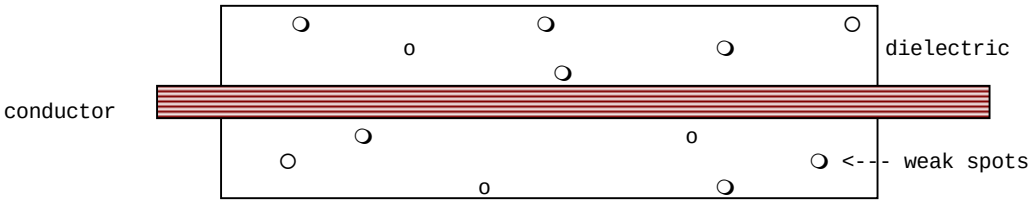

Figure 9.5 - sample of cable showing weak spots

In a Schering bridge type of measurement, since it measures the overall loss, such small individual spots cannot be detected. It is necessary that such spots are detected as these increase with time and finally cause its breakdown.

In high voltage transformers also there might be such small discharges occurring which would not be measured by the schering bridge.

The method is to apply suitable high voltage to sample, and subject it to a number of duty cycles (heat cycles, make and break cycles). Discharges caused are made to give pulses to a high frequency amplifier. The discharges caused are observed before and after such duty cycles to see whether there is any appreciable increase in the pulse intensity after the cycle of operation. The methods of discussion have been discussed in an earlier chapter.

9.3 Impulse Testing

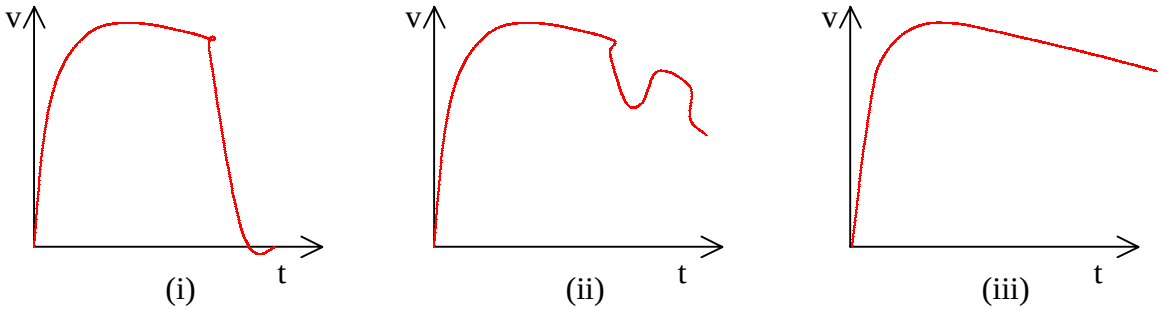

Figure 9.6 - Observed impulse waveforms

These are done as tests on sample of apparatus. The impulse test level is determined by the operating level (4 to 5 times the normal operating value) Apply on to the sample a certain number (say 10) positive impulse and 10 negative impulses of this particular value. They should withstand this voltage without any destruction.

To test the ultimate impulse strength, apply increasing amounts of impulse voltage until destruction occurs; during the tests it is necessary to see whether there is any damage. The damage may not be immediately visible, so we have it on a high frequency (single sweep and high speed) oscilloscope.
In the event of complete damage, breakdown of the insulator due to the application of the impulse voltage will be indicated as in (i). If the insulator has suffered only a minor damage the wave form would show no distortion , but would show as in (ii). If there is no damage caused due to the impulse, the waveform will be complete and undistorted as in (iii).

In testing high voltage insulators whose actual breakdown is in air (i.e flashover takes place before breakdown of insulator) the porcelain itself can be tested by immersing the whole insulator in liquid of high permeability so that there would be no outside flashover, and actual breakdown of the insulator would occur.

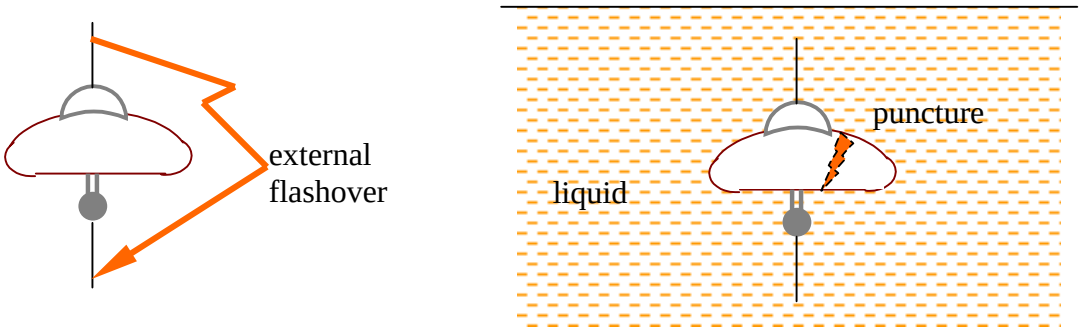

Figure 9.7 - Breakdown of insulator unit

In specifying the flashover characteristic in air we give the 50% flashover characteristic.This is done as flashover occur at the same voltage on each application of the impulse . We apply different values of test voltages (impulse) and the voltage at which there is 50% probability of breakdown is taken as 50% flashover voltage.The impulse flashover voltage also depends on the time lag of the applied impulse before flashover time lag of the applied impulse before flashover occurs. Thus we have also got to determine the time lag characteristics for breakdown.

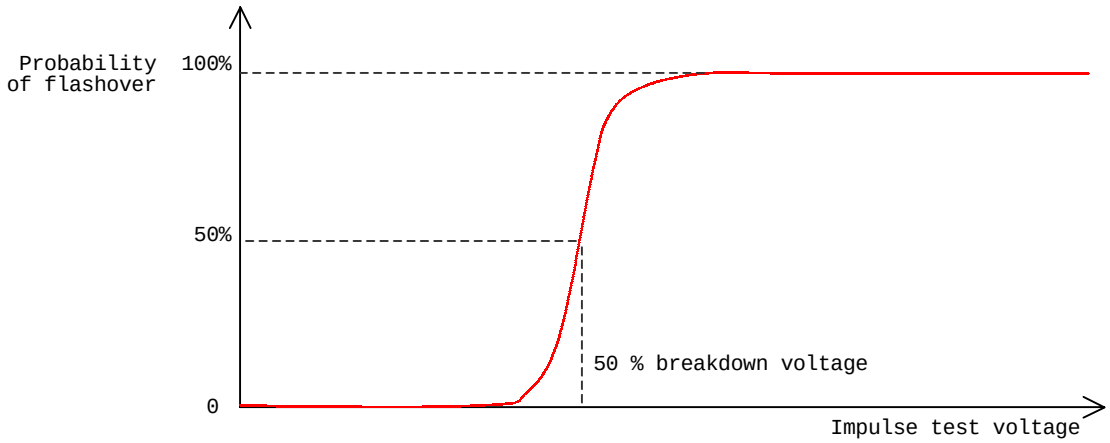

Figure 9.8 - Probability of flashover

If the voltage remains above a critical value long enough, flashover occurs.

The time lag before flashover occurs depends on the statistical time lag and on the formation time lag.

Depending on the volume of space between the gap, and also depending on the nature of shielding, a certain time will be taken for enough free electrons to be set free.This is the statistical time lag.

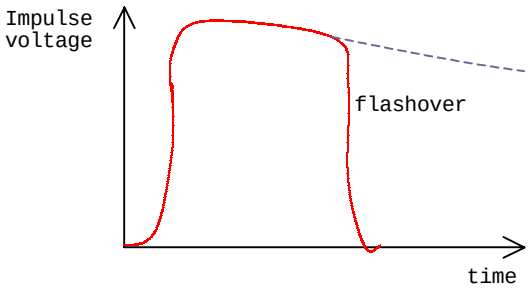

Figure 9.9 - Chopped impulse waveform

Once the electrons appear, depending on the voltage applied, they multiply and ionise the space. once the space becomes conducting, flashover occurs. This is formation time lag.

To determine the time lag characteristic of a device, we can use the impulse generator to generate impulses of gradually increasing amplitude and determine the time of breakdown. At each value, the test must be repeated a number of times so as to obtain consistent values.

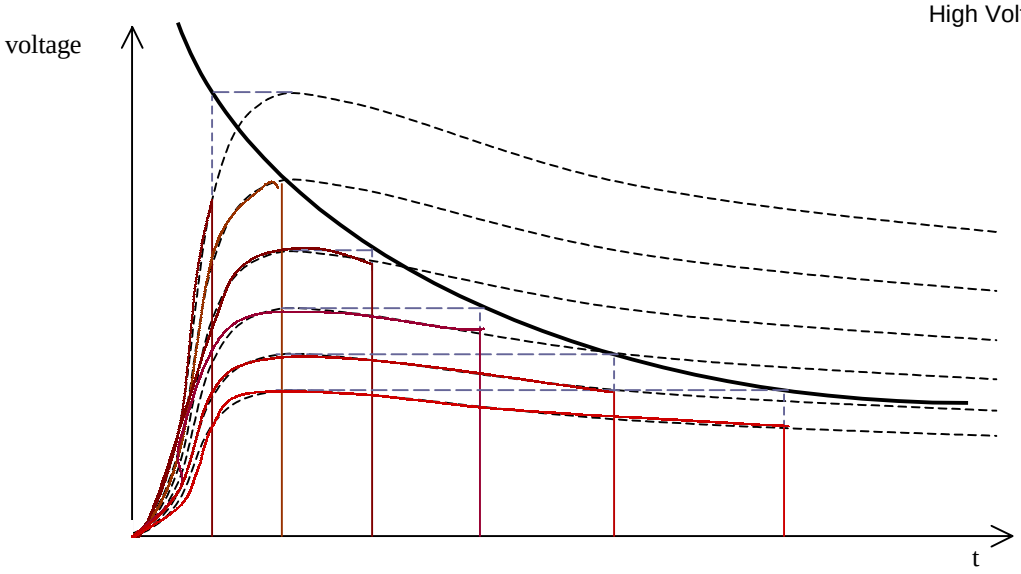

Figure 9.10 - Time lag characteristic

This type of characteristic is important in designing insulators.If a rod gap is to protect a transformer. Then the breakdown voltage characteristic of the rod gap must be less than that of the transformer so as to protect it. If the characteristic cross, protection will be offered only in the region where the rod gap characteristic is lower than that of the transformer.

System Voltage	I.E.C. Impulse Withstand Voltage
11 kV	75 kV
33 kV	170 kV
66 kV	325 kV
132 kV	550 kV
275 kV	1050 kV

In obtaining the breakdown characteristic of a transformer we do not attempt such tests that cause total destruction on transformers as they are expensive. What is done is we take a sample of the material used as insulators for the transformers and then apply these tests till puncture takes place. Thus the transformer characteristic is obtained by such tests on samples.

To obtain one point on the voltage vs time lag characteristic we would have to do a large number of tests and take the mean,as these values vary from sample to sample. The sample would have to be surrounded by a liquid material of high permittivity so that external flashover would not occur.

The impulse test voltage recommended by I.E.C. (International Electrotechnical Commission) are given in the table 9.1.

The recommendation is that device when subjected to this voltage should not suffer permanent damage or minor partial damage. The voltage is set at slightly less than the withstand voltage and gradually increase to test value. About 10 positive impulses and 10 negative impulses are applied.

9.4 Voltage Distribution in a Transformer Winding

Consider the entering of an impulse voltage on the terminating transformer, as shown in figure 9.11.

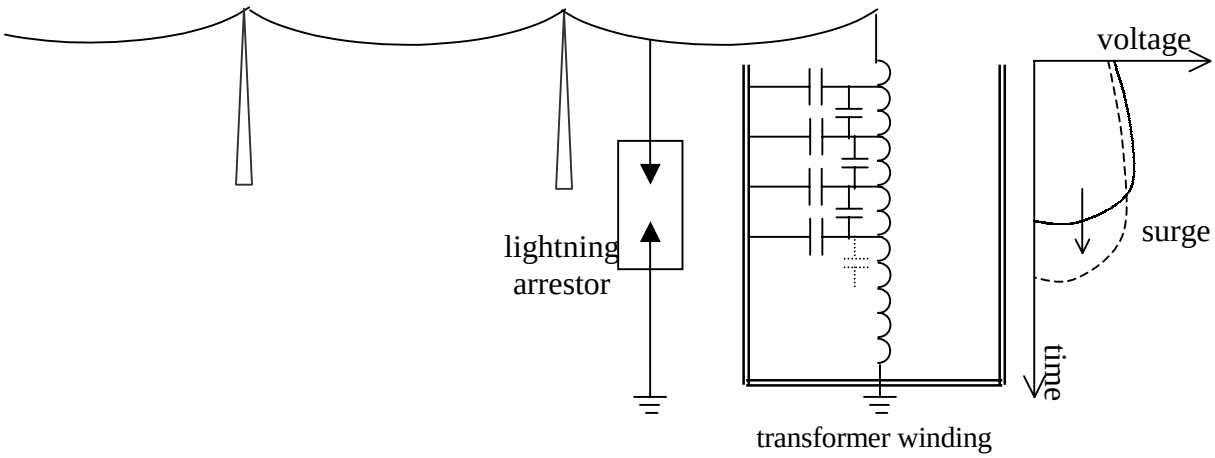

Figure 9.11 - Surge propagation in transformer winding

Due to the presence of the interwinding capacitance and the capacitances to earth of the transformer windings, the upper elements of the transformer windings tend to be more heavily stressed than the lower portions.

Due to the velocity of propagation of the impulse voltage would not be evenly distributed in the winding. Due to sharp rise of the voltage of the surge. there is a large difference of voltage caused in the winding as the wave front travels up the winding. Thus there would be an overvoltage across adjacent windings.

Depending on the termination, there will be reflections at the far end of the winding. If the termination is a short circuit, at the lowest point the voltage wave whose amplitude is same as the original wave but of opposite polarity is reflected. For a line which is open circuited, the reflected wave would be of the same magnitude and of the same sign.

Arising out of the reflections at the far end , there would be some coils heavily stressed. The position of the heavily stressed coils depending on the velocity of propagation.

If flashover occurs at the gap (lightning arrestor) the voltage of the impulse suddenly drops to zero when flashover occurs. This can be represented by a full wave, and a negative wave starting from the time flashover occurs. The chopped wave, though it reduces the voltage of the surge to zero, will have a severe effect of the winding due to sharp drop in the voltage. Thus it is always necessary to subject the transformer during tests to chopped wave conditions. Generally the method is to apply full-waves and see whether damage has occurred and then to apply the chopped waves and to see whether damage has occurred and then to apply the chopped waves and to see whether damage has occurred.

Example

A rectangular voltage V is impressed at the line terminal of a winding of a high voltage transformer , the neutral point being isolated from earth.The capacitance to earth of the complete winding is Cw.Prove that the voltage at a point in the winding distant X from the neutral is

$$v_x = V.\frac{\cosh\frac{a}{l}x}{\cosh a}, \quad \text{where } a^2 = \frac{C_g}{C_w}, \quad l = \text{length of winding}$$

If C_g = 900 pF and Cw = 10 pF , calculate the ratio of the maximum initial voltage gradient in the winding to the average voltage gradient.How will the initial voltage distribution in the winding be effected if the wavefront has a duration of several microseconds ?

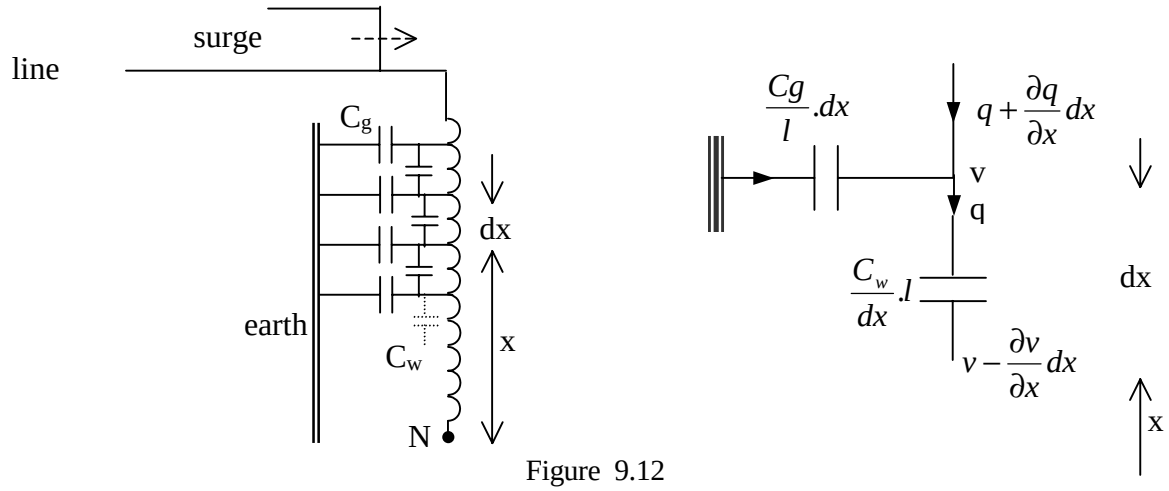

Figure 9.12

In the case of a voltage with a vertical front incident on the transformer winding , the voltage variation being instantaneous , the charging up is instantaneous and the presence of the inductance of the winding may be neglected.

$$\text{Thus,} \quad \frac{\partial q}{\partial x}.dx = \frac{C_g}{l}.dx.v, \qquad \frac{\partial v}{\partial x}.dx.\frac{C_w}{dx}.l = q$$

$$\therefore \quad \frac{\partial q}{\partial x} = \frac{C_g}{l}.v, \qquad C_w.l.\frac{\partial v}{\partial x} = q$$

$$\therefore \quad \frac{\partial^2 v}{\partial x^2} - \frac{C_g}{C_w}.\frac{1}{l^2}.v = 0$$

$$\therefore \quad v = A\cosh\frac{a}{l}x + B\sinh\frac{a}{l}x$$

$$\text{at } x = l, \ v = V; \ \text{so that } v = A\cosh\frac{a}{l}x + B\sinh\frac{a}{l}x$$

$$\text{at } x = 0, \quad q = 0, \quad \text{so that } q = C_w l.\frac{\partial v}{\partial x} = C_w l\left(A.\frac{a}{l}\sinh 0 + B.\frac{a}{l}\cosh 0\right) = 0$$

$$\therefore \quad B = 0, \quad \text{giving} \quad A = \frac{V}{\cosh a}$$

$$\therefore \quad v = \frac{V\cosh\frac{a}{l}.x}{\cosh a}, \quad \text{also} \quad \frac{\partial v}{\partial x} = \frac{V.\frac{a}{l}.\sinh\frac{a}{l}.x}{\cosh a} \quad \text{initially.}$$

$$\text{Substituting figures we have} \quad a^2 = \frac{900}{10} = 90, \quad \therefore \ a = 9.48$$

$$\text{Maximum initial voltage gradient (at } x = l) = V.\frac{a}{l}.\tanh(9.48) \approx V.\frac{a}{l}$$

$$\text{average stress} = \frac{1}{l}\int_0^l \frac{V.a}{l.\cosh a}.\sinh\frac{a}{l}.x.dx$$

$$= \frac{V}{l}.\left[1 - \frac{1}{\cosh a}\right] \approx \frac{V}{l}$$

$$\therefore \ \text{maximum stress/average stress} = a \approx 9.48 \ \text{ initially}$$

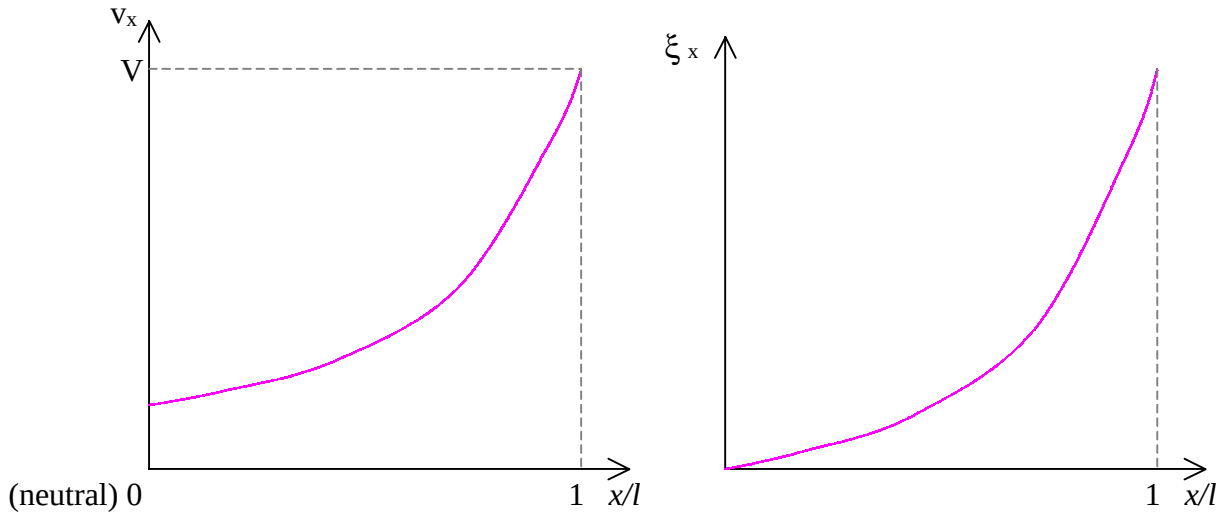

Figure 9.13 - variations of voltage and voltage gradient

The voltage distribution along the winding and the stress distribution (initially) are as shown in figure 9.13.

If the wave-front time is of several micro-seconds duration, the charging up would not be instantaneous, and the effect of the inductance during this period may not be neglected. The winding then behaves similar to a transmission line with distributed inductances and shunt capacitances. The effect of the surge would cause a lesser stress than in the case of a surge with a vertical front.

The differential equation governing the variation of the voltage would be a fourth order partial differential equation.

9.5 Tests on Insulators

The tests on insulators can be divided into three groups. These are the type tests, sample tests and the routing tests.

9.5.1 Type tests

These tests are done to determine whether the particular design is suitable for the purpose.

(a) Withstand Test: The insulator should be mounted so as to simulate practical conditions. A 1/50 μs wave of the specified voltage (corrected for humidity, air density etc.,) is applied. Flashover or puncture should not occur. [If puncture occurs, the insulator is permanently damaged]. The test is repeated five times for each polarity.

(b) Flash-over test: A 1/50 μs wave is applied. The voltage is gradually increased to the 50% impulse flash-over voltage. The test is done for both polarities. There should be no puncture of insulation during these tests.

(c) Dry One-minute test: The insulator, clean and dry, shall be mounted as specified and the prescribed voltage (corrected for ambient conditions) should be gradually brought up (at power frequency) and maintained for one minute. Thee shall not be puncture or flash-over during the test.

Dry flash-over test: The voltage shall then be increased gradually until flash-over occurs. This is repeated ten times. There shall be no damage to the insulator.

(d) One-minute Rain test: The insulator is sprayed throughout the test with artificial rain drawn from a source of supply at a temperature within 10^{o} C of the ambient temperature of the neighbourhood of the insulator. The rain is sprayed at an angle of 45 ^{o} on the insulator at the prescribed rate of 3 mm/minute. The resistivity of the water should be 100 ohm-m ± 10%. The prescribed voltage is maintained for one minute.

Wet flash-over test: The voltage shall then be increased gradually until flash-over occurs. This is repeated ten times. There shall be no damage to the insulator.

(e) Visible discharge test: This states that after the room has been darkened and the specified test voltage applied, after five minutes, there should be no visible signs of corona.

9.5.2 Sample Tests

The sample is tested fully, up to and including the point of breakdown. This is done only on a few samples of the insulator.

(a) Temperature cycle test: The complete test shall consist of five transfers (hot-cold-hot-....), each transfer not exceeding 30 s.

(b) Mechanical loading test: The insulator shall be mechanically loaded up to the point of failure. When failure occurs, the load should not be less than 2000 lbf.

(c) Electro-mechanical test: The insulator is simultaneously subjected to electrical and mechanical stress. (i.e. it shall be subjected to a power frequency voltage and a tensile force simultaneously. The voltage shall be 75% of dry flash-over voltage of the unit. There should be no damage caused.

(d) Overvoltage test: The insulator shall be completely immersed in an insulating medium (oil), to prevent external flashover occurring. The specified overvoltage must be reached without puncture. The voltage is then gradually increased until puncture occurs.

(e) Porosity test: Freshly broken pieces of porcelain shall show no dye penetration after having been immersed for 24 hours in an alcoholic mixture of fushing at a pressure of 2000 p.s.i.

9.5.3 Routine Tests

These are to be applied to all insulators and shall be commenced at a low voltage and shall be increased rapidly until flash-over occurs every few seconds. The voltage shall be maintained at this value for a minimum of five minutes, or if failures occur, for five minutes after the last punctured piece has been removed. At the conclusion of the test the voltage shall be reduced to about one-third of the test voltage before switching off.

Mechanical Routine Test: A mechanical load of 20% in excess of the maximum working load of the insulator is applied after suspending the insulator for one minute. There should be no mechanical failure of the insulator.

9.6 Tests on Transformers

The following sequence of tests is generally adopted for transformers.

System Voltage	I.E.C. Impulse Withstand Voltage
11 kV	75 kV
33 kV	170 kV
66 kV	325 kV
132 kV	550 kV
275 kV	1050 kV

(1) Apply full wave impulse at 75% I.E.C. withstand value. Since the transformer should be able to withstand the I.E.C.voltage, there should be no damage to the transformer. The values of R and C in the impulse generator are adjusted after deriving to get the required waveform.

(2) Apply full wave at 100% I.E.C. withstand value and observe whether there is any breakdown. The waveform observed should be identical to applied waveform (other than for amplitude) : then the device has passed the test.

(3) Chopped wave test at 115% fullwave amplitude : For this kind of test , the impulse generator would have to be fitted with a rod gap or controlled trigatron type gap.

Since there is no voltage across insulator after chopping takes place, from the waveform it is not possible to say whether any damage has taken place.

(4) Therefore apply full wave test again and compare the wave and at 100% of I.E.C. voltage and see whether there is any distortion in the waveform indicating damage.(same as test 2)

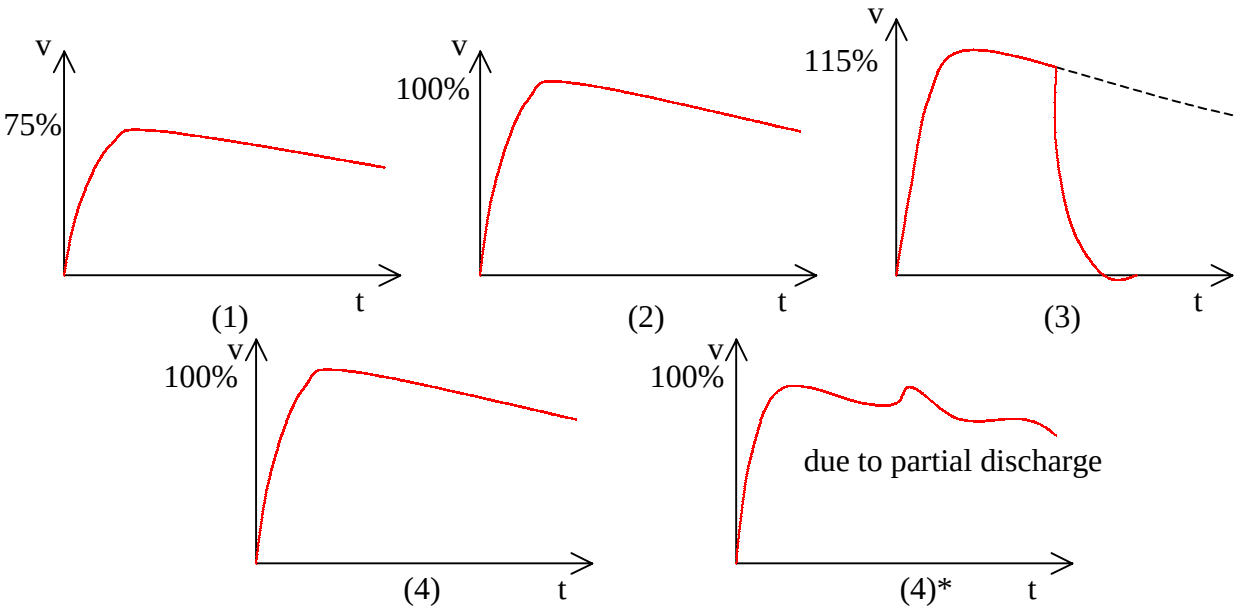

Figure 9.14 - Test waveforms

Since the chopped wave test exerts considerable stress on the winding, there is some controversy on the requirement of this test.

Thus the chopped wave requirement is not universal. In the American industry, the chopped wave is conducted at 150% full wave and such that the chopping is done at less than the peak value. In this case the stress might in fact be very much more than in the British method.

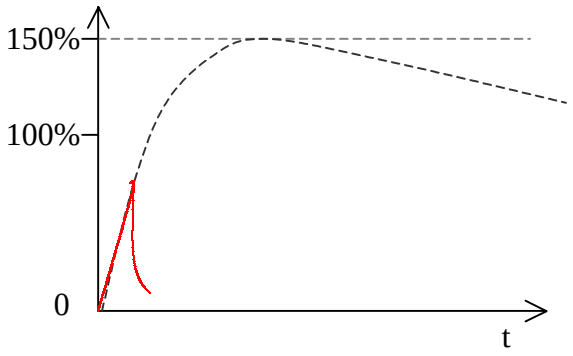

Figure 9.15 - chopped waveform at 150% voltage

9.7 Tests on Cables

For cables not in the supper voltage class the tests to be carried out are laid down in the appropriate British standard specifications.

Thus for paper impregnated insulated cables with lead or alloy sheaths, BS 480 Part I: 1954, the tests (purely electrical) are as follows;

(1) Acceptance Tests at Works

(a) Conductor resistance

(b) Voltage test: The applied voltage must be of approximately sinusoidal shape and of any frequency between 25 and 100 Hz. It must be increased gradually to the full value and maintain continuously for 15 minutes between conductors and between each conductors and sheath. The required values of the test voltages are tabulated in the specification and, as one illustration of the magnitude relative to the normal voltages, the figures for the 11 kV cables for earthed system are given in the table.

Voltage Designation	Belted Cables		Single-core, S.L. & Screened Cables
	(i)	(ii)	(ii)
	(1) (2)	(1) (2)	(1) (2)
11 kV	24 kV 36 kV	14 kV 21 kV	15 kV 22 kV

where (i) Between conductors, (ii) Between any conductor and sheath
(1) Cable as manufactured, (2) After bending test

It will be seen that a voltage test is made before and after a bending test. In this the cable has to be bent around a cylinder of specified diameter to make one complete turn: it is then unwound and the process repeated in the opposite direction . The cycle of process has to be carried out three times.

(c) Dielectric power-factor / Voltage test (for 33 kV cables only) :

Each core of every drum of completed cable is tested for dielectric power factor at room temperature at the following a.c. single phase 50 Hz voltages : 9.5 kV , 19 kV , 28.5 kV, 38.0 kV.

The measured power-factor at normal working voltage shall not the value declared by the manufacturer and shall in no case exceed 0.01 .

The ionization - ie. the difference in power-factor between half the normal working voltage and the twice the normal working voltage - shall not exceed the value declared by the manufacture and shall no case exceed 0.0006 for 3-core screened cable or 0.001 for single core and screened S.L.type cable. The manufacturer can also be asked to produced evidence to show that the power factor at normal working voltage does not exceed 0.01 at series of temperature ranging from 15 C to 65 C.

(2) Sample test at works

These include bending test above and a dripping or drainage test for cables which have to be installed vertically.

(3) Test when installed

A voltage test similar to the above is carried out in the same manner but with some what reduced voltages. Thus the value of 24 kV, 14 kV and 11 kV for belted cable as manufactured and the value 15 kV for single core, S.L. and screened cables, become 20 kV, 11.5 kV and 12 kV respectively.

9.7.1 Tests on Pressurised Cables

Type approval tests, are stipulated for each design of cable and accessory. These tests are carried out on the maximum and the minimum conductor sizes for each design and voltage rating, and if successful, no further type tests are required, except in the case of changes in the design. The dielectric thermal resistance test included in the schedule is applied only to the minimum conductor sizes.

The tests are as follows:

(a) Loading cycle test: A test loop, comprising the cable and each type of accessory to be subjected to 20 load cycles to a minimum conductor temperature 5^{o} C in excess of the design value, with the cable energised to 1.5 times the working voltage. The cable to be tested at a stipulated minimum internal pressure.

(b) Thermal stability test (132 kV cables only): After test (a), the cable to be energised to 1.5 times working voltage and the loading current adjusted to give a maximum temperature 5^{o} C in excess of the design value. The current to be maintained at this value for a period of 6 hours, with other test conditions unaltered, to prove that the cable is thermally stable. For 275 kV cables, 1.33 times the working voltage is proposed.

(c) Impulse test: A test loop, comprising cable and each type of accessory to be subjected to 10 positive and 10 negative impulses at test voltage.
[Ex: Working voltage 132 kV, Impulse test voltage 640 kV, Peak working voltage ratio during impulse test 6.0]

(d) Cold power-factor/voltage test: The power factor of a 100 m length of cable to be measured at 0.5, 1.0, 1.5 and 2 times the working voltage with the cable at the stipulated minimum internal pressure. The values not to exceed the makers' guaranteed values.

(e) Dielectric thermal resistance test: The thermal resistance of the cable is measured.

(f) Mechanical Test of metallic reinforcement: A sample of cable to withstand twice the maximum specified internal pressure for a period of seven days.

(g) Binding test: The cable to be subjected to three binding cycles round a drum of diameter 20 times the diameter of the pressure retaining sheath. The sample then to withstand the routine voltage test carried out on all production lengths of cable.

9.8 Tests on High Voltage Bushings

9.8.1 Bushing

A single or composite structure carrying a conductor or providing passage for a conductor, through a partition, such as a wall or tank cover, or through a ring type current transformer and insulating it there from, it includes the means of attachment to the partition.

(i) Solid Bushing: A bushing consisting of a single piece of solid insulating material which is continuous between its outer surface and the inner conducting surface, which may be the main conductor or a conducting layer connected thereto.

(ii) Plain Bushing: A bushing consisting of a single piece of solid insulating material, with a space between the conductor and the inner surface of the solid insulation. The space is occupied by air, oil or other insulating medium which forms part of the insulation. [See item (iii)]

(iii) Oil filled Bushing: A bushing consisting of an oil-filled insulating shell, the oil providing the major radial insulation.
[Note: The conductor may be further insulated by a series of spaced concentric cylinders which may be provided with cylindrical conducting layers with the object of controlling the internal and external electric fields.]

(iv) Condenser busing: A bushing in which cylindrical conducting layers are arranged coaxially with the conductor within a solid body of insulating materials, (including materials impregnated with oils or other impregnants),the lengths and diameters of the cylinders being designed with the object of controlling the internal and external electric fields
[Note:A conductor bushing may be provided with a weather shield, in which case the intervening space may be filled with oil or other insulating medium.it is recommended that the term **condenser bushing with oil filling** be used for this type.]

9.8.2 Tests on Bushings

Rating of bushings: Some of the relevant clauses from the standard is given in the following sections.

Clause 4: A bushing shall be rated in terms of the following:

a) voltage(refer table 1, clause 5)
b) normal current (refer tables 2 and 3 clause 6)
c) frequency (refer clause 7)
d) insulation level (see clause 8 below)

Clause 8: The insulation level of bushing is designed by a voltage which the bushing must be capable of withstanding under the specified test conditions

For impulse tested bushings the rated insulation level is expressed as an impulse voltage value i.e. the impulse withstand voltage with 1/50 μs full wave

For non-impulse tested bushings the rated insulation level is expressed as a power frequency voltage value i.e. one minute dry withstand voltage.

Type Tests

Clause 14: Power frequency test

Clause 15: Impulse test

Clause 17: Momentary dry withstand test (power frequency voltage)

Clause 18: Visible discharge test (power frequency voltage)

Clause 19: Wet withstand test (power frequency voltage)

Clause 20: Puncture withstand test (power frequency voltage)

Clause 21: Full wave withstand test (impulse voltage)

Clause 22: Puncture withstand test (impulse voltage)

Sample Tests

Clause 23: Temperature rise test

Clause 25: Thermal stability test

Clause 26: Temperature cycle test

Clause 27: Porosity test

Routine Tests

Clause 29: One minute dry withstand test (power frequency voltage)

Clause 30: Oil lightness test

Clause 31: Power factor voltage test

9.9 Tests on Porcelain and toughened glass insulators for overhead power lines

Specifications B.S.137:1960 (3.3 kV and upwards)

Classification of tests

Tests are divided into three groups, as shown.

Tests in Group I (Type tests)

These tests are intended to verify those characteristics of an insulator or set, pin or line post insulator which depend on shape and size of the insulator and of its metal parts and accessories. They are normally made once only to establish design characteristics.

Clause 18: Impulse withstand voltage tests and 50% dry impulse flashover test

Clause 19: Power frequency voltage one-minute wet test and wet flashover test

Clause 20: Visible discharge test

Tests in Group II (Sample tests)

These tests are for the purpose of verifying certain characteristics of a string insulator unit,line post insulator or pin insulator and pin and the quality of the materials used. They are made on insulators taken at random from every batch offered for acceptance.

Clause 23: Verification of dimensions

Clause 24: Temperature cycle test

Clause 25: Mechanical failing load test or

Clause 26: Electro-mechanical failing load test

Clause 27: Overvoltage tests

Clause 28: Porosity test on porcelain insulators

Clause 29: Thermal shock test on toughened glass insulators: The glass shall not shatter when the sample insulators are completely immerses in water at a temperature not exceeding 50 C, the temperature of the insulators immediately before immersion being at least 100 C higher than that of the water.

Clause 30: Galvanizing test: The galvanized samples shall be tested in accordance with B.S.729 and shall satisfy the requirements of that standard.

Tests in Group III (Sample tests)

These tests are for the purpose of eliminating insulators with manufacturing defects. They are made on every insulator offered for acceptance.

Clause 32: Electrical test on porcelain insulators

Clause 33: Thermal shock test on toughened glass insulators

Clause 34: Mechanical test on string insulator units: Every string unit shall be subjected to a tensile load of at least 40% of the specified minimum failing load, for a period of not less than 10 seconds.

Insulation Co-ordination

10.0 Insulation Co-ordination

The term Insulation Co-ordination was originally introduced to arrange the insulation levels of the several components in the transmission system in such a manner that an insulation failure, if it did occur, would be confined to the place on the system where it would result in the least damage, be the least expensive to repair, and cause the least disturbance to the continuity of the supply. The present usage of the term is broader. Insulation co-ordination now comprises the selection of the electric strength of equipment in relation to the voltages which can appear on the system for which the equipment is intended. The overall aim is to reduce to an economically and operationally acceptable level the cost and disturbance caused by insulation failure and resulting system outages.

To keep interruptions to a minimum, the insulation of the various parts of the system must be so graded that flashovers only occur at intended points. With increasing system voltage, the need to reduce the amount of insulation in the system, by proper co-ordination of the insulating levels become more critical.

10.1 Terminology

Nominal System Voltage: It is the r.m.s. phase-to-phase voltage by which a system is designated

Maximum System Voltage: It is the maximum rise of the r.m.s. phase-to-phase system voltage

For the nominal system voltages used in Sri Lanka, the international maximum system voltages are shown in table 10.1.

Nominal System Voltage (kV)	11	33	66	132	220
Maximum System Voltage (kV)	12	36	72.5	145	245

Table 10.1

Factor of Earthing: This is the ratio of the highest r.m.s. phase-to-earth power frequency voltage on a sound phase during an earth fault to the r.m.s. phase-to-phase power frequency voltage which would be obtained at the selected location without the fault.
This ratio characterises, in general terms, the earthing conditions of a system as viewed from the selected fault location.

Effectively Earthed System : A system is said to be effectively earthed if the factor of earthing does not exceed 80%, and non-effectively earthed if it does.
[Note: Factor of earthing is 100% for an isolated neutral system, while it is 57.7% (corresponding to $1/\sqrt{3}$) for a solidly earthed system. In practice, the effectively earthed condition is obtained when the ratio $x_0/x_1 < 3$ and the ratio $r_0/x_1 < 1$.

Insulation Level: For equipment rated at less than 300 kV, it is a statement of the Lightning impulse withstand voltage and the short duration power frequency withstand voltage.

For equipment rated at greater than 300 kV, it is a statement of the Switching impulse withstand voltage and the power frequency withstand voltage.

Conventional Impulse Withstand Voltages: This is the peak value of the switching or lightning impulse test voltage at which an insulation shall not show any disruptive discharge when subjected to a specified number of applications of this impulse under specified conditions.

Conventional Maximum Impulse Voltage: This is the peak value of the switching or lightning overvoltage which is adopted as the maximum overvoltage in the conventional procedure of insulation co-ordination.

Statistical Impulse Withstand Voltage: This is the peak value of a switching or lightning impulse test voltage at which insulation exhibits, under the specified conditions, a 90% probability of withstand. In practice, there is no 100% probability of withstand voltage. Thus the value chosen is that which has a 10% probability of breakdown.

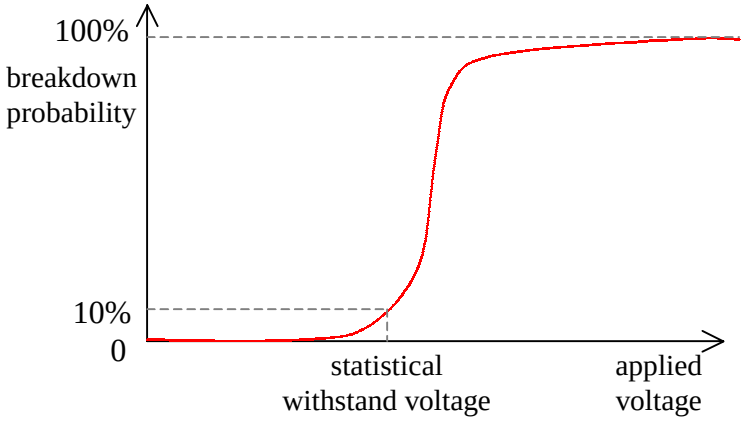

Figure 10.1 - Statistical Impulse Withstand Voltage

Statistical Impulse Voltage: This is the switching or lightning overvoltage applied to equipment as a result of an event of one specific type on the system (line energising, reclosing, fault occurrence, lightning discharge, etc), the peak value of which has a 2% probability of being exceeded.

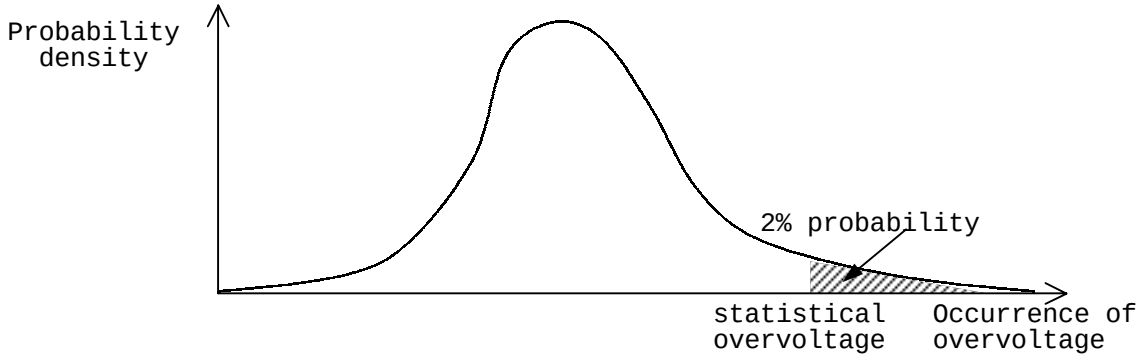

Figure 10.2 - Statistical Impulse Voltage

Rated Short Duration Power Frequency Withstand Voltage: This is the prescribed r.m.s. value of sinusoidal power frequency voltage that the equipment shall withstand during tests made under specified conditions and for a specific time, usually not exceeding one minute.

Protective Level of Protective Device: These are the highest peak voltage value which should not be exceeded at the terminals of a protective device when switching impulses and lightning impulses of standard shape and rate values are applied under specific conditions.

10.2 Conventional method of insulation co-ordination

In order to avoid insulation failure, the insulation level of different types of equipment connected to the system has to be higher than the magnitude of transient overvoltages that appear on the system. The magnitude of transient over-voltages are usually limited to a protective level by protective devices. Thus the insulation level has to be above the protective level by a safe margin. Normally the impulse insulation level is established at a

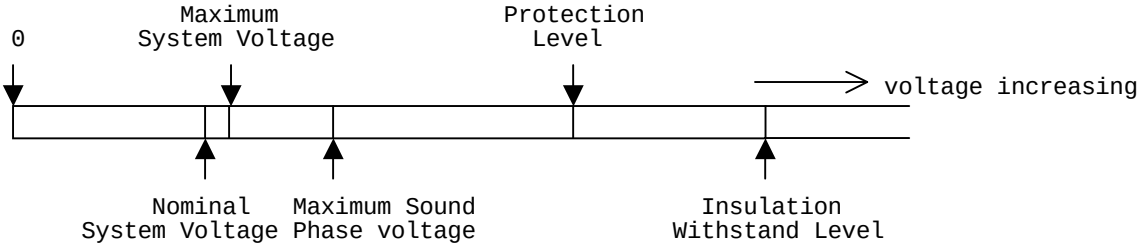

value 15-25% above the protective level.

Consider the typical co-ordination of a 132 kV transmission line between the transformer insulation, a line gap (across an insulator string) and a co-ordinating gap (across the transformer bushing).

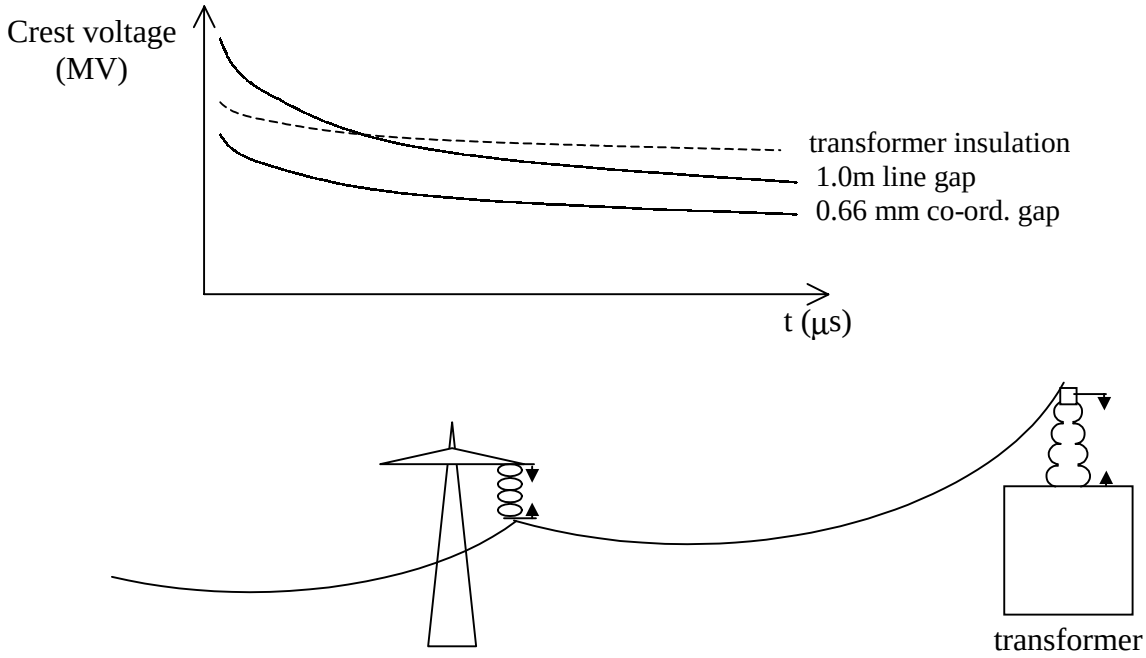

Figure 10.3 - Co-ordination using gaps

[Note: In a rural distribution transformer, a lightning arrester may not be used on account of the high cost and a co-ordinating gap mounted on the transformer bushing may be the main surge limiting device]

In co-ordinating the system under consideration, we have to ensure that the equipment used are protected, and that inadvertent interruptions are kept to a minimum. The co-ordinating gap must be chosen so as to provide protection of the transformer under all conditions. However, the line gaps protecting the line insulation can be set to a higher characteristic to reduce unnecessary interruptions.

A typical set of characteristics for insulation co-ordination by conventional methods, in which lightning impulse voltages are the main source of insulation failure, is shown in the figure 1.3.

For the higher system voltages, the simple approach used above is inadequate. Also, economic considerations dictate that insulation co-ordination be placed on a more scientific basis.

10.3 Statistical Method of Insulation Co-ordination

At the higher transmission voltages, the length of insulator strings and the clearances in air do not increase linearly with voltage but approximately to $V^{1.6}$ The required number of suspension units for different overvoltage factors is shown.

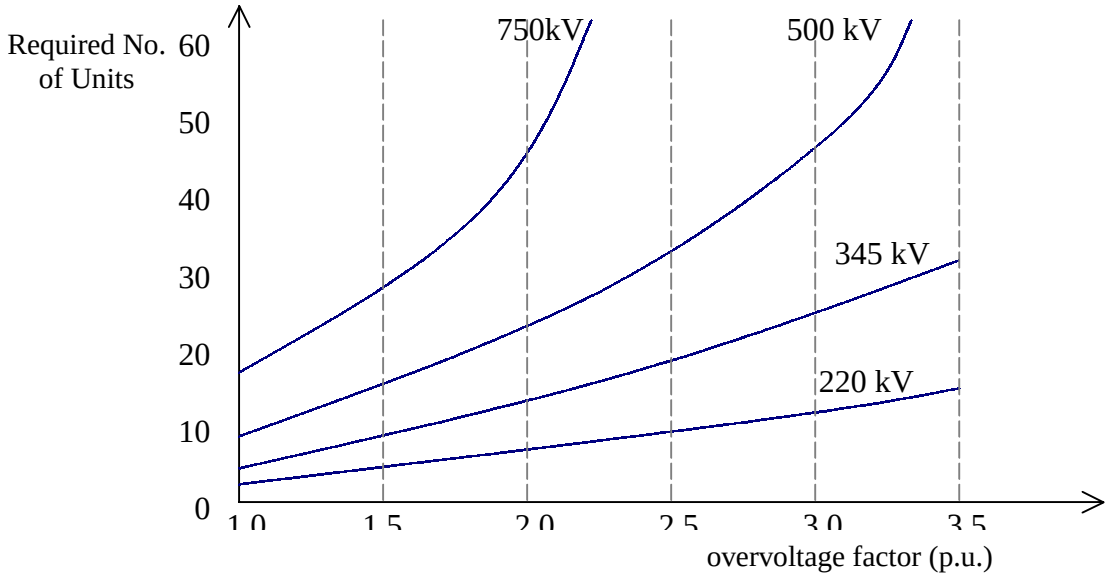

Figure 10.4 - Requirement of number of units for different voltages

It is seen that the increase in the number of disc units is only slight for the 220 kV system, with the increase in the overvoltage factor from 2.0 to 3.5, but that there is a rapid increase in the 750 kV system. Thus, while it may be economically feasible to protect the lower voltage lines up to an overvoltage factor of 3.5 (say), it is definitely not economically feasible to have an overvoltage factor of more than about 2.0 or 2.5 on the higher voltage lines. In the higher voltage systems, it is the switching overvoltages that is predominant. However, these may be controlled by proper design of switching devices.

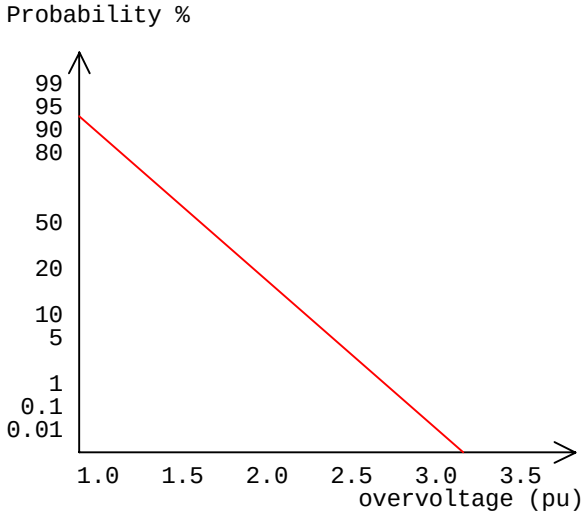

Figure 10.5 Probability of overvoltage exceeding abscissae

In a statistical study, what has to be known is not the highest overvoltage possible, but the statistical distribution of overvoltages. The switching overvoltage probability in typical line is shown. It is seen that probability of overvoltage decreases very rapidly. Thus it is not economic to provide insulation above a certain overvoltage value. In practice, the overvoltage distribution characteristic is modified by the use of switching resistors which damp out the switching overvoltages or by the use of surge diverters set to operate on the higher switching overvoltages. In such cases, the failure probability would be extremely low.

10.3.1 Evaluation of Risk Factor

The aim of statistical methods is to quantify the risk of failure of insulation through numerical analysis of the statistical nature of the overvoltage magnitudes and of electrical withstand strength of insulation.

The risk of failure of the insulation is dependant on the integral of the product of the overvoltage density function $f_0(V)$ and the probability of insulation failure P(V). Thus the risk of flashover per switching operation is equal to the area under the curve $\int f_0(V)*P(V)*dV$.

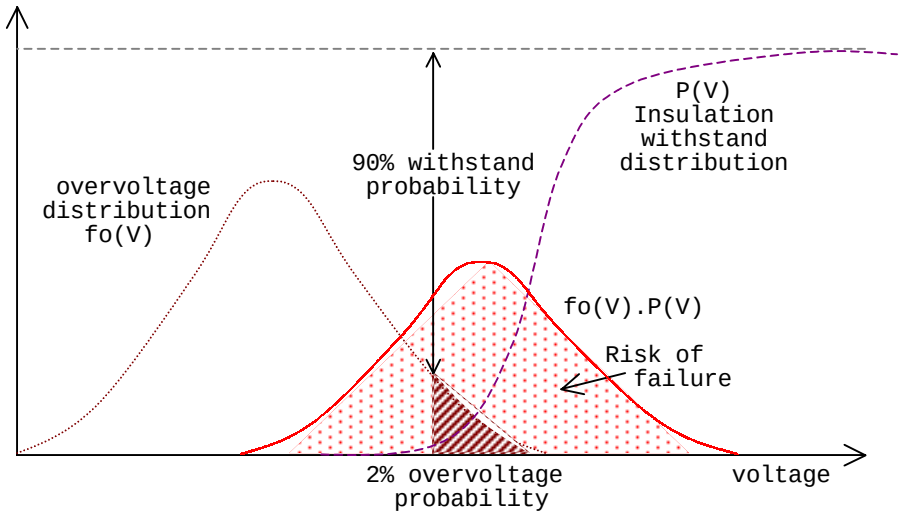

Figure 10.6 - Evaluation of risk factor

Since we cannot find suitable insulation such that the withstand distribution does not overlap with the overvoltage distribution, in the statistical method of analysis, the insulation is selected such that the 2% overvoltage probability coincides with the 90% withstand probability as shown.

10.4 Length of Overhead Shielding Wire

For reasons of economics, the same degree of protection is not provided throughout a transmission line. Generally, it is found sufficient to provide complete protection against direct strikes only on a short length of line prior to the substation. This can be calculated as follows.

Consider a surge **e** approaching the terminal equipment. When the surge magnitude exceeds the critical voltage $\mathbf{e_0}$, corona would occur, distorting the surge wavefront, as it travels. The minimum length of earth wire should be chosen such that in traversing that length, all voltage above the maximum surge that can arrive att the terminal has been distorted by corona. [The maximum permissible surge corresponds to the incident voltage that would cause insulation failure at the terminal equipment.]

10.4.1 Modification of Waveshape by Corona

When a surge voltage wave travelling on an overhead line causes an electric field around it exceeding the critical stress of air, corona will be formed. This corona formation obviously extracts the energy required from the surge. Since the power associated with corona increases as the square of the excess voltage, the attenuation of the waveform will not be uniform so that the waveform gets distorted. Further, corona increases the effective radius of the conductor giving rise to a greater capacitance for the outer layers. Since the line inductance remains virtually a constant, the surge associated with the outer layers of corona would have a lower wave velocity than in the conductor itself. These effects in practice give rise to a wavefront distortion and not a wavetail distortion, as shown in figure 10.7.

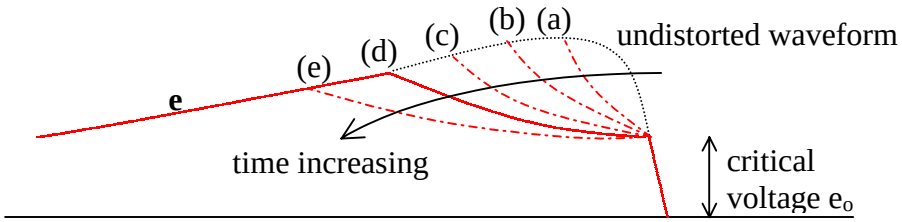

Figure 10.7 - Modification of waveshape due to corona

Corona thus reduces the steepness of the wavefront above the critical voltage, as the surge travels down the line. This means that energy is lost to the atmosphere.

Now consider the mathematical derivation.

Energy associated with a surge waveform = $\frac{1}{2} C e^2 + \frac{1}{2} L i^2$

But the surge voltage **e** is related to the surge current **i** by the equation

$$i = \frac{e}{Z_0} = e\sqrt{\frac{C}{L}}, \quad i.e. \quad \tfrac{1}{2} L i^2 = \tfrac{1}{2} C e^2$$

So that the total wave energy = $C e^2$

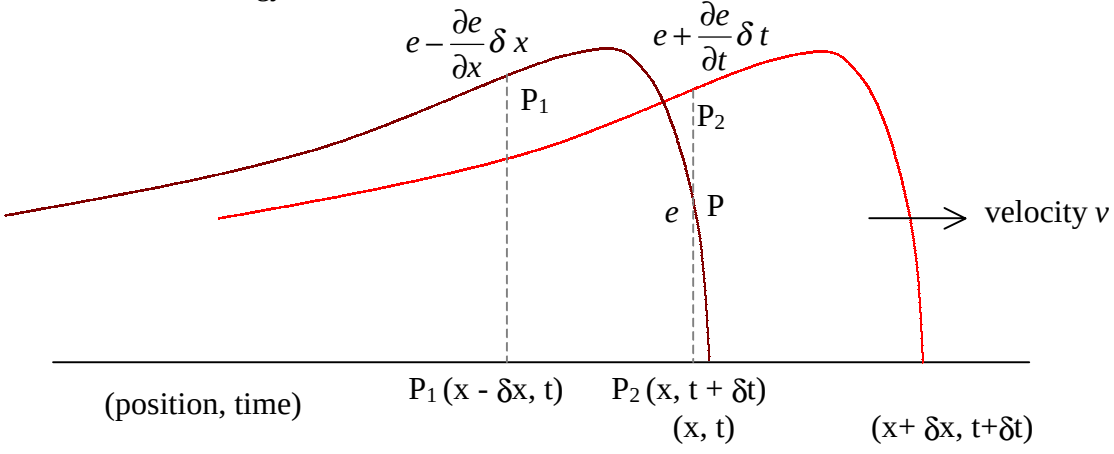

Figure 10.8 - Propagation of Surge

Consider the figure 10.8. Let the voltage at a point P at position **x** be **e** at time **t**.

Then voltage at point P_1 just behind P would be $e - \frac{\partial e}{\partial x}\delta x$ at time t, or $e - \frac{\partial e}{\partial x}.v.\delta t.$

If the voltage is above corona inception, it would not remain at this value but would attain a value $e + \frac{\partial e}{\partial t}\delta t$ at P at time $t+\Delta t$, when the surge at P_1 moves forward to P_2.

[Note: $\frac{\partial e}{\partial x}, \frac{\partial e}{\partial t}$ would in fact be negative quantities on the wavefront.]

Thus corona causes a depression in the voltage from $(e - v\frac{\partial e}{\partial x}\delta t)$ to $(e + \frac{\partial e}{\partial t}\delta t)$, with a corresponding loss of energy of $C\left[(e - v\frac{\partial e}{\partial x}\delta t)^2 - (e + \frac{\partial e}{\partial t}\delta t)^2\right]$ or $-2Ce\left[v\frac{\partial e}{\partial x} + \frac{\partial e}{\partial t}\right]\delta t$.

The energy to create a corona field is proportional to the square of the excess voltage. i.e. $k(e - e_0)^2$.

Thus the energy required to change the voltage from e to $(e + \frac{\partial e}{\partial t}\delta t)$ is given by

$$k\left[(e + \tfrac{\partial e}{\partial t}\delta t - e_0)^2 - (e - e_0)^2\right] \text{ or } 2k(e - e_0)\tfrac{\partial e}{\partial t}\delta t .$$

The loss of energy causing distortion must be equal to the change in energy required. Thus

$$-2Ce\left[v\tfrac{\partial e}{\partial x} + \tfrac{\partial e}{\partial t}\right]\delta t = 2k(e - e_0)\tfrac{\partial e}{\partial t}.\delta t$$

Rearranging and simplifying gives the equation

$$v\frac{\partial e}{\partial x} = -\left[1 + \frac{k}{C}.\frac{(e - e_0)}{e}\right]\frac{\partial e}{\partial t}$$

Wave propagation under ideal conditions is written in the form

$$v\frac{\partial e}{\partial x} = -\frac{\partial e}{\partial t}$$

Thus we see that the wave velocity has decreased below the normal propagation velocity, and that the wave velocity of an increment of voltage at **e** has a magnitude given by

$$v_e = \frac{v}{1 + \frac{k}{c}\left(\frac{e - e_0}{e}\right)}$$

Thus the time of travel for an element at **e** when it travels a distance **x** is given by

$$t = \frac{x}{v_e} = \frac{x}{v}\left[1 + \frac{k}{C}\left[\frac{e - e_o}{e}\right]\right]$$

$$i.e. \quad \left[\frac{x}{v_e} - \frac{x}{v}\right] = \frac{x}{v}.\frac{k}{C}\left[\frac{e - e_o}{e}\right]$$

$\left(\frac{x}{v_e} - \frac{x}{v}\right)$ is the time lag Δt corresponding to the voltage element at **e**. Thus

$$\frac{\Delta t}{x} = \frac{k}{v.C}\left[1 - \frac{e_0}{e}\right]$$

Example 10.1

A transformer has an impulse insulation level of 1050 kV and is to be operated with an insulation margin of 15% under lightning impulse conditions. The transformer has a surge impedance of 1600 Ω and is connected to a transmission line having a surge impedance of 400 Ω. A short length of overhead earth wire is to be used for shielding the line near the transformer from direct strikes. Beyond the shielded length, direct strokes on the phase conductor can give rise to voltage waves of the form $1000\ e^{-0.05t}$ kV (where t is expressed in μs).

If the corona distortion in the line is represented by the expression $\frac{\Delta t}{x} = \frac{1}{B}\left[1 - \frac{e_0}{e}\right]\ \mu s/m$, where B = 110 m/μs and e_0 = 200 kV, determine the minimum length of shielding wire necessary in order that the transformer insulation will not fail due to lightning surges.

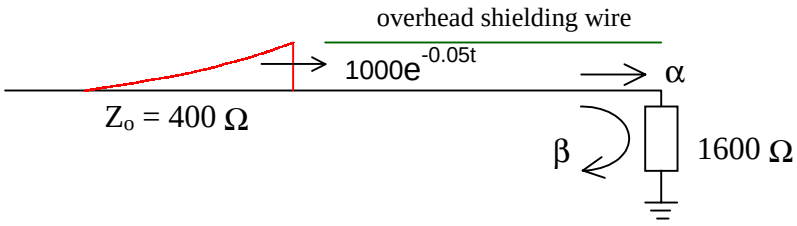

Transmission coefficient $\alpha = \frac{2 \times 1600}{1600 + 400} = 1.6$

For a B.I.L of 1050 kV, and an insulation margin of 15%,
Maximum permissible voltage = 1050 x 85/100 = 892.5 kV.

Since the voltage is increased by the transmission coefficient 1.6 at the terminal equipment, the maximum permissible incident voltage must be decreased by this factor.
Thus maximum permissible incident surge = 892.5/ 1.6 = 557.8 kV
Thus for the transformer insulation to be protected by the shielding wire, the distortion caused must reduce the surge to a magnitude of 557.8 kV.

Therefore, $1000\ e^{-0.05\ t_1} = 557.8$. This gives the delay time $t_1 = \Delta t = 11.6\ \mu s$.

Substitution in the equation gives $11.67/x = 1/100\ .\ (1 - 200/557.8)$

Solution gives x = 2002 m = 2.0 km.
Thus the minimum length of shielding wire required is 2 km.

10.5 Surge Protection

An overhead earth wire provides considerable protection against direct strikes. They also reduce induced overvoltages. However, they do not provide protection against surges that may still reach the terminal equipment. Such protection may either be done by diverting the major part of the energy of the surge to earth (surge diverters), or by modifying the waveform to make it less harmful (surge modifiers). The insertion of a short length of cable between an overhead line and a terminal equipment is the commonest form of surge modifier.

10.5.1 Spark gaps for surge protection

The simplest and cheapest form of protection is the spark gap. The selected gap spacing should no only be capable of withstanding the highest normal power frequency voltage but should flash-over when overvoltages occur, protecting the equipment.

However, this is not always possible due to the voltage-time characteristics gaps and equipment having different shapes. Also, once a gap flashes over under a surge voltage, the ionised gap allows a power frequency follow through current, leading to a system outage. Thus rod gaps are generally used as a form of back up protection rather than the main form of protection.

Typical values of gap settings for transmission and distribution voltages are as in the following table 10.3.

Nominal System Voltage (kV)	66	132	275	400
Gap setting (mm)	380	660	1240	1650

Table 10.3

One of the most extensively used protective spark gaps in distribution systems is the **duplex** rod gap, which makes use of 2 rod gaps in series. Typical settings for these gaps are as given in the table.

Nominal System Voltage (kV)	11	33
Gap setting (mm)	2 x 31	2 x 63

Table 10.4

When spark over occurs across a simple rod gap, the voltage suddenly collapses giving rise to a chopped wave. This chopped wave may sometimes be more onerous to a transformer than the original wave itself.

Expulsion Tube Lightning Arrestor

An expulsion tube arrestor consists essentially of a spark gap arranged in a fibre tube, and another series external rod gap. A typical arrangement for a 33 kV expulsion tube, with the external gap of the order of 50 mm and the internal gap of about 180 mm is shown in figure 10.9.

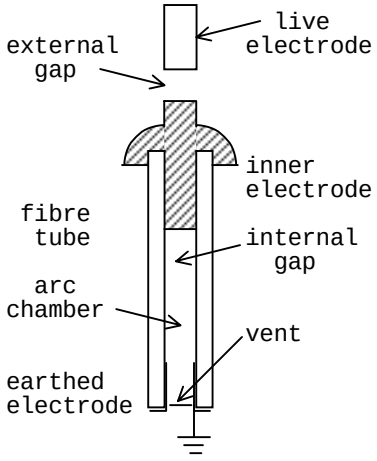

Figure 10.9 - Expulsion Tube

The purpose of the external gap is to isolate the fibre tube from normal voltages thus preventing unnecessary deterioration. When an overvoltage occurs, spark over takes place between the electrodes and the follow current arc is constrained within the small volume of the tube. The high temperature of the arc rapidly vaporises the organic materials of the wall of the tube and causes a high gas pressure (up to 7000 p.s.i.) to be built up. The high pressure and the turbulence of the gas extinguishes the arc at a natural current zero, and the hot gasses are expelled through the vent in the earthed electrode. The power frequency follow current is interrupted within one or two half cycles so that protective relays would not operate causing unnecessary interruptions.

The expulsion gaps, which are comparatively cheap, are suitable for the protection of transmission line insulators and for the protection of rural distribution transformers, where other arrestors may be too expensive and rod gaps inadequate. However, they are unsuitable for the protection of expensive terminal equipment on account of their poor voltage-time characteristics.

10.5.2 Surge Diverters

Surge diverters (or lightning arrestors) generally consist of one or more spark gaps in series, together with one or more non-linear resistors in series. Silicon Carbide (SiC) was the material most often used in these non-linear resistor surge diverters. However, Zinc Oxide (ZnO) is being used in most modern day surge diverters on account of its superior volt-ampere characteristic. In fact the ZnO arrestor is often used gapless, as its normal follow current is negligibly small. The volt-ampere characteristics of SiC and of ZnO non-linear elements are shown for comparison with that of a linear resistor in figure 10.10.

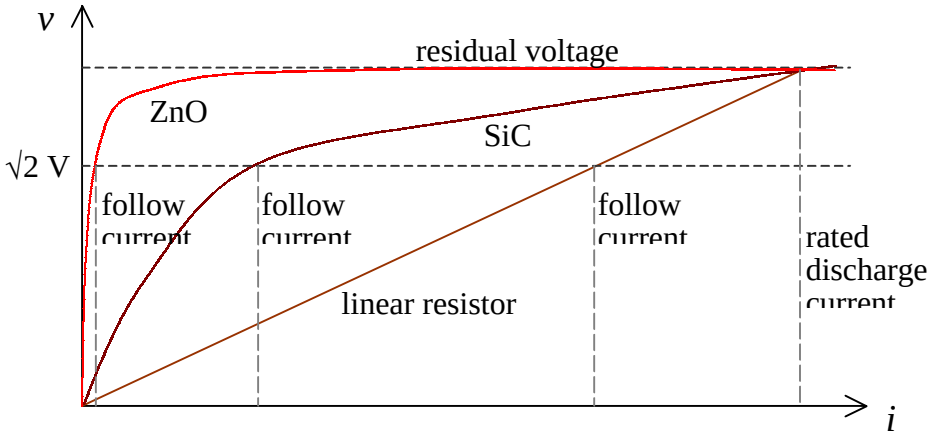

Figure 10.10 - Volt-Ampere characteristics of non-linear elements

It is seen that while a large current is drawn under overvoltage condition in all three cases, the follow current is fairly large in the linear resistor, small in the SiC resistor, and negligibly small in the ZnO resistor. Their characteristics may be mathematically expressed as follows.

$v = k_1 i$ for a linear resistor
$v = k_2 i^{0.2}$ for a Silicon Carbide resistor
$v = k_3 i^{0.03}$ for a Zinc Oxide resistor

If the current were to increase a 100 times, the corresponding increase in voltage would be 100 times for the linear resistor, 2.5 times for the SiC resistor, but only 1.15 times for the ZnO resistor. This means that for the same residual voltage and the same discharge current, the follow current would be (in the absence of a series gap) of the **kA** for a linear resistor, **A** for a SiC resistor and just **mA** for a ZnO resistor.

When a series spark gap is required for eliminating the follow current, it is preferable to have a number of small spark gaps in series rather than having a single spark gap having an equivalent breakdown spacing. This is because the rate of rise of the recovery strength of a number of series gaps is faster than that of the single gap. However, when spark gaps are connected in series, it is difficult to ensure an even voltage distribution among them due to leakage paths (Figure 10.11)

The problem is generally overcome by having high equal resistances shunting the series gaps, ensuring a uniform distribution.

When a surge appears at a surge diverter terminal, within a short time the breakdown voltage of the series gap is reached, and the arrestor discharges. Unlike in the rod gap, the voltage does not collapse to zero instantly due to the voltage across the non-linear resistor. When the surge voltage increases, there is a corresponding but rapid decrease of the resistance discharging the surge energy to earth. Once the surge passes through, the power frequency voltage remaining is insufficient to maintain a sufficient current for the arc to continue. Thus the arcs extinguish and the gaps reseal. In the case of the ZnO arrestor, due to the negligible continuous power frequency current even in the absence of a series gap, the series gap is sometimes eliminated simplifying construction.

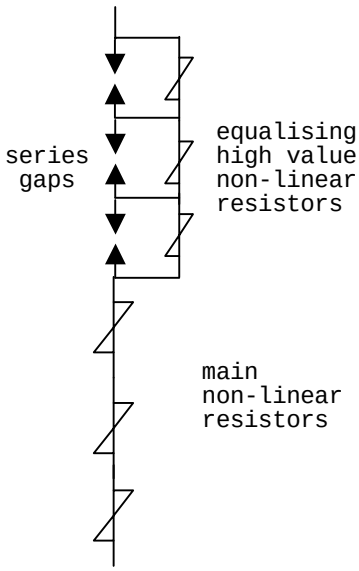

Figure 10.11 - Non-linear Arrestor

10.5.3 Selection of Surge Diverters

Surge diverters for a particular purpose are selected as follows.

(a) Rated Voltage

The designated maximum permissible r.m.s. value of power frequency voltage between line and earth terminals.

This is generally selected corresponding to 80% of the system phase-to-phase voltage for effectively earthed systems and corresponding to 100% of the system phase-to-phase voltage for non-effectively earthed systems. [Note: A surge diverter of a higher rating may sometimes have to be chosen if some of the other required criteria are not satisfied by this diverter].

(b) Discharge Current

The surge current that flows through the surge diverter after spark over.

Nominal discharge current: This is the discharge current having a designated crest value and waveshape, which is used to classify a surge diverter with respect to durability and protective characteristics.

The standard waveform for the discharge current is taken as 8/20 μs).

The nominal value of discharge current is selected from the standard values 10 kA (station type), 5 kA (intermediate line type), 2.5 kA (distribution type) and 1.5 kA (secondary type), depending on the application. The highest ratings are used for the protection of major power stations, while the lowest ratings are used in rural distribution systems. The above nominal discharge currents are chosen based on statistical investigations which have shown that surge diverter currents at the station has the following characteristic.

99 % of discharge currents are less than 10 kA
95 % of discharge currents are less than 5 kA
90 % of discharge currents are less than 3 kA
70 % of discharge currents are less than 1 kA
50 % of discharge currents are less than 0.5 kA

(c) Discharge Voltage (or Residual voltage)

The Discharge voltage is the voltage that appears between the line and earth terminals of the surge diverter during the passage of discharge currents.

The discharge voltage of the selected arrestor should be below the BIL of the protected equipment by a suitable margin (generally selected between 15% and 25%).

The discharge voltage of an arrestor at nominal discharge current is not a constant, but also depends on the rate of rise of the current and the waveshape. Typically, an increase of the rate of rise from 1 kA/μs to 5 kA/μs would increase the discharge voltage by only about 35 %.

The dependence of the discharge voltage on the discharge current is also small. Typically, an increase of discharge current from 5 kA to 10 kA would increase the discharge voltage by about 15% for Silicon Carbide arrestors and by about 2% for Zinc Oxide arrestors. {The discharge voltage is more often referred to as the residual discharge voltage].

(d) Power frequency spark over voltage

The power frequency spark over voltage is the r.m.s. value of the lowest power frequency voltage, applied between the line and earth terminals of a surge diverter, which causes spark-over of all the series gaps.
The power frequency spark over voltage should generally be greater than about 1.5 times the rated voltage of the arrestor, to prevent unnecessary sparkover during normal switching operations.

(e) Impulse spark over voltage

The impulse spark over voltage is the highest value of voltage attained during an impulse of a given waveshape and polarity, applied between the line and earth terminals of a surge diverter prior to the flow of discharge current.

The impulse spark over voltage is not a constant but is dependant on the duration of application. Thus it is common to define a wavefront impulse sparkover voltage in addition to the impulse spark-over voltage.

Arrestor Rating kV rms	Minimum Power frequency withstand	Maximum Impulse Spark-over voltage (1.2/50 μs) kV crest	Maximum Residual Voltage kV crest	Maximum Wavefront Sparkover Voltage kV crest
36	1.5 times rated voltage	130	133	150
50		180	184	207
60		216	221	250
75		270	276	310

Table 10.6

Good designs aim to keep (i) the peak discharge residual voltage, (ii) the maximum impulse sparkover voltage and (iii) the maximum wavefront impulse sparkover voltage reasonably close to each other. Table 10.6 gives a typical comparison.

Example 10.2

A lightning arrestor is required to protect a 5 MVA, 66/11 kV transformer which is effectively earthed in the system. The transformer is connected to a 66 kV, 3 phase system which has a BIL of 350 kV. Select a suitable lightning arrestor.

For 66 kV, maximum value of system rms voltage = 72.5 kV
Therefore, voltage rating for effectively earthed system = 72.5 x 0.8 = 58 kV

The selected voltage rating is usually higher by a margin of about 5%.
Selected voltage rating = 1.05 x 58 = 60.9 = 60 kV

Protective level of selected arrestor (highest of 216, 221 and 250 from table) = 250 kV
Margin of protection (crest value) = 350 - 250 = 100 kV
which is more than the required margin of 15 to 25%.
= 100/250 x 100 % = 40%
Check the power frequency breakdown voltage.
Power frequency breakdown voltage of arrestor = 60 x 15 = 90 kV

Assuming the dynamic power frequency overvoltage to be limited to 25% above maximum voltage at arrestor location,

Dynamic phase-to-neutral voltage = 1.25 x 72.5 x 0.8 = 72.5 kV

This voltage is less than the withstand voltage of the arrestor. In fact the factor of 1.5 automatically ensures that this requirement is satisfied.

Thus the chosen arrestor is satisfactory.

10.5.4 Separation limit for lightning arrestors

Best protection is obtained for terminal equipment by placing the arrestor as near as possible to that equipment. However, it is not feasible to locate an arrestor adjacent to each piece of equipment. Thus it is usually located adjacent to the transformer. However, where the BIL of the transformer permits, the arrestor may be located at a distance from the transformer to include other substation equipment within the protected zone. Thus it may be worthwhile installing them on the busbars themselves when permissible.

When arrestors must be separated from the protected equipment, additional voltage components are introduced, which add instant by instant to the discharge voltage. The maximum voltage at the terminal of a line as a result of the first reflection of a travelling wave may be expressed mathematically as

$$E_t = E_a + \beta \frac{de}{dt} x \frac{2l}{300}$$

up to a maximum of $2 \beta E_a$. The factor 2 arises from the return length from arrestor to transformer, and the factor 300 is based on a travelling wave velocity of 300 m/μs in the overhead line. l is the separation between the arrestor and the transformer location, β the reflection coefficient at the transformer location, E_a is the discharge voltage at the arrestor, and de/dt is the rate of rise of the wavefront. When the value of $ is not known, it may generally be assumed as equal to 1 without much loss of accuracy. Figure 10.12 shows how the voltage at the terminal increases with separation for typical rates of rise.

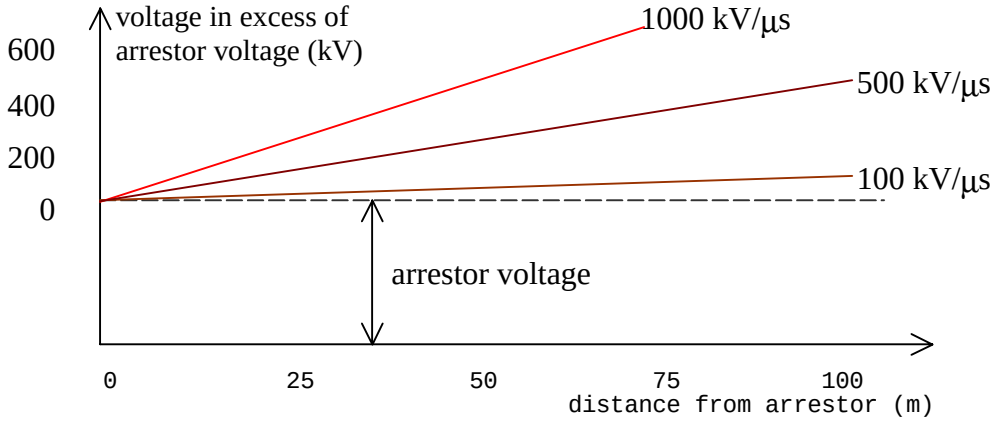

Figure 10.12 - Lightning arrestor separation

Example 10.3

A 500 kV steep fronted wave (rate of rise 1000 kV/μs) reaches a transformer of surge impedance 1600 S through a line of surge impedance 400 S and protected by a lightning arrestor with a protective spark-over level of 650 kV, 90 m from the transformer. Sketch the voltage waveforms at the arrestor location and at the transformer location. Sketch also the waveforms if the separation is reduced to 30 m.

If the separation is 90 m, travel time of line J = 90/300 = 0.3 μs

Transmission coefficient $\alpha = \frac{2 \cdot 1600}{1600+400} = 1.6$

Reflection coefficient $\beta = 1.6 - 1 = 0.6$

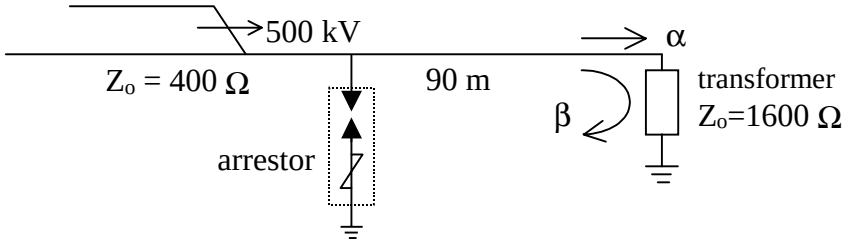

The voltage waveforms at the arrestor location and at the transformer location can be sketched as follows.

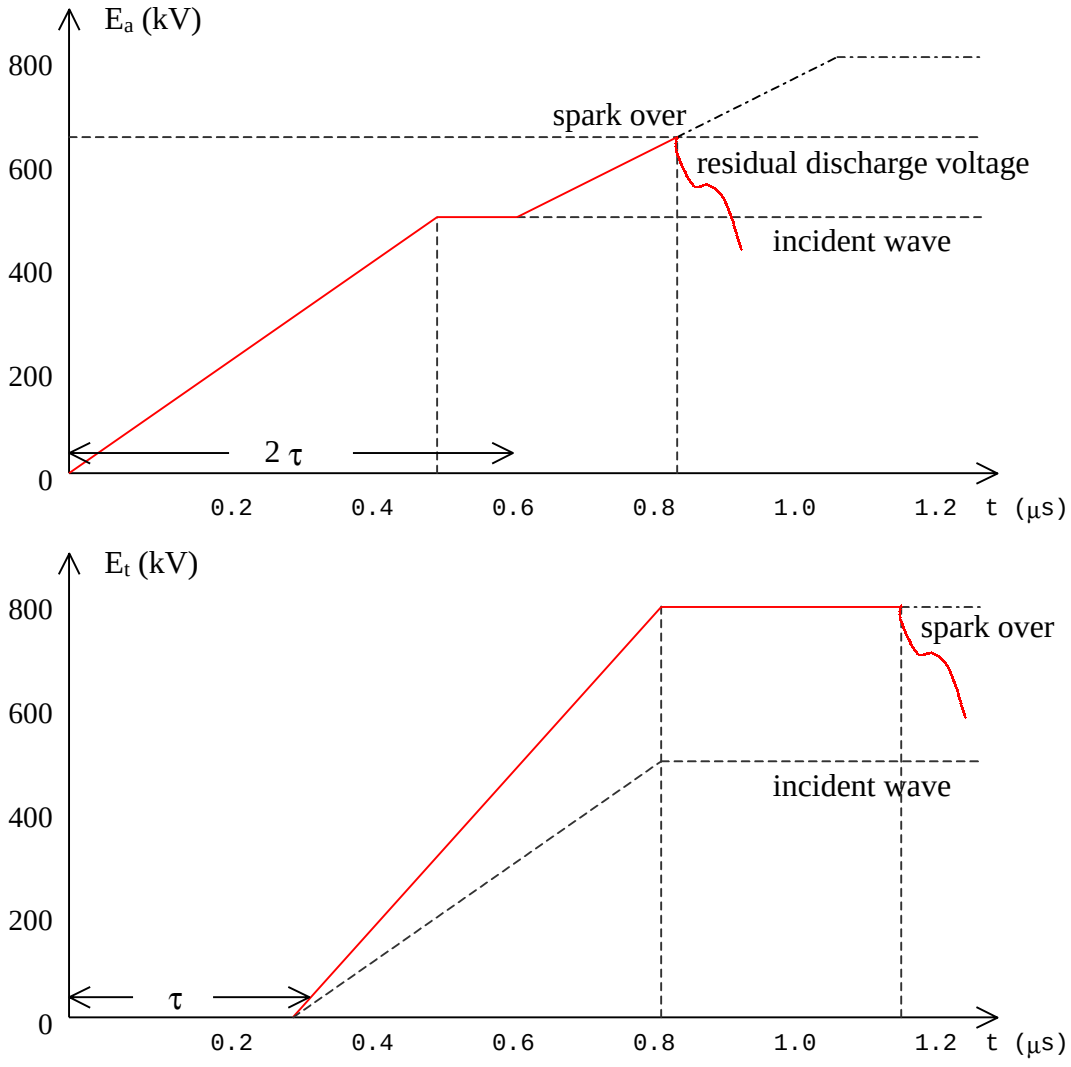

If the separation is 30 m, travel time of line J = 30/300 = 0.1 μs

In this case the voltage waveforms at the arrestor and the transformer location are as follows.

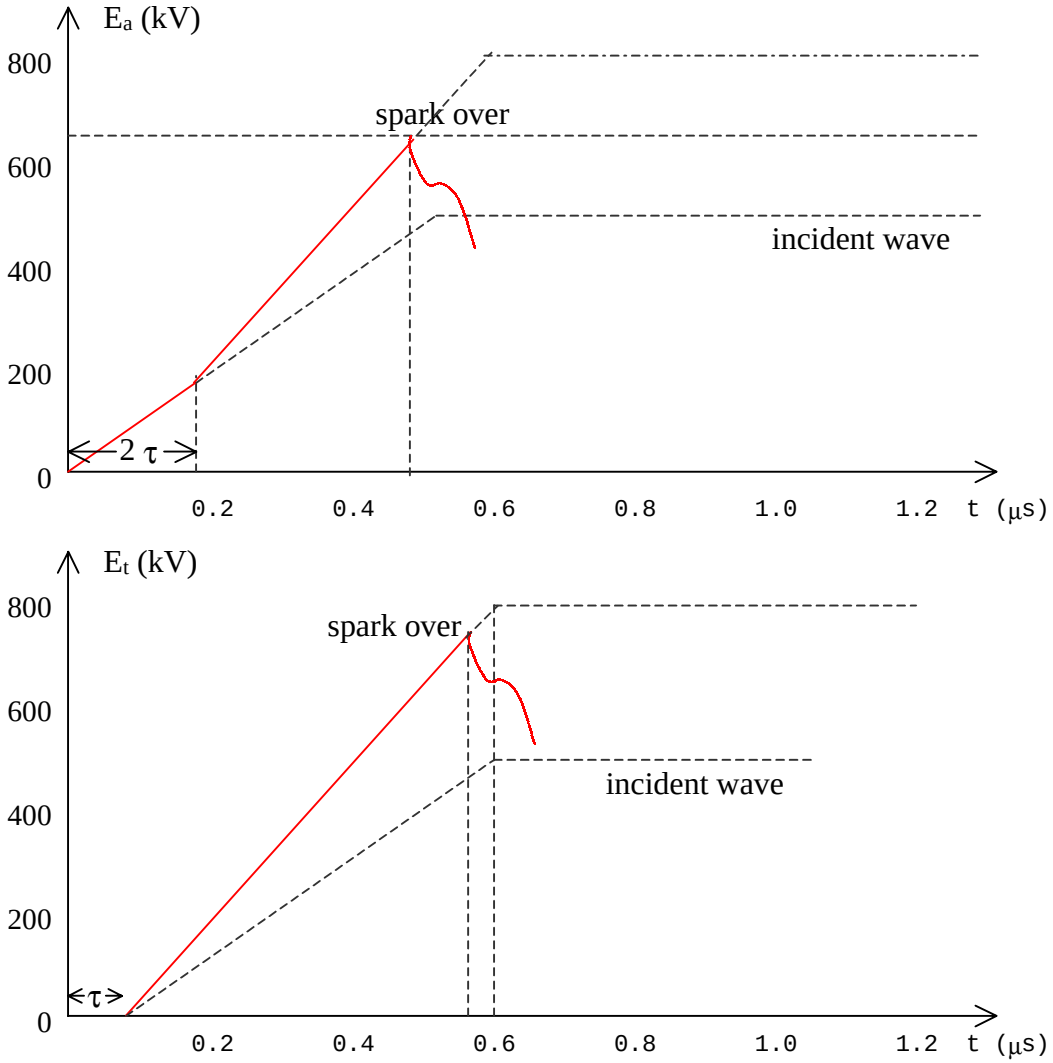

The maximum value of the voltage E_t at the terminal for each case can be determined from $E_t = E_a + 0.6 \frac{de}{dt} x \frac{2l}{300}$ up to a maximum of 0.6 E_a.

For 90 m, maximum E_t -> 650 + 0.6 x 1000 x 90 x 2 / 300 = 1010 kV > 1.6 x 500

Therefore maximum E_t = 800 kV

For 30 m, maximum E_t -> 650 + 0.6 x 1000 x 30 x 2 / 300 = 770 kV < 1.6 x 500

Therefore maximum E_t = 770 kV

What would have been the maximum separation permissible between the transformer and the lightning arrestor, if the BIL of the transformer was 900 kV and a protective margin of 25 % is required, for the above example ?
For a protective margin of 25 %, maximum permissible surge at transformer = 900/1.25 = 720 kV

Therefore 720 = 650 + 0.6 x 1000 x 2 L / 300
This gives the maximum permissible length L = 17.5 m.

If the maximum rate of rise was taken as 500 kV/μs, the maximum length would have worked out at 35 m.

Characteristics of lightning arrestors and separation limits

Table 10.7 gives the characteristics for station type lightning arrestors and separation distances permissible between arrestor location and power transformer. For line type arrestors, the discharge voltages are about 10 to 20% higher and the corresponding separation distances are roughly half. When multiple lines meet at a busbar, the voltages transmitted are lower (corresponding to 2V/n for n identical lines). It has been suggested that in the presence of multiple lines, the separation distances may be exceeded by about 9% for one additional line, 21 % for two addition lines and 39% for three additional lines for the same degree of protection.

Nominal System Voltage kV	Transformer BIL kV (peak)	Line Construction	Line Insulation kV	Arrestor Rating kV	Discharge Voltage (kV) at			Separation distance m
					5 kA	10 kA	20 kA	
23	150	wood	500	20 25	58 71	65 81	76 94	23 15
34.5	200	wood	600	30 37	88 105	101 121	117 140	27 18
69	350	wood steel	1020 600	60 73 60 73	176 210 176 210	201 241 201 241	232 279 232 279	41 23 47 29
138	550 550 650	steel	930	109 121 145	316 351 420	350 401 481	418 466 558	52 35 47
230	825 900 1050	steel	1440	182 195 242	528 568 700	605 651 800	700 756 930	44 55 58

Table 10.7

A typical co-ordination of insulation in station equipment for some system voltages is given in table 10.8 together with the corresponding line insulation.

Rated System Voltage (kV)	Impulse Withstand Voltage (kV) peak						
	Transformer	Circuit Breakers CTs,CVTs	Switch & Post Insulation	Bus Insulation		Line Insulation	
				Suspension	Tension	Steel	Wood
22	150	150	225	255	255	-	500
33	200	250	250	320	320	-	600
66	350	350	380	400	470	600	1020
132	550	650	750	700	775	930	-
220	900	1050	1050	1140	1210	1440	-

Table 10.8

Example 10.4

A lightning arrestor is to be located on the main 132 kV busbar, 30 m away from a 132/33 kV transformer. If the BIL of the transformer on the 132 kV side is 650 kV, and the transformer is effectively earthed, select a suitable lightning arrestor to protect the transformer from a surge rising at 1000 kV/μs on the 132 kV side originating beyond the busbar on a line of surge impedance 375 Ω. (Use the tables given in the text for any required additional data).

No. of discs	Dry f.o.v. kV_{rms}	Wet f.o.v. kV_{rms}	Impulse f.o.v. kV_{crest}
1	80	50	150
2	155	90	255
3	215	130	355
4	270	170	440
5	325	215	525
6	380	255	610
7	435	295	695
8	485	335	780
9	540	375	860
10	590	415	945
11	640	455	1025
12	690	490	1105
13	735	525	1185
14	785	565	1265
16	875	630	1425
18	965	690	1585
20	1055	750	1745
25	1280	900	2145
30	1505	1050	2550

Table 10.9

Maximum system voltage for 132 kV = 138 kV
Nominal rating of surge diverter = 138 x 0.8 = 110.4 kV
If this amount is increased by a tolerance of 5%
Nominal rating = 110.4 x 1.05 = 115.9 kV

From these two figures, we can see that either the 109 kV or the 121 kV rated arrestor may be used. Let us consider the 109 kV arrestor.

Line insulation for 138 kV corresponds to 930 kV. Thus this would be the maximum surge that can be transmitted by the line. Assuming doubling of voltage at the transformer, and an arrestor residual discharge voltage of E_a, the surge current and hence the arrestor discharge current would be given by

$$I_a = \frac{2E - E_a}{Z_0} = \frac{2 \times 930 - E_a}{375}$$

For the 109 kV arrestor, E_a range from 316 kV to 418 kV. For this I_a has the range 4.12 kA to 3.85 kA. Thus the 5 kA rated arrestor is suitable. For this E_a = 315 kV.

Peak value to which the transformer potential would rise on a surge rising at 1000 kV/μs is given by

$$E_t = E_a + \beta \frac{de}{dt} x \frac{2l}{300}, \text{ assuming } \beta = 1$$

Thus $E_t = 315 + 2 \times 1000 \times 30 / 300 = 515$ kV

This gives a protective margin, for the BIL of 650 kV, of = 100 x (650 - 515)/515 = 26.2%

Thus the arrestor to be selected is the 109 kV, 5 kA one which is found to be completely satisfactory.

Flashover voltages of standard discs (254 x 146 mm) is given in the table 10.9.

In selecting the number of units, it is common practice to allow one or two more units to allow for a unit becoming defective. Thus for lines up to 220 kV, one additional unit; and for 400 kV, 2 unit may be used.

Rated System Voltage kV_{rms}	Tension Insulators		Suspension Insulators	
	Impulse f.o.v. kV	No. of discs	Impulse f.o.v. kV	No. of discs
33	320	3	320	3
66	470	5	400	4
132	775	9	700	8
220	1210	15	1140	14

Table 10.10

Also tension insulator units have their axis more or less horizontal and are more affected by rain. Also a failure of tension insulators are more sever than of suspension insulators. Thus one additional disc is used on tension insulators.

Table 10.10 shows the number of disc units (254 x 146 mm) used in Busbar Insulation in a typical substation, for both tension as well as suspension insulators.

Further, for the 132 kV and 220 kV systems, if the lines are provided with proper shielding and low tower footing resistances (say less than 7 S), the number of disc units may be reduced based on a switching surge flashover voltage of $6.5 \times$ (rated phase to neutral system voltage) and a power frequency flash-over voltage of $3 \times$ (rated phase to neutral system voltage).

On this basis, 7 units are recommended for the 132 kV system and 11 units for the 220 kV system.

11

High Voltage Direct Current Transmission

11.0 Historical Background

Power Transmission was initially carried out in the early 1880s using Direct Current (**d.c.**). With the availability of transformers (for stepping up the voltage for transmission over long distances and for stepping down the voltage for safe use), the development of robust induction motor (to serve the users of rotary power), the availability of the superior synchronous generator, and the facilities of converting **a.c.** to **d.c.** when required, **a.c.** gradually replaced **d.c.** However in 1928, arising out of the introduction of grid control to the mercury vapour rectifier around 1903, electronic devices began to show real prospects for high voltage direct current (HVDC) transmission, because of the ability of these devices for rectification and inversion. The most significant contribution to HVDC came when the Gotland Scheme in Sweden was commissioned in 1954 to be the World's first commercial HVDC transmission system. This was capable of transmitting 20 MW of power at a voltage of -100 kV and consisted of a single 96 km cable with sea return.

With the fast development of converters (rectifiers and inverters) at higher voltages and larger currents, d.c. transmission has become a major factor in the planning of the power transmission. In the beginning all HVDC schemes used mercury arc valves, invariably single phase in construction, in contrast to the low voltage polyphase units used for industrial application. About 1960 control electrodes were added to silicon diodes, giving silicon-controlled-rectifiers (SCRs or Thyristors).

In 1961 the cross channel link between England and France was put into operation. The a.c. systems were connected by two single conductor submarine cables (64km) at ± 100kV with two bridges each rated at 80 MW. The mid-point of the converters was grounded at one terminal only so as not to permit ground currents to flow. Sea return was not used because of its effect on the navigation of ships using compasses. The link is an asynchronous link between the two systems with the same nominal frequency (60Hz).

The Sakuma Frequency Changer which was put into operation in 1965, interconnects the 50Hz and the 60Hz systems of Japan. It is the first d.c. link of zero length, and is confined to a single station. It is capable of transmitting 300 MW in either direction at a voltage of 250 kV.

In 1968 the Vancouver Island scheme was operated at +250 kV to supply 300 MW and is the first d.c. link operating in parallel with an a.c. link.

In 1970 a solid state addition (Thyristors) was made to the Gotland scheme with a rating of 30MW at -150kV.

Also in 1970 the Kingsnorth scheme in England was operated on an experimental basis. In this scheme transmission of power by underground d.c. cable at ± 200 kV, 640 MW is used to reinforce the a.c. system without increasing the interrupting duty of a.c. circuit breakers.

The first converter station using exclusively Thyristors was the Eel River scheme in Canada. Commissioned in 1972, it supplies 320 MW at 80 kV d.c. The link is of zero length and connects two a.c. systems of the same nominal frequency (60Hz).

The largest thyristors used in converter valves have blocking voltages of the order of kilovolts and currents of the order 100s of amperes. In order to obtain higher voltages the thyristor valve uses a single series string of these thyristors. With higher current ratings required, the valve utilizes thyristors directly connected in parallel on a common heat sink.

The largest operational converter stations have ratings of the order of gigawatts and operate at voltages of 100s of kilovolts, and maybe up to 1000 km in length.

The thyristors are mostly air cooled but may be oil cooled, water cooled or Freon cooled. With air cooled and oil cooled thyristors the same medium is used as insulant. With the Freon cooled thyristors, SF6 may be used for insulation, leading to the design of a compact thyristor valve.

Unlike an a.c. transmission line which requires a transformer at each end, a d.c. transmission line requires a convertor at each end. At the sending end rectification is carried out, where as at the receiving end inversion is carried out.

11.1 Comparison of a.c and d.c transmission

11.1.1 Advantages of d.c.

(a) **More power can be transmitted per conductor per circuit.**

The capabilities of power transmission of an a.c. link and a d.c. link are different.
For the same insulation, the direct voltage V_d is equal to the peak value ($\sqrt{2}$ x rms value) of the alternating voltage V_d.

$$V_d = \sqrt{2}\, V_a$$

For the same conductor size, the same current can transmitted with both d.c. and a.c. if skin effect is not considered.

$$I_d = I_a$$

Thus the corresponding power transmission using 2 conductors with d.c. and a.c. are as follows.

d c power per conductor $P_d = V_d I_d$

a c power per conductor $P_a = V_a I_a \cos \varphi$

The greater power transmission with d.c. over a.c. is given by the ratio of powers.

$$\frac{P_d}{P_a} = \frac{\sqrt{2}}{\cos \varphi} = \begin{cases} 1.414 & \text{at p.f = unity} \\ 1.768 & \text{at p.f = 0.8} \end{cases}$$

In practice, a.c. transmission is carried out using either single circuit or double circuit 3 phase transmission using 3 or 6 conductors. In such a case the above ratio for power must be multiplied by **2/3** or by **4/3**.

In general, we are interested in transmitting a given quantity of power at a given insulation level, at a given efficiency of transmission. Thus for the same power transmitted P, same losses P_L and same peak voltage V, we can determine the reduction of conductor cross-section A_d over A_a.

Let R_d and R_a be the corresponding values of conductor resistance for d.c. and a.c. respectively, neglecting skin resistance.

For **d.c** current $= \dfrac{P}{V_m}$

power loss $P_L = (P/V_m)^2 R_d = (P/V_m)^2.(\rho l/A_d)$

For **a.c** current $= \dfrac{P}{(V_m/\sqrt{2})\cos\varphi} = \dfrac{\sqrt{2}\,P}{V_m \cos\varphi}$.

power loss $P_L = [\sqrt{2}P/(V_m \cos\varphi)]^2 R_a$

$= 2\,(P/V_m)^2.(\rho l/A_a \cos^2\varphi)$

Equating power loss for d.c. and a.c.

$$(P/V_m)^2.(\rho l/A_d) = 2\,(P/V_m)^2.(\rho l/A_a \cos^2\varphi)$$

This gives the result for the ratio of areas as

$$\frac{A_d}{A_a} = \frac{\cos^2\varphi}{2} = \begin{cases} 0.5 \text{ at p.f. } = \text{unity} \\ 0.32 \text{ at p.f. } = 0.8 \end{cases}$$

The result has been calculated at unity power factor and at 0.8 lag to illustrate the effect of power factor on the ratio. It is seen that only one-half the amount of copper is required for the same power transmission at unity power factor, and less than one-third is required at the power factor of 0.8 lag.

(b) **Use of Ground Return Possible**

In the case of hvdc transmission, ground return (especially submarine crossing) may be used, as in the case of a monopolar d.c. link. Also the single circuit bipolar d.c. link is more reliable, than the corresponding a.c. link, as in the event of a fault on one conductor, the other conductor can continue to operate at reduced power with ground return. For the same length of transmission, the impedance of the ground path is much less for d.c. than for the corresponding a.c. because d.c. spreads over a much larger width and depth. In fact, in the case of d.c. the ground path resistance is almost entirely dependant on the earth electrode resistance at the two ends of the line, rather than on the line length. However it must be borne in mind that ground return has the following disadvantages. The ground currents cause electrolytic corrosion of buried metals, interfere with the operation of signalling and ships' compasses, and can cause dangerous step and touch potentials.

(c) **Smaller Tower Size**

The d.c. insulation level for the same power transmission is likely to be lower than the corresponding a.c. level. Also the d.c. line will only need two conductors whereas three conductors (if not six to obtain the same reliability) are required for a.c. Thus both electrical and mechanical considerations dictate a smaller tower.

(d) **Higher Capacity available for cables**

In contrast to the overhead line, in the cable breakdown occurs by puncture and not by external flashover. Mainly due to the absence of ionic motion, the working stress of the d.c. cable insulation may be 3 to 4 times higher than under a.c.

Also, the absence of continuous charging current in a d.c. cable permits higher active power transfer, especially over long lengths.

(Charging current of the order of 6 A/km for 132 kV). Critical length at 132 kV ≈ 80 km for a.c cable. Beyond the critical length no power can be transmitted without series compensation in a.c. lines. Thus derating which is required in a.c. cables, thus does not limit the length of transmission in d.c.

A comparison made between d.c. and a.c. for the transmission of about 1550 MVA is as follows. Six number a.c. 275 kV cables, in two groups of 3 cables in horizontal formation, require a total trench width of 5.2 m, whereas for two number d.c. ±500 kV cables with the same capacity require only a trench width of about 0.7 m.

(e) **No skin effect**

Under a.c. conditions, the current is not uniformly distributed over the cross section of the conductor. The current density is higher in the outer region (skin effect) and result in under utilisation of the conductor cross-section. Skin effect under conditions of smooth d.c. is completely absent and hence there is a uniform current in the conductor, and the conductor metal is better utilised.

(f) **Less corona and radio interference**

Since corona loss increases with frequency (in fact it is known to be proportional to **f+25**), for a given conductor diameter and applied voltage, there is much lower corona loss and hence more importantly less radio interference with d.c. Due to this bundle conductors become unnecessary and hence give a substantial saving in line costs. [Tests have also shown that bundle conductors would anyway not offer a significant advantage for d.c as the lower reactance effect so beneficial for a.c is not applicable for d.c.]

(g) **No Stability Problem**

The d.c. link is an asynchronous link and hence any a.c. supplied through converters or d.c. generation do not have to be synchronised with the link. Hence the length of d.c. link is not governed by stability.

In a.c. links the phase angle between sending end and receiving end should not exceed 30^o at full-load for transient stability (maximum theoretical steady state limit is 90^o).

Note: $\theta = w\sqrt{lc}$ per km $= (2\pi \times 50)/(3 \times 10^5)$ rad/km $\approx (2 \times 180 \times 50)/(3 \times 10^5) \approx 0.06^0$/km

The phase angle change at the natural load of a line is thus 0.6^o per 10 km.

The maximum permissible length without compensation $\approx$ 30/0.06 = 500 km

With compensation, this length can be doubled to 1000 km.

(h) **Asynchronous interconnection possible**

With a.c. links, interconnections between power systems must be synchronous. Thus different frequency systems cannot be interconnected. Such systems can be easily interconnected through hvdc links. For different frequency interconnections both convertors can be confined to the same station.

In addition, different power authorities may need to maintain different tolerances on their supplies, even though nominally of the same frequency. This option is not available with a.c. With d.c. there is no such problem.

(i) **Lower short circuit fault levels**

When an a.c. transmission system is extended, the fault level of the whole system goes up, sometimes necessitating the expensive replacement of circuit breakers with those of higher fault levels. This problem can be overcome with hvdc as it does not contribute current to the a.c. short circuit beyond its rated current. In fact it is possible to operate a d.c. link in "parallel" with an a.c. link to limit the fault level on an expansion. In the event of a fault on the d.c line, after a momentary transient due to the discharge of the line capacitance, the current is limited by automatic grid control. Also the d.c. line does not draw excessive current from the a.c. system.

(j) **Tie line power is easily controlled**

In the case of an a.c. tie line, the power cannot be easily controlled between the two systems. With d.c. tie lines, the control is easily accomplished through grid control. In fact even the reversal of the power flow is just as easy.

11.1.2 Inherent problems associated with hvdc

(a) **Expensive convertors**

Expensive Convertor Stations are required at each end of a d.c. transmission link, whereas only transformer stations are required in an a.c. link.

(b) **Reactive power requirement**

Convertors require much reactive power, both in rectification as well as in inversion. At each convertor the reactive power consumed may be as much at 50% of the active power rating of the d.c. link. The reactive power requirement is partly supplied by the filter capacitance, and partly by synchronous or static capacitors that need to be installed for the purpose.

(c) **Generation of harmonics**

Convertors generate a lot of harmonics both on the d.c. side and on the a.c. side. Filters are used on the a.c. side to reduce the amount of harmonics transferred to the a.c. system. On the d.c. system, smoothing reactors are used. These components add to the cost of the convertor.

(d) **Difficulty of circuit breaking**

Due to the absence of a natural current zero with d.c., circuit breaking is difficult. This is not a major problem in single hvdc link systems, as circuit breaking can be accomplished by a very rapid absorbing of the energy back into the a.c. system. (The blocking action of thyristors is faster than the operation of mechanical circuit breakers). However the lack of hvdc circuit breakers hampers multi-terminal operation.

(e) **Difficulty of voltage transformation**

Power is generally used at low voltage, but for reasons of efficiency must be transmitted at high voltage. The absence of the equivalent of d.c. transformers makes it necessary for voltage transformation to carried out on the a.c. side of the system and prevents a purely d.c. system being used.

(f) **Difficulty of high power generation**

Due to the problems of commutation with d.c. machines, voltage, speed and size are limited. Thus comparatively lower power can be generated with d.c.

(g) **Absence of overload capacity**

Convertors have very little overload capacity unlike transformers.

11.1.3 Economic Comparison

The hvdc system has a lower line cost per unit length as compared to an equally reliable a.c. system due to the lesser number of conductors and smaller tower size. However, the d.c. system needs two expensive convertor stations which may cost around two to three times the corresponding a.c. transformer stations. Thus hvdc transmission is not generally economical for short distances, unless other factors dictate otherwise. Economic considerations call for a certain minimum transmission distance (break-even distance) before hvdc can be considered competitive purely on cost.

Estimates for the break even distance of overhead lines are around 500 km with a wide variation about this value depending on the magnitude of power transfer and the range of costs of lines and equipment. The break-even distances are reducing with the progress made in the development of converting devices.

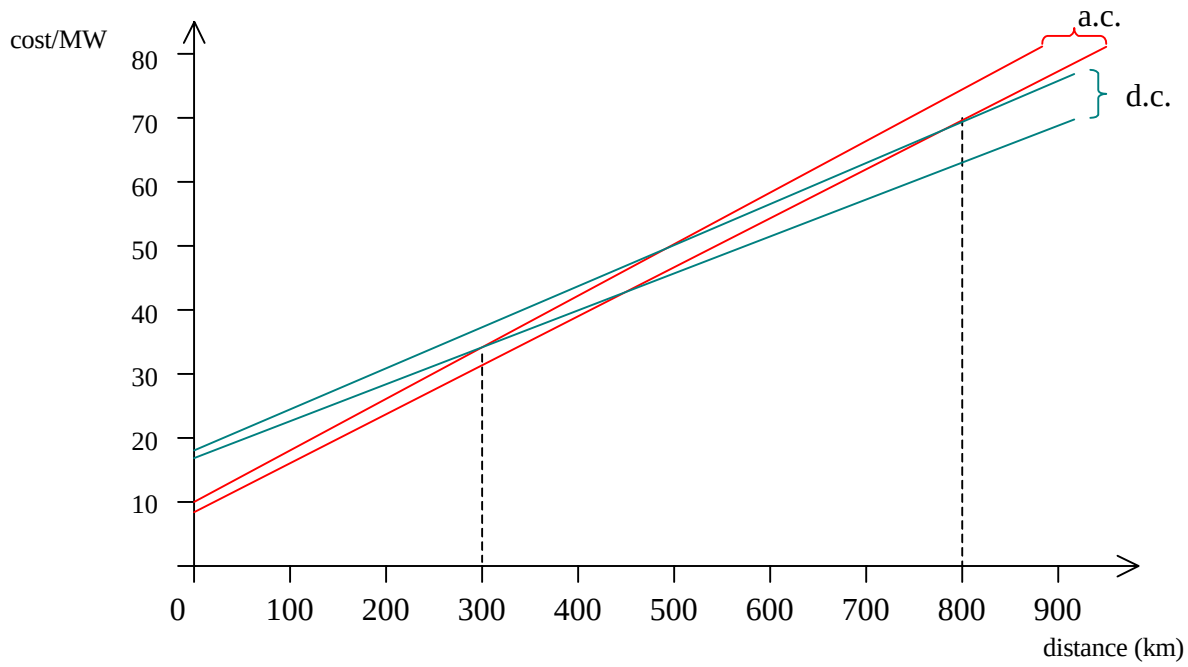

Figure 11.1 - Break-even distance for d.c. transmission

Figure 11.1 shows the comparative costs of d.c. links and a.c. links with distance, assuming a cost variation of ± 5% for the a.c. link and a variation of ± 10% for the d.c. link.

For cables, the break-even distance is much smaller than for overhead lines and is of the order of 25 km for submarine cables and 50 km for underground cables.

11.2 Convertor arrangements and operation

The three-phase six-valve bridge rectifier is almost exclusively used in high voltage direct current applications. This is shown in figure 11.2.

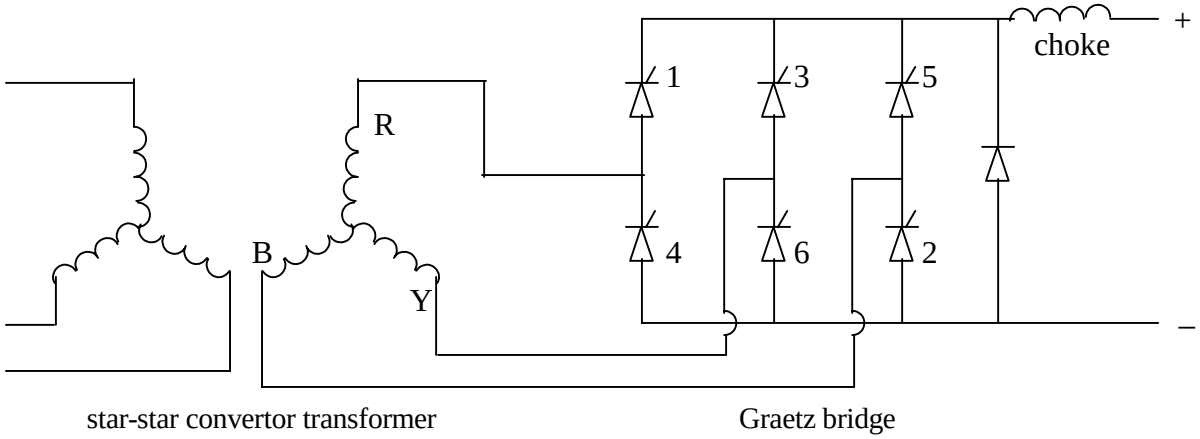

Figure 11.2 - Hexa-valve Bridge Convertor arrangement

The 6-valve bridge connection gives double the direct voltage as output compared to the simple 3-phase rectifier. The convertor transformer may either be wound star-star as shown, or as star-delta (or even as delta-star or delta-delta). The ripple of each of these connections is the same, but are phase shifted by 30^0 in output with respect to each other. To obtain a smoother output, two bridges (one star-star and the other star-delta) may be connected together to give the twelve pulse connection.

For the 6-valve bridge, with zero firing delay, the voltage waveforms across the thyristors are shown in figure 11.3. At any given instant, one thyristor valve on either side is conducting. The conducting period for the thyristor valve R1 is shown on the diagram.

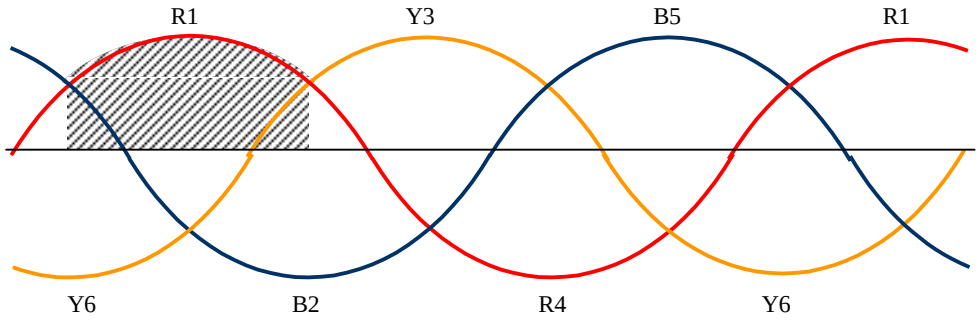

Figure 11.3 - Thyristor voltage waveforms (α = 0)

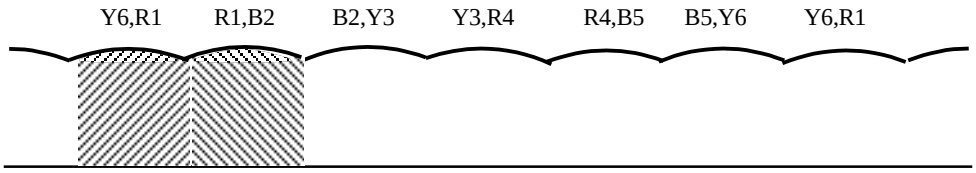

Figure 11.4 - d.c. output waveforms (α = 0)

The corresponding d.c. output voltage waveforms are shown in figure 11.4.

It can be shown that for the 6-valve bridge, the total r.m.s. ripple is of the order of 4.2% of the d.c. value (for zero delay α = 0 and zero commutation γ = 0). The ripple of course increases with the delay angle and has a value of about 30% at α= π/2.

With the 12 pulse bridge, the r.m.s. ripple is of the order of 1.03% of the d.c. value (for $\alpha = 0$ and $\gamma = 0$), and increases to about 15% at $\alpha = \pi/2$.

The use of a choke reduces the ripple appearing in the direct current transmitted.

If E is the r.m.s. line-to-line voltage, then if $\alpha = 0$, $\gamma = 0$, then the direct voltage output is given by equation (11.1).

$$V_{do} = 2 x \frac{E}{\sqrt{3}} x \sqrt{2} x \frac{3}{2\pi} \int_{-\frac{\pi}{3}}^{\frac{\pi}{3}} \cos\theta \; d\theta$$

$$= E . \frac{3\sqrt{2}}{\pi} . \frac{1}{\sqrt{3}} \left[2 x \sin\frac{\pi}{3} \right]$$

$$V_{do} = \frac{3\sqrt{2}}{\pi} . E = 1.350 E \qquad (11.1)$$

11.2.1 Control angle (Delay angle)

The control angle for rectification (also known as the ignition angle) is the angle by which firing is delayed beyond the natural take over for the next thyristor. The transition could be delayed using grid control. Grid control is obtained by superposing a positive pulse on a permanent negative bias to make the grid positive. Once the thyristor fires, the grid loses control.

Assuming no commutation (2 thyristors on same side conducting simultaneously during transfer), the voltage waveforms across the thyristors as shown in figure 11.5.

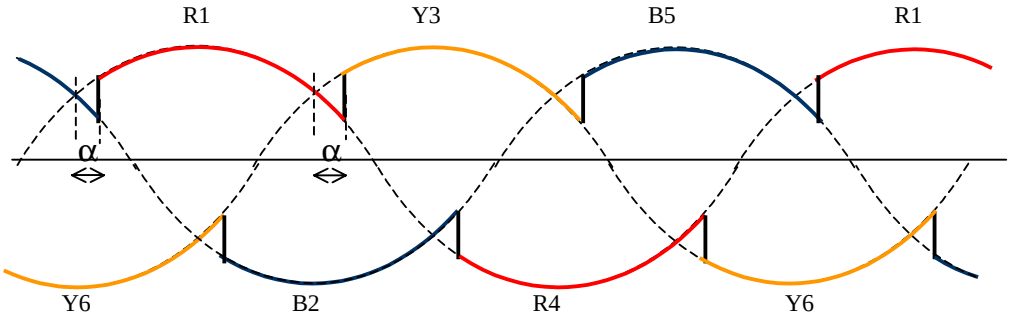

Figure 11.5 - Thyristor voltage waveforms (with delay α)

In this case, the magnitude of the direct voltage output is given by the equation (11.2).

$$V_d = 2 x \frac{E}{\sqrt{3}} x \sqrt{2} x \frac{3}{2\pi} \int_{-\frac{\pi}{3}+\alpha}^{\frac{\pi}{3}+\alpha} \cos\theta \; d\theta$$

$$= E . \frac{3\sqrt{2}}{\pi} . \frac{1}{\sqrt{3}} \left[\sin\left(\frac{\pi}{3} + \alpha\right) + \sin\left(\frac{\pi}{3} - \alpha\right) \right]$$

$$V_d = \frac{3\sqrt{2}}{\pi} E \cos\alpha = V_{do} \cos\alpha \qquad (11.2)$$

11.2.2 Commutation angle (overlap angle)

The commutation period between two thyristors on the same side of the bridge is the angle by which one thyristor commutates to the next. During this period γ, the voltage at the electrode follows mean voltage of the 2 conducting thyristors on the same side. This is shown in figure 11.6.

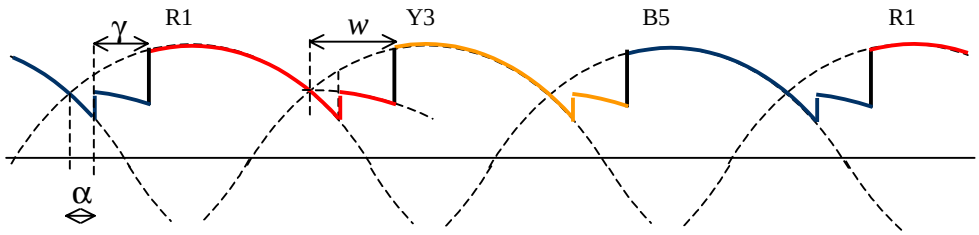

Figure 11.6 - commutation between 2 thyristors

With both the delay angle and commutation being present, the magnitude of the direct voltage may be determined from equation (11.3) as follows.

$$V_d = 2\frac{E}{\sqrt{3}}\sqrt{2}\,\frac{3}{2\pi}\int_{-\frac{\pi}{3}+\alpha}^{\frac{\pi}{3}+\alpha} f(\theta)\,d\theta$$

$$= \frac{3\sqrt{2}\,E}{\sqrt{3}\,\pi}\left[\int_{-\frac{\pi}{3}+\alpha}^{-\frac{\pi}{3}+\alpha+\gamma}\frac{1}{2}\left(\cos(\theta+\tfrac{2\pi}{3})+\cos\theta\right).d\theta + \int_{-\frac{\pi}{3}+\alpha+\gamma}^{\frac{\pi}{3}+\alpha}\cos\theta\,.d\theta\right]$$

$$V_d = \frac{V_{do}}{2}\left[\cos\alpha+\cos(\alpha+\gamma)\right] \qquad (11.3)$$

An alternate method of derivation of the result is based on comparison of similar areas on the waveform. Figure 11.7 gives the necessary information.

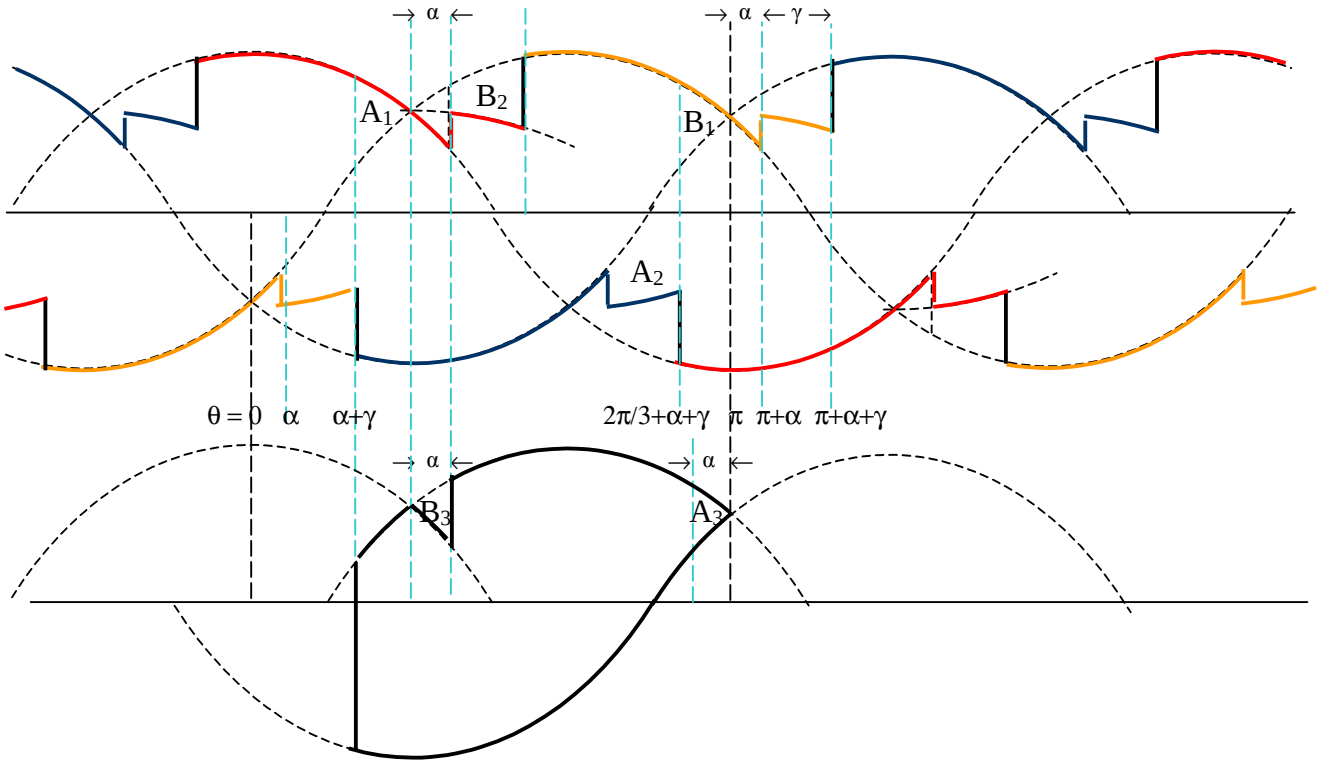

Figure 11.7 - Graphical analysis of waveform

d.c. output = average value of waveform

$$V_d = \frac{1}{2\pi/3}\int_{\alpha+\gamma}^{\alpha+\gamma+\frac{2\pi}{3}} V(\theta).d\theta$$

In this integral, in graphical form, area A_1 can be replaced by area B_1. Similarly, area A_2 can be replaced by area B_2 and area A_3 by area B_3. The integral equation then reduces to the form shown below.

$$V_d = \frac{3\sqrt{2}\,E}{2\pi} \int_{\alpha+\gamma}^{\pi-\alpha} \sin\theta \, d\theta$$

$$= \frac{3\sqrt{2}\,E}{2\pi} \left[\cos(\alpha+\gamma) - \cos(\pi-\alpha) \right]$$

where $\sqrt{2}\,E$ is the peak value of the line voltage.

Simplification gives the desired result as in equation (11.3).

$$V_d = \frac{3\sqrt{2}\,E}{2\pi} \left[\cos\alpha + \cos(\alpha+\gamma) \right]$$

$$= \frac{V_0}{2} \left[\cos\alpha + \cos(\alpha+\gamma) \right]$$

Commutation is a result of the a.c. system inductance L_c, which does not allow the current through a thyristor to extinguish suddenly. Thus the larger the current the larger the commutation angle γ.

If the extinction angle for rectifier operation w is defined as $w = \alpha + \gamma$, then V_d can be written as in equation 11.4.

Consider the commutation between thyristors 1 & 3 in the bridge circuit shown in figure 11.8. Let i_c be the commutation current. The commutation current is produced by the voltage e_c which is the line voltage between phases 1 and 2.

$$V_d = \tfrac{1}{2} \left[\cos\alpha + \cos w \right] \qquad (11.4)$$

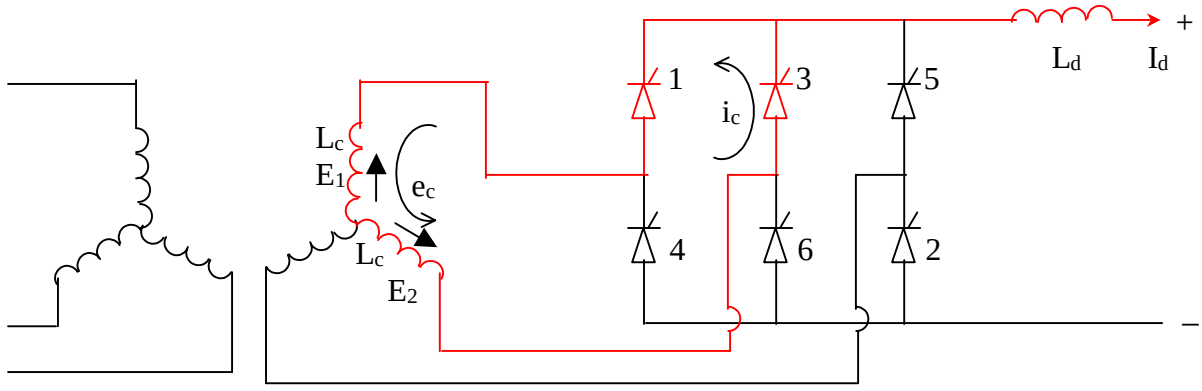

Figure 11.8 - Circuit for analysis of commutation

$$e_c = E_2 - E_1 = \frac{E\sqrt{2}}{\sqrt{3}} \left[\cos(\omega t + \frac{\pi}{3}) - \cos(\omega t - \frac{\pi}{3}) \right]$$

$$= \sqrt{2}\,E \sin\omega t$$

This can also be written in the following form, with $i_c = 0$ at the start of commutation and $i_c = I_d$ at the end of commutation.

$$e_c = 2 L_c \frac{d i_c}{d t}$$

This equation may be integrated as follows to give equation 11.5.

$$\tfrac{1}{2} \int_{\alpha}^{w=\alpha+\gamma} e_c \, d(\omega t) = \omega L_c \int_{0}^{I_d} d i_c$$

$$\tfrac{1}{2} \int_{\alpha}^{w} \sqrt{2} E \sin \omega t \, d(\omega t) = \omega L_c I_d$$

$$i.e. \quad \frac{E}{\sqrt{2}} (\cos \alpha - \cos w) = \omega L_c I_d$$

$$\cos \alpha - \cos w = \frac{\sqrt{2} \omega L_c}{E} I_d \tag{11.5}$$

$$\cos \alpha + \cos w = \frac{2 V_d}{V_o} \tag{11.6}$$

Equation 11.4 can also be written of the form of equation (11.6).

From equations (11.5) and (11.6) **w** may be eliminated to give the equation (11.7).

$$\cos \alpha = \frac{V_d}{V_0} + \frac{\omega L_c}{\sqrt{2} E} I_d$$

$$\because V_0 = \frac{3\sqrt{2} E}{\pi}, \quad \cos \alpha = \frac{V_d}{V_0} + \frac{3 \omega L_c}{\pi V_0}$$

$$\therefore \quad V_d = V_0 \cos \alpha - \frac{3 \omega L_c}{\pi} I_d \tag{11.7}$$

It can also be shown that equation (11.7) can be rewritten in terms of the extinction angle w instead of the ignition angle α as in equation (11.8).

$$V_d = V_0 \cos w + \frac{3 \omega L_c}{\pi} I_d \tag{11.8}$$

Equation (11.7) suggests that the convertor may be represented by a no load d.c. output voltage $\mathbf{V_o \cos \alpha}$

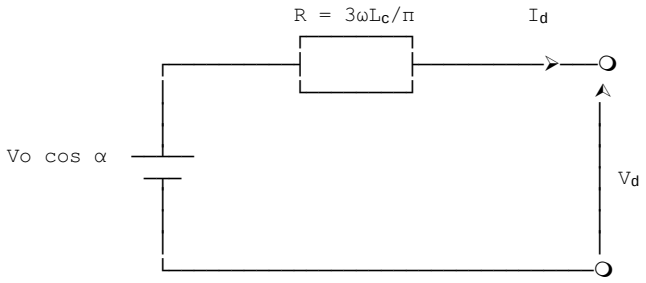

Figure 11.9 - Equivalent circuit for Rectifier

and a series fictitious resistance $\mathbf{3\omega L_c/\pi}$ as shown in figure 11.9. The fictitious resistor does not however consume any active power.

11.2.3 Current Waveforms

If Commutation is not considered, the current waveforms through each thyristor (assuming a very high value of inductance L_d in the d.c. circuit to give complete smoothing) is a rectangular pulse lasting exactly one-third of a cycle. This is shown in figure 11.10 for the cases without delay and with delay.

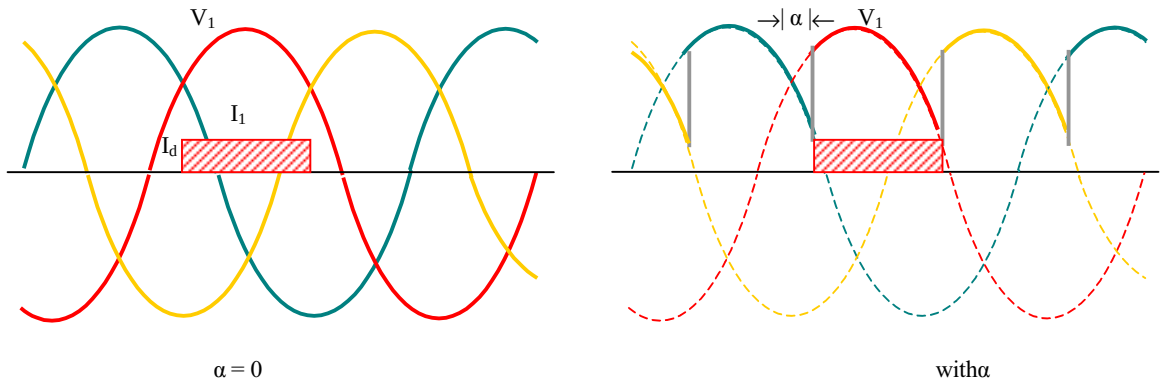

Figure 11.10 - Thyristor current waveforms (γ)

When commutation is considered, the rise and fall of the current waveforms would be modified as they would no longer be instantaneous, as shown in figure 11.11.

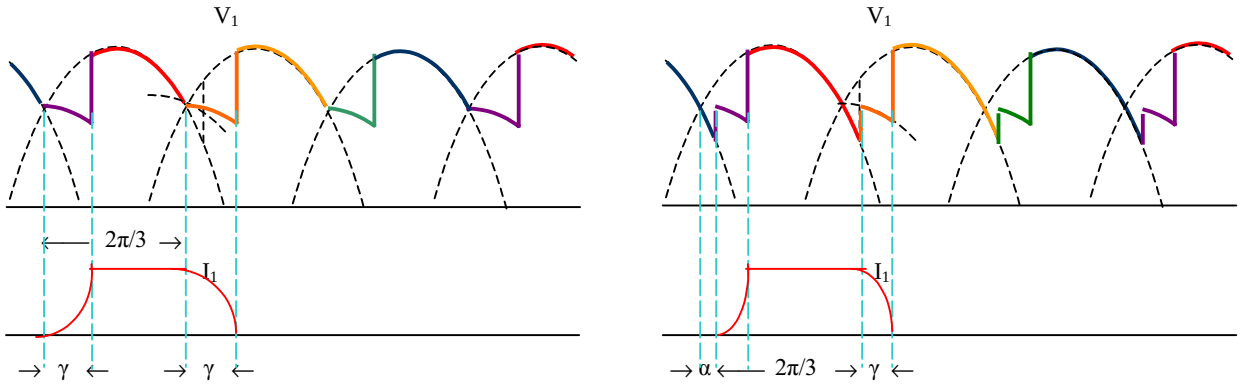

Figure 11.11 - Thyristor current waveforms

Since each phase has 2 thyristors on the opposite half cycles, the a.c. current waveform on the secondary side of the transformer has a non-sinusoidal waveform as shown in figure 11.12.

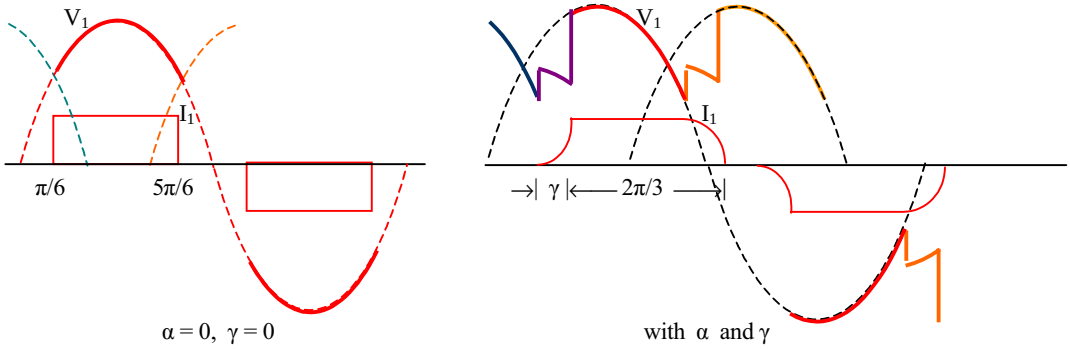

Figure 11.12 - Current waveforms on transformer secondary

If commutation angle is not considered, we can easily calculate the r.m.s. value of the a.c. current on the transformer secondary I_s as in equation (11.9).

$$I_s = \sqrt{\frac{1}{\pi} \cdot \frac{2\pi}{3} \cdot I_d^{\,2}} = \sqrt{\tfrac{2}{3}}\, I_d = 0.8165\, I_d \qquad (11.9)$$

Usually harmonic filters are provided on the a.c. system, so that only the fundamental component need to be supplied/absorbed from the a.c. system. From Fourier analysis, it can be shown that the fundamental component is given as follows, resulting in equation (11.10).

$$I = \frac{I_{\max}}{\sqrt{2}} = \frac{1}{\sqrt{2}} \cdot \frac{2}{\pi} \cdot \int_{-\frac{\pi}{3}}^{\frac{\pi}{3}} I_d \cos \omega t \, d(\omega t)$$

$$I = \frac{\sqrt{2}}{\pi} I_d \, 2 \sin \frac{\pi}{3} = \frac{\sqrt{6}}{\pi} I_d = 0.78\, I_d \qquad (11.10)$$

If filters were not provided, it can be shown, using the Fourier series analysis, that the r.m.s. ripple on the a.c. system would be 0.242 I_d (or 31 % of the fundamental)

Note: For normal operation neglecting the commutation angle, in the above calculations of the alternating current, gives rise to an error only of the order of 1%.

As can be seen from the voltage and current waveforms on the a.c. side, the current lags the voltage due to the presence of the delay angle α and the commutation angle γ. Thus since only active power is transmitted in a d.c. link, the convertor must consume the reactive power.

11.2.4 Power factor cos φ

Since the convertor consumes reactive power, there will be a power factor associated with the convertor on the a.c. side. This can be calculated as follows.

Active power supplied to d.c. link	=	$V_d I_d$
Active power supplied from a.c. system	=	$\sqrt{3}$ E I cos φ

Since the convertor does not consume any active power, there must be power balance.

$$V_d I_d = \sqrt{3}\, E\, I \cos \varphi$$

From this the power factor can be calculated as follows.

$$\cos \phi = \frac{V_d I_d}{\sqrt{3}\, E\, I}$$

$$\cos \phi = \frac{\frac{1}{2} V_0 (\cos \alpha + \cos w) \frac{\pi}{\sqrt{6}} I}{\sqrt{3} \frac{\pi}{3\sqrt{2}} V_0 I}$$

This gives the result as in equation (11.11).

$$\cos \varphi = \tfrac{1}{2} (\cos \alpha + \cos w) = \tfrac{1}{2} [\cos \alpha + \cos(\alpha+\gamma)] \qquad (11.11)$$

In the absence of commutation, this reduces to the simple relationship

$$\cos \varphi = \cos \alpha$$

Which means that α is the power factor angle in the absence of commutation. The presence of commutation reduces the effective power factor by increasing the effective angle.

With $\gamma = 0$, the active power transmitted is $\sqrt{3}$ E I cos α, and is zero in value when $\alpha = 90^o$.

Thus if a high inductance is connected with the load, the limit of power transfer under rectification is $\alpha = 90^o$. However, if no inductance were present with the load (i.e. L_d=0) then the voltage and the current waveforms would become identical in shape (since the load is purely resistive). Under these conditions, the voltage cannot go negative at any instant of time, since the current cannot flow in the opposite direction through the thyristors. The power transmitted would then become zero only at $\alpha = 120^o$. Figure 11.13 shows typical output current and voltage waveforms.

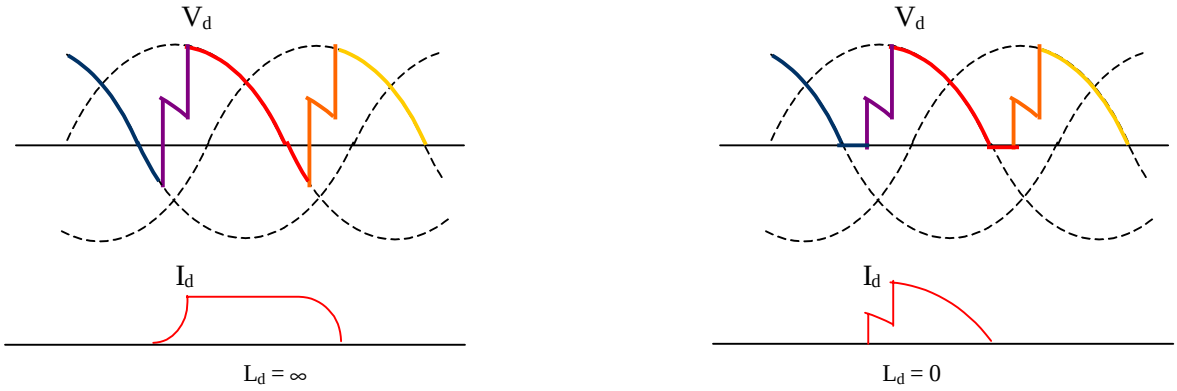

Figure 11.13 - Typical d.c. output waveforms

11.2.5 Current waveforms on a.c. system

In section 11.3.3 it was seen that the current waveform on the secondary side of the convertor transformer was as shown in figure 11.14

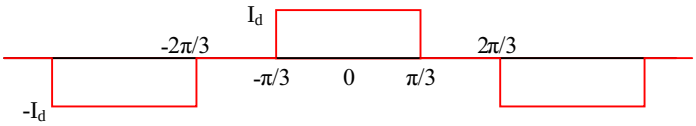

Figure 11.14 - Current waveform on a.c. system

The same current waveform appears on the primary side of the convertor transformer (a.c. system) when the winding connection is star-star, if no filters are present. If filters are present they would filter out some of the harmonics and make the a.c system currents more or less sinusoidal.

When the convertor transformer is delta-star connected, the corresponding primary current waveforms would be as shown in figure 11.15.

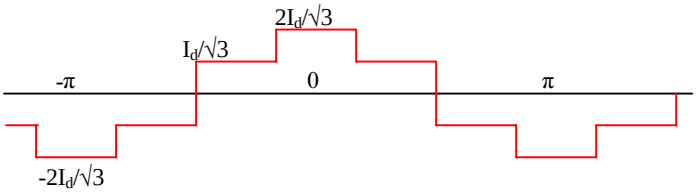

Figure 11.15 - Primary current waveform

Each of the waveforms shown in figures 11.14 and 11.15 contain the same harmonics (6k±1) with their amplitudes inversely proportional to the harmonic number. The polarities of some of the components of the two waveforms are opposite, so that when a star-star and delta-star convertor bridge are connected in cascade, only the (12k±1) harmonics remain. Thus less filtering is required. Further when commutation is present, the harmonic amplitudes reduce due to smoothing action.

Note: During normal operation of the convertor as a rectifier, the delay angle α is small (about 10^0), while the commutation angle is comparatively larger (about 20^0).

11.2.6 Inversion

Because the thyristors conduct only in one direction, the current in a convertor cannot be reversed. Power reversal can only be obtained by the reversal of the direct voltage (average value) V_d.

For inversion to be possible, a high value of inductance must be present, and the delay angle $\alpha > 90^0$, since V_d changes polarity at this angle. The theoretical maximum delay for inversion would occur at $\alpha = 180_0$.
Thus it is common practice to define a period of advance from this point rather than a delay from the previous cross-over as defined for rectification. Thus we define $\beta = \pi - \alpha$ as the ignition angle for inversion or the angle of advance. Similarly the extinction angle is also defined as $\delta = \pi - w$. The definition of the commutation angle γ is unchanged. Thus $\beta = \gamma + \delta$.

It must be noted, that unlike with rectification which can be operated with $\alpha = 0$, inversion cannot be carried out with $\beta = 0$, since a minimum angle δ_0 is required for deionisation of the arc and regaining grid control.

Thus we have the practical relationship $\delta_0 < \beta < \pi/2$. Practical values of δ_0 lie between 1^0 and 8^0.

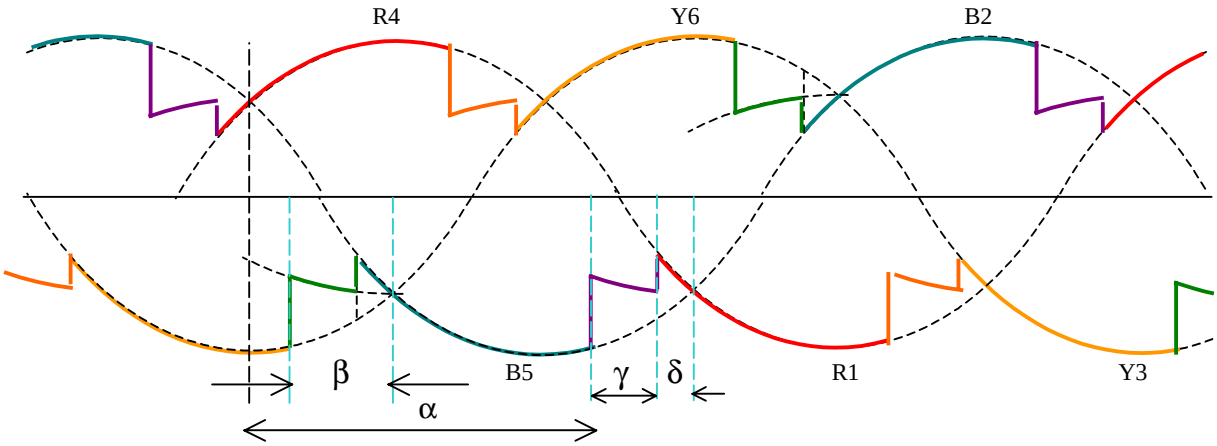

Figure 11.16 - Thyristor voltage waveforms for inversion

Inversion cannot of course be carried out without a d.c. power source. Further, to obtain the necessary frequency for the a.c. on inversion, the commutation voltage is obtained from either synchronous machines or from the a.c. system fed. In isolated systems, L C circuits may also be sometimes used for the purpose. Figure 11.16 shows the thyristor voltage waveforms for inversion.

During inversion, each thyristor conducts during the negative half cycle, so that the direct voltage waveform and the corresponding current has the form shown in figure 11.17.

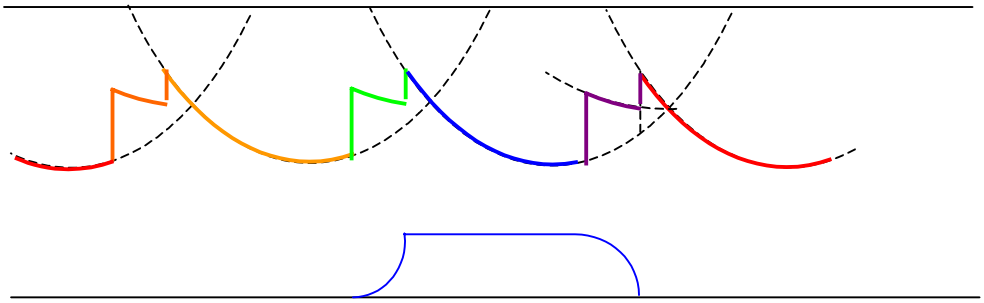

Figure 11.17 - Direct voltage waveform & thyristor current waveform

The equations derived earlier for the convertor are valid. However, they are usually written in terms of the variables β and δ instead of αand w. Thus the equation $V_d = ½ V_0 [\cos \alpha + \cos (\alpha+\gamma)]$ becomes

$$V_d = ½ V_0 [\cos (\pi - \beta) + \cos (\pi - \delta)]$$

or $$(-) V_d = ½ V_0 [\cos \beta + \cos \delta] = V_0 \cos \beta + (3\omega L_c/\pi) I_d$$

Since the direct voltage is always negative during inversion, it is common practice to omit the negative sign from the expression.

It can also be shown that

$$(-) V_d = V_0 \cos \delta - (3\omega L_c/\pi) I_d$$

As in the case of rectification, it can be shown that for inversion

$$\cos \delta - \cos \beta = \sqrt{3}\omega L_c/E \, . \, I_d \quad \text{and} \quad I = \sqrt{6}/\pi \, I_d$$

The power factor of the invertor can be shown to be given by the equation

$$\cos \varphi = ½ (\cos \delta + \cos \beta)$$

It is common practice to operate the invertor at a constant extinction angle δ (10^0 to 20^0).

11.3 Control Characteristics

The control characteristics of the convertor are the plots of the variation of the direct voltage against the direct current. These are described in the following sections.

11.3.1 Natural Voltage Characteristic (NV) and the Constant Ignition Angle (CIA) control

The Natural Voltage Characteristic corresponds to zero delay angle α = 0. This has the characteristic equation given by $V_d = V_0 - (3\omega L_c/\pi) I_d$. The Constant Ignition Angle control is a similar characteristic which is parallel to the NV characteristic with a controllable intercept $V_0 \cos \alpha$. These are shown in figure 11.18.

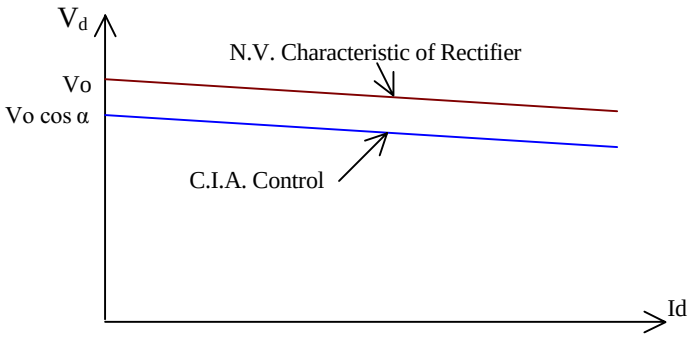

Figure 11.18 - N.V. Ch. & C.I.A. Control of Rectifier

11.3.2 Constant Extinction Angle (CEA) control

The Invertor is usually operated at constant extinction angle. This has the characteristic equation given by $V_d = V_0 \cos \delta - (3\omega L_c/\pi) I_d$. This is shown in figure 11.19.

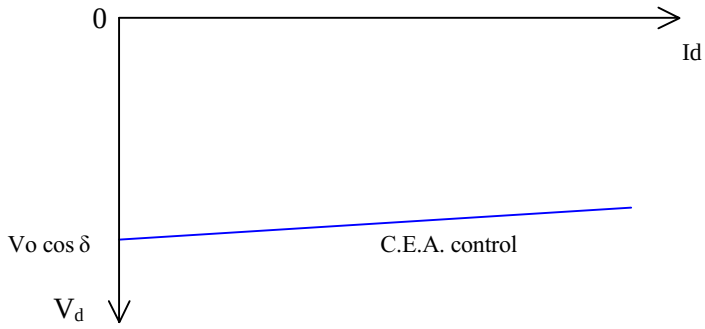

Figure 11.19 - N.V. Characteristic & C.I.A. Control of Rectifier

11.3.3 Constant Current Control (CC)

In a d.c. link it is common practice to operate the link at constant current rather than at constant voltage. [Of course, constant current means that current is held nearly constant and not exactly constant].

In constant current control, the power is varied by varying the voltage. There is an allowed range of current settings within which the current varies.

11.3.4 Full Characteristic of Convertor

The complete characteristic of each convertor has the N.V. characteristic and equipped with C.C. control and the C.E.A. control. This is shown in figure 11.20 for a single convertor.

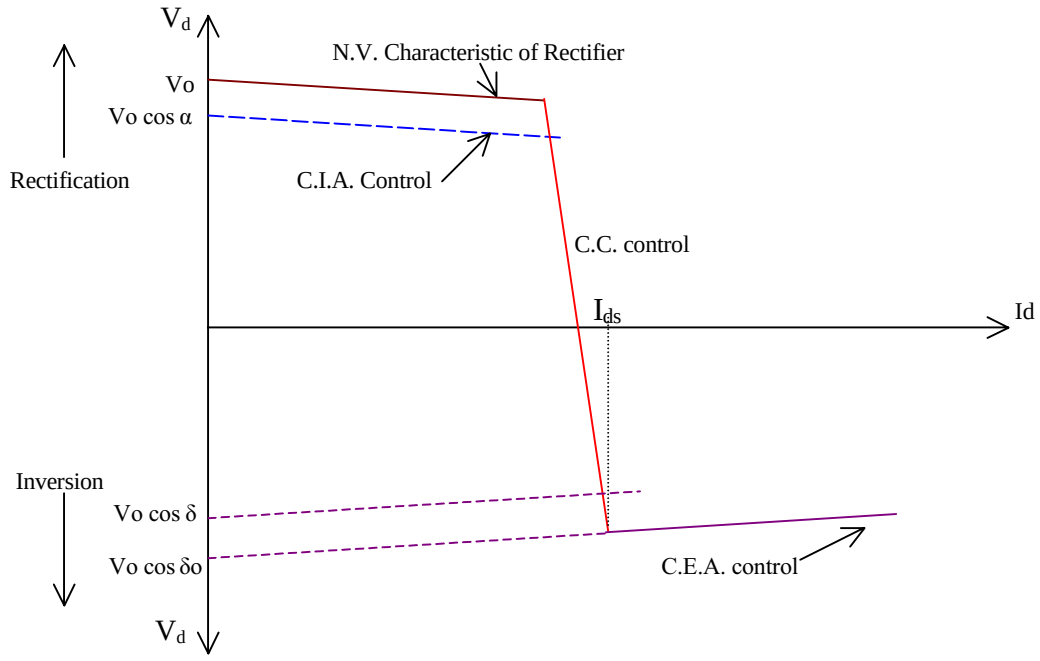

Figure 11.20 - Complete characteristic of Convertor

Note: The constant current controller adjusts the firing angle α so that the current is maintained at a set value, even for short-circuits on the d.c. line. The C.C. control is present in the invertor too, although the invertor is not usually operated in that region. The rectifier is normally operated in the C.C. region while the invertor is operated in the C.E.A. region.

11.3.5 Compounding of Convertors

Figure 11.21 shows a system of 2 convertors, connected by a hvdc link. Both convertors are provided with CEA and CC control so that either can work as a rectifier or an invertor. The compounded characteristics are shown in figure 11.22.

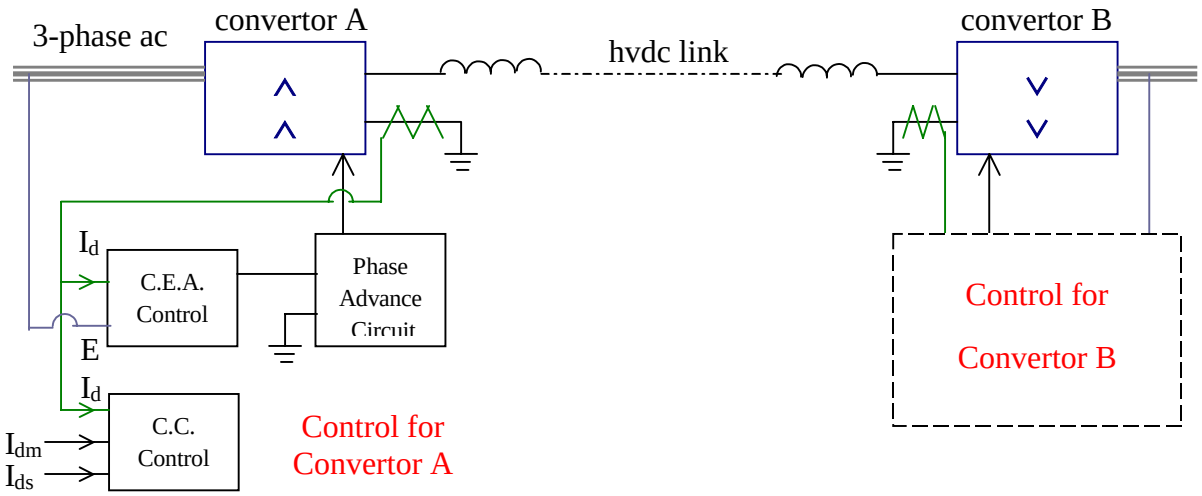

Figure 11.21 - Compounding of Convertors

The margin setting I_{dm} between the current setting I_{ds} for the invertor and for the rectifier is usually kept at about 10% to 20% of the current setting. The setting of the convertor operating as rectifier is kept higher than the setting of that as invertor by the margin setting I_{dm}.

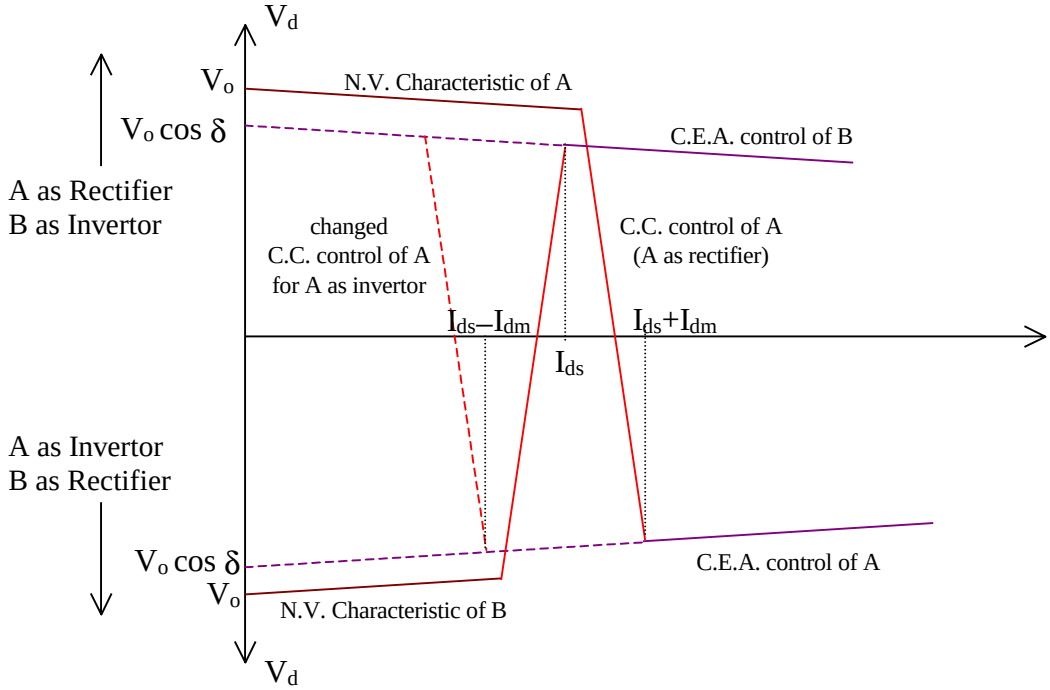

Figure 11.22 - Compounded characteristic of Convertors

The usual operating point for power transfer is the intersection of the CC control of the rectifier and the CEA control of the invertor. (For comparison, the characteristics of convertor B has been drawn inverted). It must also be ensured by proper tap changing that the N.V. characteristic of the convertor operating in the rectification mode is higher than the C.E.A. characteristic of the invertor, as V_o of the two ends are not necessarily equal.

With convertor A operating as rectifier, and convertor B operating as invertor, the steady state current under all circumstances will remain within the upper limit (I_{ds} + I_{dm}) and the lower limit I_{ds}. That is, the system direct current will not change by more than I_{dm} under all operating conditions. By reversing the margin setting I_{dm}, that is making the setting of convertor B to exceed that of A, power flow can be automatically reversed. Convertor B will then operate as a rectifier and A as an invertor. The reversal of power occurs as a result of the reversal of polarity of the voltage.

11.3.6 Per Unit Convertor Chart

The convertor operating equations for voltage V_d and current I_d are expressed as follows.

$$V_d = \frac{3\sqrt{2}\,E}{\pi}\,\frac{(\cos\alpha + \cos w)}{2}$$

$$I_d = \frac{E}{\sqrt{2}\,\omega\,L_c}(\cos\alpha - \cos w)$$

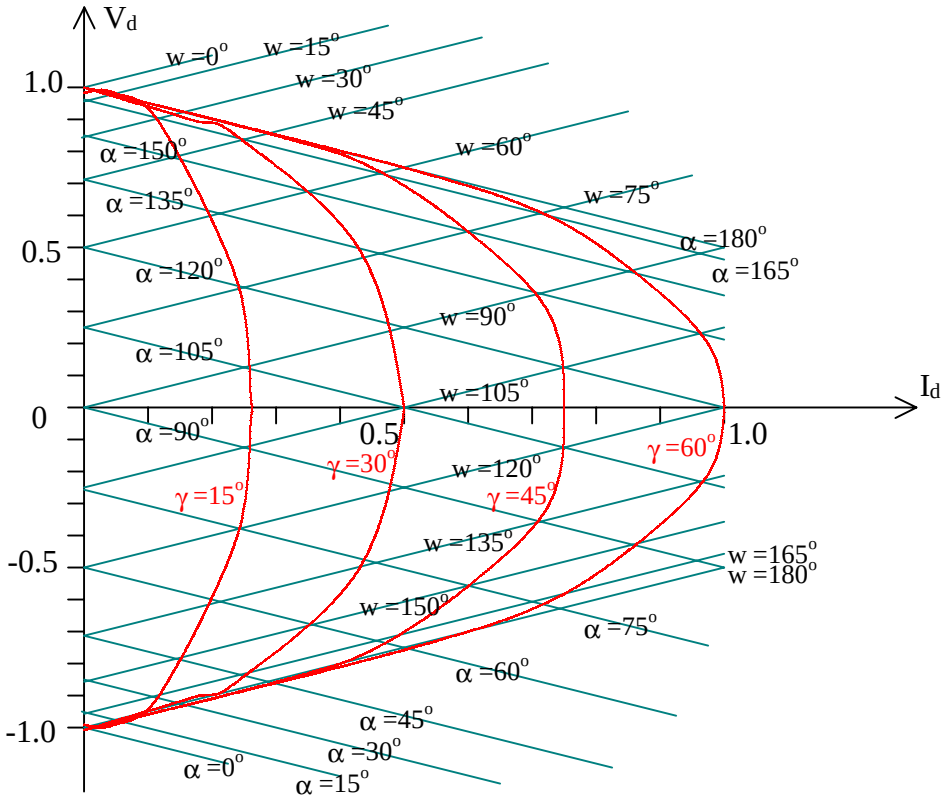

Figure 11.23 - Per unit convertor chart

It is useful to draw the convertor chart in per unit. For this purpose the natural selection for the base voltage is the maximum direct voltage output V_{do}. There is no such natural current base. Thus it is convenient to select the constant appearing in equation (11.5) for current as the base quantity. Thus the selected base quantities are as given in equation (11.15).

$$V_{base} = \frac{3\sqrt{2}\,E}{\pi}, \quad I_{base} = \frac{E}{\sqrt{2}\,\omega\,L_c} \tag{11.15}$$

With these base quantities, the per unit voltage $\mathbf{V_d}$ and per unit current $\mathbf{I_d}$ are given as follows.

$\mathbf{V_d} = ½ (\cos \alpha + \cos w)$ and $\mathbf{I_d} = \cos \alpha - \cos w$

which give the simple per unit characteristic equations (11.16) and (11.17).

$$\mathbf{V_d} + 0.5\,\mathbf{I_d} = \cos \alpha \tag{11.16}$$

$$\mathbf{V_d} - 0.5\,\mathbf{I_d} = \cos w \tag{11.17}$$

In the chosen per unit system, constant delay angle control (or the natural voltage characteristic) correspond to straight lines with slope (-) 0.5 on the per unit voltage-current chart. Similarly constant extinction angle control correspond to straight lines with slope (+) 0.5.

For inversion, the corresponding equations are as follows.

$$\mathbf{V_d} + 0.5\,\mathbf{I_d} = \cos (\pi - \beta) = (-) \cos \beta$$
$$\mathbf{V_d} - 0.5\,\mathbf{I_d} = \cos (\pi - \delta) = (-) \cos \delta$$

Since voltages are measured in the opposite direction for inversion, these equations may be rewritten in their more usual form as in equations (11.18) and (11.19).

$$\mathbf{(-)\,V_d} - 0.5\,\mathbf{I_d} = \cos \beta \tag{11.18}$$

$$(-)\,\mathbf{V_d} + 0.5\,\mathbf{I_d} = \cos \delta \tag{11.19}$$

From the characteristics, the constant commutation angle characteristic may be obtained by subtraction as follows.

$$\gamma = \beta - \delta \quad \text{or} \quad \gamma = w - \alpha$$

The constant γ characteristics can be shown to be ellipses ($\gamma < 60^0$). The per unit operating chart of the convertor is shown in figure 11.23.

11.4 Classification of d.c. links

D.C. links are classified into **Monopolar** links, **Bipolar** links, and **Homopolar** links.

In the case of the monopolar link there is only one conductor and the ground serves as the return path. The link normally operates at negative polarity as there is less corona loss and radio interference is reduced. Figure 11.23 (a) shows a monopolar link.

The bipolar links have two conductors, one operating at positive polarity and the other operating at negative polarity. The junction between the two convertors may be grounded at one or both ends. The ground does not normally carry a current. However, if both ends are grounded, each link could be independently operated when necessary. This is shown in figure 11.23 (b).

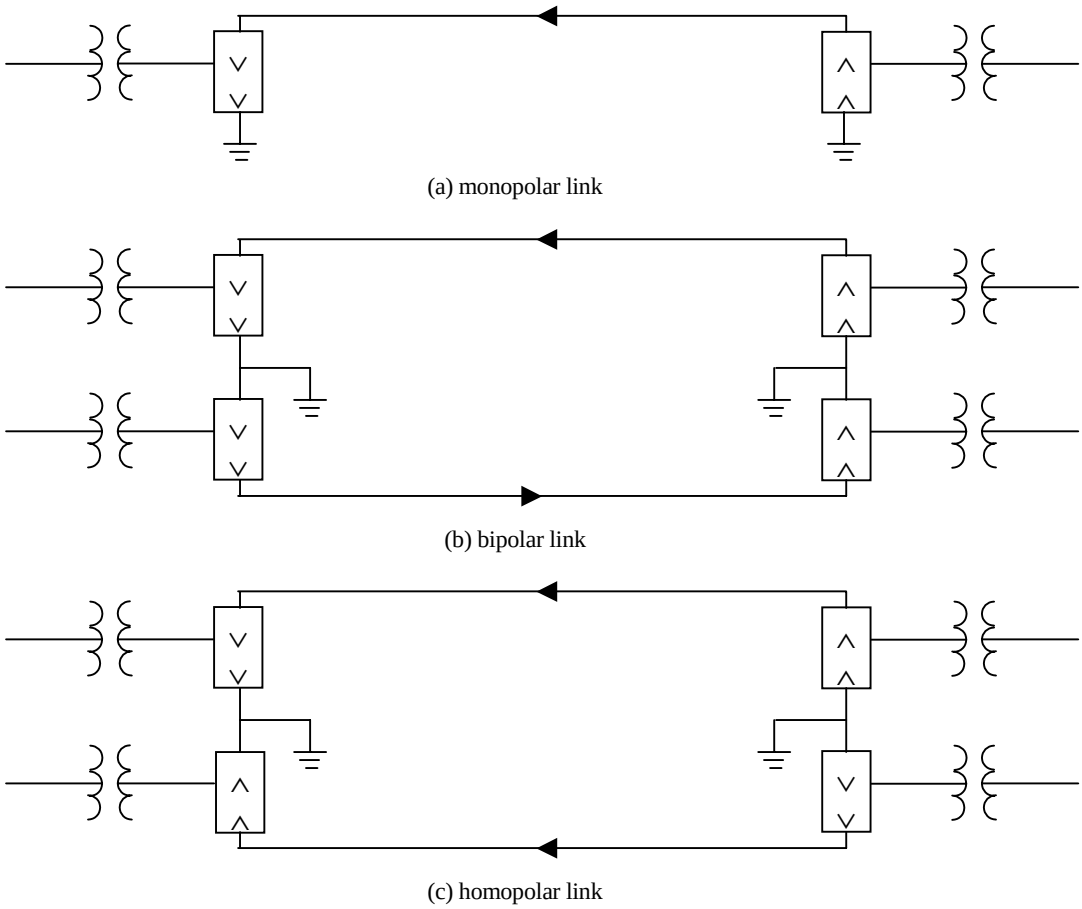

(a) monopolar link

(b) bipolar link

(c) homopolar link

Figure 11.24 - Kinds of d.c. links

The homopolar links have two or more conductors having the same polarity (usually negative) and always operate with ground path as return.

11.4.1 Harmonics and Filters

As was mentioned earlier, the harmonics present on the a.c. system are (6k±1). Thus the a.c. harmonic filters are tuned to the 5th, 7th, 11th, and 13th harmonics to reduce the harmonic content in the voltages and currents in the a.c. network to acceptable levels. Higher harmonics would not penetrate very far into the a.c. system. The harmonics are mainly present in the a.c. current as the a.c. voltage is heavily dependant on the a.c. system itself.

The Harmonics present on the d.c. side are mainly on output voltage. These are in multiples of 6 as the waveform repeats itself 6 times. The d.c. current is smoothed by the smoothing reactors.